Studies into the Synthesis of Cyclacenes

A Dissertation
SUBMITTED TO THE FACULTY OF
UNIVERSITY OF MINNESOTA
BY

Sarah Elizabeth Wegwerth

IN PARTIAL FULFILLMENT OF THE REQUIREMENTS
FOR THE DEGREE OF
DOCTOR OF PHILOSOPHY

Christopher J. Douglas

August 2017

Acknowledgements

"Now I see a lot depends on a helping hand from a few good friends."

- *The Little Blue Truck by Alice Schertle*

There are so many people I have to thank for helping me through graduate school. The Chemistry Department at the University of Minnesota is a wonderful environment to study chemistry. Thanks to all of the department staff but in particular, Nancy Tao and Nick Erickson for all the support as I navigated being the Head Organic TA. Thanks to Sean Murray and Joseph Dalluge for helping me get MS data. Thanks to Letitia for her work running the NMR facility, but even more so for her dedication to supporting and running WISE. Thank you also to the Hoye, Harned, Topczewski, Kass, and Tonks groups for sharing chemicals and the camaraderie. Thank you to the Hillmyer and Buhlmann groups, in particular Louis Pitet, for their support while I was a LANDO student, which ultimately helped me decide to pursue a Ph.D. in chemistry at UMN. Thank you to my undergraduate professors at St. Cloud State University, in particular Dr. Mechelke, for the solid education that prepared me for graduate school and for encouraging me to pursue a Ph.D. Thank you also to my high school chemistry teacher, in particular Lynn Swanson, and my elementary teacher Dave Noack, for being the first inspire my love for science.

Thank you also to Jane Wissinger and Angela Perkins for all of their support, encouragement, and mentorship while I was the Head Organic TA. I especially want to

thank you Jane for the nomination for the Bowers Award, for taking me across the country to attend a workshop on TA training, and for helping me to obtain the opportunity to teach my own section of CHEM 2302. Thanks also to Brian Woods who trained me in as an organic laboratory TA and Head Organic TA. Thank you also to all those who served as a TA while I was the Head Organic TA. You all made it an enjoyable experience and taught me many things about leadership.

A massive thank you also goes to all of the other members of the Douglas group both past and present. Thank you for creating such an amazing work environment where we have the space to work hard but also take the time to laugh together and check-in on each other. Thank you for the critiques, suggestions, and encouragement along the way. In particular, thank you Zhuoran Zhang for working so closely with me on the cyclacene project, for all the conversations we shared, and for motivating me to keep trying more reactions. Thanks Billy Ogden for obtaining the X-Ray crystal structure of my key intermediate. Thank you also to Jodi Olgivie, Katie McGarry, Ashley Dreis, Dan Everson, Matt Bruzek, Hanna Macaranas, Sadie Otte, Grant Frost, Zhuoran Zhang, Matt Eastwood, Lafe Purvis, and Jason Brethorst for all the conversations, advice, mentoring, for making me laugh, for listening when I was stressed, for letting me vent, and for creating such a supportive environment.

Thank you to my adviser Chris Douglas. While writing this dissertation I realized just how much patience you have as we learn how to be researchers. Your support has helped me to grow as both a scientist and as a professional. I am so grateful that you had the courage to pursue a seemingly impossible research project, namely the synthesis of

cyclacene, and for letting me be a part of it. Thank you for giving me the space to find my own path and not pressuring me down a traditional trajectory. I also value your support in my participation in other professional development roles, such as the Head TA position, even though it meant that less research got done. Thank you also for always making me feel like an important and valued member of the group, and for supporting me even though I chose a rather unconventional path through graduate school, and was not the most productive of graduate students. Thank you for always having the time to talk when I needed it most and for encouraging me to finish. Initially, I did not really believe I would be able to finish a Ph.D. but your support, and that of the group you have developed, has made it possible and helped me to believe in myself.

Thank you to my amazing husband Justin Wegwerth who has stood by my side through this journey and encouraged me to follow the path that is right for me. I also need to thank him and my parents, Roger and Leanne Zolldan, for all the support in caring for my son Micah so that I could continue my studies even after he was born. Thank you also to my brother David Zolldan who taught me to be tough and has dedicated himself to the protection of this great country through his service in the Army National Guard and as a Minnesota State Trooper.

Finally, to Micah, thank you for teaching me so much about what is really important in life. For teaching me to slow down and enjoy the little moments. Most of all though for just being you and bringing a smile to everyone's face. I cannot wait to see you grow but hope you will always stay my sweet little boy.

I know religion and science do not mix, but as a Christian, I would like to thank God for all the blessings, talents, and abilities He has shower on me and for working all things for my good.

Dedication

This dissertation is dedicated to my wonderful family who has supported and inspired me in so many ways.

In particular my grandmothers, Elaine Bartel and Mabel Zolldan, have been influential in my journey. I never had the chance to meet my Grandma Bartel, but by growing up hearing about how she earned her Ph.D. and a tenured faculty position at a time when not many women held that role, has inspired me to keep pursuing my own Ph.D. during the most challenging times. My Grandma Zolldan has taught me the value of hard work, to be resourceful, to care for your family, to be selfless, to be down to earth, and above all to love God and put Him first.

Abstract

Cyclacene is a unique macrocyclic hydrocarbon composed of laterally-fused benzenoid rings that has proven to be a challenging synthetic target. It is recognized as the shortest zigzag carbon nanotube (CNT) and could serve as a well-defined model to study the electronic and photophysical properties. Even prior to the discovery of CNTs, organic, physical organic, and computational chemists debated the consequences of the conjugated macrocyclic structure on the electronic and physical properties of cyclacene. This curiosity further drives the desire for experimental studies which are only possible after the successful synthesis of this molecule. Previous synthetic attempts successfully constructed the macrocyclic framework through Diels-Alder reactions, but late stage dehydrogenation and or oxidation proved problematic. Computational studies predict that one of the major challenges at the late-stage of synthetic efforts is the possibility of an open-shell singlet ground state of cyclacene, which would give the molecule a highly reactive diradical character. Another synthetic challenge associated with forming this macrocycle is its high strain energy. With these obstacles in mind, we have proposed a strategy for the synthesis of cyclacenes that should overcome these challenges because: (1) the intermediates are of approximately equal strain as the final target; (2) conjugation is completed through extrusion of a gas; (3) it allows the incorporation of substituents on the zigzag edge to increase the persistence of the final a cyclacene ring. A more detailed examination of the proposed synthetic route as well as current progress towards the synthesis of a cyclacene molecule is detailed in this dissertation.

Table of Contents

Acknowledgements i

Dedication v

Abstract vi

List of Schemes xi

List of Figures xvi

List of Tables xxi

List of Abbreviations xxii

1. INTRODUCTION 1

1.1. Background 2

1.2. Motivation 3

1.3. Structural Considerations and Computational Predictions 7

1.4. References 10

2. SUMMARY OF PREVIOUS SYNTHETIC ROUTES TOWARDS CYCLACENE AND THE PROHIBITIVE CHALLENGES ENCOUNTERED 14

2.1. Notable Synthetic Attempts Towards Cyclacene 14

2.1.1. Review of Stoddart's Attempt at [12]cyclacene 14

2.1.2. Review of Cory's Attempt at [8]cyclacene 19

2.1.3. Review of Schlüter's Macrocycle Preparation 21

2.2. Guiding Principles for Future Routes 23

2.3. References 25

3. RESEARCH PLAN: APPLYING LESSONS LEARNED TO STRATEGY 28
3.1. Strategy to Complete Conjugation 28
3.2. Strategy to Construct the Macrocycle 31
3.3. Strategy to Increase Persistence of Isolated Cyclacenes 33
3.4. General Proposed Retrosynthesis 34
3.5. References 36
4. IDENTIFYING KEY BUILDING BLOCKS 38
4.1. First Proposed Synthetic Route 38
4.1.1. Forward Synthetic Analysis 38
4.1.2. Results and Discussion 40
4.2. Design and Preparation of Benzonorbornene: A More Versatile Key-Intermediate 43
4.2.1. The Versatility of Benzonorbornenes 43
4.2.2. Identifying Fulvene and Benzyne Precursors for Benzonorbornene Preparation 46
4.3. Benzobisnorbornene Preparation and Characterization 49
4.3.1. Designing and Preparing, and Utilizing the Bisbenzyne Precursor 49
4.3.2. Optimization of Double Diels–Alder Reaction to Generate Masked Benzobisnorbornene 53
4.3.3. Isolation and Characterization of *syn*-benzobisnorbornene 60
4.4. Experimentals 64
4.5. References 75

5. ATTEMPTS TO ADVANCE KEY INTERMEDIATE BENZOBISNORBORNENE 78

5.1. Efforts to Incorporate the Cava Reaction 78

5.1.1. Precedence for the Cava Reaction and Proposed Incorporation into a Synthetic Route Towards Cyclacene 78

5.1.2. Results and Discussion 80

5.2. Generating an Electron Rich Dienophile for Inverse-Demand Diels–Alder Reactions: Attempts Toward Enamine Formation 85

5.2.1. Proposed Synthetic Route Utilizing an Inverse-Demand Diels–Alder Reaction 85

5.2.2. Results and Discussion 87

5.3. Work Towards Installation of a Cyclopentadienone 90

5.3.1. Proposed Synthesis and Utility of Cyclopentadienone 90

5.3.2. Results and Discussion 93

5.3.3. Future Work on Generating the Cyclopentadienone Unit 101

5.4. Experimentals 101

5.5. References 109

6. WORK TOWARDS BUILDING THE MACROCYCLE THROUGH DIELS–ALDER REACTIONS USING ISOBENZOFULVENE AND DIBROMOQUINONE 112

6.1. Precedence for Generating Isobenzofulvenes from Norbornene Structures 112

6.2. Proposed Routes Utilizing Isobenzofulvene Methodology 116

6.3. Model Study for Generation and Use of Isobenzofulvene 118

6.4. Application of Isobenzofulvene to the Real System: Results and Discussion.. 124

6.4.1. Preparation of key intermediates *syn*-bisquinone 6.27a and monoquinone 6.28 127

6.4.2. Attempts to Form a Macrocycle via Dimerization of Monoquinone 6.28 – Path A 137

6.4.3. Efforts to Form a Macrocycle from *syn*-bisquinone 6.27a – Path B 146

6.4.4. Conclusions and Future Work 158

6.5. Experimentals 161

6.6. References 172

BIBLIOGRAPHY 173

APPENDIX 1. 179

NMR Spectra Chapter 4 179

NMR Spectra Chapter 5 190

NMR Spectra Chapter 6 195

List of Schemes

Scheme 2.1 Retrosynthetic analysis of Stoddart's synthesis towards [12]cyclacene. 15

Scheme 2.2 Diel–Alder reactions used to prepare the macrocycle kohnkene. 18

Scheme 2.3 Deoxygenation of kohnkene to a [12]cyclacene precursor 19

Scheme 2.4 Cory's approach to preparing the macrocyclic precursor for [8]cyclacene ... 20

Scheme 2.5 Cory's attempts to advance his macrocycle 2.12. 21

Scheme 2.6 Schlüter's AB-monomers that a) dimerize and b) trimerize via Diels–Alder reactions to give macorcycles. 22

Scheme 3.1 Key end-game strategy of Chow and coworkers to prepare pure unsubstituted-hexacene via cheletropic extrusion of carbon monoxide. 29

Scheme 3.2 Proposed end-game strategy to install the final alkenes and complete the synthesis of cyclacene. 30

Scheme 3.3 Nuckolls' preparation of a pentacene derivative using an aryne and a diazapyrone. a) the overall scheme, b) the key reactive intermediates the reaction proceeds through. 32

Scheme 3.4 The Diels–Alder reaction that was performed in the organic teaching labs at the University of Minnesota. 33

Scheme 3.5 Retrosynthetic analysis of our novel proposed general strategy for synthesis of a cyclacene molecule. 35

Scheme 4.1 First proposed synthetic route towards an [8]cyclacene derivative. 39

Scheme 4.2 The palladium cross-coupling reaction reported by Miura. 41

Scheme 4.3 The attempted palladium cross-coupling reaction to prepare desired 1,3-diphenylindanone 4.15. 41
Scheme 4.4 Targeted structural motif a) the most basic structural requirement b) a suitable structure achievable by a Diels–Alder reaction. 44
Scheme 4.5 Proposed synthetic transformations of the norbornene olefin demonstrating the versatility of this key intermediate. 45
Scheme 4.6 Retrosynthetic analysis for preparation of key intermediate 3.21. 46
Scheme 4.7 Initial attempts to form the key intermediate by trapping a benzyne generated from tetrabromobenzene with a) diphenylfulvene and b) pentamethylenylfulvene. 47
Scheme 4.8 Synthesis of a) diphenylfulvene and b) pentamethylenylfulvene 48
Scheme 4.9 An example of Biju's reliable method for performing the Diels–Alder reaction between fulvenes and benzyne using the desired pentamethylenylfulvene. 49
Scheme 4.10 Wudl's use of bisbenzyne precursor 4.39 in a double Diels–Alder reaction. 49
Scheme 4.11 Brimble's efficient synthesis of 2-(trimethylsilyl)aryl triflates, 4.36. 50
Scheme 4.12 Synthetic scheme for the synthesis of bisbenzyne precursor 4.39. 50
Scheme 4.13 Initial attempt of double Diels–Alder reaction using 4.39 and Biju's conditions. 54
Scheme 5.1 Examples of the Cava reaction for adding a napthalene unit to a norbornene ring by a) Bläser and b) Paddon-Row. 79
Scheme 5.2 Proposed route to [12]cyclacene that utilizes Cava reactions to efficiently form the macrocycle. 80

Scheme 5.3 Test of the Cava reaction with our benzonorbornene system in a) a model study b) with the anti-isomer 4.32b. 82

Scheme 5.4 Formation of Diels–Alder intermediate 5.13 and alternative elimination pathways to form a) a new quinodimethane and b) isobenzofulvene. 84

Scheme 5.5 Proposed elaboration of 4.32a to prepare key intermediate, bisdiene 5.20... 86

Scheme 5.6 The various macrocycles that could potentially be formed using bisdiene 5.20..... 87

Scheme 5.7 Hydroboration of model benzonorbornene 4.37. Yields are not given as purification was saved until after oxidation to the ketone. 88

Scheme 5.8 Model study for a) oxidation of alcohol 5.24, b) one-pot hydroboration and over oxidation to ketone 5.25, and c) condensation of ketone 5.25 with pyrrolidine. *Low yield due to decomposition during purification process. 89

Scheme 5.9 Proposed addition of a cyclopentadienone unit onto 4.32a. 91

Scheme 5.10 Various pathways for proposed Diels–Alder reaction between aryne 5.31 and bisdiene 5.28. 92

Scheme 5.11 Dimerization of 5.34 to give macrocycle precursor and non-macrocyclic by-products. 93

Scheme 5.12 Swern oxidation of diol 5.36 to diketone 5.37. 98

Scheme 5.13 The observed rearrangement of a) diketone 5.38 to give 5.40 instead of the desired isobenzofulvene 5.39 and b) of diketone 5.37 to oxo-enol 5.41. 99

Scheme 5.14 Attepmts at formation of cyclopentadienone 5.42 from 5.38 and 4.2..... 100

Scheme 6.1 Chow's synthesis of hexacene starting from norbornene 6.1 and quinone 6.2 113

Scheme 6.2 Mechanism for generation of isobenzofulvene 6.9 from norbornene 6.1 and tetrazine 6.5 114

Scheme 6.3 Butler and Warrener's synthesis of pincer molecule 6.13 using isobenzofulvene 5.39 and dichloroquinone 6.10. 116

Scheme 6.4 Retrosynthetic analysis for incorporation of isobenzofulvene chemistry starting from key intermediate 4.32. 117

Scheme 6.5 The first reaction we performed generating isobenzofulvene from benzonorbornene 4.37 and trapping it with quinone 6.21 to give endo and exo dihydroquinone 6.22. 119

Scheme 6.6 Model reaction between benzonorbornene 4.37 and dibromoquinone 6.20 initiated by tetrazine 6.5. 119

Scheme 6.7 Conditions attempted to facilitate the dehydrobromination of 6.23 a) pyridine and DBU which led to decomposition and b) basic alumina successfully provided quinone 6.24 and a photo of the process showing the color change from yellow (6.23) to red-orange (6.24). 122

Scheme 6.8 Second addition of 4.37 to quinone 6.25 and elimination to give a mixture of syn and anti isomers of quinone 6.26. 124

Scheme 6.9 Attempt to form a) monoquinone 6.28 and b) bisquinone 6.27. 128

Scheme 6.10 A 3-dimensional image of the isobenzofulvene intermediate formed from a) dihydroquinone 6.29 and b) quinone 6.31. 133

Scheme 6.11 Using AB monomer 6.31, a) proposed dimerization to form [8]cyclacene precursor, b) the EXO and ENDO faces of diene 6.32 and dienophile 6.31 138

Scheme 6.12 Independent synthesis of the desired *syn* isomer of 6.32. 143

Scheme 6.13 Proposed synthesis to [12]cyclacene precursor 6.41 starting from 6.27a and 6.28..... 147

Scheme 6.14 Proposed synthesis of [10]cyclacene marcrocyclic framework. 152

Scheme 6.15 Model study of Diels–Alder cascade using aryne generated from 4.50 and 3.8 a) the reaction scheme and b) the intermediate after the first Diels–Alder reaction..... 158

Scheme 6.16 Proposed preparation of a [12]cyclacene precursor 160

List of Figures

Figure 1.1 Examples of a) benzene and selected benzene derivatives with materials applications and b) the general structure of cyclacene, where n indicates the number of benzenoid rings. 1

Figure 1.2 The alignment of the conjugated p orbitals with respect to the plane of the molecule a) parallel as in a normal aromatic system b) perpendicular as in cyclacene 7

Figure 1.3 The C–C bond lengths predicted for [8]cyclacene by Houk. 9

Figure 1.4 The proposed end-game strategy of decarbonylation to complete conjugation. 10

Figure 2.1 The differential faces of the bisdiene and bisdienophile. Note, the 1 and 2 indicate the number of olefins at the termini. 16

Figure 2.2 The unique electronic structure of Stoddart's bisdienophile 2.4 and bisdiene 2.3 a) the frontier orbitals b) the electronically favored approaches with the sterically most accessible approach boxed. 17

Figure 3.1 Anthony's persistent pentacene that is protected with TIPS acetylene groups.34

Figure 4.1 Representative ^{1}H NMRs of 4.50 and 4.32. Note the spectrum of 4.32 is enriched in one isomer due to the low solubility of the minor one. The signal at 6.91 ppm is due to the minor isomer but all other signals overlap with the major isomer. 55

Figure 4.2 a) The largest contributing resonance structures to pentamethylenylfulvene's hybrid structure and b) the proposed interaction of Cs cation with the anionic cyclopentadiene ring of the second resonance structure. 58

Figure 4.3 Characterization spetra for a sample enriched in isomer A and isomer B of 4.32 a) ^{1}H NMR, b) ^{13}C NMR, c) IR (KBr). 61

Figure 4.4 Identities of the 4.32 isomers, a) the ORTEP of the X-ray obtained for isomer A and b) a ^{1}H NMR of the benzene solvate crystals along with the assigned identities of isomer A as *syn* and isomer B as *anti*. 63

Figure 5.1 ^{1}H NMR of the matching fractions from the model studies. 82

Figure 6.1 An example of the colors observed during the washing of a Diels–Alder cascade between benzonorbornene, tetrazene, and quinone. From left to right, aqueous phases from the first and second HCl washes containing excess tetrazine and pyridazine by-product, the aqueous phase from plain water wash, and the combined organic (solvent DCM) and brine wash. The product in the DCM layer has a yellow tint. 119

Figure 6.2 ^{1}H NMR of a mixture of dihydroquinone 6.23a and 6.23b (endo and exo isomers) zoomed in on the protons of the norbornane ring. 121

Figure 6.3 ^{1}H NMR of quinone 6.24 zoomed in on the region where the norbornane protons appear. 123

Figure 6.4 ^{1}H NMR of a mixture of *syn* and *anti* isomers of quinone 6.26a. 124

Figure 6.5 General transitions state structures for the Diels–Alder reaction of an isobenzofulvene with a) dibromoquinone, a small dienophile and b) a substituted

quinone that has an EXO and ENDO face. The boxed structures are the transitions states that will lead to the desired *syn* relationship of the bridges. 126

Figure 6.6 A key for the 2-dimensional drawings of the reactions covered in this chapter, a) flat representation of bicyclic structures that will be used to improve clarity of structures of intermediates and b) definitions of R^*, py, X and Y. 127

Figure 6.7 A guide for interpreting the ^{1}H NMRs of the biquinone 6.27 a) the region of the spectra and the splitting expected for each key proton and b) identification of equivalent protons and relative order from highest ppm to lowest ppm for each isomer..... 129

Figure 6.8 ^{1}H NMR of major isomer formed from attempt to form bisquinone 6.27. Note, the apparent triplets at 4.88 ppm and 4.83ppm are actually two separate doublets that are overlapping..... 130

Figure 6.9 ^{1}H NMR of crude reaction mixture of a double cascade Diels–Alder reaction after elimination. Circled are the signals from of the minor *syn/anti* isomers..... 131

Figure 6.10 Representations of the colors observed during the cascade Diels–Alder reaction of tetrazine 6.5 with benzobisnorbornene 4.32 and after elimination. From left to right, the pink solution is tetrazine 6.5, the middle gold solution is the crude reaction mixture, the orange solution is after elimination. 135

Figure 6.11 ^{1}H NMR of monoquinone 6.31 as a mixture of *syn* and *anti* isomers..... 135

Figure 6.12 ^{1}H NMR of the dehydrohalogenated dimer of 6.28b. *Note, the labels H_{a-e} are for a general categories of key diagnostic regions, not for specific assignments. 139

Figure 6.13 A 3-dimensional image of the isobenzofulvene intermediate generated from *syn* 6.33, generated using Chem3D, showing that there is too much space between the diene and dienophile for macrocycle closure. 140

Figure 6.14 Zhuoran Zhang's Diels–Alder reaction between large isobenzofulvene 6.35 and large dienophile 6.36 to give only exo products as shown by the ^{1}H NMR spectrum. 141

Figure 6.15 The proposed plausible transition states for the Diels-Alder reaction between large isobenzofulvene 6.31 and large quinone 6.28b. 142

Figure 6.16 ^{1}H NMR of dihydroquinone 6.32 formed from the Diels–Alder cascade reaction of 4.32 and 6.27a. 143

Figure 6.17 Comparison of the ^{1}H NMR spectra of 6.32 prepared from *syn*-bisquinone 6.27a with the eliminated product 6.33. 144

Figure 6.18 Comparison of the ^{1}H NMRs of the preparation of 6.32 from *syn*-bisquinone 6.27a (top) vs a dimerization of monoquinone 6.28b. 145

Figure 6.19 ^{1}H NMR of 6.39 highlighting the singlets for the endo H for each of the 16 anticipated isomers. 148

Figure 6.20 Considering the ^{1}H NMR spectrum expected for 6.40, a) the rational for the expected number of signals for the protons on the external quinones and b) the spectrum obtained after elimination of 6.39. 150

Figure 6.21 Analysis of the mixture of isomers of 6.42 a) the isomers that would have different NMR spectra and b) the observed ^{1}H NMR spectrum for the products after

elimination of the product of the double Diels–Alder cascade reaction between 6.27a and 4.50. 154

Figure 6.22 The steric analysis Zhuoran Zhang used to explain the observed EXO–exo selectivity when he used isobenzofulvene 6.35. 155

Figure 6.23 Comparison of the NMRs of the starting material 6.42 (bottom spectrum) and after macrocyle formation attempt (top spectrum) a) ^{1}H NMR and b) ^{19}F NMR... 157

Figure 6.24 Proposed endo dihydroquinone 6.48. The ENDO face of the dienophile of this molecule could potentially be sterically hindered enough to prevent diene addition to this face. 160

List of Tables

Table 4.1 Select trials to perform the palladium cross-coupling of 4.2 to either 4.14 or 4.1 42

Table 4.2 Solvent and temperature optimization study of double Diels–Alder reaction.. 56

Table 4.3 Summary of a comparison of characterization data and properties of isomer A and isomer B of 4.32. 64

Table 5.1 Comparison of reaction conditions for the dihydroxylation of 4.37 using AD-mix β. 94

Table 5.2 Comparison of reaction conditions for the dihydroxylation of 4.37 using OsO_4 and NMO. 96

List of Abbreviations

CNT	Carbon Nanotube
CPP	Cycloparaphenylene
d	Doublet
DBN	1,5-Diazabicyclo[4.3.0]Non-5-Ene
DBU	1,8-Diazabicyclo[5.4.0]Undec-7-Ene
DCM	Dichloromethane
dd	Doublet Of Doublets
DDQ	2,3-Dichloro-5,6-Dicyano-1,4-Benzoquinone
DFT	Density Functional Theory
DMF	Dimethylformamide
DMS	Dimethyl Sulfide
DMSO	Dimethylsulfoxide
dt	Doublet Of Triplets
EPR	Electron Paramagnetic Resonance
EtOAc	Ethyl Acetate
ESI	Electrospray Ionization
FT	Fourier Transform
GC	Gas Chromatography
h	Hour
HMDS	Hexamethyldisilazane

HOMO	Highest Occupied Molecular Orbital
HRMS	High Resolution Mass Spectrometry
Hz	Hertz
i-Pr	Isopropyl
IR	Infrared
kbar	Kilobar
LDA	Lithium Diisopropyl Amide
LRMS	Low Resolution Mass Spectrometry
LUMO	Lowest Unoccupied Molecular Orbital
m	Multiplet
M	Molar
MeOH	Methanol
mL	Milliliters
mm	Millimeters
MP	Melting Point
MS	Mass Spectrometry
MTO	Methyltrioxorhenium
nm	Nanometers
NMO	*N*-Methylmorpholine *N*-Oxide
NMR	Nuclear Magentic Resonance
o	Ortho

oTf	Triflate
PCC	Pyridinium Chlorochromate
Ph	Phenyl
ppm	Parts Per Million
pTSA	*Para*-Toluene Sulfonic Acid
q	Quartet
QTOF	Quadrupole Time-Of-Flight
s	Singlet
t	Triplet
t-Bu	*Tert*-Butyl
TBAF	Tetrabutylammonium Fluoride
TEA	Triethylamine
TFAA	Trifluoroacetic Anhydride
THF	Tetrahydrofuran
TIPS	Triisopropylsilyl
TLC	Thin Layer Chromatography
TMS	Tetramethysilane
TMSCl	Chlorotrimethylsilane
TPAP	Tetrapropylammonium Perruthenate
UBS	Unrestricted Broken Spin-Symmetry
UV	Ultra Violet

V	Volt
vis	Visible
W	Watts

1. INTRODUCTION

Naturally abundant hydrocarbons, such as those found in petroleum, are vital commodities for society. Even though they are composed of only carbon and hydrogen, hydrocarbons can have vastly different properties, reactivity, and uses. Often these differences are largely influenced by the structure of the molecule. A classic example is the unusual stability of benzene in comparison to other alkenes.[1] The unusual stability is attributed to the cyclic delocalization of the π electrons – the hallmark of aromatic molecules. Recently, much attention has been given to benzene derivatives, such as

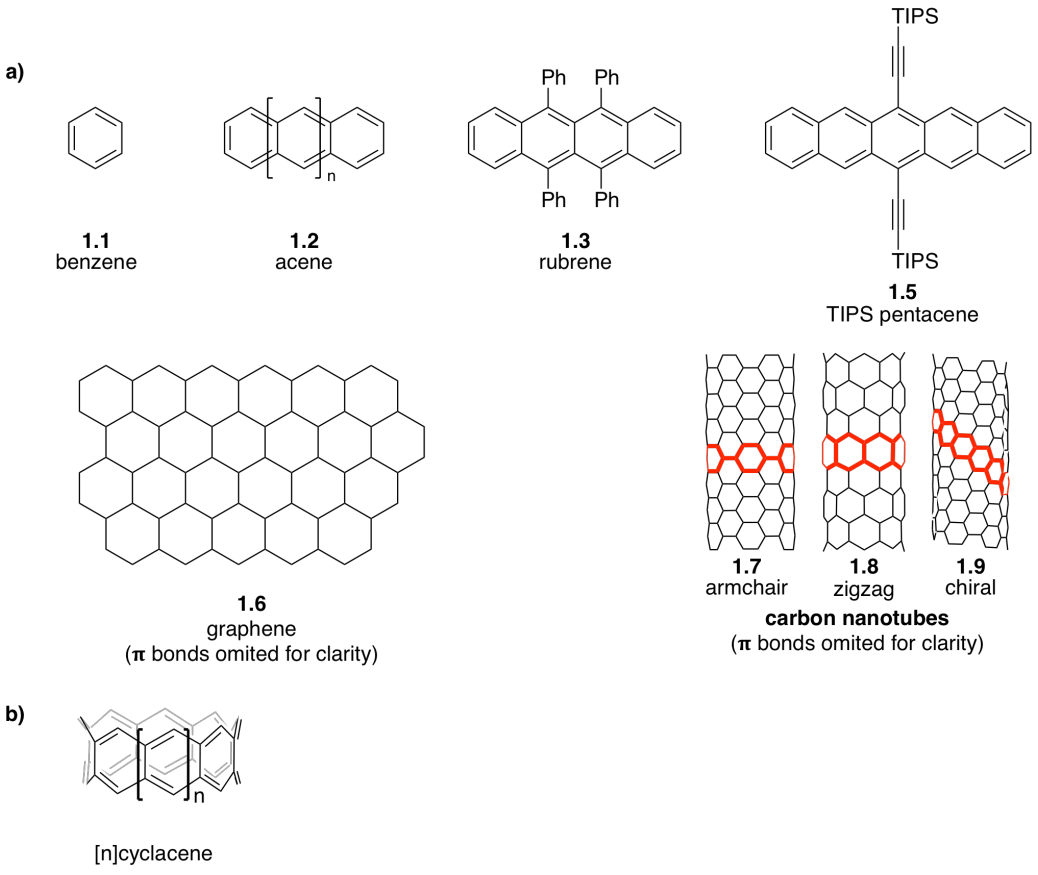

Figure 1.1 Examples of a) benzene and selected benzene derivatives with materials applications and b) the general structure of cyclacene, where n indicates the number of benzenoid rings.

graphene, acenes, and carbon nanotubes (CNTs) (Figure 1.1a), that have delivered on promises of breakthroughs in material science. A related, but unique structure, namely cyclacene (Figure 1.1b), remains a challenging synthetic target that has yet to be isolated. The research in this dissertation outlines a new synthetic strategy for the first preparation of a cyclacene molecule and reports the progress to date.

1.1. Background

In 1954 Heilbronner was the first to imagine a macrocycle composed of laterally fused benzenoid rings, now referred to as cyclacene.[2] This intriguing structure sparked many theoretical debates as to what the implications would be for such a highly conjugated structure.[3] Similar to acenes, cyclacenes are predicted to have a small energy gap between the highest occupied molecular orbital (HOMO) and lowest unoccupied molecular orbital (LUMO).[4] As a result, these systems are challenging to model even by modern computational methods. To gauge the accurateness of these sophisticated computational methods, a physical sample of a cyclacene is necessary.

Insight into the potential properties of cyclacene's structural motif was gained in the 1990s upon the discovery of carbon nanotubes (CNTs).[5] CNTs can be described as graphene sheets rolled into a cylinder.[6] Since there are multiple ways the graphene sheet can be rolled, there are three classes of CNTs, armchair, zigzag, and chiral (Figure 1.1a). The structures differ based on the connectivity of the phenyl rings of the repeating macrocyclic ring (highlighted in red in Figure 1.1a). Characteristic of the armchair structure, the phenyl rings are connected at the *para* position. The shortest armchair CNT (only one layer) has the common name cycloparaphenylene (CPP). Zigzag CNTs are

characterized by lateral fusion of the benzenoid rings in the repeat unit. The shortest zigzag CNT is therefore, the target molecule of this thesis, cyclacene. Any other connectivity of the phenyl rings belongs to the chiral class of CNTs. Characterization of CNTs revealed that these hydrocarbons have extraordinary physical and electronic properties which are dependent on the CNT structure.[6–9]

Beyond materials applications, the conjugated macrocycle of cyclacene would increase our fundamental understanding in other areas as well. The cavity within cyclacene is envisioned to be useful for host-guest chemistry.[10] A physical sample of cyclacene could also further the understanding of bonding between Csp^2 carbons in highly strained systems. For an organic chemist, the structure of cyclacene presents a unique synthetic challenge. Previous synthetic attempts towards cyclacene have been successful in preparing a macrocycle of non-conjugated six-membered rings.[10 – 14] However, oxidation and/or dehydrogenation to the fully conjugated system has proven to be challenging. Since these attempts though, many advances have been made in the area of synthesis of the linear analogue, oligoacenes.[15, 16] Based on these advances, we have a designed a new synthetic strategy to prepare the first cyclacene molecules. The core step of our route will serve as a way to test the limits of current synthetic methodology.

1.2. Motivation

Cyclacene is not a naturally occurring compound nor has it ever been isolated. Motivation for its synthesis is, in part, driven by the desire to expand on the fundamental knowledge of the structure-electronic property relationship of CNTs. In general, it is known that the armchair CNTs have metallic character whereas the zigzag and chiral

CNTs have semiconductor character.[17] It is also well established that CNTs have impressive properties that could make them powerful tools for developing new materials.[7] For instance, metallic CNTs have been shown to have current densities as high as 10^9 A/cm^2, which is orders of magnitude greater than that observed for metals which are about 10^5 A/cm^2.[18] Semiconducting CNTs on the other hand would be useful for transistors, memory, and sensory devices used in nanoelectronics. Along with the chirality, the diameter of the CNT also impacts the properties. Unfortunately, detailed studies into the structure electronic property relationship is hindered by the limited ability to synthesize or isolate specific CNTs of identical diameter and chirality.[7] As a result only bulk average properties are readily measured. Due to this limitation, cyclacene could serve as a model of chemically defined short zigzag CNTs for structure property relationship studies.

Additionally it is desirable to be able to prepare longer specific CNTs for use in devices but this also is a major synthetic challenge especially on large scale.[7] Common methods for preparing CNTs include laser ablation, electric arc discharge, and metal-catalyzed organic chemical vapor deposition. All these methods suffer from lack of ability to control both the diameter and chirality simultaneously. Additionally, separating the CNTs formed can be more challenging and costly than the synthesis itself. A solution to this problem could be the growth of CNTs from short templates through mechanistically understood and controlled reactions similar to a polymerization.[19]

Synthetically controlled growth has been realized for various chiral and armchair CNTs. For example, Zheng and Zhou demonstrated that metal-free vapor-phase epitaxy

could be used to restart the growth of short CNTs and that growth followed both the diameter and chirality set in place by the template.[20] It is hypothesized that the carbon feedstock, methane and ethanol, decompose to acetylene and or ethylene which can act as dienophiles in a Diels–Alder reaction with the edges of the template acting as the diene. Subsequent dehydrogenation results in formation of a new benzenoid ring which can also participate in another series of these reactions allowing for elongation. More recently the Itami group used synthetically prepared cycloparaphenylene (CPP), the shortest armchair CNTs, as a template to grow armchair CNTs using ethanol as a carbon source.[21] Analogously, it is hoped that cyclacene could be used as a template to synthetically prepare zigzag carbon nanotubes. However, if elongation is occurring through Diels–Alder reactions, cyclacene could not be extended using this method as its edge does not contain any suitable *s*-cis dienes. Instead conditions to facilitate reactions such as a Friedel–Crafts or C–H activation to add carbon atoms to the benzenoid rings would need to be investigated.[19] Overall cyclacene is a prime target for advancement in understanding and preparing CNTs.

Even without forming a nanotube though, samples of cyclacene could serve as a model for zigzag CNTs.[4, 17, 22] In particular, studying how the properties change in relation to the diameter of the macrocycle could reveal surprising results. For example some of the physical properties of CPP were opposite than what is observed in linear acenes.[23, 27, 36] A variety of CPPs have been prepared by the groups of by Bertozzi,[24] Jasti,[19, 25–29] Itami,[30–35] and Yamago.[36–39] Surprisingly, UV-vis studies show that the absorption maximum for CPPs is about 340 nm regardless of the macrocycle ring size,

and therefore, the number of benzenoid rings in conjugation.[27, 36, 40] Yamago and co-workers explained this phenomenon using time-dependent DFT calculations.[36] From their calculations they learned that the HOMO–LUMO transition is forbidden. Instead the absorption at 340 nm is due to a combination of the HOMO–2 to LUMO, HOMO–1 to LUMO, HOMO to LUMO+1 and HOMO to LUMO+2 transitions. In other words, the absorption is not directly related to the HOMO–LUMO gap and therefore insensitive to the ring size.

More information about the system can be gained from examining the fluorescence of CPPs in relation to the macrocycle ring size. Contrary to the linear oligoacene analogue, as the number of benzenoid ring in the macrocycle decreased, the fluorescence red-shifts.[27, 36] It is postulated that a larger Stokes shift is observed for smaller CPPs because inherently they are more strained and will therefore experience a larger structural change upon excitation.[36] Oxidation potentials have also been measured for CPPs of various sizes.[36] As the number of paraphenylene rings increases, the oxidation potential also increases and plateaus around 0.85 V, ([12]CPP). Reversible oxidation waves were also observed which indicates that the radical cation is stable. A reduction potential could not be observed under the experimental conditions used. Finally, Yamago also notes that as the CPP decreases in size the HOMO level increases and the LUMO level decreases, which is the exact opposite of what is observed for other conjugated systems.[36] This indicates that the strained CPPs' benzene rings take in a quinodimethane form thus decreasing the aromaticity giving it strong polyene character.

These unexpected results of a macrocycle analogous to cyclacene, emphasizes the need for physical samples of cyclacenes to better understand structure property relationships.

1.3. Structural Considerations and Computational Predictions

Even without relating cyclacene to CNTs, cyclacene itself is an interesting all Csp^2 hydrocarbon due to the macrocyclic delocalization and orientation of the p orbitals. Since the p orbitals are pointing towards the center of the macrocycle it is anticipated that cyclacene's cavity will act as a strong host for host-guest chemistry (Figure 1.2).[10,46] For example, the analogous CPPs have been shown to encapsulate various size fullerenes.[41] Less straightforward though is how the arrangement of the p orbitals will affect the physical and chemical properties of cyclacene.

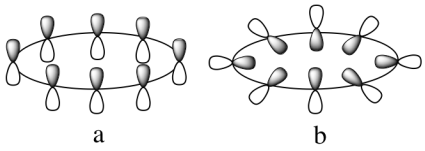

Figure 1.2 The alignment of the conjugated p orbitals with respect to the plane of the molecule a) parallel as in a normal aromatic system b) perpendicular as in cyclacene

In particular, chemists have questioned whether the cyclic arrangement of benzenoid rings will result in increased stability of the oligoacenes, as in will there be additional aromatic stabilization.[23,42] In lieu of physical data, computational chemists provide some insight into the electronic and magnetic properties expected. Houk and co-workers found the lowest energy ground state is computed when using an unrestricted, broken spin-symmetry (UBS) wavefunction for DFT and ab inito calculations.[43,4] As a result of the UBS wavefunction these calculations also predict that for [n]cyclacenes (n specifies the number of benzenoid rings) where $n \geq 6$ the lowest-energy ground state

configuration is an open-shell singlet.[4] As a result, cyclacene is predicted to have a diradical character, where the radicals are localized on the zigzag edge. This diradical character increases as the number of benzenoid rings in the macrocycle increases. The unstable diradical character of cyclacene, if true, could explain why the synthesis has proven challenging. A solution to this problem could be the addition of bulky substituents on the zigzag edge, much like the Anthony group demonstrated with oligoacenes, including nonacene derivatives exhibiting diradical character, in order to reduce its reactivity and aid in isolation of the final product.[16, 44]

This diradical like character is also observed for the acyclic version, oligoacenes, still leaving the question does the macrocycle result in additional stabilization?[43] Cramer and co-workers have shown that the difference in energy between oligoacenes and the corresponding cyclacene is about equal to the strain energy associated with bending the benzenoid rings into a macrocycle.[45] In other words there is no stabilization gained by cyclic delocalization around the macrocycle and therefore no aromatic stabilization. Bond lengths can also be used to assess aromaticity. In Houk's work, the lowest energy structure of cyclacene was predicted to have longer bonds connecting the transannular rings (1.46 Å) while the bonds around the zigzag edge were of equal length (1.41 Å) (Figure 1.3).[4] This indicates that the aromatic character of the individual benzenoid rings has been broken but there is still electron delocalization around each of the transannular rings. The validity of these results can only be confirmed by examining a physical sample of cyclacene.

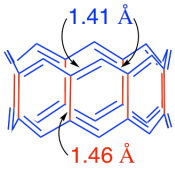

1.11

Figure 1.3 The C–C bond lengths predicted for [8]cyclacene by Houk.[4]

The synthesis of cyclacene is undoubtedly a daunting challenge primarily because of its high strain and instability as predicted by computations. Yet, motivated to answer fundamental questions about bonding, structure, and properties of a highly strained conjugated macrocycle, as well as the ability to investigate cyclacene's physical properties and uses, efforts towards its synthesis persist.[46] To date, attempts to synthesize cyclacene in order to experimentally study its physical properties have been unsuccessful. Limitations of synthetic methods, as detailed in the next chapter, appear to be late-stage dehydrogenation and/or dehydration of the macrocyclic framework. In contrast, proposed in the following chapters of this dissertation is a new route to cyclacene that relies upon an irreversible, late-stage decarbonylation to complete conjugation (Figure 1.4). In particular we are targeting macrocycles with 8–12 benzenoid rings. Smaller rings would be more strained and therefore more difficult to construct but larger macrocycles would be less stable due to the increase in diradical like character. Also proposed are modifications to the core to decrease reactivity and facilitate isolation of these compounds. It is the goal of the Douglas group to achieve a synthesis of cyclacene. Upon successful synthesis we plan to probe its structure and properties using X-ray crystallography, NMR, EPR, UV–vis, cyclic voltammetry, and Raman spectroscopy.

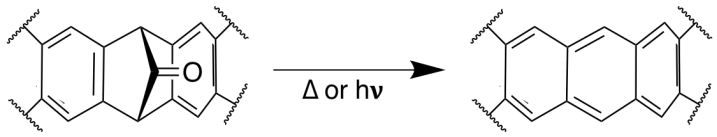

Figure 1.4 The proposed end-game strategy of decarbonylation to complete conjugation.

1.4. References

[1] Minkin, V. I.; Glukhovtsev, M. N.; Simkin, B. Y. *Aromaticity and Antiaromaticity: Electronic and Structural Aspects,* J. Wiley & Sons, New York, 1994.

[2] Heilbronner, E. *Helv. Chim. Acta* **1954**, *37*, 921–935.

[3] Tahara, K.; Tobe, Y. *Chem. Rev.* **2006**, *106*, 527–5290.

[4] Chen, Z.; Jiang, D. E.; Lu, X.; Bettinger, H. F.; Dia, S.; Schleyer, P. V.; Houk, K. N. *Org. Lett.* **2007**, *9,* 5449–5452.

[5] Iijima, S. *Nature* **1991**, *354,* 56–58.

[6] Dia, H. J. *Acc. Chem. Res.* **2002**, *35,* 1035–1044.

[7] Sgobba, V.; Guldi, D. M. *Chem. Soc. Rev.* **2009**, *38,* 165–184.

[8] Dekker, C. *Physics Today* **1999**, *52,* 22–28.

[9] Meo, M.; Rossi, M. *Composites Science and Technology* **2006**, *66,* 1597–1605.

[10] Cory, R. M.; McPhail, C. L. *Tetrahedron Lett.* **1996**, *37,* 1987–1990.

[11] Kohnke, F. H.; Slawin, A. M. Z.; Stoddart, J. F.; Williams, D. J. *Angew. Chem., Int. Ed.* **1987**, *26,* 892–894.

[12] Ashton, P. R.; Brown, G. R.; Isaacs, N.S; Giuffrida, D.; Kohnke, F. H.; Mathias, J. P.; Slawin, A. M. Z.; Smith, D. R.; Stoddart, J. F.; Williams, D. J. *J. Am. Chem. Soc.* **1992**, *26,* 6330–6353.

[13] Cory, R. M.; McPhail, C. L.; Dikmans, A. J.; Vittal, J. J. *Tetrahedron Lett.* **1996**, *37,* 1983–1986.

[14] Godt, A.; Enkelmann, V.; Schlüter, A. D. *Angew. Chem., Int. Ed.* **1989**, *28,* 1680–1682.

[15] Watanabe, M.; Chen, K. Y.; Chang, Y. J.; Chow, T. J. *Acc. Chem. Res.* **2013**, *46,* 1606–1615.

[16] Anthony, J. E.; Eaton, D. L.; Parkin, S. R. *Org. Lett.* **2002**, *4,* 15–18.

[17] Dresselhaus, M. S.; Dresselhaus, G.; Saito, R. *Carbon* **1995**, *33*, 883–891.

[18] Baughman, R. H.; Zakhidov, A. A.; de Heer, W. A. *Science* **2002**, *297*, 787–792.

[19] Jasti, R.; Bertozzie, C. R. *Chem. Phys. Lett.* **2010**, *494*, 1–7.

[20] Liu, J.; Wang, C.; Tu, X.; Liu, B.; Chen, L.; Zheng, M.; Zhou, C. *Nature Commun.* **2012**, *3*, 1199–1206.

[21] Omachi, H.; Nakayama, T.; Takahashi, E.; Segawa, Y.; Itami, K. *Nat. Chem.* **2013**, *5*, 572–576.

[22] Alvarez, M. P.; Burrezo, P. M.; Kertesz, M.; Iwamoto, T.; Yamago, S.; Xia, J.; Jasti, R.; Navarrete, J. T. L.; Taravillo, M.; Baonza, V. G.; Casado, J. *Angew. Chem. Int. Ed.* **2014**, *53*, 7033–7037.

[23] Hirst, E. S.; Jasti, R. *J. Org. Chem.* **2012**, *77*, 10473–10478.

[24] Jasti, R.; Bhattacharjee, J.; Neaton, J. B.; Bertozzi, C. R. *J. Am. Chem. Soc.* **2008**, *130*, 17646–17647.

[25] Xia, J.; Bacon, J. W.; Jasti, R. *Chem. Sci.* **2012**, *3*, 3018–3021.

[26] Darzi, E. R.; Sisto, T. J.; Jasti, R. *J. Org. Chem.* **2012**, *77*, 6624–6628.

[27] Sisto, T. J.; Golder, M. R.; Hirst, E. S.; Jasti, R. *J. Am. Chem. Soc.* **2011**, *133*, 15800–15802.

[28] Xia, J.; Jasti, R. *Angew. Chem. Int. Ed.* **2012**, *51*, 2474–2476.

[29] Evans, P. J.; Darzi, E. R.; Jasti, R. *Nature Chemistry* **2014**, *6*, 404–408.

[30] Segawa, Y.; Šenel, P.; Matsuura, S.; Omachi, H.; Itami, K. *Chem. Lett.* **2011**, *40*, 423–425.

[31] Segawa, Y.; Miyamoto S.; Omachi, H.; Matsuura, S.; Šenel, P.; Sasamori, T.; Tokitoh, N.; Itami, K. *Angew. Chem. Int. Ed.* **2011**, *50*, 3244–3248.

[32] Takaba, H.; Omachi, H.; Yamamoto, Y.; Bouffard, J.; Itami, K. *Angew. Chem. Int. Ed.* **2009**, *48*, 6112–6116.

[33] Ishii, Y.; Nakanishi, Y.; Omachi, H.; Matsuura, S.; Matsui, K.; Shinohara, H.; Segawa, Y.; Itami, K. *Chem. Sci.* **2012**, *3*, 2340–2345.

[34] Omachi, H.; Matsuura, S.; Segawa, Y.; Itami, K. *Angew. Chem. Int. Ed.* **2010**, *49*, 10202–10205.

[35] Sibbel, F.; Matsui, K.; Segawa, Y.; Studer, A.; Itami, K. *Chem. Commun.* **2013**, *50*, 954–956.

[36] Iwamoto, T.; Watanabe, Y.; Sakamoto, Y.; Suzuki, T.; Yamago, S. *Am. Chem. Soc.* **2011**, *133*, 8354–8361.

[37] Kayahara, E.; Sakamoto, Y.; Suzuki, T.; Yamago, S. *Org. Lett.* **2012**, *14*, 3284–3287.

[38] Kayahara, E.; Iwamoto, T.; Suzuki, T.; Yamago, S. *Chem. Lett.* **2013**, *42*, 621–623.

[39] Yamago, S.; Watanabe, Y.; Iwamoto, T. *Angew. Chem. Int. Ed.* **2010**, *49*, 757–759.

[40] Hirst, E. S.; Jasti, R. *J. Org. Chem.* **2012**, *77*, 10473–10478.

[41] Iwamoto, T.; Watanabe, Y.; Sadahir, T.; Haino, T.; Yamago, S. *Angew. Chem. Int. Ed.* **2011**, *50*, 8342–8344.

[42] Kivelson, S.; Chapman, O. L. *Phys. Rev. B* **1983**, *28*, 7236–7243.

[43] Bendikov, M.; Duong, H. M.; Starkey, K.; Houk, K. N.; Carter, E. A.; Wudl, F. *J. Am. Chem. Soc.* **2004**, *126*, 7416–7417.

[44] Purushothaman, B.; Bruzek, M.; Parkin, S. R.; Miller, A.; Anthony, J. E. *Angew. Chem. Int. Ed.* **2011**, *50*, 7013–7017.

[45] Sadowsky, D.; McNeill, K.; Cramer, C. J. *Faraday Discussions* **2010**, *145*, 507–521.

[46] Evans, P. J.; Jasti, R. Molecular Belts. In *Polyarenes*, Siegel J. S.; Wu, Y. T.; Topics in Current Chemistry; Springer-Verlag Berlin Heidelberg, **2014**, *349*, 249–290.

2. SUMMARY OF PREVIOUS SYNTHETIC ROUTES TOWARDS CYCLACENE AND THE PROHIBITIVE CHALLENGES ENCOUNTERED

2.1. Notable Synthetic Attempts Towards Cyclacene

During the 1980s and 1990s, the Stoddart,[1, 2] Cory,[3, 4] and Schlüter[5, 6] groups attempted to synthesize cyclacene. In all of these reports a macrocycle was successfully constructed but installation of the alkene moieties proved to be problematic. As is the nature of science, a failed result sometimes provides useful insight about the system. Therefore, it is fortunate for us that these groups reported their unsuccessful attempts. Before developing our own synthetic strategy, we reviewed these publications to ensure we would not rely on strategies that have already been shown to be ineffective. We also reviewed their work to incorporate the successful aspect of their routes, namely the efficient construction of the macrocycle. The following review focuses on highlighting the key aspects of the synthetic work towards cyclacene from the Stoddart, Cory, and Schlüter groups.

2.1.1. Review of Stoddart's Attempt at [12]cyclacene

To date, the Stoddart lab has achieved the most advanced intermediate in their effort towards the synthesis of a cyclacene molecule. The initial strategy focused on utilizing the Diels–Alder reaction to construct the six-membered benzenoid rings. However, in order to prevent polymerization that would result in a long chain, they recognized that they needed to develop curved dienes and dienophiles that would undergo

diastereoselective Diels–Alder reactions. Examining the retrosynthetic analysis, (Scheme 2.1) Stoddart envisioned that alkene installation could be achieved through a deoxygenation and dehydration of the oxo-bridges of macrocycle kohnkene **2.2** followed by oxidation. Construction of the macrocycle could be accomplished through the repetitive use of the rigid bisdiene **2.3** and rigid bisdienophile **2.4**. As will be detailed below, the Diels–Alder strategy worked remarkably well, but dehydration and oxidation to form a fully conjugated system was not possible.

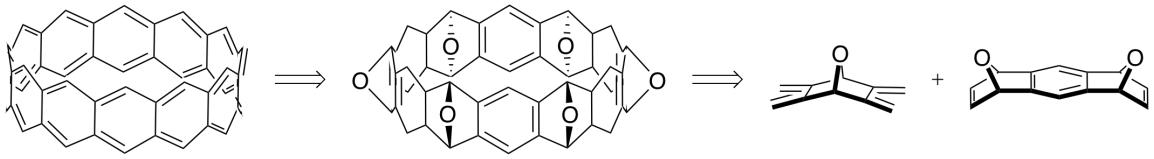

Scheme 2.1 Retrosynthetic analysis of Stoddart's synthesis towards [12]cyclacene.

Beginning with examining the construction of the macrocycle, this seemingly simple approach is actually quite strategic and complex. In fact, Stoddart notes that it took ten years for them to identify a suitable bisdiene and bisdienophile (during this time the post-doctoral students who were assigned to making starting materials for the project referred to the end target, cyclacene, as the "crazy molecule").[7, 1] Focusing on bisdiene **2.3** and bisdienophile **2.4**, these building blocks were locked into a curved conformation through inclusion of rigid [2.2.1] bicyclic systems. Less obvious though is the impact the bicycle has on the approach of the diene to the dienophile.[2] Both **2.3** and **2.4** have an EXO and ENDO face (Figure 2.1). Additionally, there is the exo and endo (lower case to differentiate from facial selectivity) alignment of the dienophile with the diene in the transition state. In total, there are four possible stereoisomers that could result from eight

different Diels–Alder transition states between bisdiene **2.3** and and bisdienophile **2.4**. Remarkably, the Stoddart group only observed one product from this reaction.

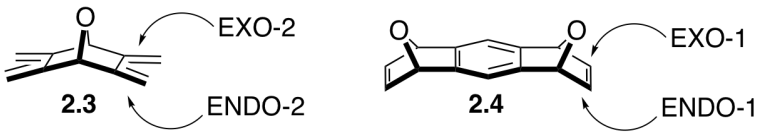

Figure 2.1 The differential faces of the bisdiene and bisdienophile. Note, the 1 and 2 indicate the number of olefins at the termini.

The selectivity of the reaction can be explained by considering the frontier orbitals and the sterics associated with the transition state.[2] Both theoretical and structural studies have shown that the norbornene olefin, such as that found in **2.4**, experiences a significant degree of pyrimidalization.[8–17] To reduce the torsional strain with the bridgehead hydrogen atoms, the olefinic hydrogen atoms are rotated toward the ENDO face. Consequently, the disrotatory tilt of the π_{π}-orbitals results in higher electron density on the EXO-1 face relative to the ENDO-1 face (Figure 2.2a).

Explaining the facial selectivity of the bidiene is less straightforward. Stoddart used the reasoning of Paquette[18–23] and Gleiter.[24] From their computational studies they found that there is a disrotatory tilt of the π_x-orbital on exocyclic methylene carbon atoms. As a result the electron density is increased on the EXO-2 face and decreased on the ENDO-2 face. To achieve a favorable interaction of the diene and dienophile the electron rich and electron poor faces must be brought together. Therefore, from considering just the electronics of the system the two approaches, Figure 2.2b, could be EXO-1/ENDO-2 or ENDO-1/EXO-2. Due to the presence of the oxo-bridge, sterically only the EXO-1/ENDO-2 pathway is possible. This pathway is also limited to an exo approach, once again for steric reasons associated with the oxo-bridge.

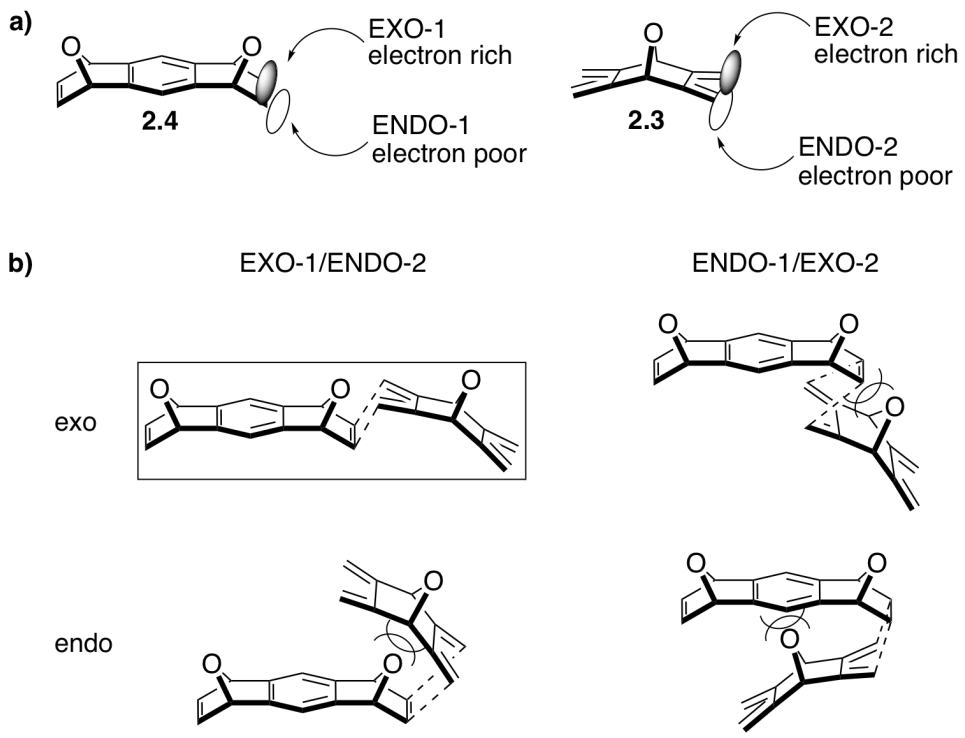

Figure 2.2 The unique electronic structure of Stoddart's bisdienophile 2.4 and bisdiene 2.3 a) the frontier orbitals b) the electronically favored approaches with the sterically most accessible approach boxed.

After identifying a bisdiene and bisdienophile that come together with "treble"[2] selectivity, Stoddart investigated how to most efficiently use these building blocks to construct the macrocycle.[1] Another latent feature of bisdiene **2.3** is that the rate of formation of monoadducts is substantially faster which allows one to control which product (mono- vs. bis-adduct) is formed. Examining the forward synthesis (Scheme 2.2), under thermal conditions **2.3** and **2.4** undergo a Diels–Alder reaction to yield the mono-cycloadduct **2.5**. Notably, **2.5** contains both a diene and a dienophile and therefore could dimerize and, after two Diels–Alder reactions, form a [12]macrocycle (where [n] indicates the number of 6-membered rings that make up the macrocycle). Refluxing **2.5** in xylene for 48 h yielded the desired macrocycle **2.2** in only 3.5% yield. Also problematic, the authors note that **2.5** readily polymerizes. Alternatively, Stoddart and co-workers chose to add another equivalent of the bisdiene **2.3** to give a new bisdiene **2.6**.

Under high pressure, 9-10 kbar, an additional equivalent of bisdienophile **2.4** could be added to **2.6**, via sequential Diels–Alder reactions. Using this route the desired macrocycle, kohnkene **2.2**, was prepared in a more satisfactory yield of 20%.

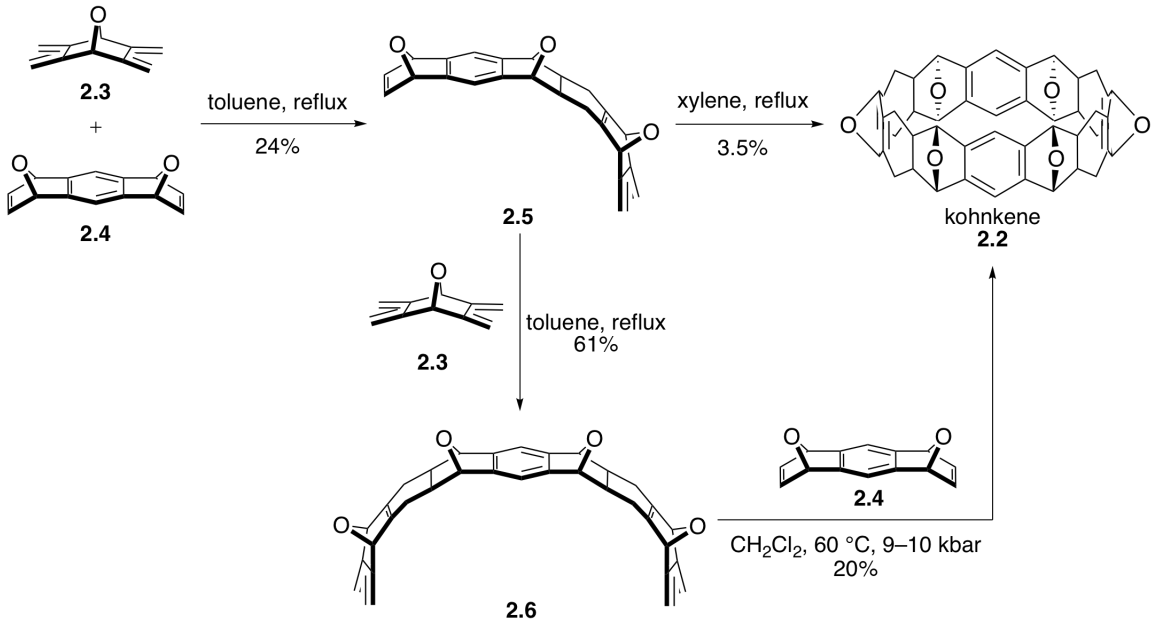

Scheme 2.2 Diel–Alder reactions used to prepare the macrocycle kohnkene.

After establishing an efficient means to construct the macrocycle,[1] they began to investigate deoxygenation and oxidation to give the target compound, [12]cyclacene (Scheme 2.3).[25] Deoxygenation of kohnkene, while possible, was surprisingly difficult. Initial efforts employing PPh_3, PI_3, and P_2I_4 were unsuccessful. Finally, following the work of Xing and Huang[26], they were able to partially deoxygenate at the 3 and 9 o'clock position using $TiCl_4$ and $LiAlH_4$. The remaining oxo-bridges of **2.7** were eliminated by heating the macrocycle in the presence of acetic anhydride and HCl. However, instead of isolating bisanthracene **2.8**, bisnaphthalene **2.9** was obtained as the major product. Presumably **2.9** is obtained from an acid-catalyzed isomerization of the less thermodynamically favorable isomer **2.8**. The anthracene units of the expected product **2.8** result in both a lower resonance energy and greater strain energy than the observed

product **2.9**. Unfortunately, this intermediate was not advanced any further towards [12]cyclacene. Instead they redirected their efforts to prepare related molecules [12]collarene and [12]beltene through reductions of **2.9**.[25] Even though they were not able to achieve a synthesis of cyclacene, they were able to apply their trebly selective Diels–Alder oligimerizations (or as Stoddart referred to it, "molecular LEGO") to construct other novel belt, collar, and cage like structures.[27]

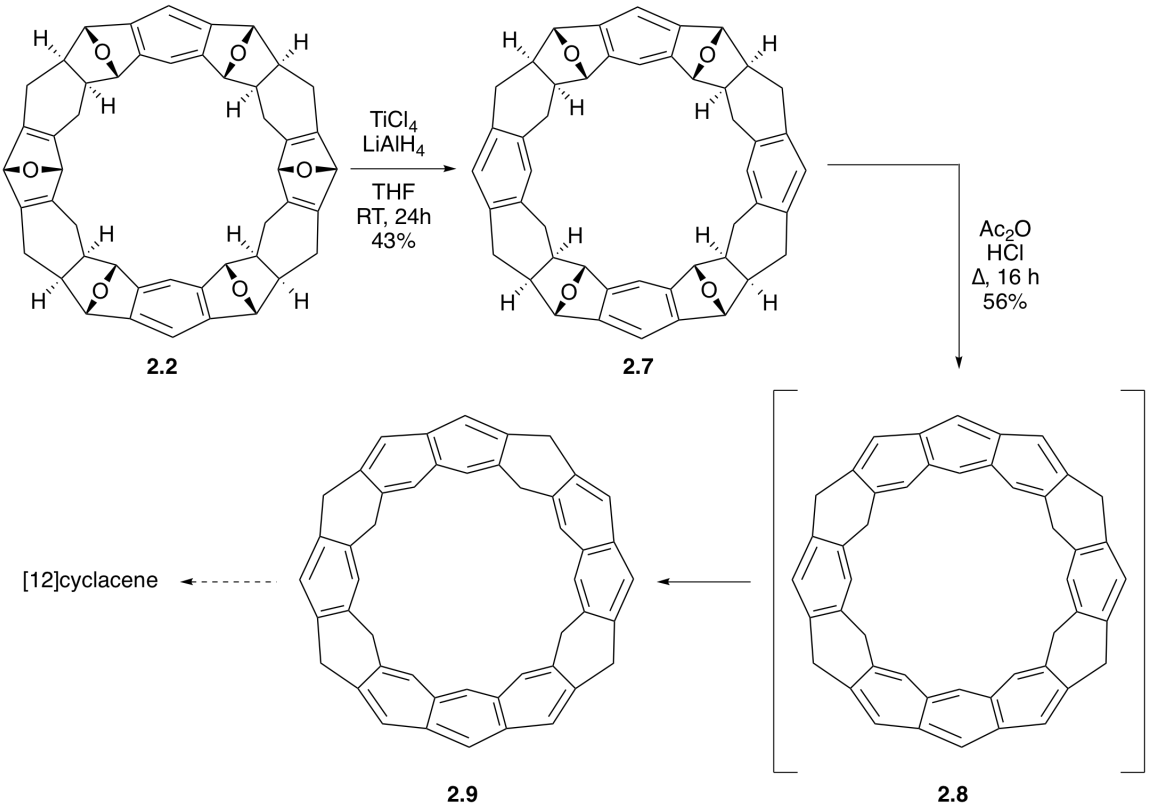

Scheme 2.3 Deoxygenation of kohnkene to a [12]cyclacene precursor

2.1.2. Review of Cory's Attempt at [8]cyclacene

Another interesting attempt at synthesizing cyclacene was carried out by the lab of Robert Cory.[3, 4] Similar to Stoddart, Cory successfully constructed the macrocycle through Diels–Alder reactions of bisdiene **2.10**[28] and bisdienophile **2.11** (Scheme 2.4). However, there are two major differences with this route. First, these building blocks are

not curved. Instead, the flexibility of the bisdiene enabled the formation of the macrocycle.[3] Second, Cory included quinone functionalities in hopes that they would serve as a synthetic handle to enable aromatization of the saturated rings. Instead he found that these macrocyclic systems led to unexpected modes of reactivity.[4]

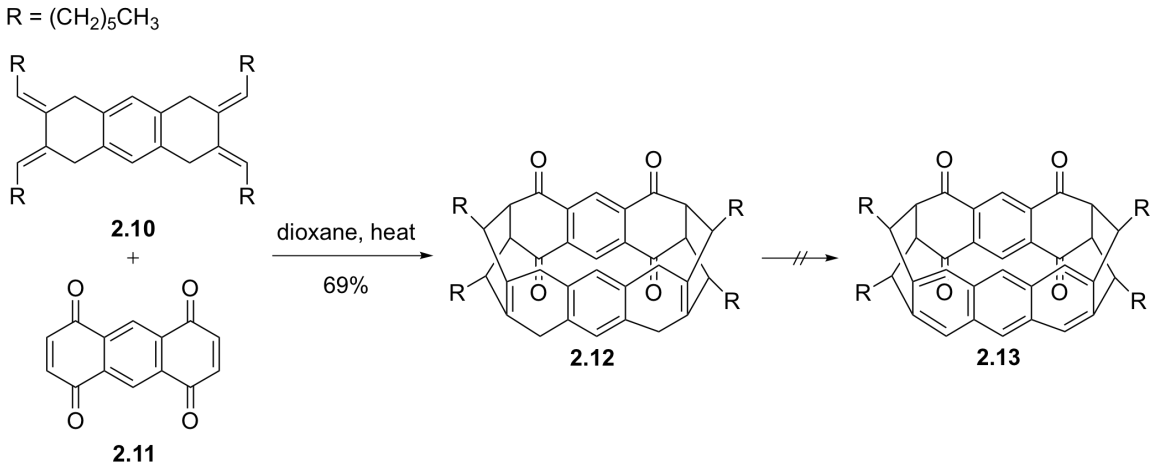

Scheme 2.4 Cory's approach to preparing the macrocyclic precursor for [8]cyclacene

Advancement of bisquinone **2.12** to the intended intermediate anthracene bisquinone **2.13** was not achieved.[4] Treatment of **2.12** with DDQ resulted in only partial oxidation to the naphthalene bisquinone **2.14**, which was not carried on further (Scheme 2.5a). Instead, bisquinone **2.12** was epoxidized to the bisepoxide **2.15** (Scheme 2.5b). From **2.15**, he attempted to install the anthracene unit through dehydration reactions using *p*-toluenesulfonic acid, but instead the bisdiene **2.16** was obtained. Abandoning the formation of the anthracene unit, Cory then attempted to instead make tetraquinone **2.17** through a PCC oxidation but instead obtained the triquione **2.18** (Scheme 2.5c). Attempts at aromatizing the unsaturated rings using aerobic oxidation resulted in the bisethoxy ketones **2.19a** and **2.19b** instead. Although Cory remained confident in his ability to fully reduce the macrocycle to cyclacene, there was never a subsequent paper reporting further progress.

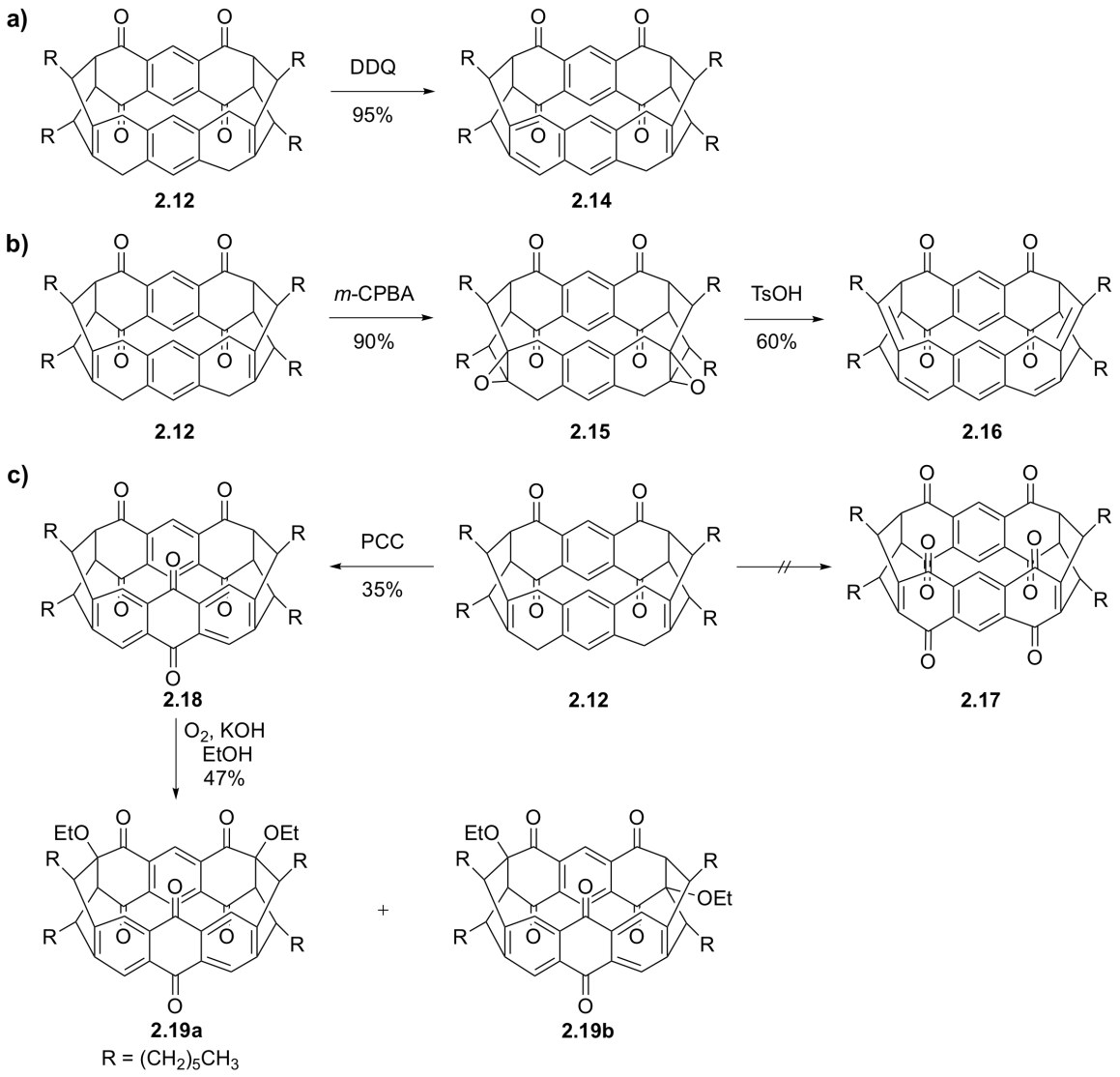

Scheme 2.5 Cory's attempts to advance his macrocycle 2.12.

2.1.3. Review of Schlüter's Macrocycle Preparation

Schlüter's approach to the macrocycle of cyclacene also relied on Diels–Alder reactions. In contrast to Stoddart and Cory though, he designed AB-monomers, **2.21** and **2.25**, that contained a diene on one end and a dienophile on the other (Scheme 2.6).[5] Monomer **2.1** (Scheme 2.6a) can make acyclic polymers, **2.23**, as well as a macrocycle, **2.24**, formed from a dimerization of **2.21**. At high concentrations (3.4 M) the acyclic polymer **2.23** predominates (3:1, polymer:macrocycle). Under dilute conditions (0.015

M) the dimer **2.24** is favored (1:4, polymer:macrocycle). Expanding on these findings, Schlüter prepared a longer AB-monomer, **2.25** (Scheme 2.6b), and studied its propensity to form linear polymers, **2.26**, versus a macrocycle, **2.27**, under various conditions.[6]

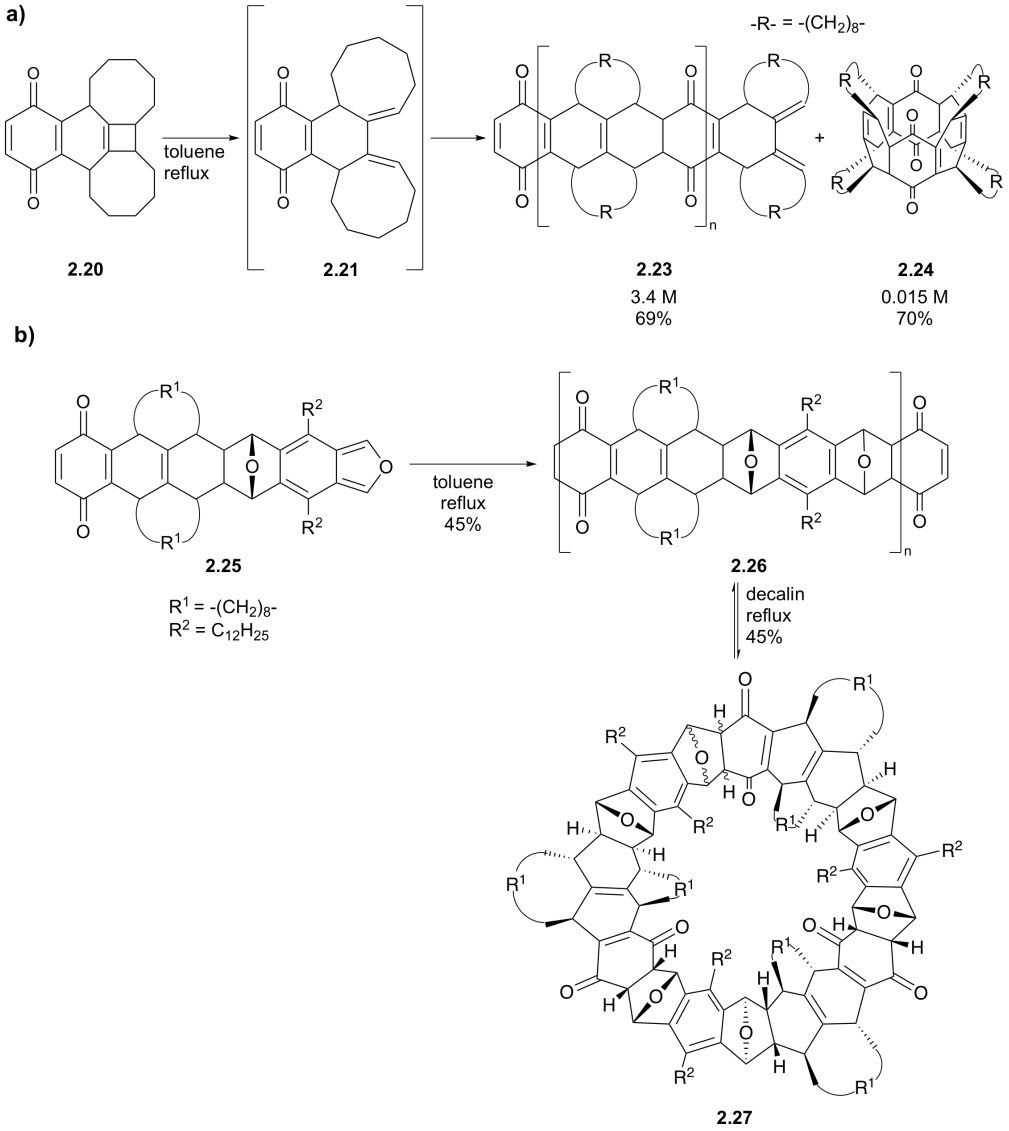

Scheme 2.6 Schlüter's AB-monomers that a) dimerize and b) trimerize via Diels–Alder reactions to give macorcycles.

When monomer **2.25** is refluxed in toluene the polymer, **2.26**, predominates (45% yield) and only a small amount of a trimeric macrocycle, **2.27**, is formed (6%). At higher temperatures (refluxing decalin) the retro-Diels–Alder reaction can occur and an equilibrium between the polymer and macrocycle is established. By refluxing polymer

2.26 in decalin Schlüter and co-workers were able to isolate the macrocycle **2.27** in 45% yield. While Schlüter does recognize that the macrocycles he prepared are precursors to cyclacene molecules he does not report any attempts to advance the macrocycles towards that target compound.

2.2. Guiding Principles for Future Routes

These attempts at synthesizing cyclacene confirm that it is not a straightforward or simple task to prepare this class of molecules. In particular, the demise for Stoddart and Cory appeared to be converting flexible macrocycles to the rigid strained structures. Other lessons from their work and Schlüter's are highlighted below.

Stoddart's remarkable advances towards cyclacene is rich with valuable chemistry. First, he proved that the macrocycle can be prepared via stereoselective Diels–Alder reactions. However, deoxygenation was challenging, presumably for two reasons. First, deoxygenation results in formation of a benzene ring, which increases the strain energy of the macrocycle, so energetically this is an up-hill process. Second, the conditions employed for deoxygenation allowed for the isomerization of the macrocycle to an isomer of lower energy, thus effectively increasing the energy barrier to oxidize the macrocycle to a fully conjugated system. If a strategy were to include removal of a bridge in future routes, it needs to be an irreversible process.

Cory's attempt further underscores the viability of constructing the macrocycle by Diels–Alder reactions. Based on his attempts to advance his macrocycle, it seems that once the macrocyle is formed, it is difficult to transform the flexible 6-membered rings to rigid 6-membered rings. Future attempts to prepare cyclacene need to build up strain as

the macrocycle is built to lessen the unfavorable energetics related to forming rigid benzenoid like rings.

The insight gained from Schlütler's work is limited to the possibility of constructing the macrocycle from a monomer with ends of complimentary reactivity. This strategy has the benefit of removing the need to worry about mono- vs. bis- addition that is possible with using bisdienes and bisdienophile. Additionally, one does not need to worry about the relative equivalence of diene to dienophile. Future use of this strategy could be to purposefully design an AB-monomer where after the first Diels–Alder reaction, the other reactive centers are locked in close proximity. The close proximity of the diene and dienophile would ensure closure to give the macrocycle and limit the amount of acyclic polymer formed.

Based on our review of these reports from Stoddart, Cory, and Schlüter, we have identified that late-stage dehydration, deoxygenation, or dehydrogenation of a macrocyclic cyclacene scaffold should be avoided. These transformations have proven to be challenging even with well-established methodologies. It is likely these strategies failed because the attempted transformations were not thermodynamically or kinetically feasible due to an increase in ring strain, the construction of 'local' aromaticity in isolated benzene rings (as in **2.9**), incompatibility/instability of the cyclacene product with harsh reaction conditions or some combination of these factors. We kept this knowledge at the forefront of our minds as we developed our synthetic route toward cyclacene.

2.3. References

[1] Kohnke, F. H.; Slawin, A. M. Z.; Stoddart, J. F.; Williams, D. J. *Angew. Chem., Int. Ed.* **1987**, *26,* 892–894.

[2] Ashton, P. R.; Brown, G. R.; Isaacs, N.S; Giuffrida, D.; Kohnke, F. H.; Mathias, J. P.; Slawin, A. M. Z.; Smith, D. R.; Stoddart, J. F.; Williams, D. J. *J. Am. Chem. Soc.* **1992**, *26,* 6330–6353.

[3] Cory, R. M.; McPhail, C. L.; Dikmans, A. J.; Vittal, J. J. *Tetrahedron Lett.* **1996**, *37,* 1983–1986.

[4] Cory, R. M.; McPhail, C. L. *Tetrahedron Lett.* **1996**, *37,* 1987–1990.

[5] Godt, A.; Enkelmann, V.; Schlüter, A. D. *Angew. Chem., Int. Ed.* **1989**, *28,* 1680–1682.

[6] Kintzel, O.; Luger, P.; Weber, M.; Schlüter, A. –D. *Eur. J. Org. Chem.* **1998**, 99–105.

[7] Stoddart, J. F. *J. Inclusion Phenom. And Molecular Recognition in Chem.* **1989**, *7*, 227–245.

[8] Houk, K. N. *Stereochemistry and Reactivity of Systems Containing π-Electrons*; Watson, W. H., Ed.; Verlag-Chemie: Deerfield Beach, FL, 1983; 1–40.

[9] Alder, K.; Stein, G. *Liebigs Ann. Chem.* **1931**, *485*, 211–222.

[10] Alder, K; Stein, G. *Liebigs Ann. Chem.* **1935**, *515*, 185–200.

[11] Schleyer, P. v. R. *J. Am. Chem. Soc.* **1967**, *89*, 701–703.

[12] Brown, H. C.; Hammer, W. J.; Kawakami, J. H.; Rotberg, I.; Van Der Jugt, D. L. *J. Am. Chem. Soc.* **1967** *89*, 6381–6382.

[13] Brown, H. C.; Kawakami, J. H.; Liu, K.-T. *J. Am. Chem. Soc.* **1973**, *95*, 2209-2216.

[14] Watson, W. H.; Galloy, J.; Bartlett, P. D.; Roof, A. A. M. *J. Am. Chem. Soc.* **1981**, *103*, 2022-2031.

[15] Bartlett, P. D.; Combs, G. L., Jr.; Thi Li, A.-X.; Watson, W. H.; Galloy, J.; Kimura, M. *J. Am. Chem. Soc.* **1982**, *104*, 3131–3138.

[16] Pinkerton, A. A.; Schwarzenbach, D.; Stibbard, J. H. A.; Carrupt, P.-A.; Vogel, P. *J. Am. Chem. Soc.* **1981**, *103*, 2095–2096.

[17] Hagenbuch, J.-P.; Vogel, P.; Pinkerton, A. A.; Schwarzenbach, D. *Helv. Chim. Acta* **1981**, *64*, 1818–1832.

[18] Paquette, L. A.; Carr, R. V. C.; Böhm, M. C.; Gleiter, R. *J. Am. Chem. Soc.* **1980**, *102*, 1186–1188.

[19] Böhm, M. C.; Carr, J. V. C.; Gleiter, R.; Paquette, L. A. *J. Am. Chem. Soc.* **1980**, *102*, 7218–7228.

[20] Paquette, L. A.; Carr, R. V. C.; Arnold, E.; Clardy, J. *J. Org. Chem.* **1980**, *45*, 4907–4913.

[21] Paquette, L. A.; Charumilind, P.; Kravetz, T. M.; Böhm, M. C.; Gleiter, R. *J. Am. Chem. Soc.* **1983**, *105*, 3126–3135.

[22] Paquette L. Al; Schaefer, A. G.; Blount, J. F. *J. Am. Chem. Soc.* **1983**, *105*, 3642–3649.

[23] Paquette, L. A.; Green, K. E.; Hsu, L.-Y. *J. Org. Chem.* **1984**, *49*, 3650–3652.

[24] Paquette, L. A.; Kravetz, T. M.; Böhm, M. C.; Gleiter, R. *J. Org. Chem.* **1983**, *48*, 1250–1257.

[25] Ashton, P. R.; Isaacs, N. S.; Kohnke, F. H.; Slawin, A. M. Z.; Spencer, C. M.; Stoddart, J. F.; Williams, D. J. *Angew. Chem. Int. Ed.* **1988**, *27*, 966–969.

[26] Xing, Y. D.; Huang, N. Z. *J. Org. Chem.* **1982**, *47*, 140–142.

[27] Ashton, P. R.; Girreser, U.; Giuffrida, D.; Kohnke, F. H.; Mathias, J. P.; Raymo, F. M.; Slawin, A. M. Z.; Stoddart, J. F.; Williams, D. J. *J. Am. Chem. Soc.* **1993**, *115*, 5422–5429.

[28] Cory, R. M.; McPhail, C. L.; Dikmans, A. J. *Tetrahedron Lett.* **1993**, *34*, 7533–7536.

3. RESEARCH PLAN: APPLYING LESSONS LEARNED TO STRATEGY

Undertaking the synthesis of a cyclacene molecule can be broken into two major challenges. The first, and unsolved challenge, is installing all the alkenes to form a fully conjugated system. The second challenge is to develop a route that provides the macrocyclic scaffold in good yield. It has been shown that Diels–Alder reactions are a reliable way to build the macrocycle,[1–4] but the identity of the diene and dieneophile depend on the end-game strategy. Below is an outline of our proposed general strategy for synthesizing a cyclacene molecule governed by our guiding principles that we developed based on our review of previous attempts.

3.1. Strategy to Complete Conjugation

Since the work of Stoddart,[1, 5, 6] and Cory,[2, 7] advances have been made in the synthesis of linear acene molecules.[8] Unsubstituted acenes longer than pentacene were believed to be inaccessible due to their vulnerability to air oxidation and or self-dimerization. This reactivity is a major barrier for using extended acenes in organic electronic devices. To access this reactive class of molecules, a new strategy has been developed that generates the acene on demand from stable precursors. In general, the acene precursor contains a bicycle whose bridge can be extruded as a gas, such as carbon monoxide or carbon dioxide, and thereby complete aromatization.

An example of this methodology is the synthesis of unsubstituted hexacene (Scheme 3.1) by Chow and co-workers.[9] The hexacene precursor (**3.1**) contained a [2.2.1] ring system with a ketone bridge. Upon heating or irradiation, a cheletropic extrusion of

carbon monoxide occurred resulting in the completely conjugated system of hexacene **3.2** in near quantitative yield. This strategy has found wide use in the preparation of numerous acene molecules.[8] It has proven to be a particularly useful strategy because the acene precursors are stable, extrusion of the bridge proceeds with high yields, the by-product is a gas so no purification is required, and the process is irreversible. The stability of the acene precursors stems from the disruption of the conjugated system by the bridge. An additional feature of these precursors is the bridge interrupts π-stacking and thereby aids in solubility.

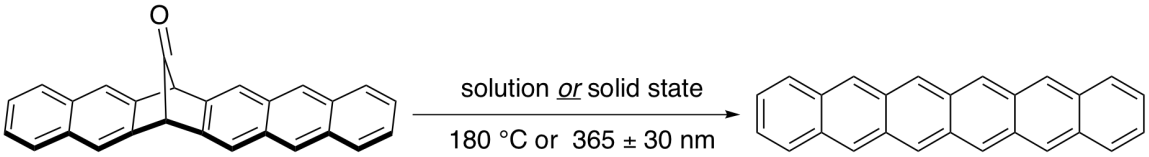

3.1 **3.2**

Scheme 3.1 Key end-game strategy of Chow and coworkers to prepare pure unsubstituted-hexacene via cheletropic extrusion of carbon monoxide.

While its application to the synthesis of acene molecules is relatively new, cheletropic decarbonylation is actually a classic pericyclic reaction. However, when the product is a short acene, such as naphthalene or anthracene, decarbonylation is relatively rapid at room temperature.[10–13] Computational studies have shown that the shorter the acene system, the more exothermic the process is due to the increase in available resonance energy of the product.[14] Therefore, isolating the corresponding [2.2.1]-bridged ring systems can be challenging. If it is necessary to isolate the bridged intermediate, then an alkene can be used as a ketone equivalent that could be unmasked via oxidative cleavage. This strategy has been employed previously to prepare anthracene as well as in the hexacene example.[10, 9]

We envision using this methodology, cheletropic extrusion of carbon monoxide, as our end-game strategy to complete the conjugation of a cyclacene molecule (Scheme 3.2). This is a novel approach, and potential solution for the long-standing challenge of installing the last alkenes for cyclacene. In particular, we were attracted to this strategy as it circumvents the need for late-stage dehydrogenation, dehydration, or oxidation. The cheletropic reaction is initiated by heat or light, thus eliminating the number of reaction pathways to side products, and at the same time simplifies the purification process since no external reagents are required. Also, since extrusion of carbon monoxide is irreversible, the system will not have the opportunity to reorganize itself to create areas of 'local' aromaticity. This is because in the cyclacene precursor, **3.4**, all the carbons atoms are in the same oxidation state as in cyclacene (**3.3**). Additionally, as discussed above, this methodology is well established and has successfully been applied in the preparation of other unstable molecules. To avoid premature decarbonylation, all intermediates prior to the final step will have the alkene bridge as a masked ketone (**3.5**). With a vision for the structure of our key cyclacene precursor, we were then able to strategize how the macrocycle could be constructed.

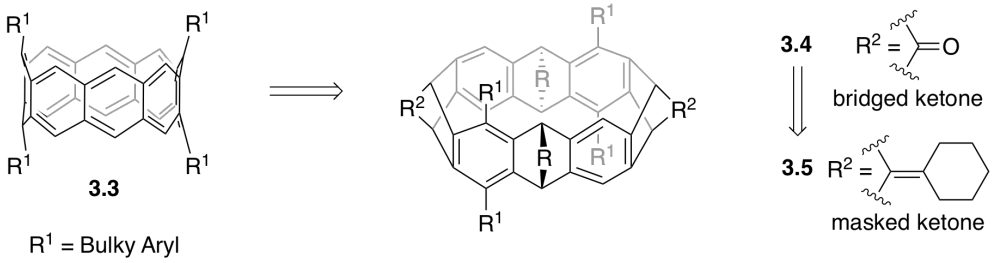

Scheme 3.2 Proposed end-game strategy to install the final alkenes and complete the synthesis of cyclacene.

3.2. Strategy to Construct the Macrocycle

Following the lead of Stoddart,[1] Cory,[2] and Schlüter,[3,4] we are confident that the macrocycle can be constructed using Diels–Alder reactions. A major disadvantage of the dienes and dienophiles used in prior strategies is the need to oxidize the resultant six-membered ring. Ideally, the product of the reaction would have carbon atoms that are in the same oxidation state as those in cyclacene. Therefore, in designing our route we focused on incorporating [4+2] cycloaddition reactions that facilitated aromatization. Again, looking to the acene literature for inspiration, we found that this goal could be achieved through the use of arynes, retro-Diels–Alder reactions, and elimination reactions.

In particular, Nuckolls' synthesis of a pentacene derivative, **3.9**, caught our attention (Scheme 3.3a).[15] The central ring of pentacene **3.9** was constructed via a consecutive series of [4+2] and retro-Diels–Alder reactions (Scheme 3.3b), yielding an aromatic ring. There are two unique key features of this methodology that allow for formation of an aromatic ring rather than a cyclohexene ring. First, the dienophile of the initial [4+2] reaction is an aryne (**3.7** generated from **3.6**). As a result, after the cycloaddition an alkene, rather than an alkane, is left in place of the dienophile (**3.10**). Second, use of the diene, diazapyrone **3.8**, initiates a cascade reaction. The product of the initial Diels–Alder reaction includes a diazene (**3.10)**. Spontaneously, a retro-[4+2] reaction occurs releasing N_2 and simultaneously creating a new diene, **3.11**. This diene then participates in a second Diels–Alder reaction with an additional equivalent of aryne (**3.7**). The product of this reaction (**3.12**) is unstable and another retro-Diels–Alder reaction occurs with loss of carbon dioxide and thereby completing the aromatization of

the central ring. This ability to generate aromatic rings through Diels–Alder reactions with arynes and subsequent retro-Diels–Alder reactions became our primary strategy.

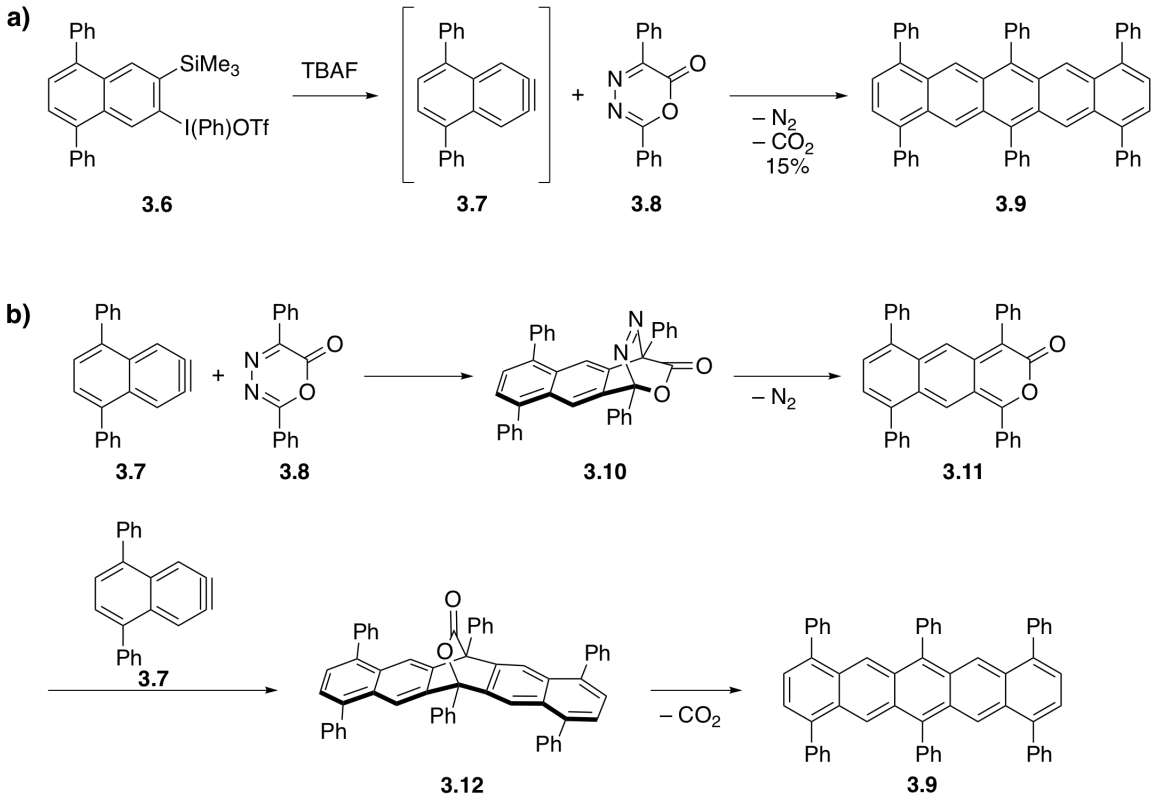

Scheme 3.3 Nuckolls' preparation of a pentacene derivative using an aryne and a diazapyrone. a) the overall scheme, b) the key reactive intermediates the reaction proceeds through.

A second requirement of the intermediates for macrocycle formation was that they needed to be curved and rigid as in Stoddart's approach.[1] However, the retro-Diels–Alder reactions of Nuckolls' method are spontaneous and therefore result in rigid planar products. Inspiration for a modification of this methodology suitable for our goals came from the organic teaching labs here at the University of Minnesota.[16] In previous semesters, a Diels–Alder reaction between tetraphenylcyclopentadieneone **3.12** and benzyne (**3.13**) formed the [2.2.1]-bicycloheptanone intermediate **3.14**. Cheleotropic loss of carbon monoxide facilitated aromatization to give naphthalene derivative **3.15**. Since

this chemistry has been reproduced by thousands of undergraduate students, we know it is robust and believe it will be well suited for applications in challenging contexts.

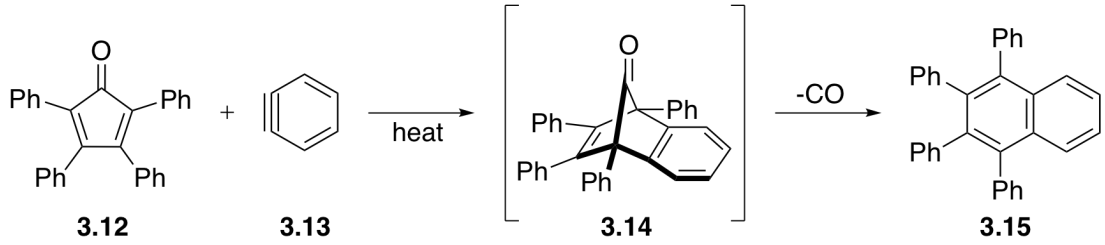

Scheme 3.4 The Diels–Alder reaction that was performed in the organic teaching labs at the University of Minnesota.

Adapting this methodology for our route we initially targeted cyclopentadieneone derivatives. After the Diels–Alder reaction to form the [2.2.1] ring we would then protect the ketone to prevent premature decarboxylation. In hindsight, this may not be a realistic goal for early intermediates that would have generated anthracene precursors. Alternatively, we recognized, and later incorporated, the use of fulvenes. Fulvenes furnish a [2.2.1] with an alkene bridge when used as a diene in [4+2] reactions. Details on the attempts to form cyclopentadieneone and choice of fulvenes is given in later sections.

3.3. Strategy to Increase Persistence of Isolated Cyclacenes

Based on computational studies and our knowledge of acene compounds, we anticipate that cyclacene will be an unstable compound that posses a diradical like character.[17, 18] Fortunately, a solution to this problem has been found for the closely related compounds, linear oligoacenes. Anthony has shown that one effective strategy to increase the persistence of acenes is to include substituents, such as TIPS acetylene, along the zigzag edge (Figure 3.1).[19] This method works because the steric bulk of the TIPS group prevents the edges from coming in contact with each other or the π-face of the acene backbone for dimerization at 6,13-poisitions. He has even successfully used

this strategy to prepare nonacene derivatives.[20] These substituents also have the added benefit of increasing the solubility (insolubility is a major challenge when trying to synthesize, purify, and utilize acenes) of acene molecules. Therefore, our final goal in developing a route to construct the macrocycle was the ability to include functional groups on the zigzag edge. Ideally, these groups would be added on at late stage to facilitate an investigation into the impact of different groups on the persistence and stability of cyclacene.

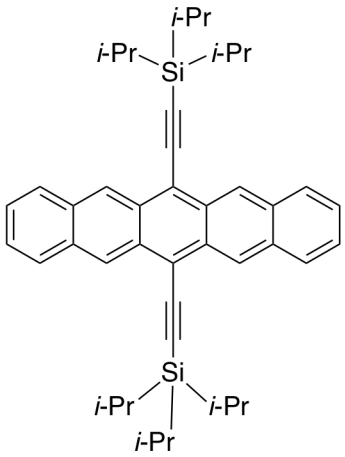

3.16

Figure 3.1 Anthony's persistent pentacene that is protected with TIPS acetylene groups.

3.4. General Proposed Retrosynthesis

Upon identifying requirements of future proposed syntheses towards a cyclacene we developed a general retrosynthetic scheme as a guide (Scheme 3.5). Our primary target was to establish a method for the synthesis of a family of cyclacene compounds. To test our proposed strategy we targeted macrocycles with 8–12 benzenoid rings. First, starting from cyclacene (**3.17**), instead of making a bond disconnection, we added [2.2.1] rings, in line with our strategy for installation of the final alkenes. The bridge would be a masked ketone (**3.19**) which once revealed (**3.18**) would undergo decarbonylation to

complete conjugation of the macrocycle. To actually form the macrocycle we envisioned using Diels–Alder reactions between arynes and dienes that generate a leaving group in the product. Additionally, in order to form a macorcycle we recognized that both ends of every intermediate need to be reactive or able to be readily transformed into a diene or dieneophile. We initially decided to avoid using a diene-dienophile AB monomer like Schlüter since this strategy tends to proceed with low yield due to the competing long chain polymerization pathway.[1,3,4] Instead, we focused on forming bisdienes (**3.20**) and bisdieneophiles (**3.21** and **3.22**). As starting building blocks, we identified the usefulness of a molecule that could generate two benzynes sequentially (**3.22**) and cyclopentadiene derivatives (**3.23**). The following chapters detail investigation of various dienes and their inadequacies, as well as the preparation of a bisbenzyne equivalent.

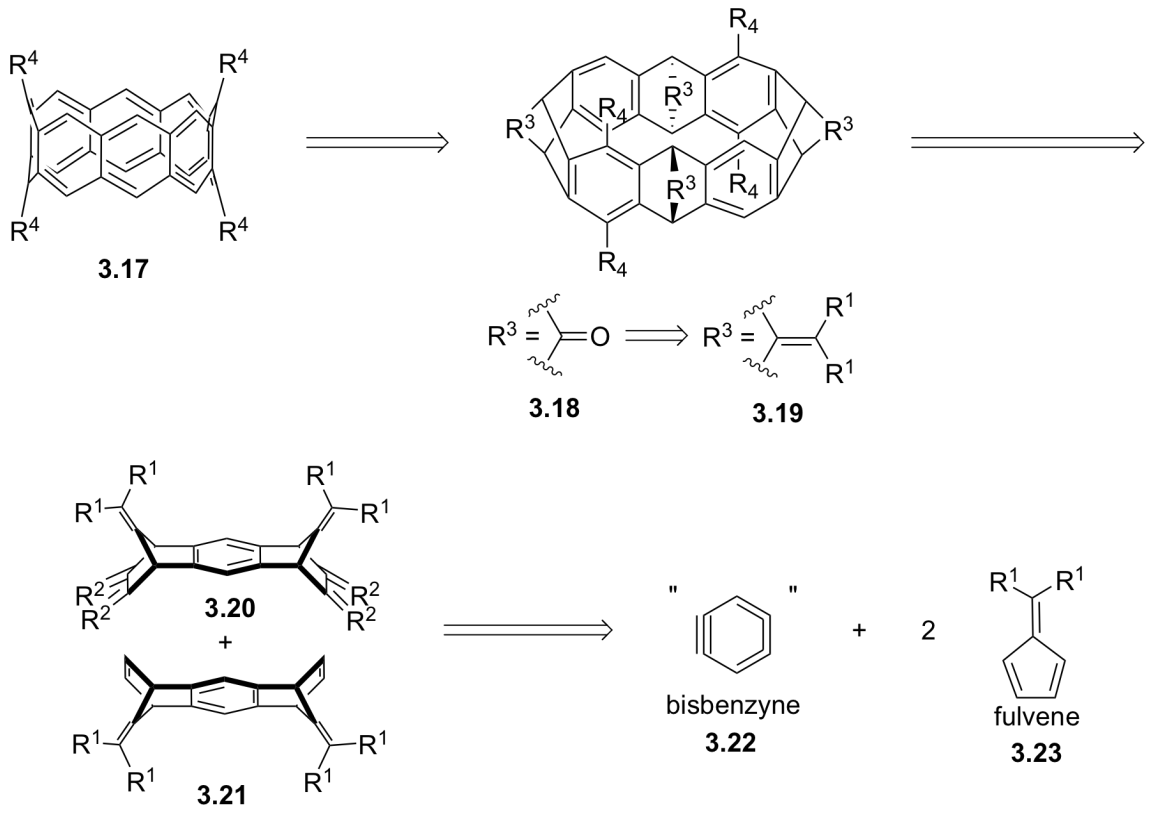

Scheme 3.5 Retrosynthetic analysis of our novel proposed general strategy for synthesis of a cyclacene molecule.

3.5. References

[1] Kohnke, F. H.; Slawin, A. M. Z.; Stoddart, J. F.; Williams, D. J. *Angew. Chem., Int. Ed.* **1987**, *26,* 892–894.

[2] Cory, R. M.; McPhail, C. L.; Dikmans, A. J.; Vittal, J. J. *Tetrahedron Lett.* **1996**, *37,* 1983–1986.

[3] Godt, A.; Enkelmann, V.; Schlüter, A. D. *Angew. Chem., Int. Ed.* **1989**, *28,* 1680–1682.

[4] Kintzel, O.; Luger, P.; Weber, M.; Schlüter, A. –D. *Eur. J. Org. Chem.* **1998**, 99–105.

[5] Ashton, P. R.; Isaacs, N. S.; Kohnke, F. H.; Slawin, A. M. Z.; Spencer, C. M.; Stoddart, J. F.; Williams, D. J. *Angew. Chem. Int. Ed.* **1988**, *27*, 966–969.

[6] Ashton, P. R.; Brown, G. R.; Isaacs, N.S; Giuffrida, D.; Kohnke, F. H.; Mathias, J. P.; Slawin, A. M. Z.; Smith, D. R.; Stoddart, J. F.; Williams, D. J. *J. Am. Chem. Soc.* **1992**, *26,* 6330–6353.

[7] Cory, R. M.; McPhail, C. L. *Tetrahedron Lett.* **1996**, *37,* 1987–1990.

[8] Watanabe, M.; Chen, K.-Y.; Chow, T. J. *Acc. Chem. Res.* **2013**, *46*, 1606–1615 and references therein.

[9] Watanabe, M.; Chang, Y. J.; Liu, S. W.; Chao, T. H.; Goto, K.; Islam, M. M.; Yuan, C. H.; Tao, Y. T.; Shinmyozu, T.; Chow, T. J. *Nat. Chem.* **2012**, *4*, 574–578.

[10] Irie, T.; Tanida, H. *J. Org. Chem.* **1979**, *44*, 1002–1003.

[11] Yankelevich, S.; Fuchs, B. *Tetrahedron Lett.* **1967**, *8*, 4945–4949.

[12] McCulloch, R.; Rye, A. R.; Wege, D. *Tetrahedron Lett.* **1969**, *10*, 5231–5234.

[13] Meinwald, J.; Miller, E. G. *Tetrahedron Lett.* **1961**, *2*, 253–258.

[14] Lai, C.-H.; Li, E. Y.; Chen, K.-Y.; Chow, T. J.; Chou, P.-T. *J. Chem. Theory Comput.* **2006**, *2*, 1078–1084.

[15] Miao, Q.; Chi, X.; Xiao, S.; Zeis, R.; Lefenfeld, M.; Siegrist, T.; Steigerwald, M. L.; Nuckolls, C. *J. Am. Chem. Soc.* **2006**, *128*, 1340–1345.

[16] Wissinger, J. E. *Laboratory Manual for Organic Chemistry 2311*. Eighth Ed.; Cengage Learning: Mason, Ohio, 2008; pp 67–69.

[17] Bendikov, M.; Duong, H. M.; Starkey, K.; Houk, K. N.; Carter, E. A.; Wudl, F. *J. Am. Chem. Soc.* **2004**, *126*, 7416–7417.

[18] Chen, Z.; Jiang, D. E.; Lu, X.; Bettinger, H. F.; Dia, S.; Schleyer, P. V.; Houk, K. N. *Org. Lett.* **2007**, *9,* 5449–5452.

[19] Anthony, J. E.; Eaton, D. L.; Parkin, S. R. *Org. Lett.* **2002**, *4*, 15–18.

[20] Purushothaman, B.; Bruzek, M.; Parkin, S. R.; Miller, A.-F.; Anthony, J. E. *Angew. Chem. Int. Ed.* **2011**, *50*, 7013–7017.

4. IDENTIFYING KEY BUILDING BLOCKS

While we had a clear idea of the requirements for our dienes and dienophiles to build a macrocycle, it was challenging to design a pair that would fit our needs. In particular it was difficult to design molecules where both sides were reactive and not prone to polymerization. In this chapter our first route towards cyclacene is described and an account of our efforts on this route are briefly covered. As often happens with multistep synthesis projects, we ended up designing a completely new route. A major benefit of the new route was the versatility of an early key intermediate as will be discussed. Also covered in this chapter is the design and synthesis of this key intermediate.

4.1. First Proposed Synthetic Route

4.1.1. Forward Synthetic Analysis

In this first route, we had narrowed in on using Diels–Alder reactions where the dienophile is an aryne species and the diene is diazapyrone **3.8** or cyclopentadienones (Scheme 4.1). To produce intermediates with curvature, the first [4+2] reaction needed to use a cyclopentadienone derivative. Ideally, this diene would be annulated to a benzene ring with functionality that would allow for the formation of an aryne on the opposing side of the ring. However, this diene, a benzocyclopentadienone would be highly reactive and need to be generated *in situ*.[2] We envisioned accomplishing this by using a palladium-catalyzed cross-coupling reaction between tetrabromobenzene **4.1** and 1,3-diphenylpropanone **4.2** to form monodihydroindenone **4.3**.[1] The *ortho* bromines on the

opposite side of the phenyl ring would be left untouched and serve as a synthetic handle for later transformations. Bromination at the carbon atoms α to the ketone would furnish dibromoindanone **4.4**, which could serve as a precursor to the benzocyclopentadienone **4.5**.[2]

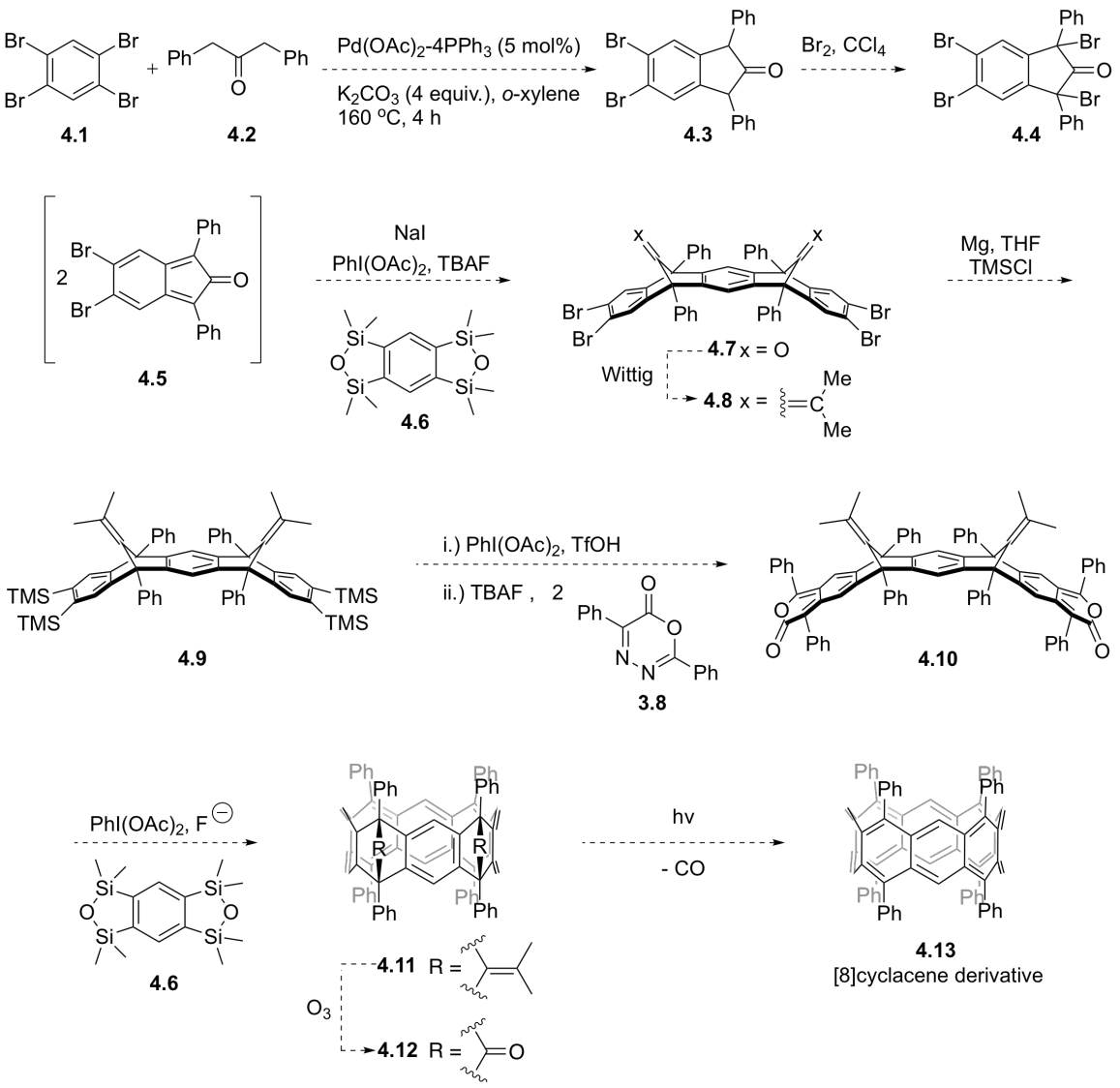

Scheme 4.1 First proposed synthetic route towards an [8]cyclacene derivative.

The next step would have been challenging due to the need to generate two reactive species *in situ* simultaneously. Reduction of **4.4** with NaI could generate the reactive diene **4.5**,[2] which would trap the dienophilic benzyne, generated from

benzobisoxadisilole **4.6**.[3,4] Sequentially, the second benzyne of benzobisoxadisilole **4.6** could be revealed and trapped with a second equivalent of benzocyclopentadienone **4.5** to give the bisbicyclic intermediate **4.7**. However, with respect to the position of the bridges, a 1:1 mixture of *syn:anti* products would be expected. We were confident that these isomers could be separated based on reports of the isolation of similar compounds by column chromatography.[5] Upon isolating the *syn* isomer the ketone would need to be protected as the alkene, **4.8**, which could be accomplished by a Wittig reaction.

To move forward, the termini of **4.8** would need to be converted to a reactive species. Transforming the bromides to Grignard reagents in the presence of TMSCl would give the tetra-TMS substituted intermediate **4.9**.[6] The *ortho*-TMS groups serve as a benzyne precursor.[3,4] Treatment with $PhI(OAc)_2$ and triflic acid exchanges a TMS group on each end with a hypervalent iodine. Upon introduction of a fluoride source the benzyne is revealed. We envisioned trapping these benzynes with diazapyrone **3.8**. A subsequent retro-[4+2] with loss of nitrogen would leave bispyrone **4.10** as a reactive diene.[7] Introduction of the bisbenzyne equivalent **4.6** could be used to close **4.10** to furnish macrocycle **4.11**. The synthesis could then be completed by ozonolysis of the alkene bridges to provide **4.12**, followed by decarbonylation to yield the target compound, [8]cyclacene derivative **4.13**.[5,8]

4.1.2. Results and Discussion

In retrospect, there are many steps in the above-proposed synthesis that would be highly challenging. Surprisingly, in practice, the route failed at the first step. We had proposed that a palladium-catalyzed cross-coupling could be used to generate dihydroindenone **4.3**. This coupling was adopted from the reaction developed by Miura

and co-workers (Scheme 4.2) who successfully formed 1,3-diphenylindanone **4.15** from *o*-dibromobenzene **4.14**, and 1,3-diphenylpropanonone **4.2**.[1] Initial attempts at implementing this cross-coupling to our system resulted in about a 65% conversion (Table 4.1, trial 1) of the starting material to the singly cross-coupled intermediate **4.16** (Scheme 4.3), as determined by NMR and GC-MS, and none of the desired product **4.3**.

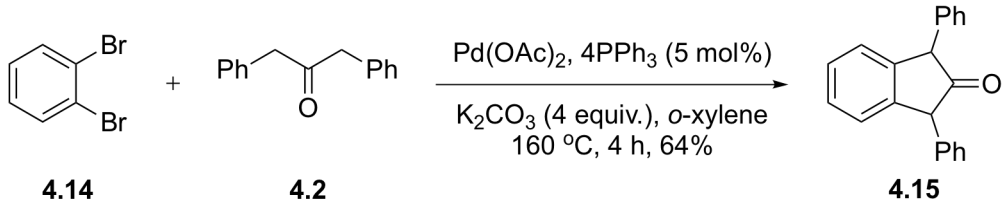

Scheme 4.2 The palladium cross-coupling reaction reported by Miura.

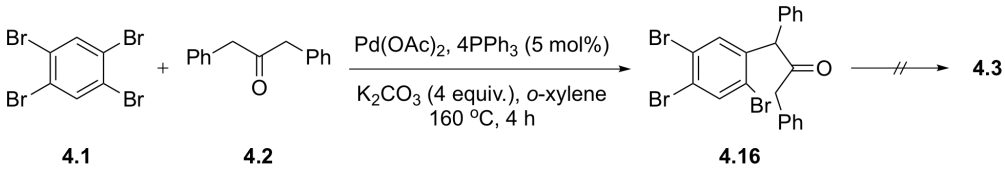

Scheme 4.3 The attempted palladium cross-coupling reaction to prepare desired 1,3-diphenylindanone 4.15.

To probe the failure to produce **4.3**, attempts to reproduce the exact reaction reported in the literature were performed (trial 2). Following the reported conditions gave only trace amounts of 1,3-diphenylindanone **4.15** and a significant amount of the singly cross-coupled intermediate **4.17**. Increasing the reaction time (trial 3) improved the conversion, however the ratio of intermediate to desired product was still 1.8:1. Previously, the Miura group reported that DMF was a good solvent for palladium-catalyzed arylations with aryl halides.[9] When DMF was used for the reaction of interest (trial 4) the yield of the desired product decreased significantly.

Table 4.1 Select trials to perform the palladium cross-coupling of 4.2 to either 4.14 or 4.1.

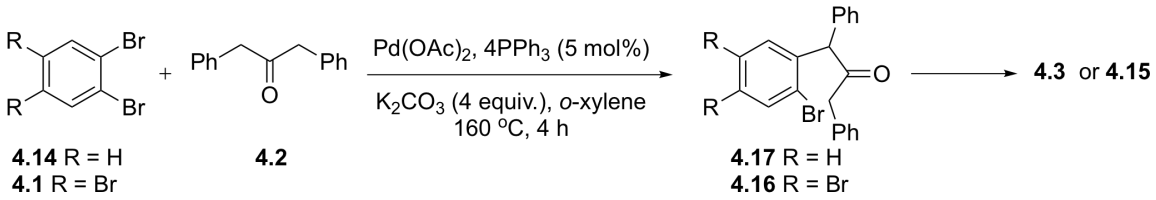

4.14 R = H
4.1 R = Br

4.2

4.17 R = H
4.16 R = Br

Trial	Base	Catalyst	Ligand	Solvent	Temp (°C)	Time (h)	Ratio 4.3 (4.15) : 4.17 (4.16) : 4.14 (4.1)
1[a]	K_2CO_3	$Pd(OAc)_2$	PPh_3	*o*-xylene	160	4	0 : 1 : 0.5
2[b]	K_2CO_3	$Pd(OAc)_2$	PPh_3	*o*-xylene	160	4	1 : 20 : 84
3[b]	K_2CO_3	$Pd(OAc)_2$	PPh_3	*o*-xylene	160	24	1 : 1.8 : 1
4[b]	K_2CO_3	$Pd(OAc)_2$	PPh_3	DMF	120	24	1 : 3 : 132
5[b]	K_2CO_3	$Pd(OAc)_2$	X-Phos	*o*-xylene	160	4	1 : 0 : 0.5
6[a]	K_2CO_3	$Pd(OAc)_2$	X-Phos	*o*-xylene	160	5	0 : 0 : 1
7[a]	K_2CO_3	$Pd(OAc)_2$	X-Phos	DMF	120	4	0 : 0 : 1
8[a]	K_2CO_3	$Pd(OAc)_2$	X-Phos	dioxane	120	4	0 : 0 : 1
9[a]	K_2CO_3	$Pd(OAc)_2$	X-Phos	TFT	120	4	0 : trace : 1
10[a]	NaO*t*-Bu	$Pd(OAc)_2$	X-Phos	THF	70	4	0 : 0 : 1
11[a]	$CsCO_3$	$Pd(OAc)_2$	X-Phos	*o*-xylene	160	4	0 : 0 : 1
12[a]	NaO*t*-Bu	PEPPSI-IPR	–	THF	70	4	0 : 0 : 1
13[a]	K_2CO_3	$Pd_2(dba)_3$	X-Phos	*o*-xylene	160	4	0 : 0 : 1

[a] Starting material was **4.1**; [b] Starting material was **4.14**.

Since all of our trials indicated that more of the intermediate was formed than the desired product this suggested that the integrity of the catalyst was compromised after the first coupling. In an attempt to help facilitate the second oxidative addition, we investigated the use of electron rich ligands. The ligand X-Phos has been shown in the

literature to improve palladium catalyzed α-ketone arylations and was chosen to try and improve the yields of the desired product.[10, 11] Gratifyingly, employing X-Phos (trial 5) appeared to have facilitated the second oxidative addition into the aryl halide as no intermediate and only desired product was observed. Yet, there was still only approximately a 66% conversion of starting material.

Unfortunately, when the modified conditions were applied to the real system (trial 8), with tetrabromobenzene **4.1**, no conversion was observed. Still convinced that the desired dihydroindenone should be accessible, we attempted screening solvents (trials 7–9), bases (trial 10–11), and palladium sources (trials 12–13) but found no viable conditions. Additionally, we found that the intermediate co-eluted with the desired product further complicating efforts to prepare **4.3**. Despite persistent efforts, we were unable to produce the desired dihydroindenone **4.3** in reasonable yield and purity, especially for the first step of a total synthesis. Instead, we decided it was time to develop a new route.

4.2. Design and Preparation of Benzonorbornene: A More Versatile Key-Intermediate

4.2.1. The Versatility of Benzonorbornenes

Returning to our fundamental design principals, the ultimate goal was to build intermediates that have a [2.2.1] bicycle fused to an aromatic ring, such as that found in **4.18** (Scheme 4.4a). Upon transforming the terminal end of the norbornane system to an olefin, **4.19**, (Scheme 4.4b) the synthesis of such a structure is straightforward. A Diels–Alder reaction between benzyne **3.13** and a cyclopentadiene derivative would readily

prepare the desired structural motif. Additionally, fulvenes, **3.23**, could be used in place of cyclopentadienone, thereby removing a protection step. The question that remained though was, how could the olefin of the norbornene ring be utilized as a synthetic handle?

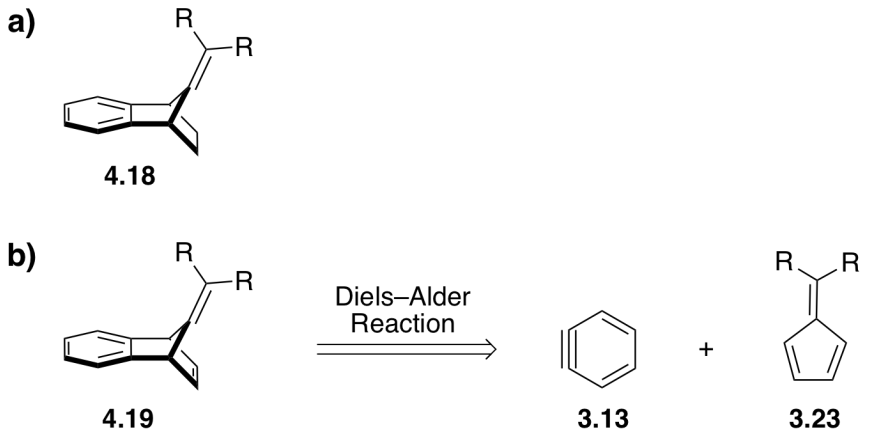

Scheme 4.4 Targeted structural motif a) the most basic structural requirement b) a suitable structure achievable by a Diels–Alder reaction.

First instinct may be to try and use the alkene as a dienophile in a [4+2] reaction. However, the rigid boat conformation of norbornene causes the endocyclic alkene to be strained with an electron rich exo-face.[12, 13] As a result, this alkene is not commonly used in normal electron demand Diels–Alder reactions. Intuitively, this makes sense as otherwise Diels–Alder reactions would result in polymerizations when cyclopentadienes are employed. Additionally, when Stoddart made use of a norbornene like olefin as a dienophile the reactions only proceeded at high temperature or extreme high pressures.[14] Although with a highly reactive diene, such as *o*-quinodimethane **4.21** (generated from tetrabromoxylene **4.20**), this Diels–Alder reaction can readily occur.[15–17] Therefore, there was potential that this alkene could serve as a dienophile to form an anthracene unit as found in **4.22** (Scheme 4.5a).

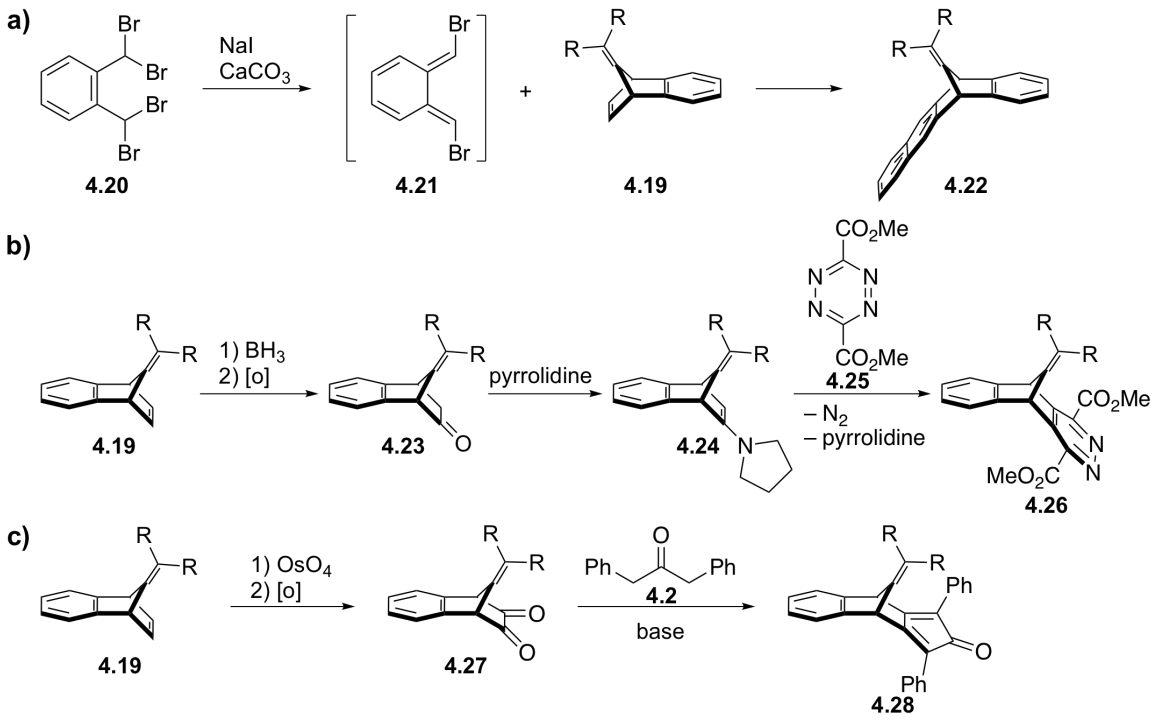

Scheme 4.5 Proposed synthetic transformations of the norbornene olefin demonstrating the versatility of this key intermediate.

We also considered other transformations of the norbornene olefin. Another viable option would be to convert the alkene to ketone **4.23** and then generate enamine **4.24** (Scheme 4.5b). Enamines are electron-rich dienophiles that readily participate in an inverse demand Diels–Alder reactions with tetrazine molecules such as **4.25**.[18,19] Use of tetrazine would result in a cascade reaction where the [4+2] product expels N_2 followed by elimination of the amine to generate the pyridazine moiety of **4.26**. The pyridazine contains a diene, which could potentially participate in a Diels–Alder reaction with benzyne.

A third option would be to use the alkene to append a cyclopentadieneone unit (Scheme 4.5c). We envisioned this could be achieved by dihydroxylating the alkene, followed by oxidation to the dione **4.27**. A double Aldol condensation reaction with

diphenyl acetone **4.2** would furnish the diphenylcyclopentadienone **4.28**. These are known to be excellent dienes for use in the Diels–Alder reaction, especially with arynes.

The diversity of the different proposed pathways convinced us that the norbornene olefin was an adaptable intermediate. However, to construct the macrocycle, we needed two norbornene units on opposite sides of the benzene ring, as in **3.21**. Conceivably, both bicycles could be constructed via a Diels–Alder reaction between arynes **3.22** and fulvenes **3.23**. At the time we started this work, there was little precedence though for forming two arynes sequentially on the same ring. Also, we were unsure as to how important the identity of the R groups on the fulvene would be. Our work towards preparing masked anthracene **3.21** began with testing known benzyne precursors and defining the substituent on the fulvene.

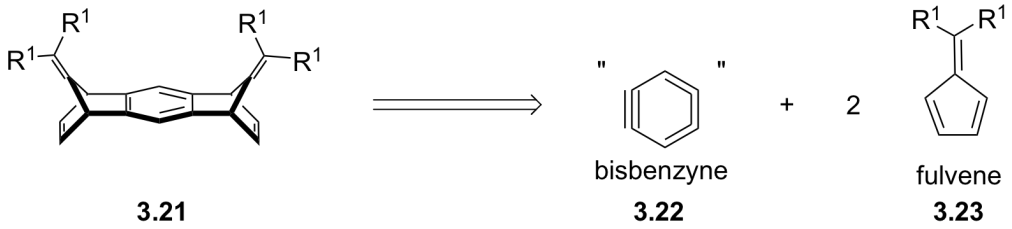

Scheme 4.6 Retrosynthetic analysis for preparation of key intermediate 3.21.

4.2.2. Identifying Fulvene and Benzyne Precursors for Benzonorbornene Preparation

To keep the synthesis simple, we initially tried to generate the arynes through a double lithiation-elimination sequence of tetrabromobenzene **4.1** (Scheme 4.7). Stoddart successfully used this method to generate his bisdienophile **2.4**.[13] Unlike Stoddart though, we needed to trap the arynes with a fulvene instead of furan. Originally, we arbitrarily chose diphenylfulvene **4.29**. Fulvene **4.29** was readily generated, following literature procedures, through a condensation reaction between cyclopentadiene **4.33** and

diphenylacetone **4.34** (Scheme 4.8a).[20] Employing **4.29** as a diene to trap the arynes generated from tetrabromobenzene following literature procedures[13, 21] was not productive. As detected by ^{1}H NMR, only trace amounts of the desired product, **4.30**, along with other unidentified by-products were formed. Instead the primary component of the crude reaction mixture was unreacted fulvene **4.29**. Furthermore only a trace amount of tetrabromobenzne **4.1** could be detected. This indicated that the benzyne was formed however it is not efficiently trapped by the fulvene. It is also important to note that in working up the reaction, there was difficulty in keeping the starting material and by-product(s) in solution. This was an indication that the phenyl rings on the fulvene may hinder solubility of future intermediates and thereby make isolation and purification more challenging.

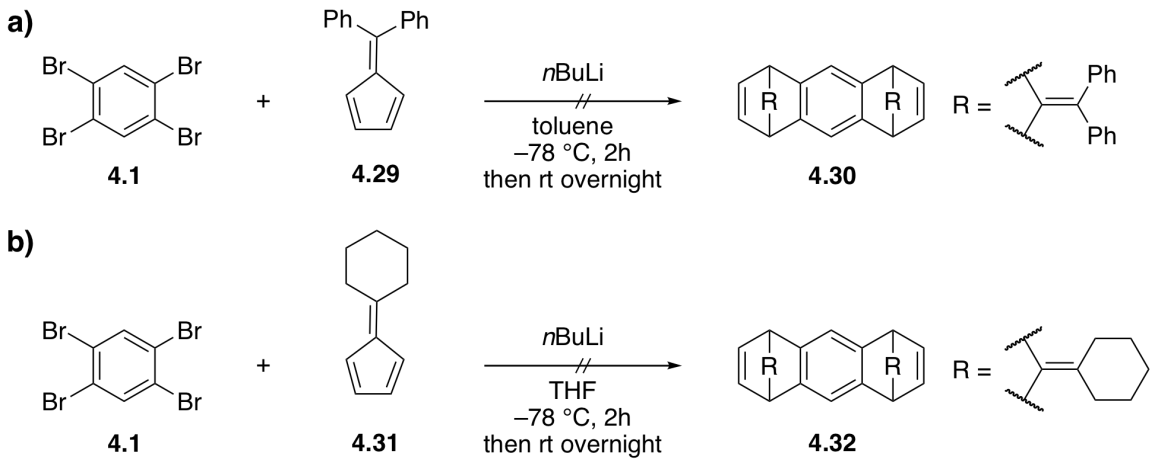

Scheme 4.7 Initial attempts to form the key intermediate by trapping a benzyne generated from tetrabromobenzene with a) diphenylfulvene and b) pentamethylenylfulvene.

To improve solubility, we opted to replace the phenyl groups on the fulvene with a relatively greasier cyclohexane ring, **4.31**. This fulvene can be prepared in gram quantity in high yield (95%) following literature procedures (Scheme 4.8b).[22] Additionally, the cyclohexane fulvene is a yellow oil, where as the diphenyl fulvene was an orange solid. This supports the hypothesis that incorporation of the cyclohexane ring

should reduce intermolecular interactions and therefore help improve solubility. Unfortunately, the cyclohexylfulvene, **4.31**, was not able to efficiently trap the arynes generated from tetrabromobenzene **4.1**. We postulate, that compared to furan, fulvene is too poor of a diene for this reaction to be efficient at the low temperatures (–78 °C) necessary to generate the aryne species. Fortuitously, during these attempts the Biju group reported an efficient method for the exact desired transformation.[23]

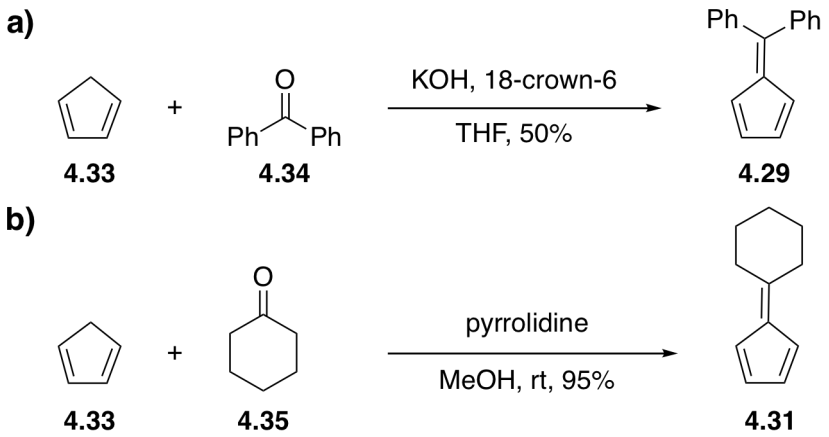

Scheme 4.8 Synthesis of a) diphenylfulvene and b) pentamethylenylfulvene

In their paper, Biju and co-workers recount the unreliability and low yields associated with trapping benzynes by fulvenes.[23] They attribute the low yield to the harsh reaction conditions. Instead, they found that if the benzyne is generated by the fluoride-induced elimination of 2-(trimethylsilyl)aryl triflates, **4.36**, then fulvenes can efficiently act as the diene. Generation of the benzyne under these conditions[24] is done at room temperature without the need for any additives such as a strong acid or strong base. Indeed, following their reported conditions we were able to readily prepare the desired model benzonorbornene **4.37** using cyclohexylfulvene **4.31**. Convinced that this overall methodology would meet our needs we worked on applying this to our real system.

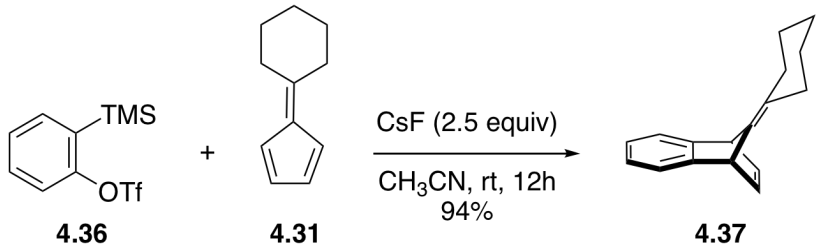

4.36 4.31 4.37

Scheme 4.9 An example of Biju's reliable method for performing the Diels–Alder reaction between fulvenes and benzyne using the desired pentamethylenylfulvene.

4.3. Benzobisnorbornene Preparation and Characterization

4.3.1. Designing and Preparing, and Utilizing the Bisbenzyne Precursor

For the real system, we needed the ability to functionalize at the 4 and 5 positions of the benzene ring of **4.37**. In the prior route, bromine atoms at these positions served as handles for functionalization post benzyne formation. Instead, we decided that the route would be more efficient overall if we could prepare a molecule capable of forming arynes sequentially. We were pleased to find in the literature a report of the preparation of the bisbenzyne precursor **4.39**, the analogue of the benzyne precursor **4.36** used by Biju, depicted in Scheme 4.10.[25] Additionally, the Wudl group successfully used **4.39** for tandem Diels–Alder reactions with cyclopentadieneone **4.38** as the diene to give twistacene **4.40** in 22% yield.[26] Not surprisingly though **4.39** is not commercially available and the reported synthesis[25] is likely not the most efficient route.

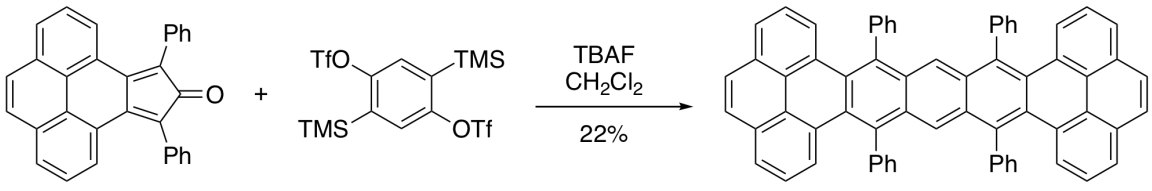

4.38 4.39 4.40

Scheme 4.10 Wudl's use of bisbenzyne precursor 4.39 in a double Diels–Alder reaction.

In recent years, there has been an increased interest in benzyne chemistry. As a result, work has been done to develop efficient and fascicle syntheses of the 2-(trimethylsilyl)aryl triflates **4.36** since the cited synthesis of bisbenzyne precursor **4.39**.[27–29] We decided to adapt the procedure of Brimble[29] to prepare **4.39**. The authors highlight the benefit of their route is the overall short reaction time and high yield. The synthesis is four steps starting from *o*-chlorophenol. First, phenol **4.41** is protected as the TMS ether, **4.42**, then the chloride is substituted with a TMS substituent, **4.43**, followed by deprotection, **4.44**, and triflation to provide **4.36** (Scheme 4.11). For our route (Scheme 4.12), we could obtain an *o*-chlorophenol **4.41** equivalent by dibrominating hydroquinone **4.45**. The remaining steps could follow the work of Brimble except for the triflation, which had been optimized by Wudl for the bisbenzyne precursor. Below is an account of the optimization of each step for our synthesis of bisbenzyne precursor **4.39**.

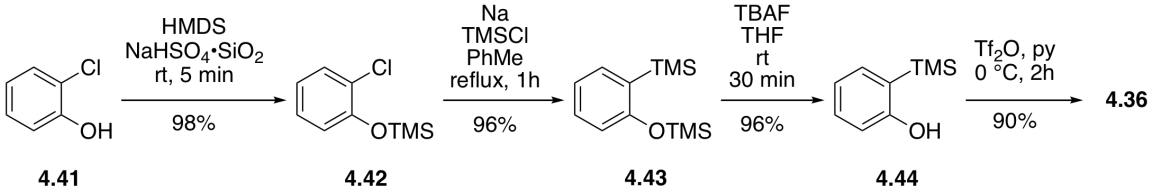

Scheme 4.11 Brimble's efficient synthesis of 2-(trimethylsilyl)aryl triflates, 4.36.

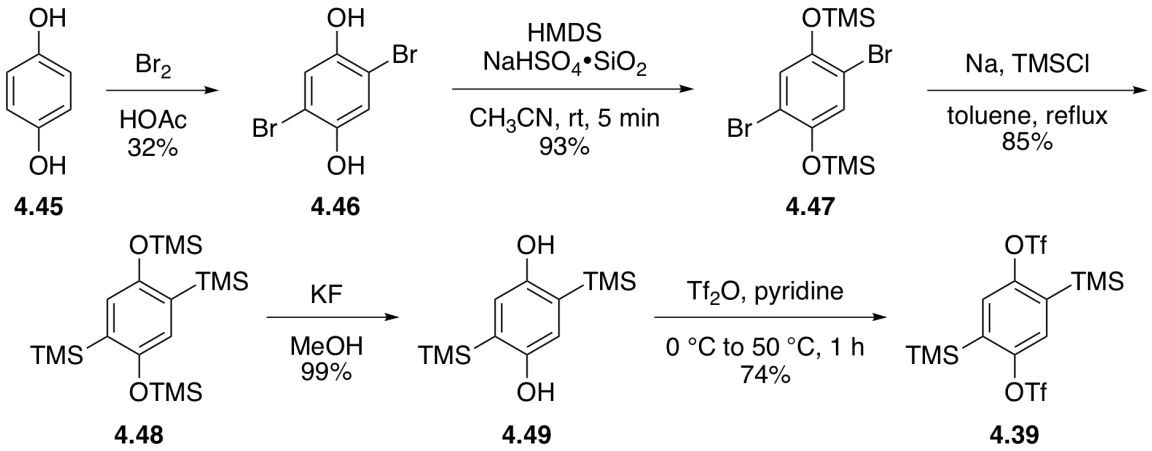

Scheme 4.12 Synthetic scheme for the synthesis of bisbenzyne precursor 4.39.

The synthesis began with a double electrophilic aromatic substitution of hydroquinone, **4.45**, with bromine in the presence of acetic acid at room temperature.[30] Due to the exothermic nature of this reaction, the bromine needed to be added slowly and an internal temperature probe was used to ensure the temperature did not rise above 35 °C. The major product of this reaction was 2,5-dibromohydroquinone **4.46**, however a by-product, 2,3-dibromohydroquinone, was also formed. The desired 2,5-isomer is less soluble in acetic acid and partially precipitated out of solution (~12%) and was collected and carried forward in the synthesis with out additional purification. However, if the reaction was run at lower temperatures (15 °C) then the 2,3-isomer also precipitated out and purification was necessary. Additional product **4.46** could be obtained by concentrating the reaction mixture but then both the 2,5 and 2,3-isomers precipitated out of solution. Literature reports[30] on purification for this reaction can be achieved by recrystallization in acetic acid however this method was found to be unreliable and only worked if there was a small amount of the undesired 2,3-isomer present. Alternatively, it was found that the two isomers could be separated via column chromatography. However, the low solubility of the products required the use of a large column (6 × 20 cm) and only 2 g of material could be separated at a time. An additional safety note is the by-product of the reaction is HBr. On large scale (20 mmol of hydroquinone) the resultant reaction mixture is difficult to handle due to the extreme fuming of HBr. On a 10 mmol scale, 2,5-dibromohydroquinone **4.46** can be prepared in 32% yield (could be higher with more scalable purification procedures) as a colorless solid.

Next, the alcohols of **4.46** were protected as TMS-ethers, which proceeded smoothly.[29] Treatment with HMDS in the presence of sodium bisulfate on silica gel[31]

afforded the desired product, **4.47**, in quantitative yield within 5 minutes. The product was purified by recrystallization from hexanes to give disilyl ether **4.47** in 93% yield as a colorless crystalline solid. Subsequently, the bromines were substituted with TMS groups.[29] The desired transformation was achieved by adding **4.47** in toluene drop-wise to a refluxing solution of TMSCl in toluene with molten sodium. The resulting solution was dark blue indicating the presence of a solvated electron. For safety reasons, the largest scale this reaction was run on was about 17 mmol of **4.47**, which would require 1.7 g of sodium metal. The yield of this reaction was highly dependent on vigorous stirring of the reaction mixture to prevent the sodium metal chunks from agglomerating after melting, thus reducing the surface area of sodium metal. If the sodium metal did agglomerate, then surface became oxidized and the reaction did not proceed. After the reaction was complete, a Schlenk filter was used to safely remove the excess sodium metal and a clear yellow solution was obtained. Concentration provided the tetra-TMS intermediate **4.48** as a colorless solid in up to 85% yield. This product was taken on into the next step without additional purification.

Initially, attempts to deprotect the TMS silylethers used TBAF.[29] However, the resulting mixture was difficult to purify and did not appear to give the desired product as indicated by ^{1}H NMR. Instead, it was found that heating **4.48** in MeOH at 50 °C using KF as the fluoride source, achieved the deprotection to give 2,5-(trimethysilyl aryl)hydroquinone **4.49**.[32] Unsurprisingly, **4.49** was prone to air oxidation to give, presumably, the corresponding quinone, 2,5-(trimethysilyl)quinone. Running the reaction in degassed MeOH under a N_2 atmosphere afforded the desired product in 99% yield as a colorless solid and could be carried on into the next step without further purification. If

necessary, the product could be purified via recrystallization from hexanes however the yield dropped (65–73%) and the resulting crystals were very fine, like glitter, and difficult to collect and transfer. Due to its vulnerability to oxidation, **4.49** should be taken on directly into the next reaction or stored under an intert atmosphere.

The final step for the preparation of the bisbenzyne precursor **4.39** was triflation of the phenols of **4.49**.[26] This was achieved by heating **4.49** with triflic anhydride in pyridine. To achieve a high yield for this reaction it was important to use triflic anhydride that had not been exposed to moisture (even from the atmosphere). The resulting product was purified by recrystallization from hexanes to give a colorless crystalline solid (cubes) of **4.39** in 74% yield. This product is stable under ambient conditions for long periods of time (at least 4 years). From 2,5-dibromohydroquinone, **4.39** can be prepared in overall 58% yield without the use of any column chromatography.

4.3.2. Optimization of Double Diels–Alder Reaction to Generate Masked Benzobisnorbornene

Once the bisbenzyne precursor **4.39** was in hand, investigations into its use in a double Diels–Alder reaction with pentamethylenylfulvene **4.31** began (Scheme 4.13). Initial attempts used the same procedure reported by Biju for generation of the benzyne from the corresponding monobenzyne precursor **4.36**. Gratifyingly the desired product **4.32** was formed providing proof of concept. However, **4.32** (as a mixture of diastereomers in which the bridges are *syn* or *anti*, a discussion on their separation and characterization is covered in 4.3.3) was only isolated in 25% yield along with the mono Diels–Alder adduct **4.50** in 7% yield. Separation of **4.32** and **4.50** enabled the identification of key diagnostic peaks in the ^{1}H NMR spectra belonging to each structure.

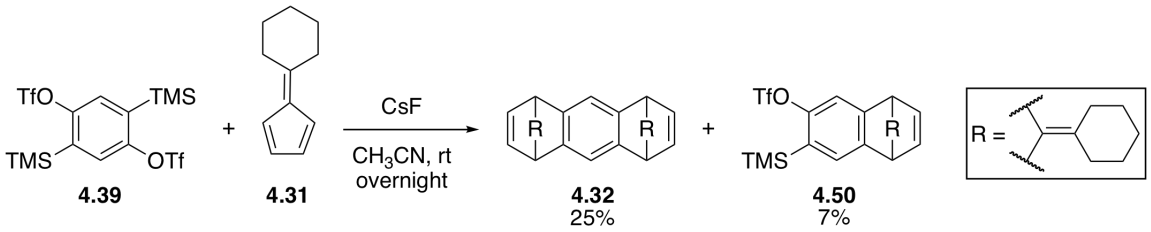

Scheme 4.13 Initial attempt of double Diels–Alder reaction using 4.39 and Biju's conditions.

Upon separation of the mono and double Diels–Alder adducts, **4.32** and **4.50** respectively, ^{1}H NMR was used to readily determine the respective identities. The presence of a large signal corresponding to a TMS group at δ = 0.33 ppm in the ^{1}H NMR spectrum, as well as a singlet at δ = -74.19 ppm in the ^{19}F NMR spectrum, indicated the presence of the aryne precursor from the mono adduct **4.50**. Further supporting this assignment was the presence of two singlets in the aromatic region at δ = 7.27 and 7.19 ppm, corresponding to the protons *ortho* to the remaining aryl triflate and aryl TMS groups respectively. In contrast, for the double Diels–Alder adduct **4.32** there is only one singlet at δ = 7.12 ppm in the aromatic region, as the aromatic hydrogens are equivalent for this compound.

Analyzing these ^{1}H NMRs was also instructive as the position of signals corresponding to the hydrogen atoms attached to the norbornene is non-intuitive. Particularly, the protons on the alkene are surprisingly deshielded and show up around δ = 6.9 ppm. In comparison, the olefinic hydrogens of norbornene appear around δ = 6.02 ppm,[33] which suggests that these hydrogens are influenced by the aromatic ring even though conjugation is broken by the bridgehead carbons. This is possibly similar to the homoconjugation, through-space interactions across an allegedly insulating aliphatic bridge, observed for quinone molecular clips.[34] Finally, the hydrogen atoms at the bridgehead are also highly deshielded, as compared to most aliphatic hydrogen atoms,

and appear around δ = 4.3 ppm. As will be highlighted later (Chapter 6), this was quite a convenient diagnostic peak as not much else appears in this region of the ^{1}H NMR. Confident in our NMR analysis and ability to estimate relative amounts of the mono and double Diels–Alder product in the crude NMR we proceeded to optimize our double Diels–Alder reaction.

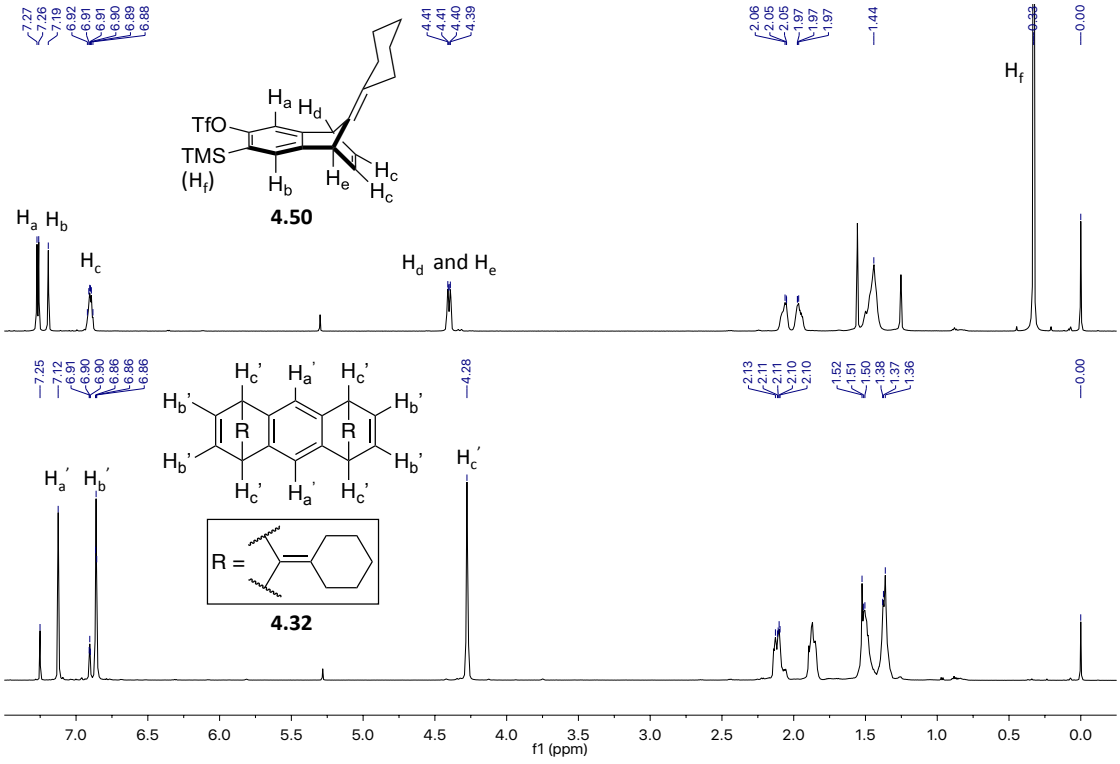

Figure 4.1 Representative ^{1}H NMRs of 4.50 and 4.32. Note the spectrum of 4.32 is enriched in one isomer due to the low solubility of the minor one. The signal at 6.91 ppm is due to the minor isomer but all other signals overlap with the major isomer.

The optimization study began by examining the effect of solvent and temperature on the outcome of the reaction. All of the reactions were run in parallel and yields were determined from the ^{1}H NMR of the crude reaction mixture using 1,3,5-trimethoxybeznene as an internal standard. Unfortunately, new impurities with peaks that slightly overlap with those of the internal standard prevented the ability to obtain exact

yields (a range is given) however clear trends still emerged. The solvent screen included acetonitrile (as a standard), along with dichloromethane (DCM), tetrahydrofuran (THF), and dioxane. For each solvent, one reaction was run at room temperature and one was run at 50 °C.

Table 4.2 Solvent and temperature optimization study of double Diels–Alder reaction.

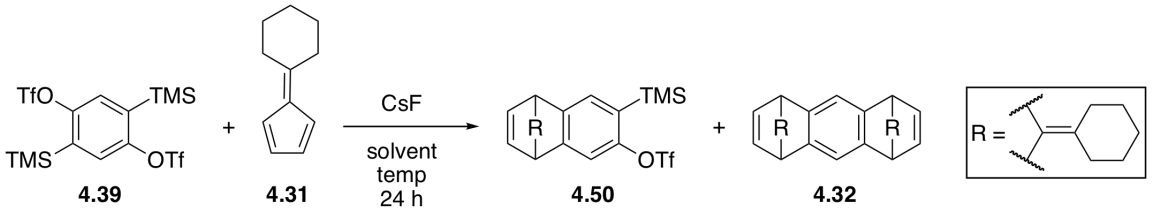

Entry	Solvent	Temperature (°C)	Mono D.A. product 4.50	Double D.A. product 4.32
1	CH_3CN	rt	17%	8%
2	CH_3CN	50	0%	9%
3	DCM	rt	0%	0%
4	DCM	50	0%	0%
5	THF	rt	53-58%	0%
6	THF	50	56-59%	0%
7	dioxane	rt	45-47%	0%
8	dioxane	50	47-53%	0%

The first reaction (Table 4.1, entry 1) used the same conditions as reported by Biju and served as a reference. Under these standard conditions more of the mono product **4.50** is formed than the double Diels–Alder product **4.32**. Increasing the

temperature to 50 °C (entry 2) did aid in pushing the reaction to completion to give only the double product, **4.32**, but the yield did not significantly improve (~9%, **4.32**). Therefore, increasing the temperature was not an adequate solution. Trials using DCM (entries 3 and 4) resulted in no reaction. Presumably this was because DCM is too non-polar to dissolve any of the CsF. Next, using THF and dioxane at room temperature gave high yields of the intermediate product **4.50** (entries 5 and 7) however, none of the double adduct **4.32** was formed. Increasing the temperature for both solvents (entries 6 and 8) slightly increased the yield of the mono adduct **4.50** but, unlike the acetonitrile trial, did not afford the desired product **4.32**. THF gave slightly higher yields than dioxane.

From the study it was determined that THF at room temperature was optimal. THF was chosen because, even though it gives only the mono adduct, it proceeded with the highest conversion of the bisbenzyne precursor **4.39**. The higher conversion is likely due to the increased solubility of the bisbenzyne precursor **4.39** in THF as oppose to acetonitrile. The problem with THF though is it is less polar than acetonitrile and therefore the CsF is less soluble. In fact, these reactions are not homogenous as not all the CsF is able to go into solution. In contrast, solubility of the reagents is not a concern when using the monobenzyne precursor **4.36** as the reagent is a liquid. Room temperature was chosen, even though it gives lower yields, because less unidentified by-products are formed. These unidentified products are proposed to be from fulvene dimerization, polymerization, or decomposition. With the optimal solvent and temperature determined the problems of low CsF solubility and fulvene instability needed to be addressed.

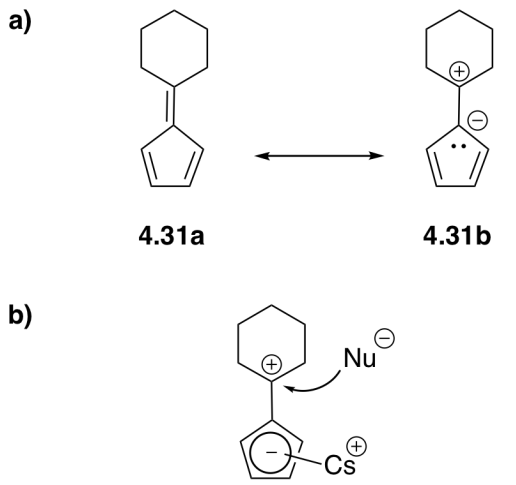

Figure 4.2 a) The largest contributing resonance structures to pentamethylenylfulvene's hybrid structure and b) the proposed interaction of Cs cation with the anionic cyclopentadiene ring of the second resonance structure.

Focusing on the fulvene piece, fulvene are commonly drawn with an exocyclic alkene. However, a resonance structure can be drawn in which the π electrons are associated with the cylopentadiene ring forming an aromatic ring (Figure 4.2a). This alternative resonance structure is likely a strong contributor to the resonance hybrid. My initial hypothesis was that perhaps the Cs cation from CsF was interacting with the pseudo aromatic ring of fulvene leaving the cyclohexyl ring susceptible to nucleophilic attack (Figure 4.2b).[35, 36] Additionally, if the Cs cations were interacting with the cyclopentadiene ring this would make it less electron rich and therefore less reactive in the Diels–Alder reaction with benzyne. To test this hypothesis, three control reactions were run in acetonitrile. The first two reactions only contained fulvene in CH_3CN, one at room temperature, the other at 50 °C. In both cases no reaction occurred. The third control was run at room temperature with the addition of CsF. This resulted in the formation of the same impurities observed during the double Diels–Alder reaction optimization.

From the control reaction I was convinced that the free Cs cation in solution was leading to decomposition of the fulvene and that was the main problem. As a solution I proposed that by switching to KF the cation, K^+, could be encapsulated by 18-crown-6 and thereby allow the reaction to proceed.[23] Indeed, running the reaction in THF at room temperature with KF and 18-crown-6 ether afforded the desired double Diels–Alder product **4.32** in 60% yield. Additionally using these conditions no mono product **4.50** and little by-product was observed. However, now I believe this method works as it generates more free F^- anion *not* because it reduces fulvene decomposition and reactivity. In retrospect, the problem with CsF/THF conditions was the inability to generate the second benzyne, not the instability or reactivity of fulvene. Regardless, a satisfactory method for sequential aryne formation on a single aryl ring under mild conditions was achieved allowing the synthesis to move forward.

It should be noted that two years after the work to optimize the double Diels–Alder reaction with **4.39**, Peña and Pérez published an article on the use of bisbenzyne precursor **4.39** in mono Diels–Alder reactions with various cyclopentadienones.[37] They encountered similar problems of incompatible solubility of **4.39** and CsF. The authors' solution was to run the reaction in a 2:1 mixture of acetonitrile–DCM. They propose that their reactions stopped after the first [4+2] reaction because the mono Diels–Alder product precipitates out of solution and thereby prevents the formation of the second aryne. However, it is unclear how thoroughly they investigated their hypothesis as they were not trying to achieve a double Diels–Alder reaction. Also, unclear was the conditions they used or were planning to use to unmask the second benzyne in future

reactions. These results along with ours though show the utility of bisbenzyne precursors and the ability to use them selectively for either mono or double Diels–Alder reactions.

4.3.3. Isolation and Characterization of *syn*-benzobisnorbornene

The successful preparation and isolation of the benzobisnorbornene product **4.32** was good. However, based on the proposed routes (Scheme 4.5), only the isomer in which the bridges are *syn* **4.32a** (Figure 4.4) can be carried forward. Unsurprisingly, the second Diels–Alder reaction occurs with no stereospecificity as there are no steric or electronic factors to govern the approach of the diene to the dienophile. As a result a 1:1 mixture of the *syn* and *anti* isomers of **4.32** are produced. Separation of these isomers was difficult to achieve by flash chromatography due to their low polarity and similar structures. However, in hexanes one isomer (A) was soluble where as the other was only slightly soluble (isomer B). (Since isomer B has low solubility in chloroform, ^{1}H NMR could not be used to accurately determine the relative ratio of *syn*:*anti* isomers in a concentrated sample as not all of isomer B was in solution, other NMR solvents should be investigated.) This property allowed for the isolation of a pure sample of isomer B and a sample enriched in isomer A.

Attempts were made to isolate isomer A by flash chromatography but were unsuccessful. Isomer B eluted from the column first but it also streaked, thereby contaminating the fractions containing isomer A. Increasing the polarity of the column did decrease the observed streaking, however, it also reduced the resolution between the isomers so that no separation was achieved. Gratifyingly, it was found that recrystallization in benzene produced cube crystals highly enriched in isomer A (16:1, isomer A: isomer B). With the isomers separated full characterization was used to attempt

to identify which isomer was had the *syn* configuration and which one had the *anti* configuration.

a) ^{1}H NMR

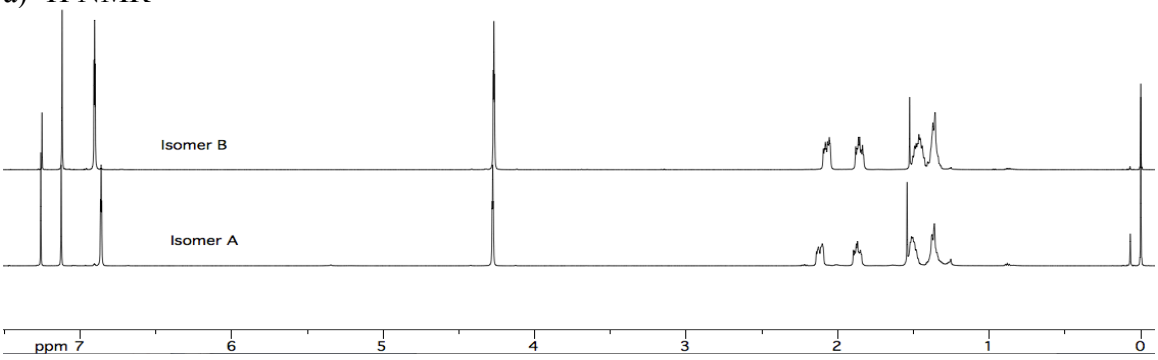

b) ^{13}C NMR

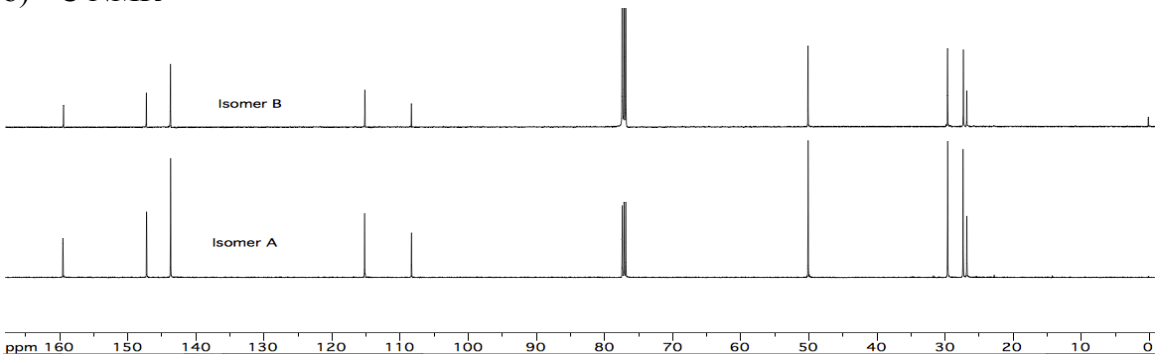

c) IR (KBr)

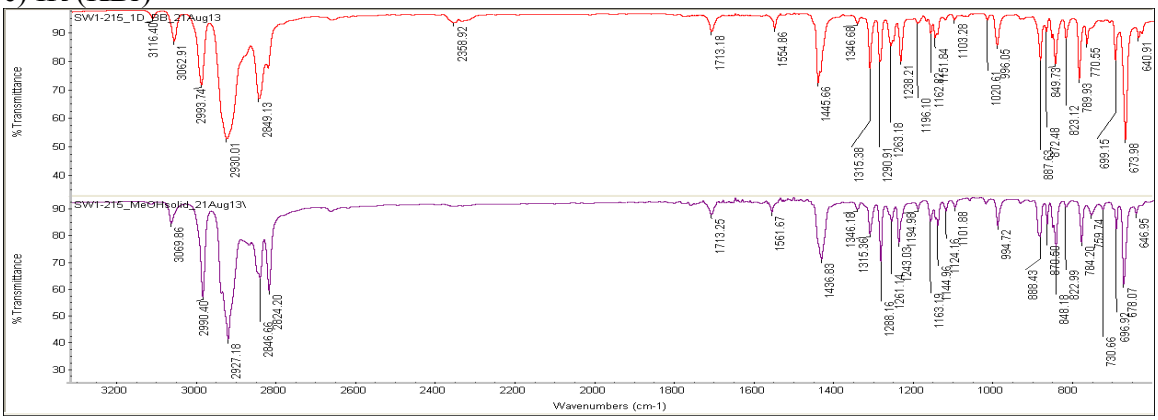

Figure 4.3 Characterization spetra for a sample enriched in isomer A and isomer B of 4.32 a) ^{1}H NMR, b) ^{13}C NMR, c) IR (KBr).

The spectrum of the ^{1}H NMR for isomers A and B are nearly identical (Figure 4.3a). The largest difference is observed at the norbornene olefinic hydrogens but there is

no way to reason if these protons would be more deshielded in the *syn* or *anti* configuration. The spectrums for the ^{13}C NMR (Figure 4.3b) and the IR (Figure 4.1c) of the two isomers were identical. Shockingly, when the melting points were taken isomer A melted at 164–171 °C where as isomer B melted at 362–370 °C. This was the first firm indication that isomer B possessed the *anti* relationship of the bridges as this configuration allows for tighter packing. This would also explain why isomer B has a lower solubility in hexanes. Isomer B also comes off the column first, and the *anti* configuration would make the structure overall slightly less polar.

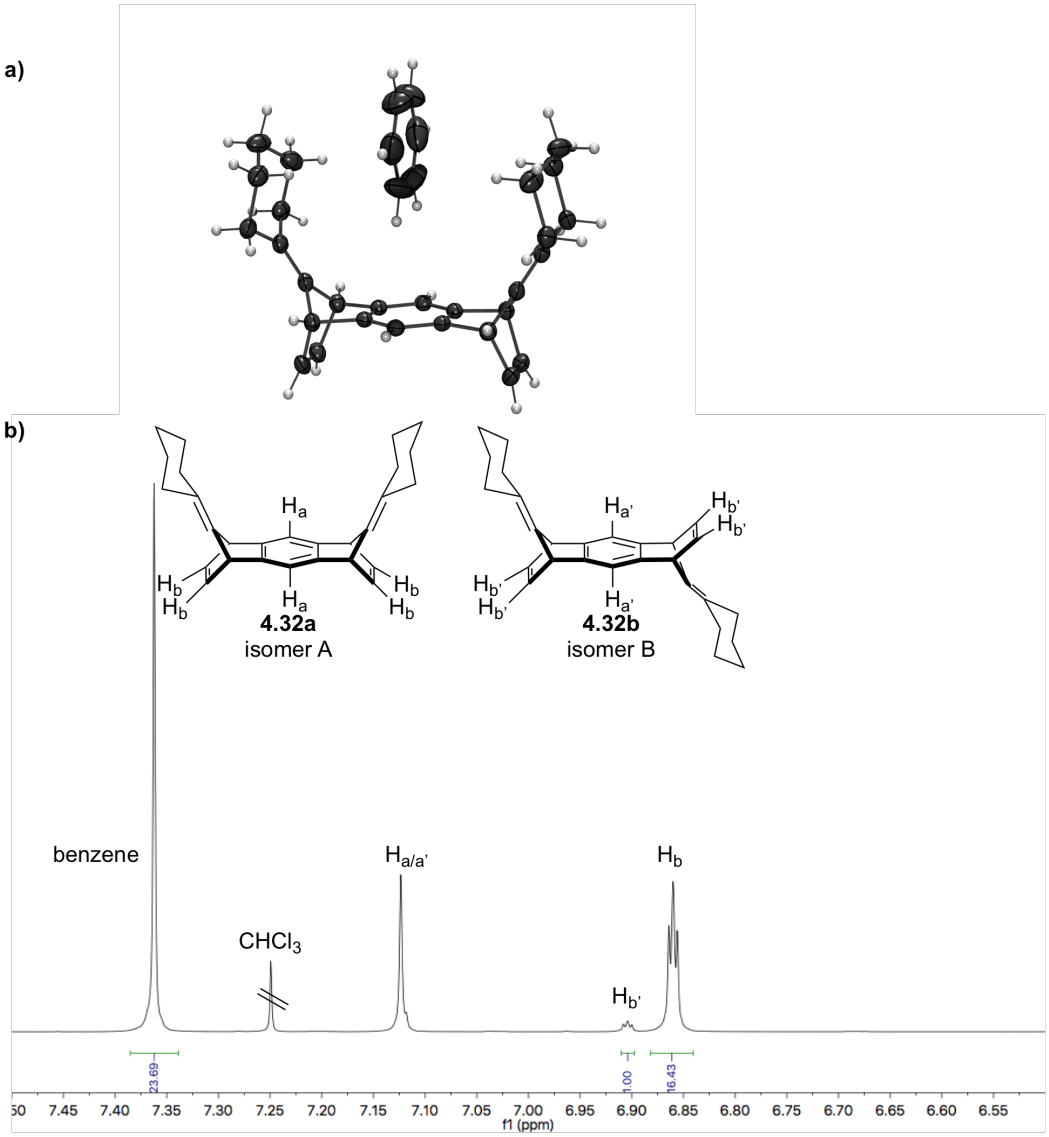

Figure 4.4 Identities of the 4.32 isomers, a) the ORTEP of the X-ray obtained for isomer A and b) a ^{1}H NMR of the benzene solvate crystals along with the assigned identities of isomer A as *syn* and isomer B as *anti*.

Recrystallization of the each isomer results in single crystals with different morphologies. When isomer A is recrystallized from benzene it yields crystals that are cubes, where as when isomer B is recrystallized from hexanes needle like crystals are formed. X-ray crystallography (Figure 4.4a) using the crystals obtained from recrystallization of a sample enriched in isomer A (in the sample subjected to recrystallization the mol ratio of isomer A to isomer B was 16:1), in benzene indicated

that isomer A was in fact they *syn* isomer (Figure 4.4b). The *syn* isomer preferentially formed a crystal because it formed a solvate with a benzene molecule nestled between the *syn* cyclohexane rings. A ^{1}H NMR of the crystal (Figure 4.4b) confirms that isomer A is the isomer that formed the benzene solvate as can be seen by the 1:1 mole ratio of benzene to isomer A. We are also fairly confident in this assignment as only approximately 5% of solution contained isomer B. However, to firmly conclude the structural assignment a crystal structure of pure isomer B could be obtained. With a synthesis and isolation of the key intermediate *syn*-benzobisnorbornene **4.32a** in hand efforts to investigate the utility of the norbornene alkene could be initiated.

Table 4.3 Summary of a comparison of characterization data and properties of isomer A and isomer B of 4.32.

Characterization/Properties	**4.32** isomer A	**4.32** isomer B
Solubility in hexanes	soluble	partially insoluble
^{1}H NMR	nearly identical	nearly identical
^{13}C NMR	identical	identical
IR	nearly identical	nearly identical
Melting Point	164–171 °C	362–370 °C
Recrystallization Solvent	benzene (cube)	hexanes (needles)
Column Elution Order	second	first

4.4. Experimentals

All reactions were carried out using flame-dried glassware under nitrogen atmosphere unless aqueous solutions were employed as reagents. Tetrahydrofuran (THF) was dried by distillation from benzophenone/sodium under nitrogen. Dichloromethane

(DCM), toluene, acetonitrile, hexanes, pyridine, and TMSCl were dried by distillation from CaH_2 under nitrogen. All other chemicals were used as received unless otherwise noted.

Analytical thin layer chromatography (TLC) was carried out using 0.25 mm silica plates from Silicycle. Eluted plates were visualized first with UV light. Flash chromatography was performed using 230–400 mesh (particle size 0.04–0.063 mm) silica gel purchased from Silicycle. ^{1}H NMR (500 MHz), ^{13}C NMR (126 MHz), ^{19}F NMR (471 MHz) spectra were obtained on Varian FT NMR or Bruker FT NMR instruments. NMR spectra were reported as δ values in ppm relative to TMS for ^{1}H (0.00 ppm), and chloroform for ^{13}C (77.16 ppm). ^{1}H NMR coupling constants are reported in Hz; multiplicity was indicate as follows; s (singlet); d (doublet); t (triplet); q (quartet); m (multiplet); dd (doublet of doublets); ddd (doublet of doublet of doublets); dt (doublet of triplets); app (apparent); br (broad).

Infrared (IR) spectra were obtained as films from DCM or $CDCl_3$ on sodium chloride plates or as KBr pellets on a Thermo Scientific FT-IR. High-resolution mass spectra (HRMS) in electrospray (ESI) experiments were performed on a Bruker BioTOF II. HRMS using GC-MS (QTOF) was performed on an Agilent 7200-QTOF GC/MS, GC column RTX-5MS 30 m length, 0.255 mm ID, 0.25 μm. Method: inlet temperature 250 °C, source temperature 280 °C. th initial column temperature was 120 °C and was held for 4 minutes after injection. Column temperature was ramped to 325 °C over 10 minutes and then held for 31 minutes. Alternatively the column was by-passed by using a solid injection probe. Method: Initial temperature was 80 °C was ramped at a rate of 45 °C/min up to 320 °C and held at 320 °C for 3 minutes.

2,5-dibromobenzene-1,4-diol 4.46

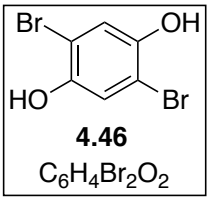

4.46

$C_6H_4Br_2O_2$

In a 3-armed round bottom flask equipped with a thermometer, a dropping funnel, and an outlet into a solution of 1M sodium thiosulfate, hydroquinone (11.0 g, 100 mmol) was suspended in glacial acetic acid (100 mL) at room temperature. To this, bromine (10.3 mL, 200 mmol) in glacial acetic acid (10 mL) was added drop wise (~1 drop/s) using a dropping funnel. The internal temperature was monitored to ensure the temperature did not rise above 35 °C. After about 1/3 of the bromine solution was added all of the hydroquinone dissolved to give a clear golden solution. Once all of the bromine was added a precipitate crashed out of solution. The reaction was allowed to stir for 1 h at room temperature. The dropping funnel was then replaced with a gas dispersion tube and nitrogen was bubbled through the reaction mixture to facilitate removal of excess bromine. The reaction mixture was then filtered and the colorless solid (3.20 g, 11.9 mmol, 12%) was collected as sufficiently pure product (>99:1, product:by-product). Concentrating the mother liquor to about half the original volume and collecting the resultant solid could be performed to obtain additional product. However, this product was contaminated with the *o*-dibromohydroquinone isomer but this could be removed via flash chromatography (60% hexanes : 40% EtOAc).[1]

R_f = 0.56, 60% hexanes : 40% EtOAc.

[1] This is a known compound and was synthesized via the reported procedure so full characterization was not performed. An experimental was written to provide more insight into running the reaction for future reference.

^{1}H NMR (500 MHz, DMSO-d_6) δ ^{1}H NMR (500 MHz, DMSO-d_6) δ 9.84 (s, 2H), 7.04 (s, 2H).

^{13}C NMR (126 MHz, DMSO-d_6) δ 147.7, 119.9, 108.7.

IR (KBr) 3277, 2921, 1617, 1424, 1196, 1060, 852 cm^{-1}.

Mp 187–190 °C.

Silyl ether 4.47

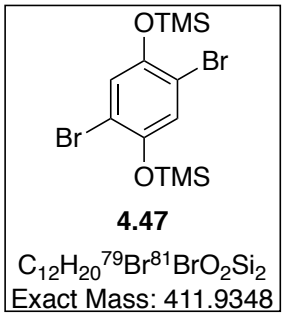

4.47

$C_{12}H_{20}{}^{79}Br^{81}BrO_2Si_2$

Exact Mass: 411.9348

The catalyst $NaHSO_4{\cdot}SiO_2$ (51.2 mg) was suspended in a solution of dibromohydroquinone **4.46** (2.68 g, 10 mmol) in acetonitrile (5 ml) at room temperature. While stirring, HMDS (4.17 mL, 20 mmol) was added drop wise. After the addition was complete the reaction was allowed to stir for an additional 5 min. The reaction mixture was then diluted with DCM (5 mL), filtered to remove the catalyst, and concentrated to give a colorless solid. Recrystallization from hexanes afforded **4.47** (3.82 g, 9.3 mmol, 93%) as a colorless solid.

^{1}H NMR (500 MHz, Chloroform-*d*) δ 7.04 (s, 2H), 0.29 (s, 18H).

^{13}C NMR (126 MHz, Chloroform-*d*) δ 147.4, 124.3, 114.1, 0.4.

IR (film) 2959, 2898, 1055, 1476, 1254, 1210, 841, cm^{-1}.

Mp 63–66 °C.

HRMS (QTOF) *m/z* 411.9344 (411.9343 $C_{12}H_{20}Br_2O_2Si_2$, $(M)^+$).

1,4-bisTMS benzene 4.48

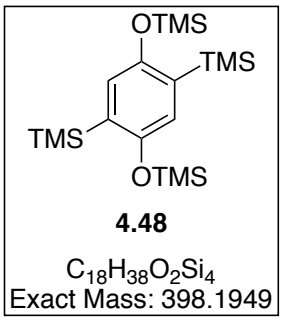

4.48

$C_{18}H_{38}O_2Si_4$
Exact Mass: 398.1949

Safety Note: This reaction involves the use of sodium metal so great care must be taken to ensure all glassware, solvents, and reagents are dry. Small pieces of sodium metal (0.9656 g, 42 mmol) were vigorously stirred in a solution of TMSCl (1.5 mL, 12 mmol) in toluene (6.4 mL) and then heated to reflux. Once the sodium metal had melted,[2] silyl ether **4.47** (4.12 g, 10 mmol) in toluene (5 mL) was added drop wise via syringe pump and simultaneously TMSCl (1.5 mL, 12 mmol) in toluene (2.5 mL) was added drop wise manually over the course of 0.5 h. Caution, the reaction is exothermic so the addition rate may need to be adjusted or the temperature of the oil bath may need to be lowered to prevent excessive refluxing. During the addition the reaction turns a dark blue color. Upon complete addition of **4.47** and TMSCl, the reaction is allowed to reflux for an additional 0.75 h. The reaction was allowed to cool to room temperature and a Schlenk filter was used to safely remove the remaining sodium metal under an inert atmosphere. Distilled toluene (10 mL) and distilled hexanes (10 mL) was used to help facilitate the transfer of material through the filter. The filtered material was a clear yellow solution with a strong pungent odor. The reaction mixture was then concentrated to give pure **4.48** as a colorless solid (3.38 g, 8.5 mmol, 85%).

$\mathbf{R_f}$ = 0.47 (100% hexanes).

[2] vigorous stirring is extremely important at this point to prevent the sodium from agglomerating into one large piece

^{1}H NMR (500 MHz, Chloroform-*d*) δ 6.76 (s, 2H), 0.29 (s, 18H), 0.24 (s, 18H).

^{13}C NMR (126 MHz, Chloroform-*d*) δ 154.1, 131.7, 122.6, 0.8, –0.9.

IR (film) 2955, 1450, 1339, 1254, 1205, 1106, 935, 837, 746 cm^{-1}.

Mp 123–126 °C.

HRMS (QTOF) *m/z* 398.1927 (398.1943 calcd for $C_{18}H_{38}O_2Si_4$, $(M)^+$).

1,4-bisTMS hydroquinone 4.49

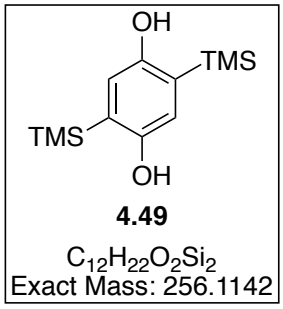

Silyl ether **4.48** (2.59 g, 6.5 mmol) was dissolved in MeOH (65 mL). Nitrogen gas was then bubbled through the solution for 0.5 h to deoxygenate the reaction. KF (0.79 g, 13.7 mmol) was quickly added to the flask and the reaction was vigorously stirred at room temperature for 1.25 h. The reaction mixture was poured onto ice-cold water (250 mL). The product was extracted from the aqueous mixture using chloroform (4 × 150 mL). The combined organic phases was washed with brine (1 × 200 mL), dried (Na_2SO_4) and concentrated to give pure **4.49** as a tan solid (1.64 g, 6.4 mmol, 99%).

R_f = 0.16 (100% hexanes).

^{1}H NMR (500 MHz, Chloroform-*d*) δ 6.67 (s, 2H), 4.46 (s, 2H), 0.29 (s, 18H).

^{13}C NMR (126 MHz, Chloroform-*d*) δ 154.1, 128.1, 120.8, – 0.9.

IR (film) 3426, 2957, 1507, 1365, 1244, 1166, 1103, 836, 745 cm^{-1}.

Mp 178–183 °C.

HRMS (QTOF) *m/z* 256.1155 (256.1142 calcd for $C_{12}H_{22}O_2Si_2$, $(M)^+$).

Bisbenzyne Precursor 4.39

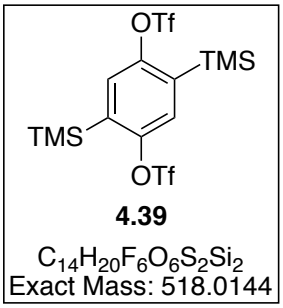

4.39

$C_{14}H_{20}F_6O_6S_2Si_2$
Exact Mass: 518.0144

The 1,4-bisTMS hydroquinone **4.49** (1.80 g, 7.1 mmol) was dissolved in pyridine (45 mL). The solution was cooled in an ice bath then, while stirring, triflic anhydride[3] (5.00 g, 17.7 mmol) was added drop wise to give a bright orange solution. Once the addition was complete the reaction was allowed to warm to room temperature and then was placed in a 50 °C bath for 2 h. The resulting reaction mixture was cooled to room temperature and then concentrated to give a black sludge. This residue was triturated with hexanes (4 × 20 mL, 50 °C, 5 min). The combined hexane fractions were then concentrated to give a yellow solid (3.52 g). The crude product was recrystallized from hexanes to give bisbenzyne precursor **4.39** as a colorless solid (2.74 g, 5.3 mmol, 74%).

$\mathbf{R_f}$ = 0.69 (90% hexanes : 10% EtOAc).

^{1}H NMR (500 MHz, Chloroform-*d*) δ 7.44 (s, 2H), 0.38 (s, 18H).

^{13}C NMR (126 MHz, Chloroform-*d*) δ 153.1, 137.4, 127.0, 126.9, 118.5 (q, *J* = 320 Hz), -1.3.

[3] The reaction works best if a fresh ampule of triflic anhydride is used.

^{19}F NMR (471 MHz, Chloroform-*d*) δ -73.78.

IR (film) 2961, 2904, 1421, 1339, 1218, 1141, 1080, 909, 844, 734 cm^{-1}.

Mp 107–108 °C.

Monobenzonorbornene aryne precursor 4.50

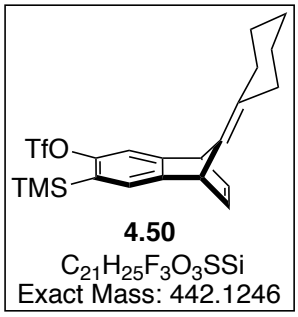

4.50
$C_{21}H_{25}F_3O_3SSi$
Exact Mass: 442.1246

In a round bottom flask, the bisbenzyne precursor **4.39** (518.6 mg, 1 mmol), fulvene **4.31** (219.3 mg, 1.5 mmol), and CsF (379.8 mg, 2.5 mmol) were stirred vigorously in THF (4 mL) at room temperature overnight. The reaction mixture was then diluted with DCM (5 mL) and filtered through a plug of silica gel, which was rinsed with DCM (4 × 5 mL). The organic solution was concentrated to give a thick brown oil (444.4 mg). Purification via flash chromatography (5% toluene : 95% hexanes to 10% toluene : 90% hexanes) provided the mono Diels–Alder product as a yellow oil (309.4 mg, 0.70 mmol, 70%).

R_f = 0.34 (1% toluene : 95% hexanes).

^{1}H NMR (500 MHz, Chloroform-*d*) δ 7.27 (s, 1H), 7.19 (s, 1H), 6.91 – 6.89 (m, 2H), 4.41 – 4.39 (m, 2H), 2.12 – 2.02 (m, 2H), 2.01 – 1.92 (m, 2H), 1.52 – 1.39 (m, 6H), 0.33 (s, 9H).

^{13}C NMR (126 MHz, Chloroform-*d*) δ 158.6, 155.1, 152.3, 149.9, 143.4, 142.9, 127.1, 126.7, 113.1, 111.9, 50.6, 49.7, 29.7, 27.4, 27.4, 26.7, – 0.5 (unable to extract from the

noise the expected quartet for the carbon of the triflate group but the presence of the triflate is confirmed by ^{19}F NMR spectrum).

^{19}F NMR (471 MHz, Chloroform-*d*) δ -74.19.

HRMS (QTOF) *m/z* 442.1239 (442.1240 calcd for $C_{21}H_{25}F_3O_3SSi$, $(M)^+$).

Benzobisnorbornene 4.32

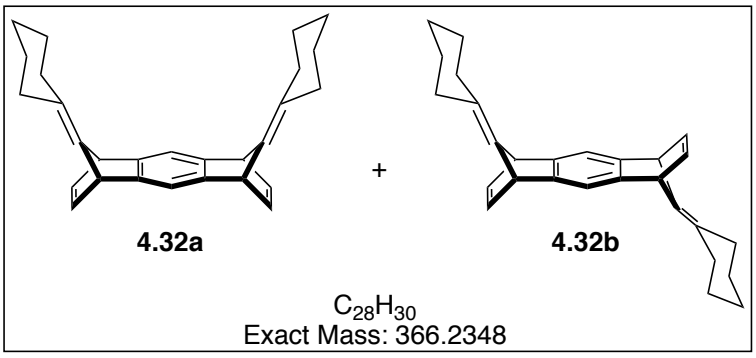

Fulvene **4.31** (0.73 g, 5 mmol) and bisbenzyne precursor **4.39** (1.04 g, 2 mmol) were weighed into a scintillation vial that was then brought into a glove box[4]. Inside the glove box 18-crown-6 [5](2.64 g, 10 mmol), KF (0.58 g, 10 mmol), THF (8 mL) and a stir bar were added. The vial was capped and the reaction was brought out of the glove box and left to stir vigorously at room temperature overnight. The reaction mixture was then diluted with DCM (25 mL) and filtered through a plug of silica gel, which was rinsed with DCM (5 × 10 mL) to ensure all the product is eluted. The organic solution was then concentrated to give a brown solid (4.02 g). Purification via flash chromatography[6,7] (5% DCM : 95% hexanes,

[4] Glove box is used for a dry atmospher because KF extremely hydroscopic.
[5] Best if used recrystallized 18-crown-6 (Organic Syntheses, Coll. Vol. 6, p. 301 (1988); vol. 57, p. 30 (1977); DOI: 10.15227/orgsyn.057.0030).
[6] Column can be easier if you first take up the crude product in hexanes and filter off the solid which is the anti isomer **4.32b**
[7] Sometimes multiple columns are necessary.

then 30% DCM : 70% hexanes) to give a mixture of *syn* and *anti* isomers of **4.39** as a colorless solid (424.46 g, 1.16 mmol, 58%).

4.32a

R_f = 0.09 (5% DCM : 95% hexanes).

^{1}H NMR (500 MHz, Chloroform-*d*) δ 7.12 (s, 2H), 6.86 (t, *J* = 2.0 Hz, 4H), 4.28 (t, *J* = 2.1 Hz, 4H), 2.15 – 2.08 (m, 4H), 1.90 – 1.87 (m, 4H), 1.53 – 1.46 (m, 6H), 1.38 – 1.36 (m, 6H).

^{13}C NMR (126 MHz, Chloroform-*d*) δ 159.6, 147.3, 143.8, 115.3, 108.4, 50.1, 29.6, 27.4, 26.8.

IR (KBr) 3063, 2994, 2930, 2849, 1713, 1555, 1446, 1315, 1291, 1263, 1238, 888, 850, 673 cm^{-1}.

Mp 164–171 °C.

HRMS (EI) *m/z* 366.2362 (366.2347 calcd for $C_{28}H_{30}$, $(M)^+$).

The structure was confirmed by X-Ray crystallography.

4.32b

R_f = 0.09 (5% DCM : 95% hexanes).

^{1}H NMR (500 MHz, Chloroform-*d*) δ 7.12 (s, 2H), 6.90 (t, *J* = 2.1 Hz, 4H), 4.27 (t, *J* = 2.1 Hz, 4H), 2.10 – 2.05 (m, 4H), 1.88 – 1.83 (m, 4H), 1.51 – 1.42 (m, 6H), 1.42 – 1.31 (m, 6H).

^{13}C NMR (126 MHz, Chloroform-*d*) δ 159.5, 147.3, 143.8, 115.2, 108.4, 50.1, 29.6, 27.3, 26.8.

IR (KBr) 3070, 2990, 2927, 2847, 2824, 1713, 1562, 1437, 1315, 1288, 1261, 1243, 888, 848, 678 cm^{-1}.

Mp 362–370 °C.

HRMS (EI) *m/z* 366.2366 (366.2347 calcd for $C_{28}H_{30}$, $(M)^+$).

4.5. References

[1] Terao, Y.; Satoh, T.; Miura, M.; Nomura, M. *Bull. Chem. Soc. Jpn.* **1999**, *72*, 2345–2350.

[2] Holland, J. M.; Jones, D. W. *J. Chem. Soc. C: Organic* **1971**, 608–612.

[3] Kitamura, T.; Yamane, M.; Inoue, K.; Todaka, M.; Fukatsu, N.; Meng, Z. H.; Fujiwara *J. Am. Chem. Soc.* **1999**, *121*, 11674–11679.

[4] Chen, Y. L.; Sun, J. Q.; Wei, X.; Wong, W. Y.; Lee, A. W. M. *J. Org. Chem.* **2004**, *69*, 7190–7197.

[5] Butler, D. N.; Smits, R.; Evans, D. A. C.; Vinidra Weerasuria, K. D.; Warrener, R. N. *Tetrahedron Lett.* **1996**, *37*, 2157–2160.

[6] Lorbach, A.; Reus, C.; Bolte, M.; Lerneer, H. W.; Wagner, M. *Adv. Synth. Catal.* **2010**, *352*, 3443–3449.

[7] Miao, Q.; Chi, X.; Xiao, S.; Zeis, R.; Lefenfeld, M.; Siegrist, T.; Steigerwald, M. L.; Nuckolls, C. *J. Am. Chem. Soc.* **2006**, *128*, 1340–1345.

[8] Irie, T.; Tanida, H. *J. Org. Chem.* **1979**, *44*, 1002–1003.

[9] Satoh, T.; Inoh, J.; Kawamura, Y.; Kawanura, Y.; Miura, M.; Nomura, M *Bull. Chem. Soc. Jpn.* **1998**, *71*, 2239–2246.

[10] Cao, C.; Wang, L.; Cai, Z.; Zhang, L.; Guo, J.; Pang, G.; Shi, Y. *Eur. J. Org. Chem.* **2011**, 1570–1574.

[11] Hellal, M.; Singh, S.; Cuny, G. D. *J. Org. Chem.* **2012**, *77*, 4123–4130.

[12] Inagaki, S.; Fujimoto, H.; Fukui, K *J. Am. Chem. Soc.* **1976**, *98*, 4054-4061.

[13] Ashton, P. R.; Brown, G. R.; Isaacs, N.S; Giuffrida, D.; Kohnke, F. H.; Mathias, J. P.; Slawin, A. M. Z.; Smith, D. R.; Stoddart, J. F.; Williams, D. J. *J. Am. Chem. Soc.* **1992**, *26,* 6330–6353, and references therein.

[14] Kohnke, F. H.; Slawin, A. M. Z.; Stoddart, J. F.; Williams, D. J. *Angew. Chem., Int. Ed.* **1987**, *26,* 892–894.

[15] Cava, M. P.; Napier, D. R. *J. Am. Chem. Soc.* **1957**, *79*, 1701–1709.

[16] Cava, M. P.; Shirley, R. L. *J. Am. Chem. Soc.* **1960**, *82*, 654–656.

[17] Paddon-Row, M. N.; Patney, H. K.; Harish, K. *Synthesis* **1986**, 328–330.

[18] Boger, D. L.; Panek, J. S.; Meier, M. M. *J. Org. Chem.* **1982**, *47*, 895–897.

[19] Boger, D. L. *Chemtracts: Org. Chem.* **1996**, *9*, 149–189.

[20] Alper, H.; Laycock, D. E. *Synthesis* **1980**, 799.

[21] Hart, H.; Lai, C.-Y.; Nwokogu, G. C.; Shamouilian, S. *Tetrahedron* **1987**, *43*, 5203–5224.

[22] Reynaud, C; Fall, Y.; Feuerstein, M.; Doucet, H.; Santelli, M. *Tetrahedron* **2009**, *65*, 7440–7448.

[23] Bhojgude, S. S.; Kaicharia, T.; Bhunia, A.; Biju, A. T. *Org. Lett.* **2012**, *14*, 4098–4101, and references therein.

[24] Himeshima, Y.; Sonoda, T.; Kobayashi, H. *Chem. Lett.* **1983**, 1211.

[25] Bock, H.; Nick, S.; Ruppert, K. Z. *Naturforsch* **1995**, *50*, 595–602.

[26] Duong, H. M.; Bendikov, M.; Steiger, D.; Zhang, Q.; Sonmez, G.; Yamada, J.; Wudl, F. *Org. Lett.* **2003**, *5*, 4433–4436.

[27] Wu, Q. –C.; Li, B.-S.; Shi, C.-Q; Chen, Y.-X. *Hecheng Huaxue*, **2007**, *15*, 111.

[28] Bronner, S. M.; Garg, N. K. *J. Org. Chem.* **2009**, *74*, 8842–8843.

[29] Atkinson, D. J.; Sperry, J.; Brimble, M. A. *Synthesis* **2010**, 911–913.

[30] Tietze, L. F.; Eicher, T.; Diederichsen, U.; Speicher, A. *Reactions and Syntheses in the Organic Chemistry Laboratory*; Wiley-VCH Verlag GmbH & Co. KGaA: Weinheim, Germany, 2007; pp 174.

[31] Breton, G. W. *J. Org. Chem.* **1997**, *62*, 8952–8954.

[32] Douglas, C. J. Evaluation of Ferrocenyloxazoline Palladacyclic Catalysts for the Asymmetric Allylic Imidate Rearrangement and Studies toward an Enantioselective Synthesis of Sarain A. Ph.D. Dissertation, University of California at Irvine, 2005.

[33] Pretsch, E.; Bühlmann, P.; Badertscher, M. *Stucture Determination of Organic Compounds Tables of Spectral Data*; Springer: Verlag Berlin Heidelberg, 2009; 174.

[34] Jansen, G.; Kahler, B.; Klärner, F.-G.; Boese, R.; Bläser, D. *J. Am. Chem. Soc.* **2010**, *132*, 8581–8592.

[35] Schleyer, P. V.; Jiao, H. J. *Pure Appl. Chem.* **1996**, *68*, 209–218.

[36] Bergmann, E. D. *Chem. Rev.* **1968**, *68*, 41–84.

[37] Rodríguez-Lojo, D.; Peña, D.; Pérez, D.; Guitián, E. *Synlett* **2015**, *26*, 1633–1637.

5. ATTEMPTS TO ADVANCE KEY INTERMEDIATE BENZOBISNORBORNENE

Key intermediate benzobisnorbornene **4.32a** was proposed to be a versatile intermediate due to the number of proposed transformations of the norbornene alkene to a useful diene or dienophile. To investigate the actual feasibility of these transformations, benzonorbornene **4.37** was used as a model substrate. Detailed below are three different transformations that were investigated.

5.1. Efforts to Incorporate the Cava Reaction

5.1.1. Precedence for the Cava Reaction and Proposed Incorporation into a Synthetic Route Towards Cyclacene

The Cava reaction is a Diels–Alder reaction that utilizes a dibromoquinodimethane intermediate, such as **4.21** (examples given in Scheme 5.1), as the diene.[1,2] This highly reactive intermediate can be readily generated *in situ* by treating tetrabromo-*o*-xylene **4.20** with sodium iodide. The resulting [4+2] product **5.2** is not isolated; instead, elimination of two equivalents of HBr furnishes a naphthalene derivative, **5.3**. Both Bläser[3] (Scheme 5.1a) and Paddon-Row[4] (Scheme 5.1b) have reported the successful trapping of the olefin of a norbornene ring using the Cava reaction. Encouraged by these reports and attracted to the efficiency with which conjugated systems could be formed, efforts to utilize the Cava reaction in our synthesis of cyclacene were initiated.

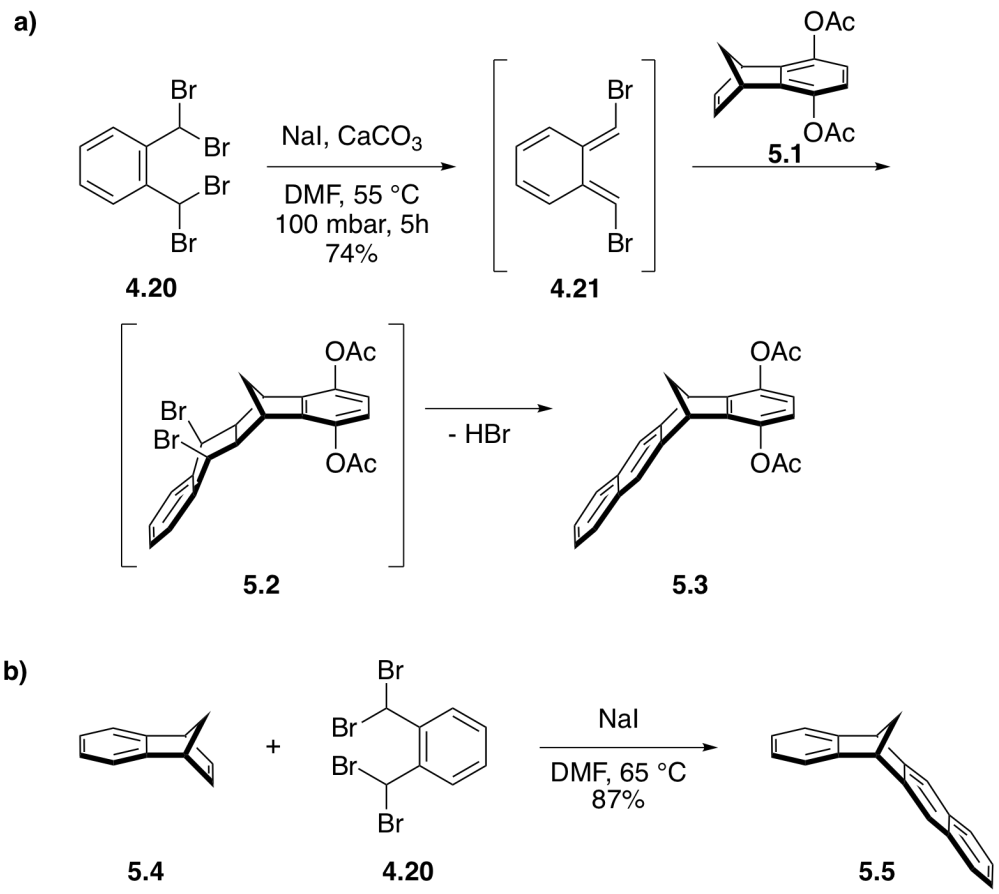

Scheme 5.1 Examples of the Cava reaction for adding a napthalene unit to a norbornene ring by a) Bläser and b) Paddon-Row.

We envisioned that the key intermediate **4.32a** could serve as a bisdienophile in a double Cava reaction with bis(tetrabromo-*o*-xylene) **5.6**. Although **5.6** is not a typical diene source, we planned to investigate the use of **5.6** to generate bis(dibromoquinodimethane) precursor **5.7**. In the next step, we envisioned that macrocycle **5.8** could be closed through a double Cava reaction between **5.7** and bisdienophile **4.32a**. From here, we would implement our end-game strategy: oxidation of the alkene bridges to give **5.9**, followed by cheletropic extrusion of carbon monoxide to afford the target molecule [12]cyclacene **2.1**. This route was particularly appealing as

it had the potential to provide a succinct method to obtain the macrocycle and it utilized relatively mild and easy-to-perform reactions.

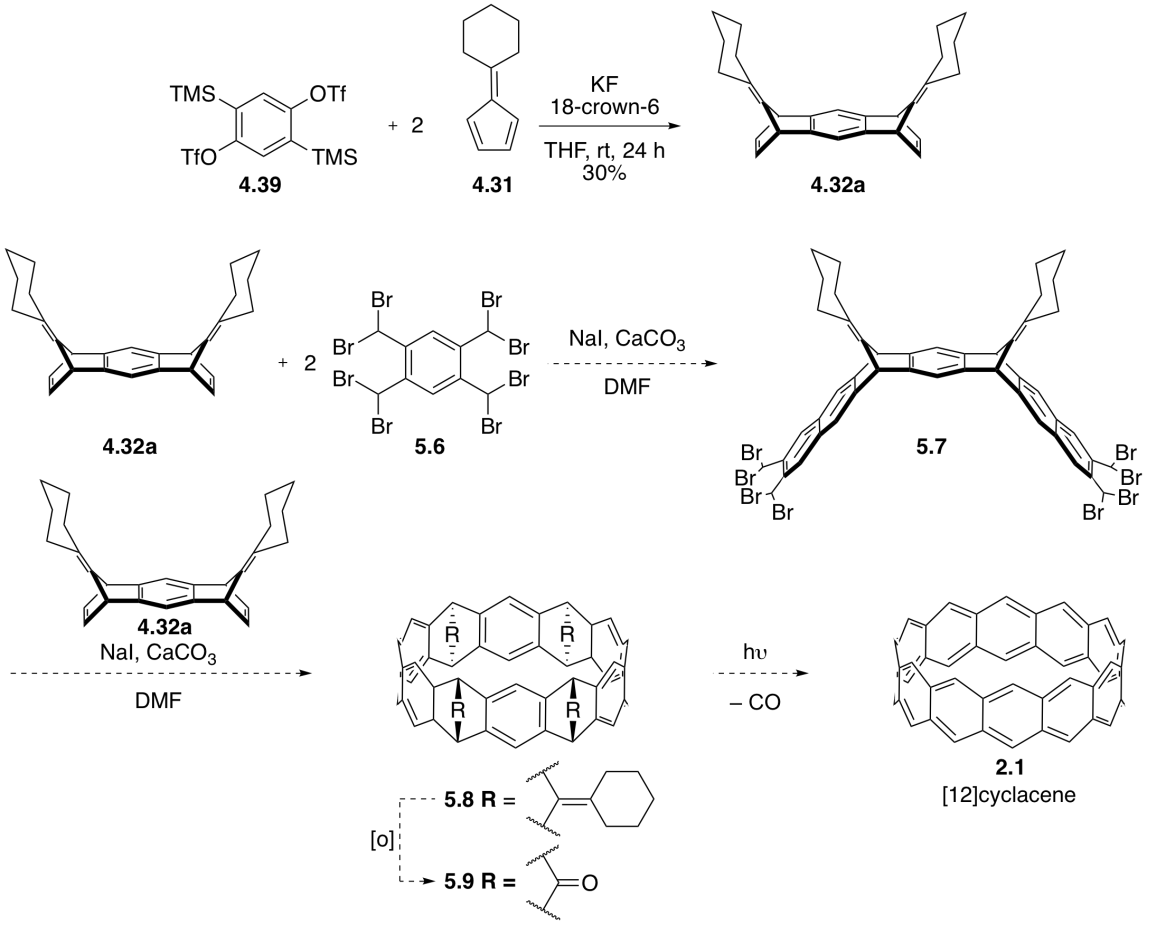

Scheme 5.2 Proposed route to [12]cyclacene that utilizes Cava reactions to efficiently form the macrocycle.

5.1.2. Results and Discussion

Investigations into the viability of using norbornene **4.32a** in the Cava reaction began with a model study. This model study used benzonorbornene **4.37** with the traditional dibromoquinodimethane precursor **4.20** (Scheme 5.3a).[3] By using a combination of a monodienophile and a monodiene, we eliminated the possibility for the formation of a complex mixture of products due to mono and double Diels–Alder

reactions. However, subjection of **4.20** and **4.37** to the conditions reported by Bläser[3] still resulted in a complex mixture by both TLC and ^{1}H NMR. Based on the ^{1}H NMR, it looks like both starting materials were consumed, but it is not clear what products were formed. Column chromatography was used to try to isolate products or by-products, but the resulting fractions were still complex mixtures. Attempts were also made to run the double Diels–Alder reaction by replacing **4.37** with **4.32b** (Scheme 5.3b), which only led to a different complex mixture. Column chromatography was again used to try and identify the products but no clear conclusions could be made.

There was one column fraction from each model system whose ^{1}H NMR spectra matched. The spectrum (Figure 5.1) is simple, containing two AA'BB' signals in the aromatic region (indicative of a symmetric *o*-disubstituted benzene ring) and one singlet at δ = 5.44 ppm in a 1:1:1 ratio. Notably, there are no signals in the alkyl region. This indicates that the norbornene system was not incorporated, as one would expect to see signals from the hydrogen atoms of the cyclohexane ring. Instead, this product is likely due to some sort of decomposition of the common reactant between the two model systems, **4.20**. One possibility is this could be the electrocyclized analogue **5.12a** of **4.21**; however, this could not be confirmed as no ^{1}H NMR spectrum for **5.12a** could be found in the literature. This seems rather unlikely as the reverse, an electrocyclic ring opening, should readily occur to regenerate the diene allowing the desired Diels–Alder reaction to take place.[5] Another possibility is that **4.21** dimerized followed by a double elimination to give **5.12b**, but a ^{1}H NMR has been reported[6] for this compound and the spectra do not match. Regardless of the definite identity of this by-product, its presence suggests that

either the reaction between the diene and dienophile is slower than decomposition of the starting materials or that the resultant [4+2] product is unstable and decomposing.

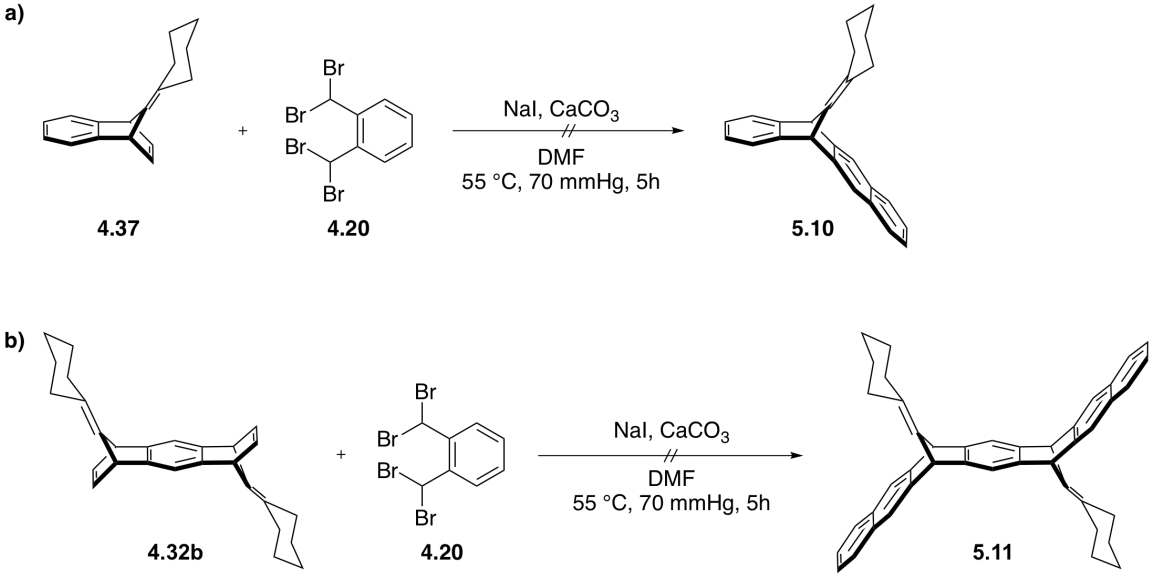

Scheme 5.3 Test of the Cava reaction with our benzonorbornene system in a) a model study b) with the anti-isomer 4.32b.

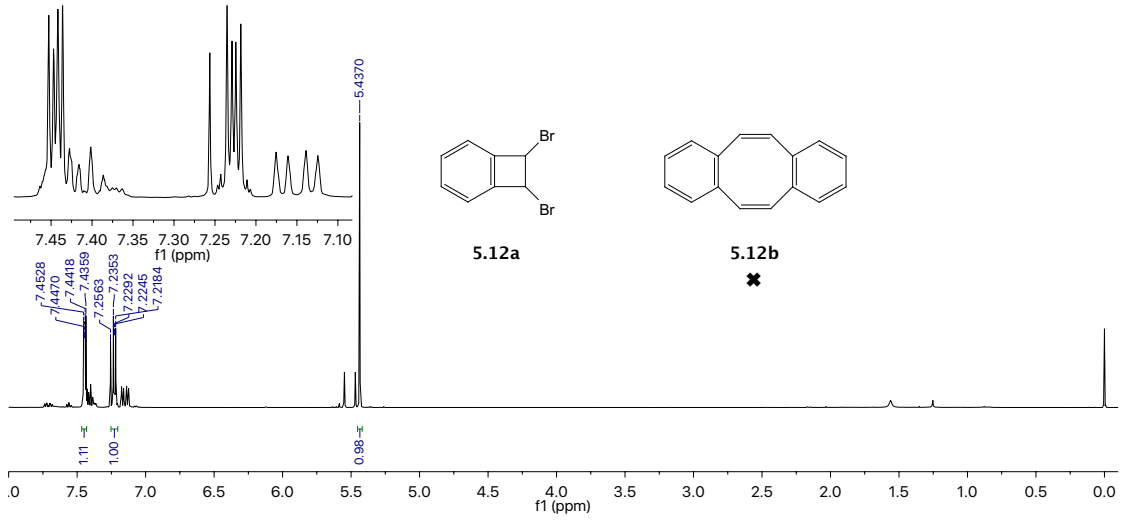

Figure 5.1 ^{1}H NMR of the matching fractions from the model studies.

Analysis of the ^{1}H NMR of the crude reaction mixture revealed that norbornene derivative, **4.37** was consumed under the reaction conditions. A control reaction was

performed using **4.32b** and subjecting it to the reaction conditions (NaI, $CaCO_3$, DMF, 55 °C, 75 mmHg) but in the absence of **4.20**. Only starting material, was recovered, indicating it is stable under the reaction conditions and is only consumed when **4.20** is present. Another concern was that HBr was being released during the generation of the **4.21**, thereby enabling the formation of a norbornyl cation, which is prone to rearrangement.[7,8] A control reaction, treatment of **4.32b** with $HCl{\cdot}Et_2O$, resulted in no decomposition suggesting that norbornene **4.32** is not extremely acid sensitive.

Alternatively, it is possible that the desired Diels–Alder reaction took place but that the intermediate prior to elimination, **5.13**, proceeds through other pathways (Scheme 5.4a). Reports can be found of elimination proceeding to generate, instead of a naphthalene unit, a second quinodimethane intermediate **5.14**.[9] Conceivably, an alternative elimination could occur through the benzonorbornane side to generate an isobenzofulvene **5.15** and naphthalene **5.16** (Scheme 5.4b). Both **5.14** or **5.15** are reactive dienes which could participate in other reactions, which would help to explain why such a complex reaction mixture is formed.

Since we were unable to identify the products of the Cava reaction and worried that the problem was due to undesired and uncontrollable elimination pathways, we decided to pursue alternative methods for elaboration of the key intermediate **4.32a**.

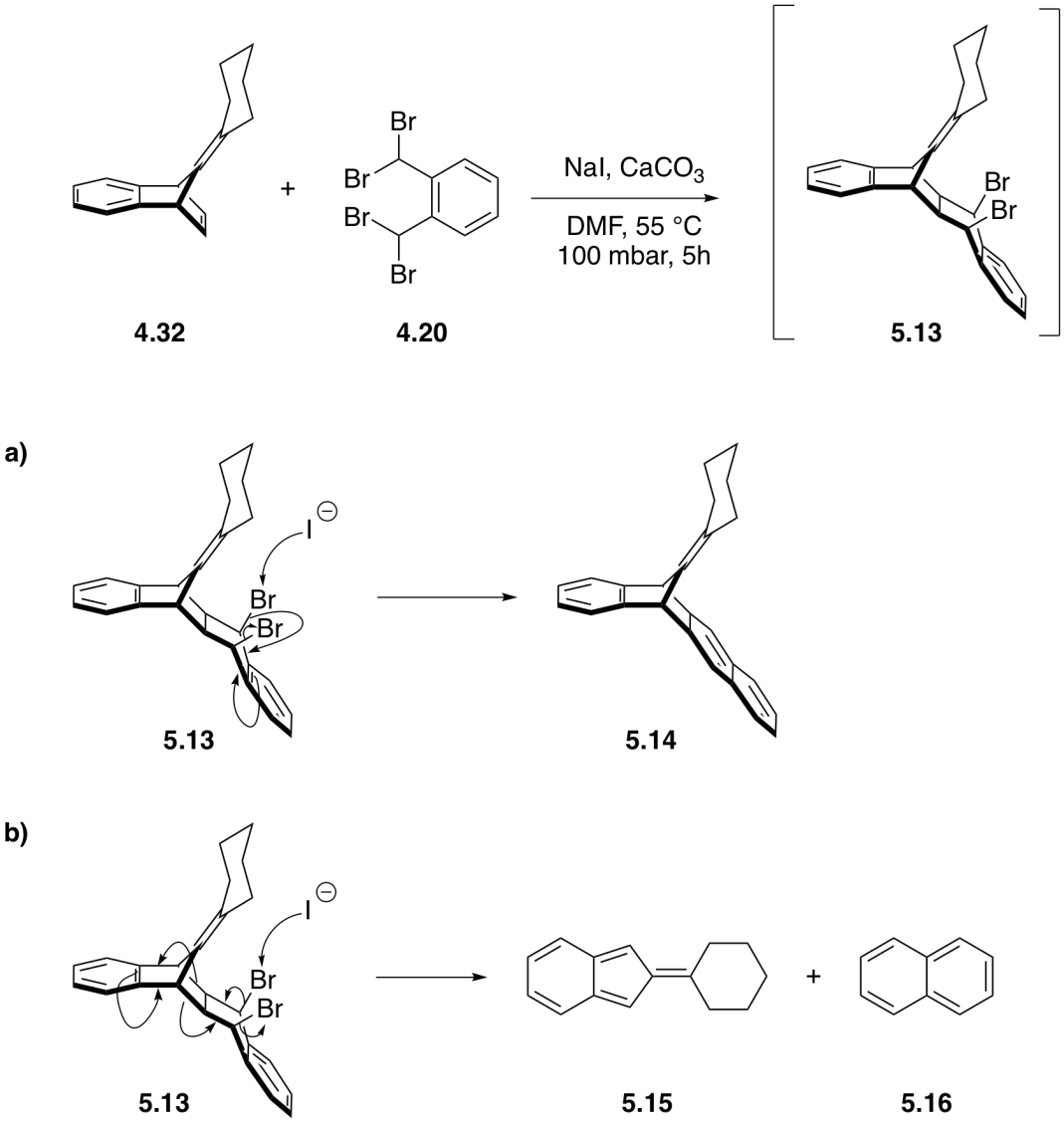

Scheme 5.4 Formation of Diels–Alder intermediate 5.13 and alternative elimination pathways to form a) a new quinodimethane and b) isobenzofulvene.

5.2. Generating an Electron Rich Dienophile for Inverse-Demand Diels–Alder Reactions: Attempts Toward Enamine Formation

5.2.1. Proposed Synthetic Route Utilizing an Inverse-Demand Diels–Alder Reaction

To meet our guideline of constructing the macrocycle by Diels–Alder reactions, we investigated methods to make the norbornene alkenes of **4.32a** better dienophiles. A potential solution was to go through an inverse demand Diels–Alder reaction instead of trying to force a normal [4+2] reaction (Scheme 5.5).[10,11] We proposed that the disubstituted olefins of **4.32a** could selectively undergo hydroboration/oxidation to give *meso* diketone **5.17** as an inconsequential mixture with chiral diastereomers. Condensation with pyrrolidine could then afford electron-rich bisenamine **5.18**. Following the work of Boger, enamines are known to readily participate in Diels–Alder reactions with tetrazines (electron-poor dienes) **5.19**. The resultant intermediate could then undergo a retro-[4+2] reaction to release N_2, followed by aromatization through pyrrolidine elimination to provide a pyridazine **5.20**. This cascade sequence was particularly attractive as the eliminations are spontaneous, thereby meeting another one of our proposed guidelines.

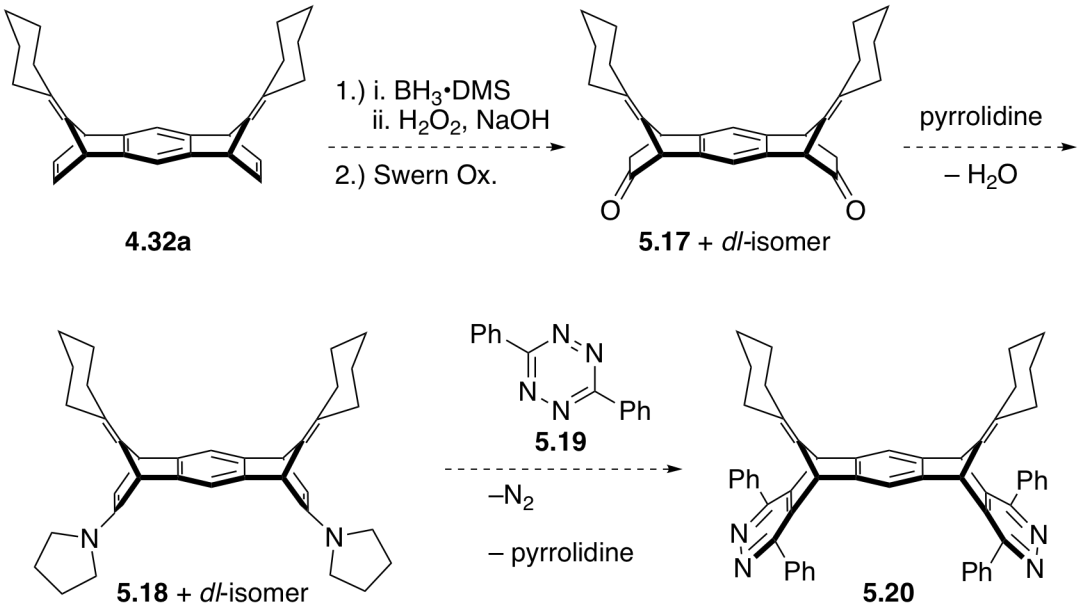

Scheme 5.5 Proposed elaboration of 4.32a to prepare key intermediate, bisdiene 5.20.

Pyridazine **5.20** was identified as an adaptable key intermediate. We envisioned that the pyridazine rings could serve as dienes in hetero-Diels–Alder reactions, followed by spontaneous loss of N_2 through a retro-[4+2] reaction to extend conjugation. We envisioned that several different dienophiles could be trapped by the pyridazine moieties allowing for different sized macrocycles to be formed (Scheme 5.6). Potentially, the scaffold for [8]cyclacene derivative **3.5** could be set though a Diels–Alder reaction of **5.20** with bisdienophile **5.17**. Alternatively, a single [4+2] reaction with benzyne generated from bisbenzyne precursor **4.39** would furnish an AB like monomer (an intermediate with both a diene and dienophile precursor). In the presence of excess fluoride, the second aryne could be generated and two monomer units could come together in a dimerization to give [12]macrocycle **5.21**. Finally, we also postulated that each side of bisdiene **5.20** could trap an aryne generated from **4.39** to give a new bisdienophile precursor **5.22**. Dimerization of **5.22** could be achieved by treatment with a

fluoride source in the presence of diazapyrone **3.8** to give [16]macrocycle **5.23**. Excited by all the potential uses of bispyridazine **5.20**, efforts to prepare it were explored using model benzonorbornene **4.37** (Scheme 5.7).

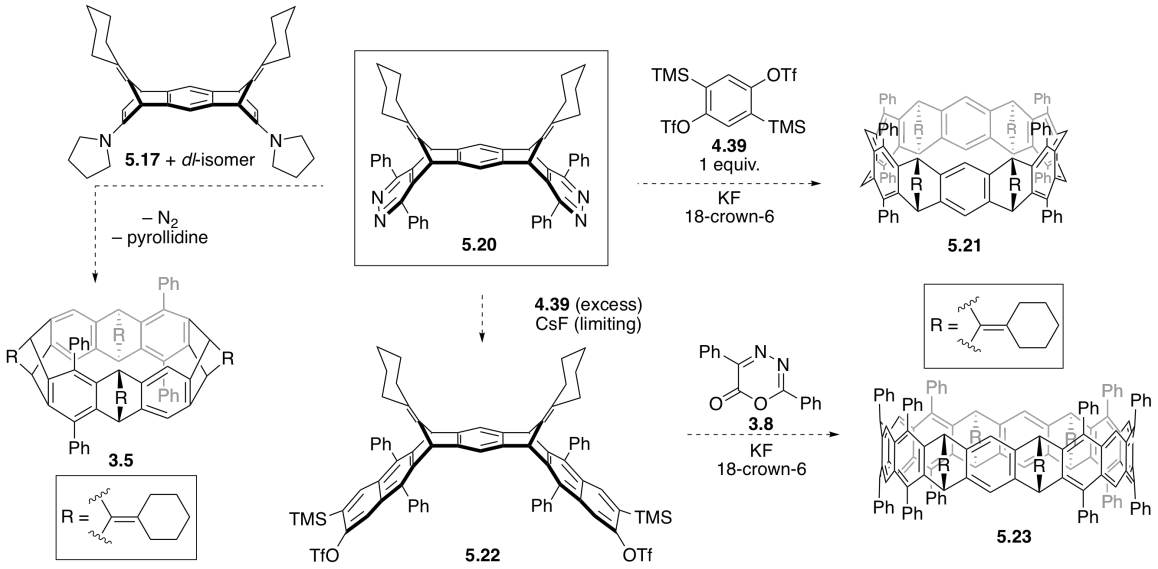

Scheme 5.6 The various macrocycles that could potentially be formed using bisdiene 5.20.

5.2.2. Results and Discussion

We anticipated that the initial hydroboration would regioselectively occur at the less hindered alkene of the norbornene ring, rather than the tetrasubstituted olefin on the bridgehead. Treatment of **4.37** with BH_3·DMS followed by base and hydrogen peroxide resulted in a complex mixture as indicated by ^{1}H NMR (Scheme 5.7a).[12, 13] It appeared that the desired product was probably made but there were several by-products present as well. We hypothesized that the tetrasubstituted olefin was also being oxidized, thereby leading to multiple products. Instead, we decided to try using 9-BBN[13] as the hydroboration reagent for two reasons: first, the bulkiness of the reagent should be more selective for the relatively less hindered alkene and second, it is easier to control the

equivalents of active reagent. Gratifyingly, switching to 9-BBN resulted in a much cleaner conversion to alcohol **5.24** in a high yield of 99% based on recovered starting material (Scheme 5.7b). An inconsequential mixture of exo and endo isomers was formed and efforts were not made to isolate the individual isomers. To test our prior theory that BH_3·DMS reduced the tetrasubstituted olefin, alcohol **5.24** was treated with BH_3·DMS. By ^{1}H NMR, **5.24** was consumed and a complex mixture of products was observed. Since the mixture of isomers was inconsequential, crude **5.24** was brought forward into the next step.

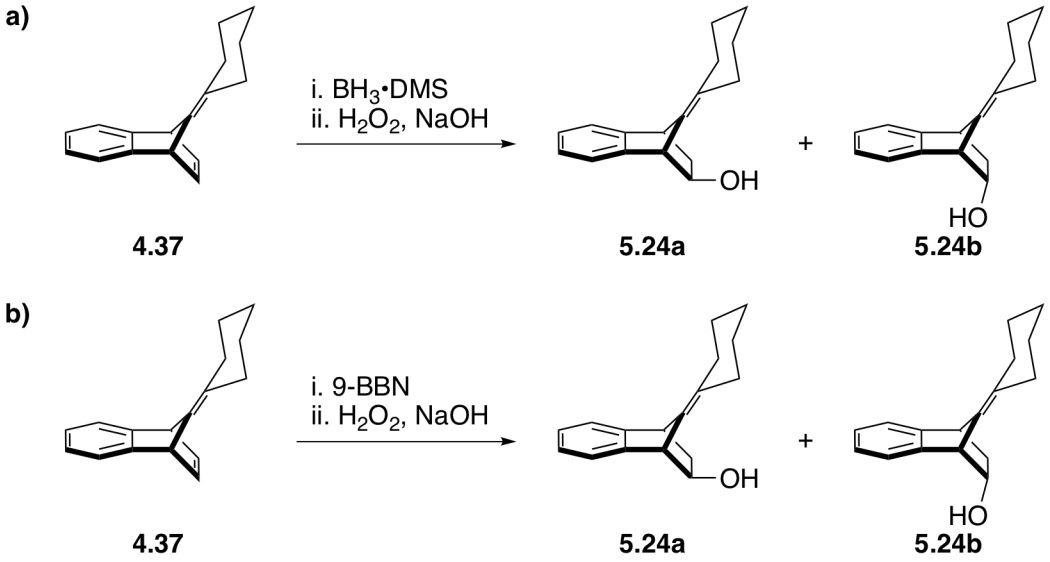

Scheme 5.7 Hydroboration of model benzonorbornene 4.37. Yields are not given as purification was saved until after oxidation to the ketone.

Efforts to oxidize alcohol **5.24** with oxone were unsuccessful.[14] Instead, a Swern oxidation smoothly afforded ketone **5.25** in quantitative yield based on crude material (Scheme 5.8a).[15] Unfortunately, when subjected to a column chromatography, the product appears to have decomposed. Attempts were made do the hydroboration and oxidation to the ketone in one-pot reaction via a Ley oxidation. However, this method

proved to be unsuccessful, resulting in mixtures of unreacted starting material, intermediates, and very little desired product (Scheme 5.8b).[16,13] Condensation of ketone **5.25** with pyrrolidine to give enamine **5.26** was also more challenging than expected (Scheme 5.8c). Surprisingly, the literature reports that related condensations (such as formation of the pyrrolidone enamine of camphor) are challenging to achieve.[17–19] It is postulated that both steric hindrance of the carbonyl as well as the reversibility of the reaction are responsible for the observed low yields and poor conversions for these systems. In favor of more promising and scalable methods, this route was set aside.

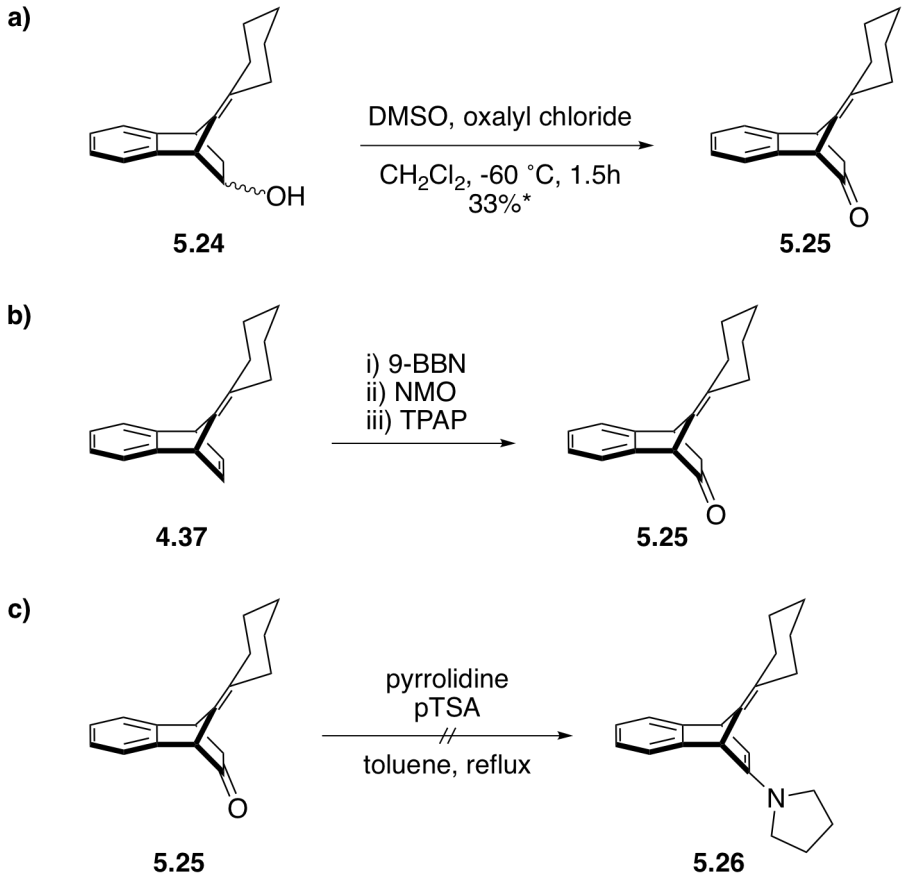

Scheme 5.8 Model study for a) oxidation of alcohol 5.24, b) one-pot hydroboration and over oxidation to ketone 5.25, and c) condensation of ketone 5.25 with pyrrolidine. *Low yield due to decomposition during purification process.

5.3. Work Towards Installation of a Cyclopentadienone

5.3.1. Proposed Synthesis and Utility of Cyclopentadienone

As shown previously (Scheme 3.4), cyclopentadienone is an excellent diene for trapping benzyne in a Diels–Alder reaction. Spontaneous cheletropic loss of CO typically follows this Diels–Alder reaction, removing the need for an elimination step, which is another desirable feature. We envisioned that a cyclopentadienone unit could be readily appended onto key intermediate **4.32a** as shown in Scheme 5.9. Beginning with dihydroxylation, we planned to use AD-Mix to ensure the norbornene alkenes were oxidized before the tetrasubstituted alkenes through steric control.[20,21] We anticipated that the resultant tetrol could be readily oxidized to give tetraketone **5.27**. Effective methods that oxidize 2,3-norbornanediols to diketones, rather than causing oxidative cleavage, have been reported.[22–24] Next, the cyclopentadienones of **5.28** could be formed through double aldol condensation reactions with 1,3-diphenylacetone.[25,26] Once the cyclopentadienone rings are in place, macorcycle formation (**5.29** or **5.30**) with bisbenzyne precursor **4.39** could be investigated.

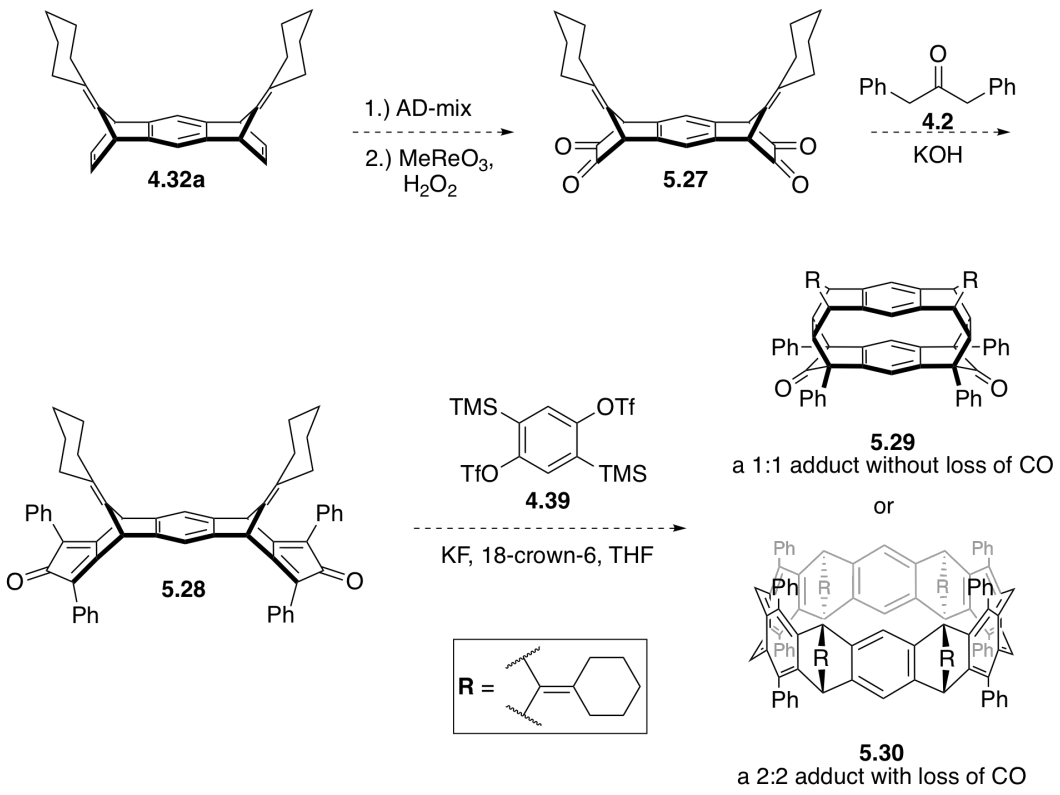

Scheme 5.9 Proposed addition of a cyclopentadienone unit onto 4.32a.

The outcome of the proposed macrocycle forming Diels–Alder reaction would be governed by both the approach of the dienophile and by the relative rates of decarbonylation and second aryne formation. We anticipated, based on steric arguments, that the convex face of **5.28** is more accessible for approach by the benzyne generated from **4.39** (Scheme 5.10). If, however, some of aryne **5.31** was able to approach from the concave face to give **5.32**, two different macrocycles could potentially be accessed. If decarbonylation of **5.32** is slower than second aryne formation, a second intramolecular [4+2] reaction could occur to give [6]macrocycle **5.29**. If instead decarbonylation is faster, naphthalene derivative **5.34** would be generated and an intramolecular Diels–Alder reaction would no longer be possible. Instead, a dimerization could occur to give

[12]macrocycle **5.30**. Naphthalene derivative **5.34** could also be accessed if the initial [4+2] reaction occurs on the convex face of **5.28**, to give **5.33**, followed by loss of carbon monoxide.

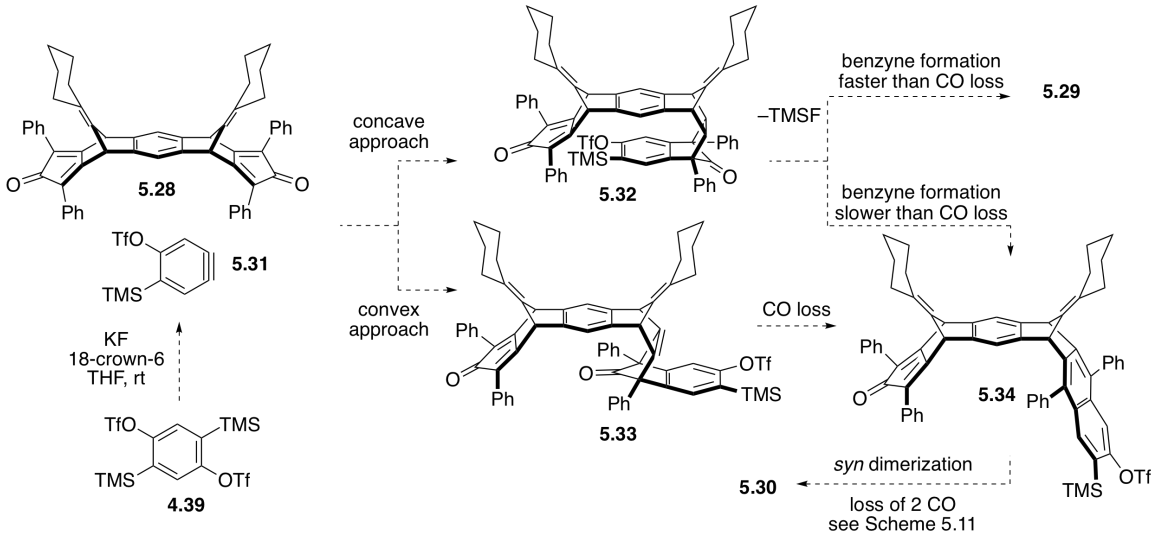

Scheme 5.10 Various pathways for proposed Diels–Alder reaction between aryne 5.31 and bisdiene 5.28.

We also recognized that the Diels–Alder reaction for the dimerization of **5.34** has both productive and nonproductive pathways. The approach of the dienophile to the convex or concave face is inconsequential as extrusion of CO will ablate the stereocenters of the newly formed ring. Of greater concern is the relative orientation of the pre-existing [2.2.1]-bicycloheptane units of the monomers. In this dimerization, likely both *syn* and *anti* stereoisomers would be formed. However, only the *syn* isomer, **5.35a**, would bring the diene and dienophile in close enough proximity to allow for the second [4+2] reaction to occur to close the macrocycle (Scheme 5.11). Conversely, the *anti* isomer **5.35b** would likely just oligomerize. Confident that a macrocycle would be attainable with the chosen diene and dienophile, work was done to establish a method for preparing the cyclopentadienone units.

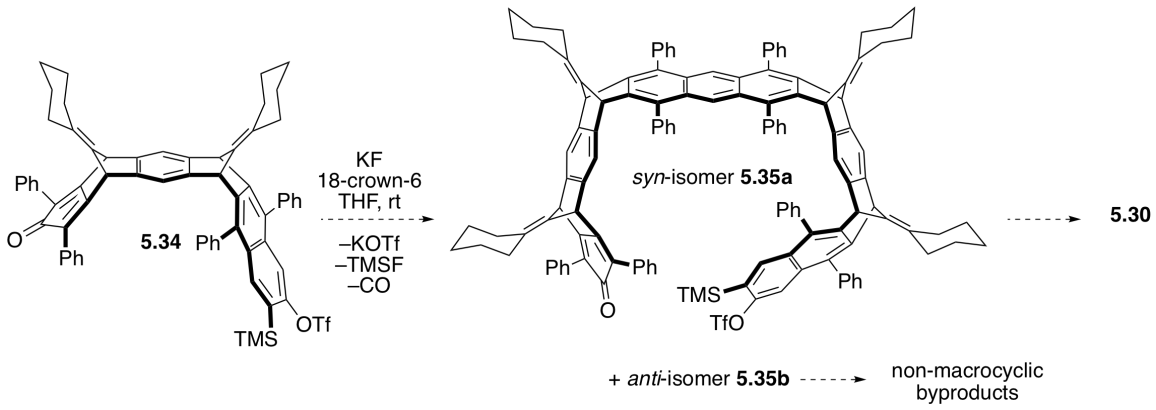

Scheme 5.11 Dimerization of 5.34 to give macrocycle precursor and non-macrocyclic by-products.

5.3.2. Results and Discussion

A model study for the synthesis of the cyclopentadienone unit began with attempts to dihydroxylate the norbornene alkene of **4.37** using AD-mix β.[27] Following literature procedures[28] (Table 5.1, entry 1), very little conversion of **4.37** to diol **5.36** was observed. Since we were not concerned about the diastereoselectivity of the reaction, we decided to try increasing the reaction temperature. Increasing the temperature from 0 °C to room temperature (entry 2) increased the conversion but it was still unsatisfactory. Sharpless reports that often the slow step in the dihydroxylation of nonterminal alkenes is hydrolysis of the intermediate osmate ester and recommends the use of an organic sulfonamide to aid this step.[29] Introduction of $CH_3SO_2NH_2$ to the reaction at 0 °C (entry 3) drastically improved the conversion. Running the same reaction at room temperature (entry 4) allowed for the same conversion in about one-third the time. Increasing the temperature further to 40 °C only moderately improved the conversion. While we were able to obtain desired diol **5.36**, the reaction was sluggish and the observed conversion was never greater than 25%. Originally, we had chosen to use the AD-mix as the source

of osmium to ensure the tetrasubstituted olefin would not get dihydroxylated as well. We were having a difficult time dihydroxylating the disubstituted olefin, indicating perhaps we were being overly cautious. We were also worried that the ligands included in the AD-mix were making the catalyst too bulky, which could be partially responsible for the slow reaction rate. We decided to move forward with trying to achieve the desired transformation using OsO_4 in water with *N*-methylmorpholine *N*-oxide (NMO) as the oxidant.

Table 5.1 Comparison of reaction conditions for the dihydroxylation of 4.37 using AD-mix β.

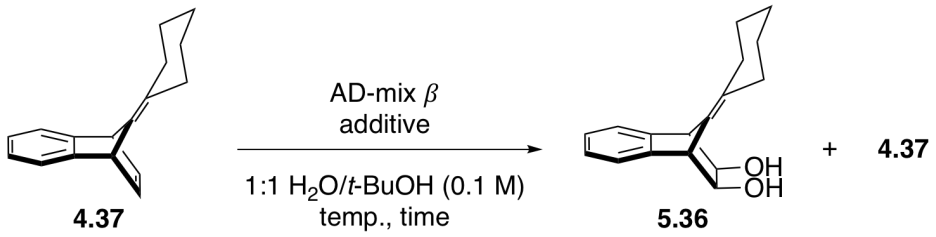

Entry	Additive	Temp (°C)	Time (h)	Diol **5.36** : Alkene **4.37**[a]
1	None	0	24	1 : 67
2	None	25	41	1 : 24
3	$CH_3SO_2NH_2$	0	136	1 : 4
4	$CH_3SO_2NH_2$	25	48	1 : 4
5	$CH_3SO_2NH_2$	40	90	1 : 3

[a] Ratios determined from ^{1}H NMR of crude reaction mixtures

First, we were excited to see moderate conversion when switching to using OsO_4 and NMO with no additive (Table 5.2, entry 1).[30] In setting up the reaction it was noted that the starting alkene came out of solution upon addition of water, which was remedied

by heating the reaction at 40 °C to get everything to go into solution. Worried about solubility with the acetone/H_2O system, we decided to return to the old solvent system (*t*BuOH/H_2O). When this was employed, no reaction occurred even when additive(s) were present (entries 2–5). These reactions were also cloudy, indicating that perhaps the alkene was not going into solution. In reviewing observations for reactions using AD-mix it was found that the reaction mixture became cloudy upon addition of the alkene, indicating solubility problems. At the time the AD-mix trials were being done, the cloudy appearance was not a concern as the reference for the reaction conditions indicated that the reaction should turn cloudy as inorganic salts precipitate out.[27] We decided to return to the acetone/H_2O solvent system at 40 °C since everything went into solution and the conversions were clean even at the elevated temperature.

Unexplainably, using conditions similar to those of entry 1 gave significantly lower conversions (entry 6). The only hypothesis I have is that the OsO_4 may have degraded over time between entries 1 and 6. In comparison to entry 6, adding pyridine[31] to the reaction greatly increased the conversion (entry 7), whereas addition of the sulfonamide only led to a small improvement (entry 8). Running the reaction with both pyridine and sulfonamide (entry 9) only improved the conversion slightly over having pyridine alone. Pyridine serves as a ligand to the OsO_4 (instead of the chiral ligands included in AD-mix) and accelerates the formation of the osmate ester; in contrast, the sulfonamide helps with hydrolysis of the complex. These results suggest that with our system, the slow step is the binding of the OsO_4 to the olefin, not hydrolysis of the osmate ester.

Table 5.2 Comparison of reaction conditions for the dihydroxylation of 4.37 using OsO_4 and NMO.

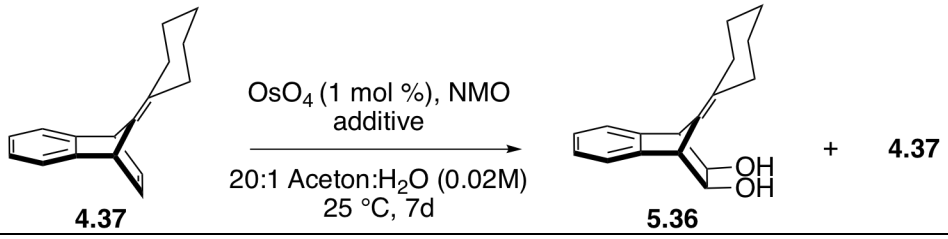

4.37 **5.36**

Entry	Solvent	Concentration (M)	Additive	Temp (°C)	Time (h)	Diol **5.36** : Alkene **4.37**
1	Acetone : H_2O 4:1	0.3	none	40	24	1 : 7
2	*t*BuOH : H_2O 1:1	0.1	none	25	24	0 : 1
3	*t*BuOH : H_2O 1:1	0.1	pyridine	25	24	0 : 1
4	*t*BuOH : H_2O 1:1	0.1	$CH_3SO_2NH_2$	25	24	0 : 1
5	*t*BuOH : H_2O 1:1	0.1	pyridine and $CH_3SO_2NH_2$	25	24	0 : 1
6	Acetone : H_2O 4:1	0.2	none	40	18	1 : 50
7	Acetone : H_2O 4:1	0.2	pyridine	40	18	1 : 11
8	Acetone : H_2O 4:1	0.2	$CH_3SO_2NH_2$	40	18	1 : 44
9	Acetone : H_2O 4:1	0.2	pyridine and $CH_3SO_2NH_2$	40	18	1 : 10
10	Acetone : H_2O 9.3:1	0.02	none	25	24	1 : 9
11	Acetone : H_2O 4:1	0.2	pyridine	40	6 d	1 : 0.7
12	Acetone : H_2O 20:1	0.02	pyridine	25	7 d	1 : 0.57

[a] Ratios determined from ^1H NMR of crude reaction mixtures

At this point we had optimized the additive, deciding just pyridine needed to be added to accelerate the reaction. Returning to the drastic dependence on solvent choice and solubility issues, we re-examined the effects of solvent and concentration. Running

the reaction ten times more dilute with the ratio of acetone to water at 9:1, a decent conversion was observed at room temperature even without the addition of pyridine (entry 10).[32] By allowing the reaction to run for a prolonged period of time, 6 d, we finally were able to achieve a greater than 50% conversion of starting material to product (entry 11). Running the reaction under optimized conditions (entry 12), a 56% isolated yield of diol **5.36** was obtained. We were satisfied with these conditions as virtually no by-product is formed, meaning the remaining starting material can be readily recovered and resubjected to the reaction conditions, thereby reducing the overall loss of material.

With diol **5.36** in hand, we began investigating oxidation conditions to give diketone **5.37**. First, a Corey-Kim oxidation was attempted using *N*-chlorosuccinimide and dimethyl sulfide followed by treatment with TEA.[33] As observed by ^{1}H NMR, no product was formed, starting material remained, and many unidentifiable by-products were detected. Next, oxidation using methyltrioxorhenium (MTO) with H_2O_2 was attempted.[34] This also did not yield any appreciable amount of the desired diketone. Finally, a Swern oxidation using trifluoroacetic anhydride (TFAA) rather than oxalyl chloride provided the desired diketone **5.37** as a bright orange solid with full consumption of the starting diol **5.36** (Scheme 5.12).[35] However, during purification it was noticed that the product was decomposing over time as shown by TLC and ^{1}H NMR resulting in only a 75% isolated yield.

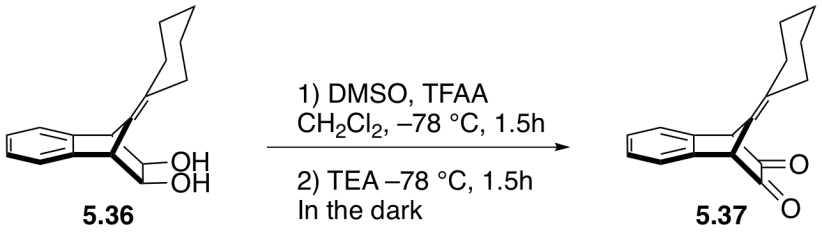

Scheme 5.12 Swern oxidation of diol 5.36 to diketone 5.37.

We did not believe that diketone should be conjugated enough to be susceptible to air oxidation to form an endoperoxide.[36] By 2D TLC, the compound appeared to be stable to the chromatography conditions used to isolate **5.37**. We hypothesized that the decomposition pathway must involve light. Indeed, repeating the Swern oxidation of **5.36** in the dark provided **5.37** without any indication of the decomposition product. A search in the literature reveals that the presence of the alkene on the bridgehead of the norbornane ring allows for a photochemical suprafacial 1,3-sigmatropic rearrangement to give a fused tricyclic oxo-enol.[37] This was observed when Warrener and co-workers were trying to generate isobenzofulvene **5.39** through a light induced decarboxylation of **5.38** and instead isolated oxo-enol **5.40** (Scheme 5.13a). To confirm this same rearrangement was the observed decomposition pathway, a sample of diketone **5.37** was dissolved in $CDCl_3$ and exposed to light by placing it in a dewar with a light bulb. After three hours, almost all of the starting material (orange) had decomposed to oxo-enol **5.41** (yellow) as indicated by ^{1}H NMR and IR (Scheme 5.13b).

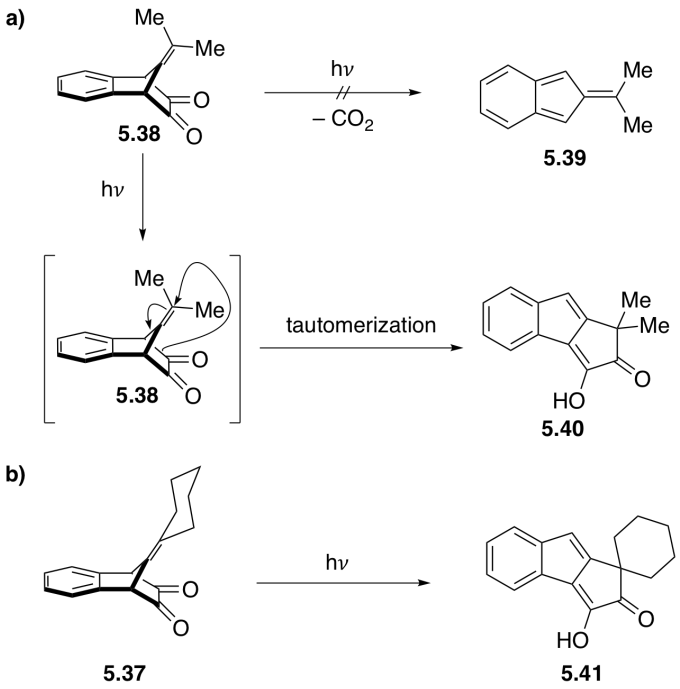

Scheme 5.13 The observed rearrangement of a) diketone 5.38 to give 5.40 instead of the desired isobenzofulvene 5.39 and b) of diketone 5.37 to oxo-enol 5.41.

Upon isolating diketone **5.37**, efforts to form the cyclopentadienone **5.42** were initiated with the hopes that **5.42** would be a more stable intermediate (Scheme 5.14). During the first attempts at the double aldol condensation reaction, we were not yet aware that **5.37** was light sensitive so care was not taken to run the reaction in the dark. Even so, only trace amounts of the rearranged product were observed. Instead, upon treating a solution of diketone **5.37** and diphenylacetone **4.2** with KOH at 80 °C yielded no trace of the desired product **5.42**.[38] Instead, by TLC and ^{1}H NMR, it appears that **5.37** decomposed and **4.2** did not react. Worried that diketone may be heat senstitive, **5.37** was dissolved in d_4-MeOH and heated at 80 °C for 0.5 h in the dark. The ^{1}H NMR before and after heating were similar indicating that **5.37** is heat stable. Running the reaction at 100 °C in the dark and using triton B as the base instead yielded similar results to the KOH

trial.[25] What was most troubling about the ^{1}H NMR of the crude reaction mixtures for these reactions was the lack of new peaks to help shed light on what was happening to the diketone **5.37**. In particular, there was no indication of the presence of the alkyl protons from the cyclohexane ring.

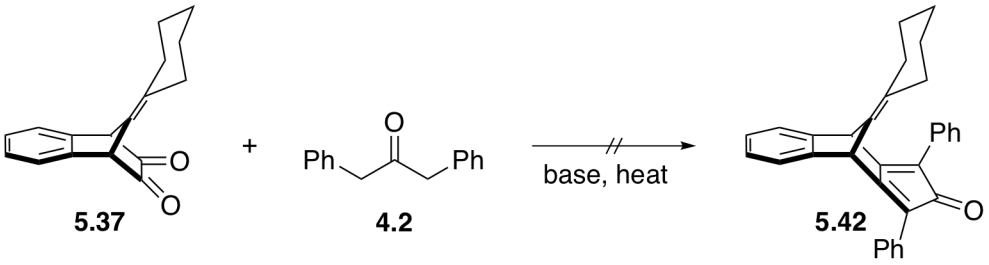

Scheme 5.14 Attepmts at formation of cyclopentadienone 5.42 from 5.38 and 4.2.

In an attempt to try to understand what was happening, the reaction was run in d_6-DMSO at room temperature (a mild temperature) using KOH as the base and was monitored by ^{1}H NMR. When **5.37** and **4.2** were mixed together followed by addition of base, new singlets in the region of the bridgehead protons and the α-methylene protons of **4.2** began to appear after one hour, indicating at least one aldol reaction may have occurred. ^{1}H NMR spectra at later time points (5h and 23h) did not indicate any significant progression of the reaction. Interestingly, when **4.2** was first mixed with base then added to **5.37**, the same new signals from the prior reaction were observed again and at much higher intensity within 15 minutes. After 3 hours, these new signals had decreased in intensity as new singlets grew in nearby, indicating that either a dehydration or a second aldol reaction had occurred. Heating the reaction at 75 °C for 10 minutes to try to facilitate dehydration did not lead to any change in the ^{1}H NMR spectrum. While

this study was promising, it did not provide firm evidence that cyclopentadienone was formed.

5.3.3. Future Work on Generating the Cyclopentadienone Unit

Even though the dihydroxylation of norbornene is slow and the norbornane diketone is unstable, there is still potential for the cyclopentadienone unit to be formed. Future work on this route would be to further investigate the double aldol condensation reaction. Results for the attempts at the aldol reaction when diphenylacetone **4.2** was first treated with base were promising. Additionally, the dione appears to be stable in the presence of base at room temperature. It would be interesting to first form the enolate of **4.2**, perhaps through treatment with LDA, then add it to **5.37**. At this point, there is no reason to believe that it is not possible to generate cyclopentadienone **5.42**.

Although I am optimistic that the cyclopentadienone can be accessed, this route has been set aside. During efforts to perform the double aldol condensation reaction, preliminary studies on a new route were performed. As will be covered in the next chapter, these preliminary studies were extremely promising and rapidly gave encouraging results.

5.4. Experimentals

All reactions were carried out using flame-dried glassware under nitrogen atmosphere unless aqueous solutions were employed as reagents. Tetrahydrofuran (THF) was dried by distillation from benzophenone/sodium under nitrogen. Dichloromethane

(DCM) and triethylamine (TEA) were dried by distillation from CaH_2 under nitrogen. All other chemicals were used as received unless otherwise noted.

Analytical thin layer chromatography (TLC) was carried out using 0.25 mm silica plates from Silicycle. Eluted plates were visualized first with UV light then $KMnO_4$ stain unless stated otherwise. Flash chromatography was performed using 230–400 mesh (particle size 0.04–0.063 mm) silica gel purchased from Silicycle. ^{1}H NMR (500 MHz), ^{13}C NMR (126 MHz), ^{19}F NMR (471 MHz) spectra were obtained on Varian FT NMR or Bruker FT NMR instruments. NMR spectra were reported as δ values in ppm relative to TMS for ^{1}H (0.00 ppm), and chloroform for ^{13}C (77.16 ppm). ^{1}H NMR coupling constants are reported in Hz; multiplicity is indicated as follows; s (singlet); d (doublet); t (triplet); q (quartet); m (multiplet); dd (doublet of doublets); ddd (doublet of doublet of doublets); dt (doublet of triplets); app (apparent); br (broad).

Infrared (IR) spectra were obtained as films from DCM or $CDCl_3$ on sodium chloride plates or as KBr pellets on a Thermo Scientific FT-IR. High-resolution mass spectra (HRMS) in electrospray (ESI) experiments were performed on a Bruker BioTOF II. HRMS using GC-MS (QTOF) was performed on an Agilent 7200-QTOF GC/MS, GC column RTX-5MS 30 m length, 0.255 mm ID, 0.25 μm. Method: inlet temperature 250 °C, source temperature 280 °C. the initial column temperature was 120 °C and was held for 4 minutes after injection. Column temperature was ramped to 325 °C over 10 minutes and then held for 31 minutes. Alternatively, the column was by-passed by using a solid injection probe. Method: Initial temperature of 80 °C was ramped at a rate of 45 °C/min up to 320 °C and held at 320 °C for 3 minutes.

Alcohols 5.24

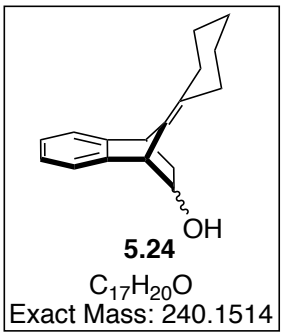

Benzonorbornene **4.37** (167.3 mg, 0.75 mmol) was dissolved in THF (2 mL). To this, 9-BBN (0.5M in THF, 1.88 mL, 0.94 mmol) was added drop wise (~1 drop/s) and allowed to stir at room temperature for 24 h. Then EtOH (0.45 mL, 7.7 mmol), NaOH (20%, 0.16 mL, 1.1 mmol), and H_2O_2 (30%, 0.3 mL, 3.5 mmol) were added. The reaction was then heated at 50 °C for 1 hour. After cooling back to room temperature, the crude reaction mixture was partitioned between DCM (10 mL) and H_2O (20 mL). The product was extracted from the aqueous phase using DCM (3 × 10 mL). The combined organic extracts were then washed with brine (1 × 10 mL), dried (Na_2SO_4) and concentrated to give a colorless solid (197.2 mg, >100%). The crude product was used without further purification. Characterization data reported below is for the mixture of isomers.

R_f = 0.85 (5% EtOAc : 95% Hexanes).

^{1}H NMR (500 MHz, Chloroform-*d*) δ 7.22 – 7.17 (m, 1H), 7.14 – 7.10 (m, 1H), 7.08 – 7.02 (m, 2H), 3.92 (app t, *J* = 7.3 Hz, 1H), 3.83 – 3.77 (m, 2H), 3.76 (s, 1H), 2.31 – 2.23 (m, 2H), 2.12 – 2.06 (m, 2H), 1.63 – 1.56 (m, 3H), 1.54 (dd, *J* = 4.2, 2.1 Hz, 1H), 1.51 (dd, *J* = 4.3, 2.1 Hz, 1H), 1.49 – 1.45 (m, 3H).

^{13}C NMR (126 MHz, Chloroform-*d*) δ 148.8, 143.7, 143.3, 126.3, 125.7, 125.1, 121.8, 120.1, 72.7, 71.9, 52.6, 42.8, 41.6, 36.5, 31.2, 31.2, 28.6, 28.3, 26.8, 20.2.

IR (film) 3353, 3927, 2852, 1462, 1447, 1007, 908, 733 cm^{-1}.

MP 134–136 °C.

Ketone 5.25

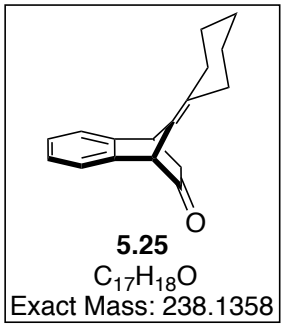

DMSO (0.22 mL, 3.1 mmol) was diluted with DCM (4.7 mL) and cooled in a –78 °C bath. Oxalyl chloride (2M in DCM, 0.78 mL, 1.6 mmol) was added drop wise and the resulting mixture was allowed to stir for 10 min. Alcohol **5.24** (300.4 mg, 1.3 mmol) in DCM (12.5 mL) was then added via syringe pump at a rate of 1 mL/min. After the addition was complete, the reaction was allowed to stir for 1 h, then triethylamine (3.5 mL, 25 mmol) was added dropwise. The reaction was then allowed to warm to room temperature overnight. The reaction mixture was then poured into $NaHCO_3$ (25 mL) and diluted with H_2O (30 mL). The product was extracted from the aqueous solution using DCM (3 × 20 mL). The collected organic extracts were then washed with H_2O (2 × 30 mL), and brine (1 × 40 mL), dried ($MgSO_4$), and concentrated to give a brown oil mixed with a tan solid (299.8 mg, >100%). The crude mixture was

purified by flash chromatography (5% EtOAc : 95% Hexanes) to give a colorless solid (100 mg, 0.42 mmol, 33%).

R_f = 0.332 (5% EtOAc : 95% Hexanes).

^{1}H NMR (500 MHz, Chloroform-*d*) δ 7.26 (app t, *J* = 6.6 Hz, 2H), 7.14 (app td, *J* = 7.6, 1.2 Hz,1H), 7.10 (app td, *J* = 7.5, 0.9 Hz,1H), 4.19 (d, *J* = 4.1 Hz, 1H), 4.14 (s, 1H), 2.43 (dd, *J* = 16.7, 4.1 Hz, 1H), 2.29 – 2.22 (m, 1H), 2.19 – 2.12 (m, 2H), 2.10 (d, *J* = 16.8 Hz, 1H), 2.07 – 2.00 (m, 1H), 1.60 – 1.43 (m, 6H).

^{13}C NMR (126 MHz, Chloroform-*d*) δ 209.4, 148.4, 142.9, 139.7, 127.2, 126.6, 126.0, 122.8, 121.0, 60.0, 43.7, 43.6, 30.9, 30.6, 27.8, 27.8, 26.6.

IR (film)3045, 2927, 2852, 1745, 1460, 1447, 1261, 1074, 911, 761, 733 cm^{-1}.

Diol 5.36

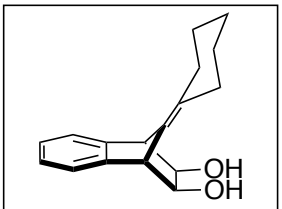

5.36

$C_{17}H_{20}O_2$

Exact Mass: 256.1463

In a round bottom flask, benzonorbornene **4.37** (222 mg, 1 mmol) was dissolved in acetone (47.6 mL). While stirring, water (2.4 mL), NMO (175 mg, 1.5 mmol), pyridine (80 μL, 1 mmol) and OsO_4 (74 μL of a 0.135 M sol'n in water, 1%) were added to the solution in order. The reaction mixture was allowed to stir at room temperature for 1 week. The reaction was quenched by adding Na_2SO_3 (1.5 g) and water (60 mL) and stirring for 1 h. The product was then extracted from the aqueous reaction

mixture using EtOAc (3 × 30 mL). The combined organic fractions were washed with brine (1 × 30 mL), dried ($MgSO_4$), and concentrated to give a tan solid (239 mg). Purification by flash chromatography (15% EtOAc : 85% hexanes) provided pure diol **5.36** (144 mg, 0.56 mmol, 56%) as a colorless solid.

$\mathbf{R_f}$ = 0.15 (15% EtOAc : 85% hexanes).

^{1}H NMR (500 MHz, Chloroform-*d*) δ 7.18 (AA'BB', *J* = 7.7, 0.7, 7.4, 1.1 Hz, 2H), 7.09 (AA'BB', *J* = 7.6, 0.6, 7.4, 1.1 Hz, 2H), 3.79 (br s, 2H), 3.72 (s, 2H), 2.84 (br s, 2H), 2.33 – 2.29 (m, 2H), 2.09 – 2.04 (m, 2H), 1.62 – 1.58 (m, 3H), 1.47 – 1.45 (m, 3H).

^{13}C NMR (126 MHz, Chloroform-*d*) δ 144.2, 141.1, 129.0, 126.6, 121.7, 71.0, 51.1, 31.4, 28.6, 26.8.

IR (film) 3341, 2995, 2925, 2851, 1443, 1161, 1054, 987, 743 cm^{-1}.

Mp 149–151 °C.

HRMS (QTOF) *m/z* 256.1448 (256.1458 calcd for formula, $(C_{17}H_{20}O_2)^+$).

Diketone 5.37

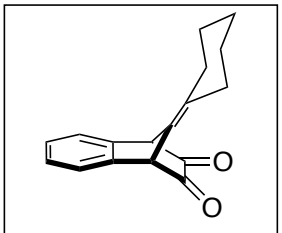

5.37
$C_{17}H_{16}O_2$
Exact Mass: 252.1150

In a round bottom flask, DMSO (1.68 mL, 23.7 mmol) in DCM (19.2 mL) was cooled to –78 °C. While stirring, trifluoroacetic anhydride (1.62 mL, 11.7 mmol) was added dropwise and the resulting mixture was allowed to stir for 25 minutes.

A solution of diol **5.36** (76.8 mg, 0.3 mmol) in DCM (15.3 mL) and DMSO (1.68 mL, 23.7 mmol) was added slowly (0.25 mL/min via syringe pump). The reaction was allowed to stir at –78 °C for 1.5 h. The round bottom flask was then shielded from light. Triethylamine (0.64 mL, 4.6 mmol) was added drop wise and the reaction was allowed to stir for 1.5 h at –78 °C. While keeping the reaction mixture in the dark as much as possible, the flask was removed from the cold bath and allowed to warm to room temperature. The reaction mixture was diluted with DCM (10 mL) and washed with water (3 × 50 mL), and brine (1 × 50 mL), dried ($MgSO_4$), and concentrated to give a dark orange oil (387.9 mg). Purification by recrystallization (5% EtOAc : 95% Hexanes) gave pure diketone **5.37** (28.0 mg, 0.11 mmol, 37%) as a bright orange solid. Additional pure product (14.1 mg, 0.06 mmol, 19%) could be obtained by filtering the filtrate through a 1 cm pad of silica gel in a pipet, collecting only the orange fractions, concentrating the solution, then subjecting the resulting solid to high vacuum.

R_f = 0.30 (20% EtOAc : 80% Hexanes).

^{1}H NMR (500 MHz, Chloroform-*d*) δ 7.35 (AA'BB', *J* = 7.5, 0.6, 7.5, 1.1 Hz, 2H), 7.28 (AA'BB', *J* = 6.7, 0.6, 7.4, 1.3 Hz, 2H), 4.47 (s, 2H), 2.30 – 2.19 (m, 4H), 1.67 – 1.48 (m, 6H).

^{13}C NMR (126 MHz, Chloroform-*d*) δ 192.3, 140.6, 139.9, 132.4, 129.2, 123.6, 58.5, 31.3, 27.9, 26.4.

IR (film) 3009, 2927, 3862, 1754, 1455, 1236, 1089, 994, 764, 716 cm^{-1}.

Mp 152–154 °C.

HRMS (ESI) *m/z* 275.1049 (275.1042 calcd for $C_{17}H_{16}O_2Na$, $(M)^+$).

Oxo-enol 5.41

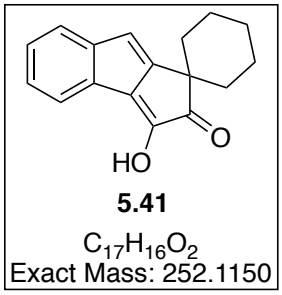

Diketone **5.37** (14.1 mg, 0.06 mmol) was dissolved in $CDCl_3$ (0.55 mL) and placed in an NMR tube. The NMR tube was then placed in a dewar along side a 15 W fluorescent light bulb for 3 h.[8] NMR indicated almost full conversion of **5.37** to **5.41** and no purification was performed.

^{1}H NMR (500 MHz, Chloroform-*d*) δ 7.72 (dd, *J* = 7.3, 1.0 Hz 1H), 7.33 – 7.26 (m, 2H), 7.15 (td, *J* = 7.3, 1.5 Hz, 1H), 6.56 (s, 1H), 1.83 – 1.74 (m, 5H), 1.70 – 1.61 (m, 5H).

^{13}C NMR (126 MHz, Chloroform-*d*) δ 149.4, 147.9, 130.1, 128.8, 125.4, 124.8, 121.5, 119.5, 47.9, 33.0, 25.2, 22.8.

IR (film) 3283, 2929, 2853, 1699, 1688, 1605, 1449, 1381, 1326, 1133, 1005, 965, 754 cm^{-1}.

HRMS (QTOF) *m/z* 238.0990 (238.0988 calcd for $C_{16}H_{14}O_2$, $(M)^+$).

[8] Used the following apparatus for photoreactions. See Pound, S. M. Development of an Intramolecular Alkene Aminocyanation Reaction and Progress Toward the Total Synthesis of Drimentine C, Ph.D. Dissertation, University of Minnesota, Minneapolis, MN, July, 2016.

5.5. References

[1] Cava, M. P.; Napier, D. R. *J. Am. Chem. Soc.* **1957**, *79*, 1701–1709.

[2] Cava, M. P.; Shirley, R. L. *J. Am. Chem. Soc.* **1960**, *82*, 654–656.

[3] Jansen, G.; Kahlert, B.; Klärner, F.-G.; Boese, R.; Bläser, D. *J. Am. Chem. Soc.* **2010**, *132*, 8581–8592.

[4] Paddon-Row, M. N.; Patney, H. K.; Harish, K. *Synthesis*, **1986**, 328–330.

[5] Segura, J. L.; Martin, N. *Chem. Rev.* **1999**, *99*, 3199–3246.

[6] Bornhöft, J.; Siegwarth, J.; Näther, C.; Herges, *Eur. J. Org. Chem.* **2008**, *9*, 1619–1624.

[7] Winstein, S.; Trifan, D. S. *J. Am. Chem. Soc.* **1949**, *71*, 2953–2953.

[8] Anslyn, E. V.; Dougherty, D. A. Organic Reaction Mechanisms, Part 2 *Modern Physical Organic Chemistry*; University Science Books, 2006, 662 and references therein.

[9] Parakka, J. P.; Sadanandan, E. V.; Cava, M. P. *J. Org. Chem.* **1994**, *59*, 4308–4310.

[10] Boger, D. L.; Panek, J. S.; Meier, M. M. *J. Org. Chem.* **1982**, *47*, 895–897.

[11] Boger, D. L. *Chemtracts: Org. Chem.* **1996**, *9*, 149–189.

[12] Michael, J. P.; Maqutu, T. L.; Howard, A. S. *J. Chem. Soc., Perkin Trans, 1* **1989**, 2389–2395.

[13] Boger, D. L.; Lerner, R. A.; Cravatt, B. F. *J. Org. Chem.* **1994**, *59*, 5078–5079.

[14] Schulze A.; Pagona, G.; Giannis, A. *Syn. Comm.* **2006**, *36*, 1147–1156.

[15] Scarso, A.; Pellizzaro, L.; De Lucchi, O.; Linden, A.; Fabris, F. *Angew. Chem. Int. Ed.* **2007**, *46*, 4972.

[16] Yates, M. H. *Tetrahedron Lett.* **1997**, *38*, 2813–2816.

[17] Pashkovskii, F. S.; Lakhvich, F. A.; Koval'skaya, S. S.; Kozlov, N. G. *Russ. J. Org. Chem.* **2001**, *37*, 375–381.

[18] Carlson, R.; Nilsson, Å. *Acta Chemica Scandinavica* **1985**, *39B*, 181–186.

[19] Carlson, R.; Nilsson, Å. *Acta Chemica Scandinavica* **1984**, *38B*, 49–53.

[20] Becker, H.; Soler, M. A.; Sharpless, B. K. *Tetrahedron* **1995**, *51*, 1345–1376.

[21] Français, A.; Bedel, O.; Haudrechy, A. *Tetrahedron* **2008**, *64*, 2495–2524.

[22] Regen, S. L.; Whitesides, G. M. *J. Org. Chem.* **1972**, *37*, 1832–1833.

[23] Jain, S. L.; Sharma, V. B.; Sain, B. *Tetrahedron Lett.* **2004**, *45*, 1233–1235.

[24] Lokan, N.; Paddon-Row, M. N.; Smith, T. A.; La Rosa, M.; Ghiggino, K. P.; Speiser, S. *J. Am. Chem. Soc.* **1999**, *121*, 2917–2918.

[25] Burgstahler, A. W.; Boger, D. L.; Naik, N. C. *Tetrahedron* **1976**, *32*, 309–315.

[26] Greenfield, S.; Mackenzie, K. *J. Chem. Soc., Perkin Trans. 2* **1986**, 1651–1666.

[27] Kolb, H. C.; VanNieuwenhze, M. S.; Sharpless, K. B. *Chem. Rev.* **1994**, *94*, 2483–2547.

[28] Takano, S.; Yoshimitsu, T.; Ogasawara, K. *J. Org. Chem.* **1994**, *59*, 54–57.

[29] Sharpless, B. K.; Amberg, W.; Bennani, Y. L.; Crispino, G. A.; Hartung, J.; Jeong, K.-S.; Kwong, H.-L.; Morikawa, K.; Wang, Z.-M.; Xu, D.; Zhang, X.-L. *J. Org. Chem.* **1992**, *57*, 2768.

[30] Wu, F.; Mandadapu, V.; Day, A. I. *Tetrahedron* **2013**, *70*, 9957–9965.

[31] Ray, R.; Matteson, D. S. *Tetrahedron Lett.* **1980**, *21*, 449–450.

[32] Watanabe, M.; Chang, Y. J.; Liu, S.-W.; Chao, T.-H.; Goto, K.; Islam, Md. M.; Yuan, C.-H.; Tao, Y.-T.; Shinmyozu, T.; Chow, T. J. *Nat. Chem.* **2012**, *4*, 574–578.

[33] Russell, R. A.; Harrison, P. A.; Warrener, R. N. *Aust. J. Chem.* **1984**, *37*, 1035–1041.

[34] Jain, S. L.; Sharma, V. B.; Sain, B. *Tetrahedron Lett.* **2004**, *45*, 1233–1235.

[35] Mondal, R.; Adhikari, R. M.; Shah, B. K.; Neckers, D. C. *Org. Lett.* **2007**, *9*, 2505–2508.

[36] Maliakal, A.; Raghavachari, K.; Katz, H.; Chandross, E.; Siegrist, T. *Chem. Mater.* **2004**, *16*, 4980–4986 and references therein.

[37] Warrener, R. N.; Harrison, P.A.; Russell, R.A. *J. Chem. Soc., Chem. Commun.*, **1982**, 1134-1136.

[38] Johnson, J. R.; Grummitt, O. *Org. Syn.* **1955**, *3*, 806.

6. WORK TOWARDS BUILDING THE MACROCYCLE THROUGH DIELS–ALDER REACTIONS USING ISOBENZOFULVENE AND DIBROMOQUINONE

Advancing benzobisnorbornene **4.32** towards a macrocycle was more challenging than anticipated. During optimization efforts of older routes, we kept our minds open to and were searching for alternative methods to achieve our goals. As detailed below, after revisiting the hexacene synthesis,[1] we learned of a one-step process to generate isobenzofulvene from norbornene. Gratifyingly, the first time we used this chemistry in our system the reaction proceeded smoothly. To date, we have settled on focusing efforts to construct the macrocycle using isobenzofulvene and dibromoquinone as our diene and dienophile respectively. Also, at this point my colleagues Zhuoran Zhang and Lafe Purvis joined the project and have helped develop the chemistry that will be presented below.

6.1. Precedence for Generating Isobenzofulvenes from Norbornene Structures

Initially, for our purposes, Chow's synthesis of nonsubstituted hexacene served as a reference for the oxidative cleavage and decarbonylation of the alkene bridge of a [2.2.1]bicyclic system (Scheme 6.1, intermediate **6.4** to **3.2**).[1] When we first examined the synthesis to prepare bicycle **6.4** (Scheme 6.1 intermediate **6.1** to **6.4**) we deemed their methods unsuitable for our target as it required the reduction and dehydration of a quinone to achieve aromatization. This broke our guideline that late-stage dehydration must be avoided and Cory had shown quinones in a macrocycle can lead to unexpected

transformations.[2] With our attention so focused on using this synthesis as precedence for our end-game strategy and the fact that aromatization involved reduction and dehydration of a quinone, we missed some remarkable chemistry that actually turns benzonorbornene into an isobenzofulvene.

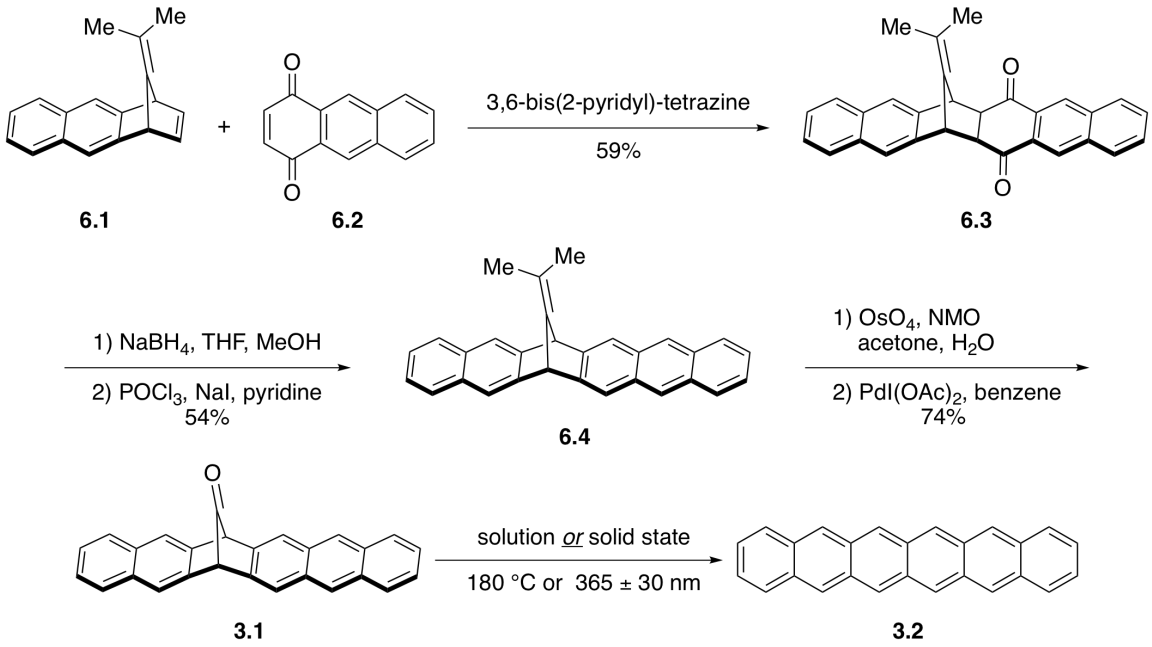

Scheme 6.1 Chow's synthesis of hexacene starting from norbornene 6.1 and quinone 6.2

The main reason we missed this transformation is because the mechanism for this reaction is not obvious. The actual synthesis of hexacene was only included in the SI[1] and there is no expansion on the chemistry beyond a scheme and experimental. Looking at the first reaction of Scheme 6.1, all that is shown is, in the presence 3,6-bis(2-pyridyl)-tetrazine **6.5**, norbornene **6.1** and quinone **6.2** can come together to provide dihydroquinone **6.3**. Upon reviewing this synthesis later and thinking harder about this first transformation, it struck us as odd. How did the norbornene bridgehead carbons get attached to the quinone and how did two carbon and two hydrogen atoms get lost? The answer is in the mechanism.[3]

The role of tetrazine **6.5** (Scheme 6.2), a diene, is to initiate a cascade of [4+2] and retro[4+2] reactions. Normally both norbornene **6.1** and quinone **6.2** could act as dieneophiles, but remember tetrazines are electron-poor dienes. The strain induced by the bicyclic system of **6.1** renders it more reactive as a dieneophile in this case.[3] Therefore, tetrazine **6.5** reacts selectively with norbornene **6.1** to give azabicycle **6.6**. As seen in Boger's[4] work, N_2 spontaneously leaves to give dihydropyridazine **6.7**. This intermediate is also unstable and undergoes a retro-[4+2] reaction to give pyridazine **6.8** and the extremely reactive diene, isobenzofulvene **6.9**. Presumably the driving force for this step is the generation of the aromatic pyridazine ring **6.8**. The isobenzofulvene **6.9** is trapped by quinone **6.2** to give the desired product dihydroquinone **6.3** in a reasonable yield of 59%. For simplicity, this reaction of benzonorbornenes with tetrazine and quinones will be referred to as the Diels–Alder cascade reaction.

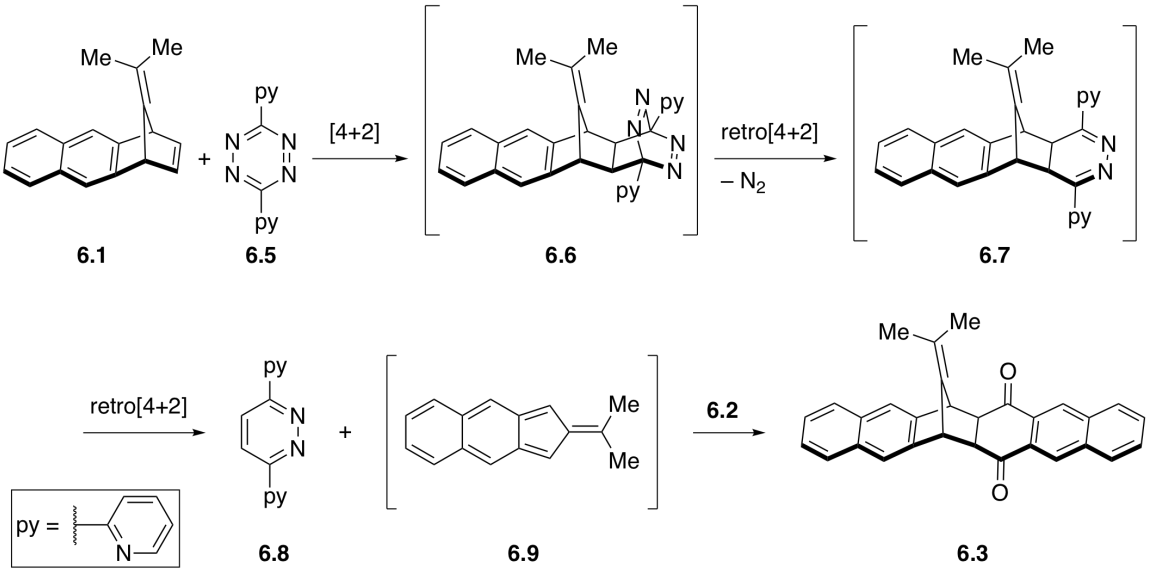

Scheme 6.2 Mechanism for generation of isobenzofulvene 6.9 from norbornene 6.1 and tetrazine 6.5

Warrener and coworkers developed this methodology in the 1970s. The system was described with great detail in their 1972 *Australian Journal of Chemistry* paper and

only key aspects of their work will be highlighted as necessary here.[3] One interesting thing to point out though is that they never obtained spectroscopic evidence for the presence of the isobenzofulvene intermediate. They could however isolate the dihydropyridazine intermediate at low temperatures and under basic conditions. Also, the pyridazine by-product, from isobenzofulvene generation, was isolated. Finally, in the presence of various dieneophiles the expected Diels–Alder products were isolated. Therefore, by inference the isobenzofulvene was generated from a reaction between a norbornene and tetrazine **6.5**.

While considering how this chemistry could be applied to our system, we found that Butler and Warrener used this chemistry to generate pincer like molecules (example **6.13** in Scheme 6.3) with structures strikingly similar to what we are targeting.[5] To achieve these molecules, dichloroquinone **6.10** was used as the trapping agent for isobenzofulvene **5.39**. This proved to be extremely convenient as treatment with a non-nucleophilic base such as collidine, DBN, or basic alumina regenerated the quinone through, formally, a dehydrohalogenation. This process is much easier than performing an oxidation to reform the quinone. Additionally, they showed that the other olefin of the quinone could trap another equivalent of isobenzofulvene **5.39** followed by treatment with base to generate a 1:1 mixture of *syn*:*anti* isomers of quinone **6.12**. Encouraged by the seemingly simplistic nature of these reactions we decided to reconsider whether it was reasonable to include the incorporation of quinones into our macrocycle.

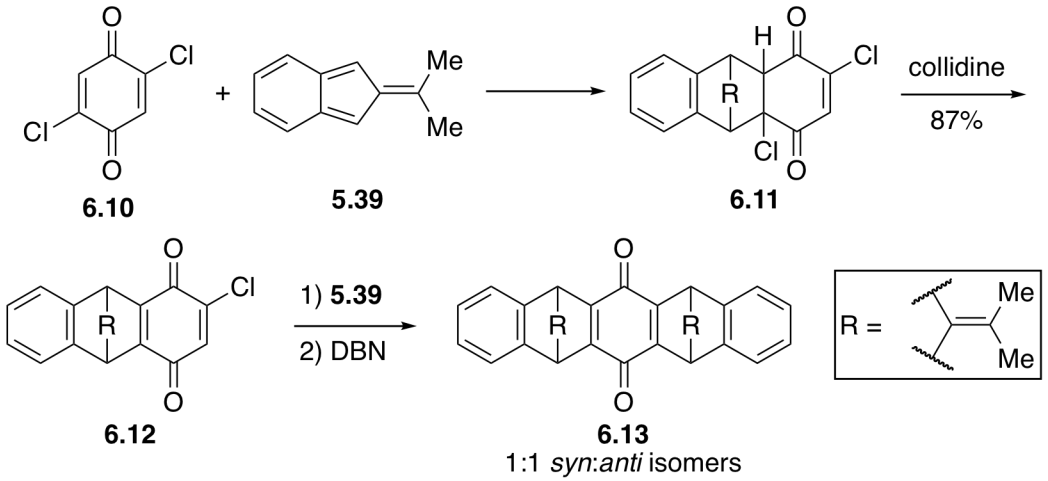

Scheme 6.3 Butler and Warrener's synthesis of pincer molecule 6.13 using isobenzofulvene 5.39 and dichloroquinone 6.10.

Part of our fear in including quinones stemmed from Cory's work (Section 2.1.2).[2] However, in reviewing his work, he never reported trying to manipulate the quinones in the macrocycle. Instead, he was unsuccessful in installing anthracene like units. Going through a route that traps isobenzofulvene with quinone would generate quinones that are isolated from aromatic rings by the bridging bicycles. Therefore we propose that these quinones should be easier to functionalize. Additionally, the quinones could serve as synthetic handles for late-stage introduction of a bulky substituent on the zigzag edge of the macrocycle.[6,7] If this strategy works it would fulfill our last requirement by enabling the study of the effects of substituents on the persistence of a cyclacene. Persuaded that quinones were acceptable to include in our macrocycle, we began proposing how key intermediate **4.32** could be transformed to an isobenzofulvene for use toward macrocycle construction.

6.2. Proposed Routes Utilizing Isobenzofulvene Methodology

In looking at the retrosynthetic analysis, we envisioned using the same end-game strategy, decarbonylation of **6.15** generated from **6.16**, as proposed previously.

Installation of the aryl groups (R^1) could be achieved through addition of a Grignard or organolithium to the carbonyl groups of **6.17** followed by reductive aromatization to give **6.16**. Two different pathways could achieve formation of the macrocycle of quinone **6.17**. Path A utilizes AB monomer **6.18** which could provide various sized macrocycles through oligomerization upon treatment with tetrazine **6.5** to generate the isobenzofulvene moiety. Alternatively, Path B could construct the macrocycle through a series of Diels–Alder reactions between bisdienophile **6.19** and bisdiene precursor **4.32**. Both **6.18** and **6.19** could be generated through a coupling of key intermediate **4.32** to dibromoquinone **6.20** as dicated by varying the equivalence of tetrazine **6.5**.

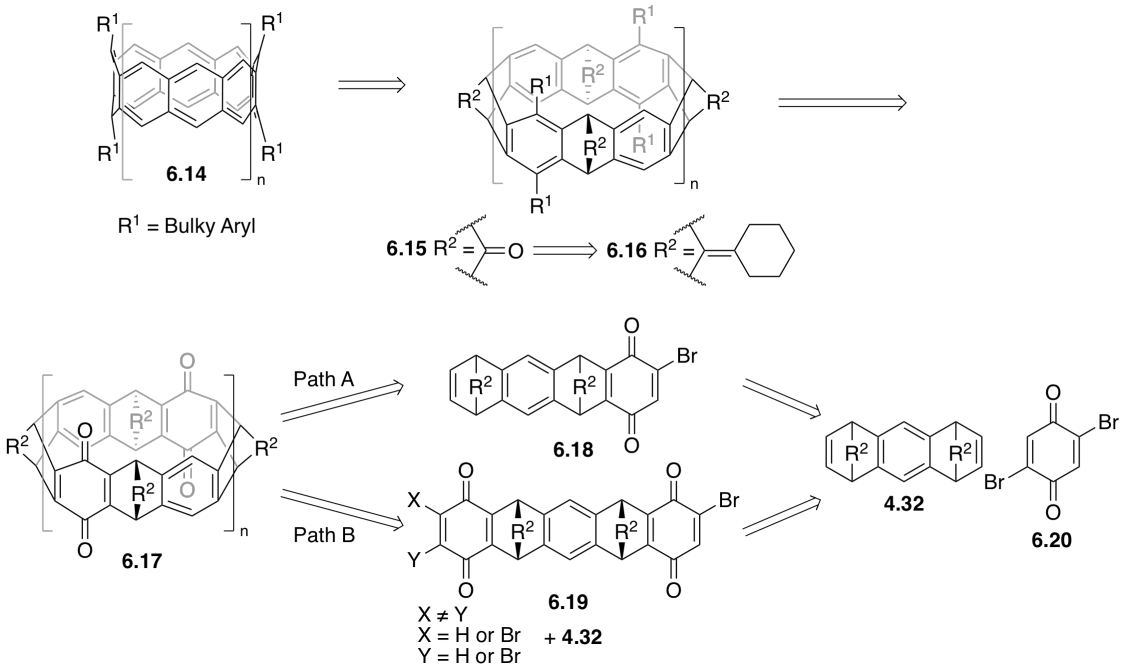

Scheme 6.4 Retrosynthetic analysis for incorporation of isobenzofulvene chemistry starting from key intermediate 4.32.

We decided to propose use of dibromoquinone **6.20** as it can be readily prepared through an oxidation of dibromohydroquinone **4.46** which we had from the synthesis of bisbenzyne precursor **4.39**.[8] A major advantage to this proposed route is the ability to use both the *syn* and *anti* isomers of **4.32**, as generation of the isobenzofulvene ablates the

relative configuration of the bridges. However, upon incorporation of quinones on both sides of **4.32** (such as in **6.19** or a dimerized product of **6.18**) once again a mixture of *syn* and *anti* isomers would be produced and only the *syn* isomer could be advanced. Another benefit of the route is that it allows for different sized macrocycles to be constructed. Finally, one could also envision combining the key intermediates in paths A and B as well. In short, this route is adaptable and had the potential to allow for rapid construction of macrocycle. We valued adaptability as we were not sure what the diastereoselectivities would be of these Diels–Alder cascade reactions, or if the selectivity would change for each intermediate. To try and get an idea of the practicality of the reaction, we tested the proposed chemistry in a model study using benzonorbornene **4.37**.

6.3. Model Study for Generation and Use of Isobenzofulvene

The very first model reaction we ran used benzonorbornene **4.37** and naphthoquinone **6.21** (Scheme 6.5). Carrying out the reaction was surprisingly simple as well. Since benzonorbornene **4.37**, naphthoquinone **6.21**, and tetrazine **6.5** are all solids, they can all be added to the flask and the reaction is initiated upon the addition of solvent. The reaction was complete within 3.5 h and the pyridazine by-product **6.8** and excess tetrazine **6.5** could be removed by washing the reaction mixture with 1M HCl. In fact, **6.5** and **6.8** give the solution an intense pink-red color allowing one to visually determine if all of **6.5** and **6.8** been removed from the organic phase, which becomes yellow (Figure 6.1). The resultant crude product was surprisingly pure and a crude yield of 94% was obtained. By ^{1}H NMR it appeared that a mixture of endo and exo isomers of **6.22** had formed (detailed analysis for how this was determined is given later (Figure 6.2)). ^{13}C

NMR, IR, and GCMS also confirmed the product's identity. These results were extremely impressive and encouraging based on our experiences with prior routes.

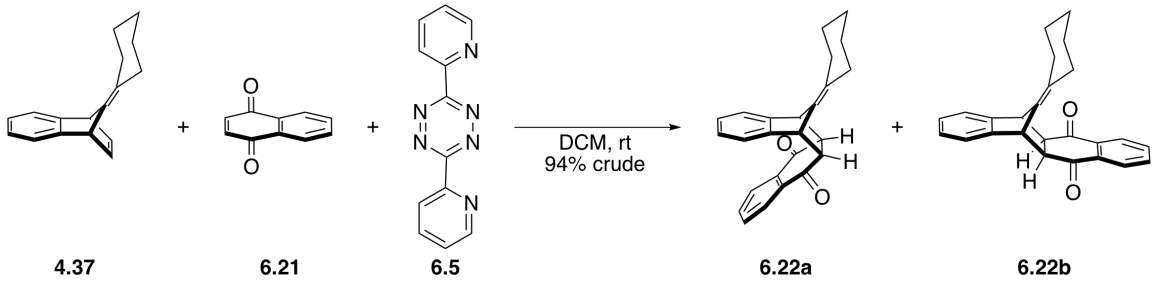

Scheme 6.5 The first reaction we performed generating isobenzofulvene from benzonorbornene 4.37 and trapping it with quinone 6.21 to give endo and exo dihydroquinone 6.22.

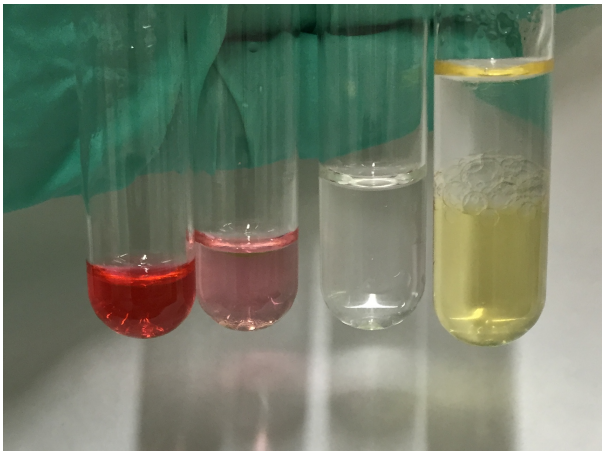

Figure 6.1 An example of the colors observed during the washing of a Diels–Alder cascade between benzonorbornene, tetrazene, and quinone. From left to right, aqueous phases from the first and second HCl washes containing excess tetrazine and pyridazine by-product, the aqueous phase from plain water wash, and the combined organic (solvent DCM) and brine wash. The product in the DCM layer has a yellow tint.

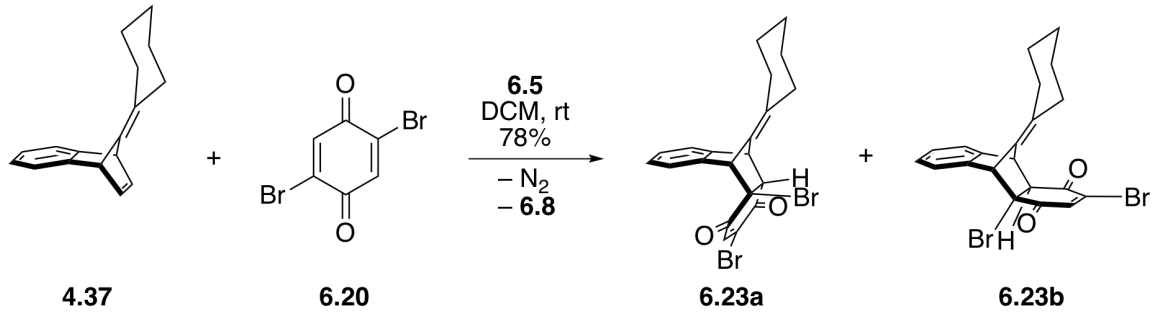

Scheme 6.6 Model reaction between benzonorbornene 4.37 and dibromoquinone 6.20 initiated by tetrazine 6.5.

We continued our model study by switching to dibromoquinone to test how readily we could accomplish the dehydrohalogenation. Gratifyingly, the Diels–Alder cascade

proceeded smoothly to provide an inconsequential mixture of endo and exo isomers of dihydroquinone **6.23**. These isomers are distinguishable by ^{1}H NMR as shown in Figure 6.2. In particular, the splitting pattern and chemical shift of the protons of the norbornane ring (H_a–H_c in Figure 6.2) can be used to confidently determine the presence and ratio of the exo and endo isomers. In both isomers, the bridgehead protons split each other with a small coupling constant of about 1.6 Hz. If the quinone is in the endo position though then additional splitting is seen between H_c and H_b with a coupling constant of 4.4 Hz. Therefore, H_b is a doublet-of-doublets and H_c is a doublet. Conversely, if the quinone is in the exo position then the dihedral angle between $H_{b'}$ and $H_{c'}$ is near 90° and therefore, as predicted by the Karplus curve, the coupling constant is near 0 Hz. As a result $H_{b'}$ is a doublet and $H_{c'}$ is a singlet. Additionally, since $H_{c'}$ is in the endo position it is actually shielded by the aromatic ring and appears about 1 ppm downfield of all the other protons. Based on this analysis, the ratio of endo **6.23a**:exo **6.23b** is about 5:1, and is in agreement with the endo rule. Ultimately the ratio of endo:exo isomers is inconsequential in this case as the next step, dehydrohalogenation, will convert them to the same compound. Examining the spectral data on this simplified system though is of great use as a reference for understanding the spectra of future, more complex, systems.

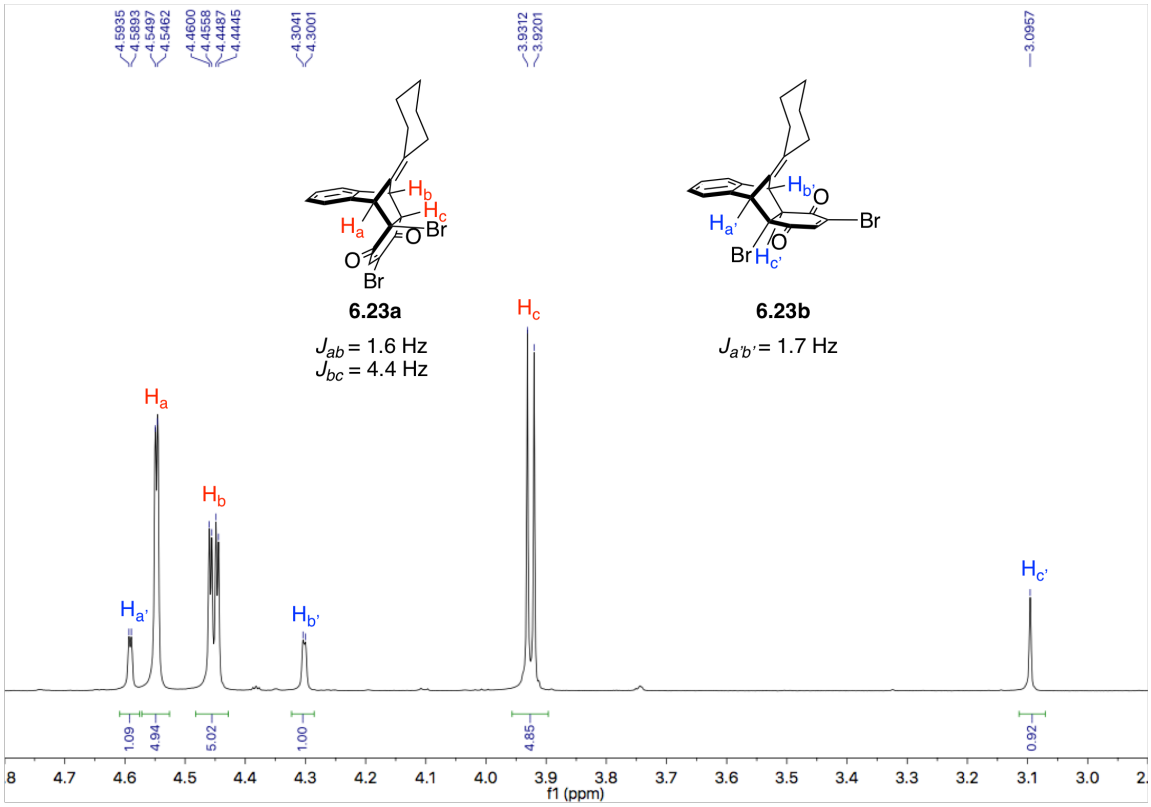

Figure 6.2 ^{1}H NMR of a mixture of dihydroquinone 6.23a and 6.23b (endo and exo isomers) zoomed in on the protons of the norbornane ring.

During attempts to accomplish the dehydrohalogenation we found that dibromodihydroquinone **6.23** was surprisingly sensitive to base (Scheme 6.7). When **6.23** was treated with pyridine or DBU it instantly turned from pale yellow to a black cloudy mixture (Scheme 6.7a). ^{1}H NMR confirmed decomposition had occurred. Interestingly, when **6.23** was subjected to column chromatography, the ^{1}H NMRs of the end fractions suggest that the desired elimination to give a quinone **6.24** had occurred. Reviewing the literature, Warrener did report that extremely mild conditions, such as treatment with alumina, could induce the dehydrohalogenation.[5] Indeed, upon dissolving **6.23** in DCM and passing it through a short column of basic alumina in a pipet the desired transformation to quinone **6.24** was achieved with 94% yield. It is important to note that the best yields are given when dry basic alumina (dried in a 500 °C kiln) is used. In fact,

we found that that approximately a 10% increase in yield could be obtained by using dried alumina over basic alumina stored on the bench top. Surprisingly, an attempt to purify a dihydrobromoquinone on a neutral alumina column (as basic alumina absorbs water it becomes less basic) resulted in complete decomposition of the product. Visually it could be seen that the desired transformation was taking place. The starting material, **6.23**, was yellow but as soon as it came in contact with the alumina it turned to a red-orange color (Scheme 6.7b).

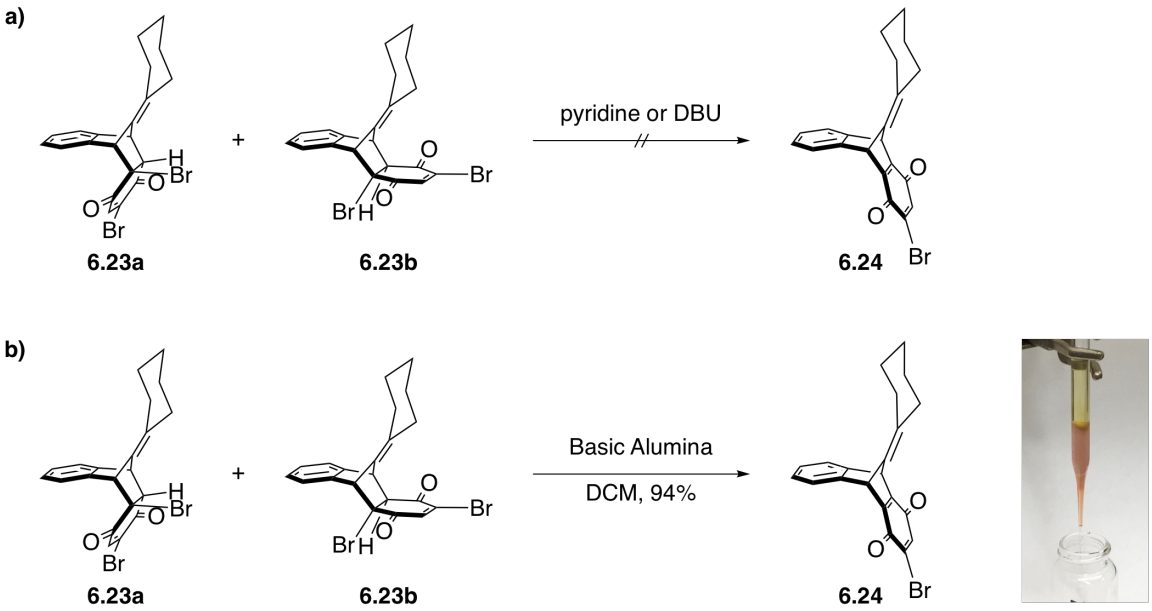

Scheme 6.7 Conditions attempted to facilitate the dehydrobromination of 6.23 a) pyridine and DBU which led to decomposition and b) basic alumina successfully provided quinone 6.24 and a photo of the process showing the color change from yellow (6.23) to red-orange (6.24).

^{1}H NMR confirmed that the elimination had occurred as evident by the change in the shift and splitting of the norbornane protons (Figure 6.3). Immediately obvious is the absence of the hydrogen from the quinone (formerly H_c and $H_{c'}$ in Figure 6.2). Also, the signals for the bridgehead protons have been shifted downfield. Each proton appears as a doublet with a coupling constant of 1.7 Hz due to them splitting each other. The lack of additional splitting indicates that there are no other protons on neighboring carbon atoms.

IR further confirmed the desired elimination as the wavenumber of the carbonyls (1672 cm^{-1} for **6.23**, 1665 and 1649 cm^{-1} for **6.24**) decreased, indicating an increase in conjugation.

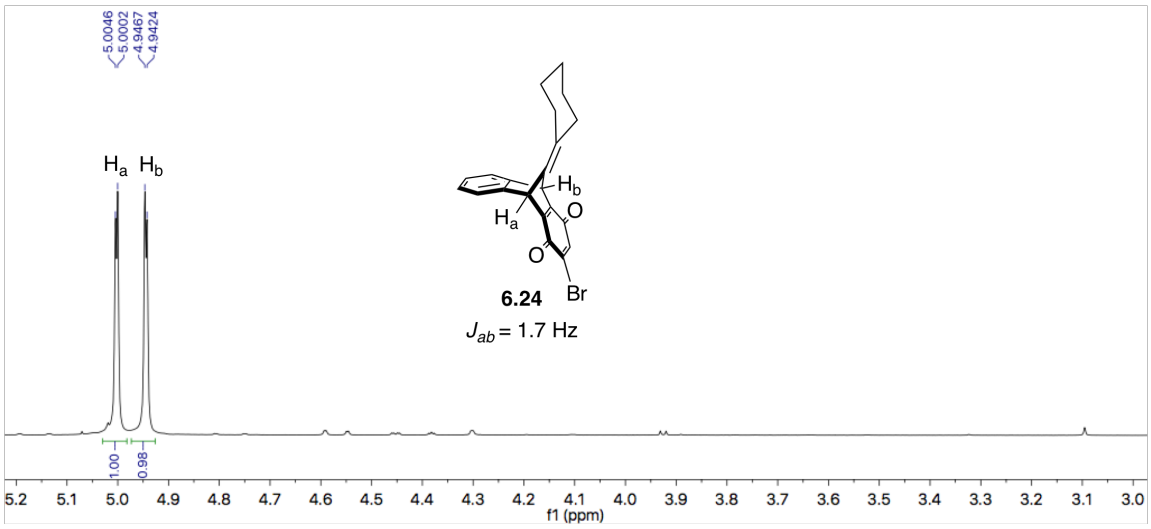

Figure 6.3 ^{1}H NMR of quinone 6.24 zoomed in on the region where the norbornane protons appear.

We next investigated if it was feasible to add a second equivalent of norbornene **4.37** on the other side of the quinone of **6.24**. One concern that we had was that the cyclohexane ring of the generated the isobenzofulvene, would render it too bulky to access the relatively bulky quinone **6.24**. Fortunately, treatment of **4.37** with tetrazine **6.5** in the presence of quinone **6.24** provided dihydroquinone **6.25** as a mixture of isomers (endo/exo and *syn*/*anti*). Treatment of **6.25** with basic alumina, reduced the complexity of the mixture to two isomers (*syn/anti*) of quinone **6.26**.

The presence of both the *syn* and *anti* isomers was verified by ^{1}H NMR (Figure 6.4). Due to the high symmetry of quinone **6.26**, only three signals for each isomer should be observed between 7.5 and 4.6 ppm. Furthest upfield are two overlapping singlets. Each singlet represents all the bridgehead protons, which are now equivalent, from an isomer. In the aromatic region, two AA'BB' signals can be found for each

isomer. Satisfied that two equivalents of the isobenzofulvene generated from **4.37** could be added onto dibromoquinone **6.20**, that the dehydrobromination was facile, and that both *syn* and *anti* isomers of **6.26** were formed we decided to move forward and began investigations into the real system.

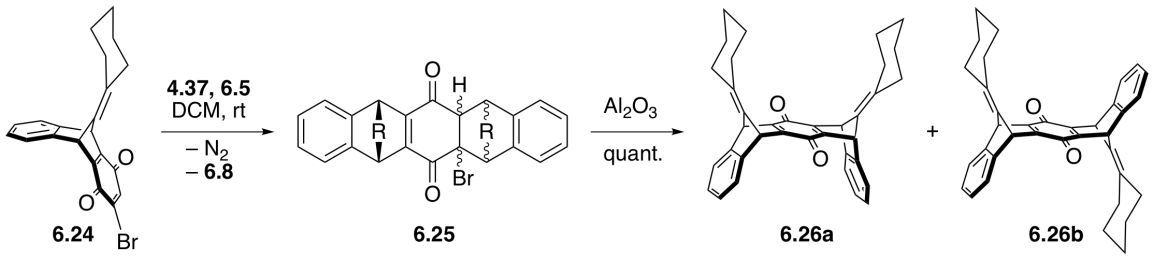

Scheme 6.8 Second addition of 4.37 to quinone 6.25 and elimination to give a mixture of syn and anti isomers of quinone 6.26.

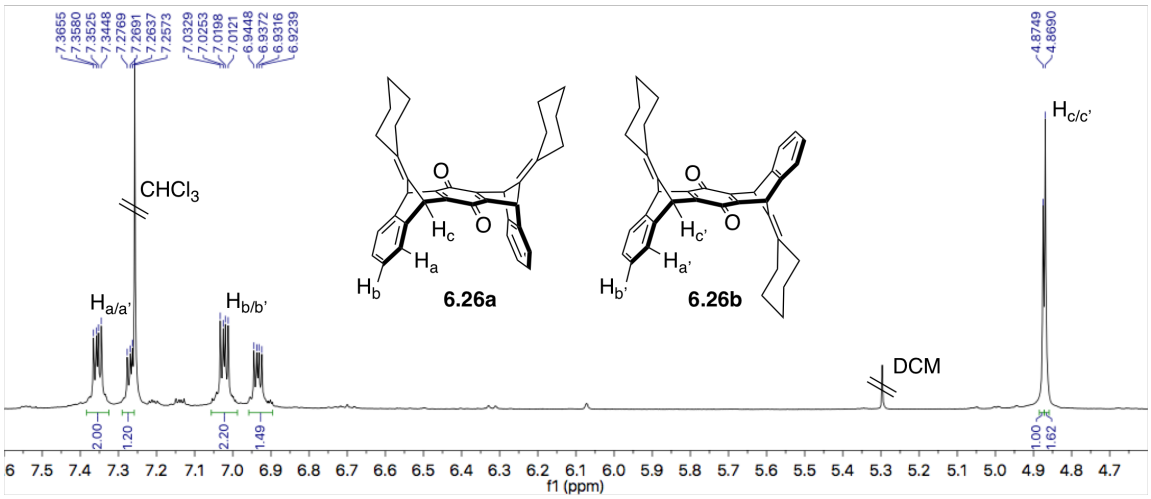

Figure 6.4 ^{1}H NMR of a mixture of *syn* and *anti* isomers of quinone 6.26a.

6.4. Application of Isobenzofulvene to the Real System: Results and Discussion

An unavoidable major challenge with this route is the number of stereoisomers that are produced in each step. Once a norbornene ring has been transformed to isobenzofulvene and trapped a quinone then the *syn* or *anti* configuration of the bridge is locked in place. To form a macrocycle, only the isomers with a *syn* relationship of the

bridges can be carried forward. By considering the different transition states, rationalization of experimental outcomes and strategies to achieve *syn* isomers can be made.

In considering the different transition states, Figure 6.5a, when the dienophile is small, such as unsubstitued dibromoquinone **6.20**, then secondary orbital effects should dominate and the endo approach should be favored. If however the quinone is substituted with a [2.2.1] ring, Figure 6.5b, then steric effects should dominate causing the endo approach to be unfavorable. This would be especially true if there are large substituents on the six-membered ring of the isobenzofulvene. Additional transition states must be considered though as the bridge causes the dienophile to have both an EXO and ENDO face. Of the four possible transition states only exo/EXO and endo/ENDO will provide the desired isomer. Likely though, only the exo/EXO arrangement will be accessible and in competition with the undesirable exo/ENDO approach. While we could make predictions using models, we needed experimental data to refine our assumptions.

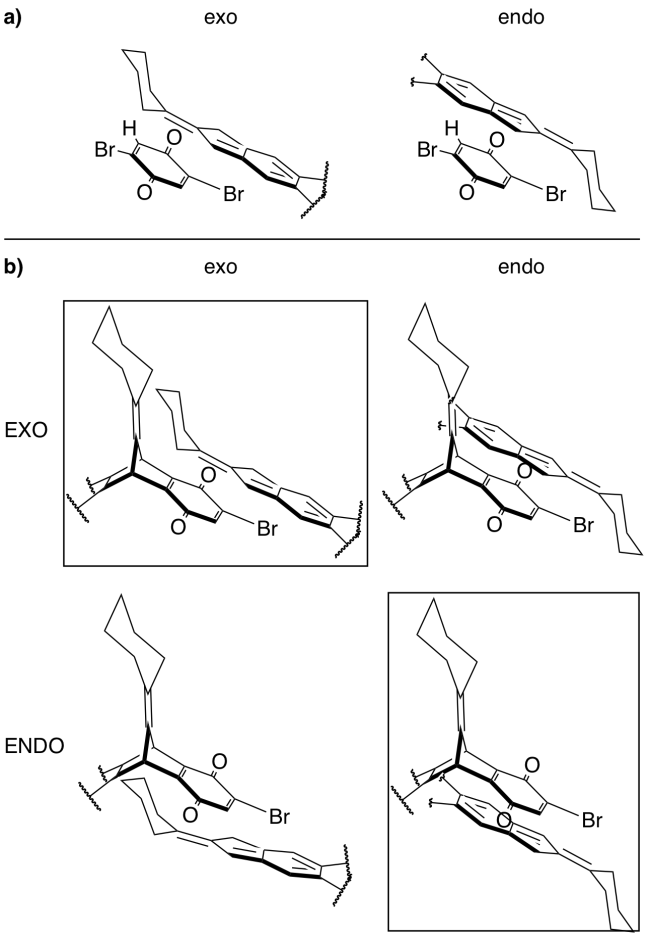

Figure 6.5 General transitions state structures for the Diels–Alder reaction of an isobenzofulvene with a) dibromoquinone, a small dienophile and b) a substituted quinone that has an EXO and ENDO face. The boxed structures are the transitions states that will lead to the desired *syn* relationship of the bridges.

Use of 3-dimensional structures is helpful to understand outcomes of the reactions presented in this chapter. However, to improve clarity of the structures of the intermediates, a flat representation as shown in Figure 6.6a will be used for most reaction schemes. As needed the 3-dimensional structure will be used to help explain and or rationalize reaction outcomes.

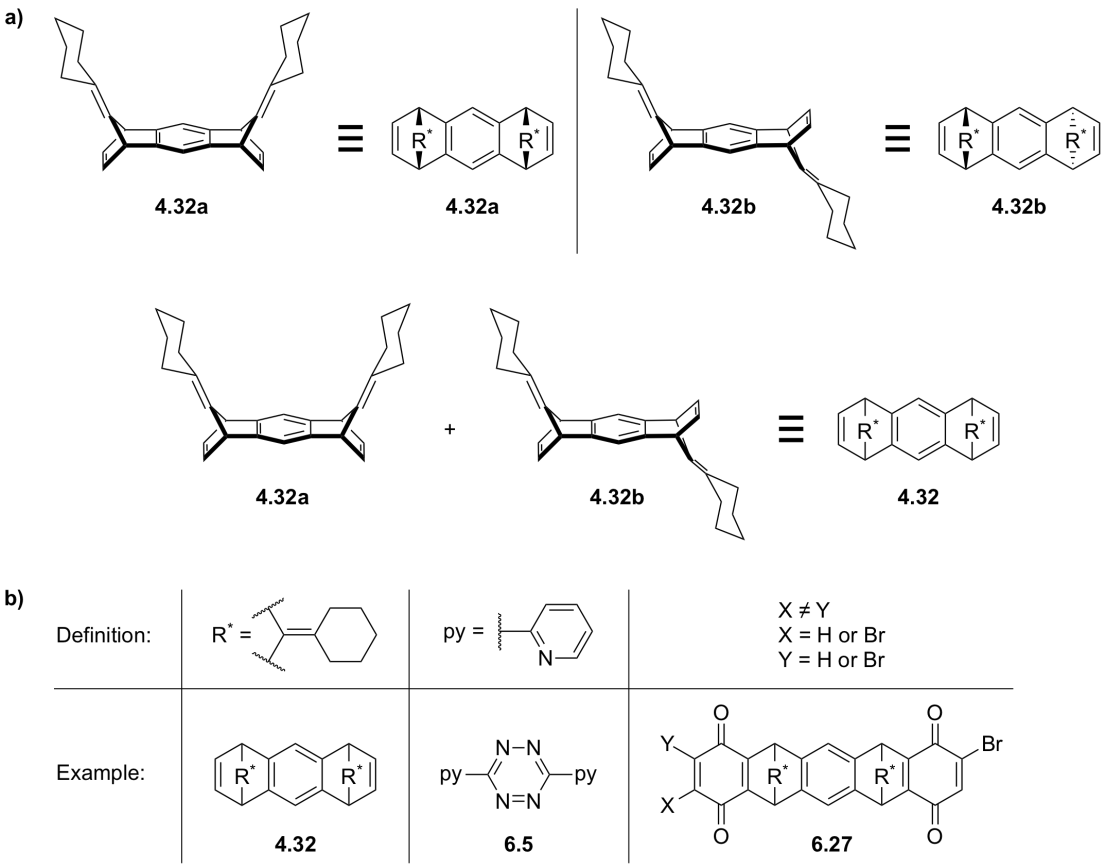

Figure 6.6 A key for the 2-dimensional drawings of the reactions covered in this chapter, a) flat representation of bicyclic structures that will be used to improve clarity of structures of intermediates and b) definitions of R*, py, X and Y.

6.4.1. Preparation of key intermediates *syn*-bisquinone 6.27a and monoquinone 6.28

Initially, we attempted to install only one quinone on key intermediate **4.32**. However, the rate of formation of the second isobenzofulvene is competitive with the rate of formation of the first isobenzofulvene of **4.32**. As a result, we observed about a 2:1 ratio of the mono **6.28**:bis **6.27** adducts (Scheme 6.9a). Seeing that formation of the second isobenzofulvene was so facile, we decided to try a double Diels–Alder cascade to make exclusively **6.27**. This was readily accomplished by treating **4.32** with two equivalents of tetrazine **6.5** in the presence of over two equivalents of dibromoquinone **6.20**. The subsequent elimination was readily achieved using basic alumina.

Theoretically, four different isomers of **6.27** (bridges *syn/anti* and bromine atoms *cis/trans*) could be formed. These isomers should all have similar looking ^{1}H NMR spectra. Therefore, before attempting to interpret the ^{1}H NMR of the reaction mixture, it was helpful to consider what key differences in the spectra would be for each isomer.

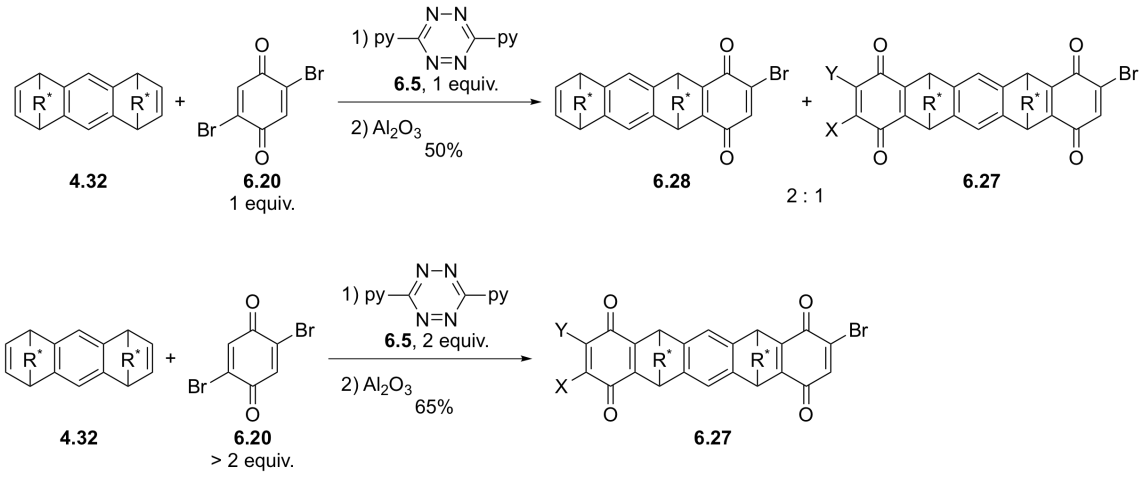

Scheme 6.9 Attempt to form a) monoquinone 6.28 and b) bisquinone 6.27.

As introduced by the model study, on the core of **6.27** there are three diagnostic types of hydrogens, each in a distinct region of the ^{1}H NMR spectra, Figure 6.7a. Furthest upfield between 4.8 and 5.1 ppm, are hydrogens of the bridgehead (Figure 6.7b, H_d/H_e of **6.27a/c** and H_c/H_e of **6.27b/d**). Due to the bromine substituents, the hydrogens across the bridges are inequivalent, so they split each other with a coupling constant of about 1.7 Hz. Therefore, for each isomer, one would expect to see two doublets. Moving downfield, the next diagnostic peaks come in at around 6.9 and 7.1 ppm, corresponding to the hydrogens of the quinone (Figure 6.7b, H_c of **6.27a/c** and H_b of **6.27b/d**). Regardless of whether the bromines are *cis* or *trans* across the molecule, the hydorgens of the quinone should be equivalent and appear as a single singlet for each isomer. Last, are the hydrogens of the central aromatic ring (Figure 6.7b, H_a/H_b of **6.27a/c** and H_a of **6.27b/d**). When the bromines are *cis*, as in **6.27a/c** these hydrogens are inequivalent and

appear as separate singlets. Conversely, when the bromines are *trans* then the protons are equivalent and appear as one singlet.

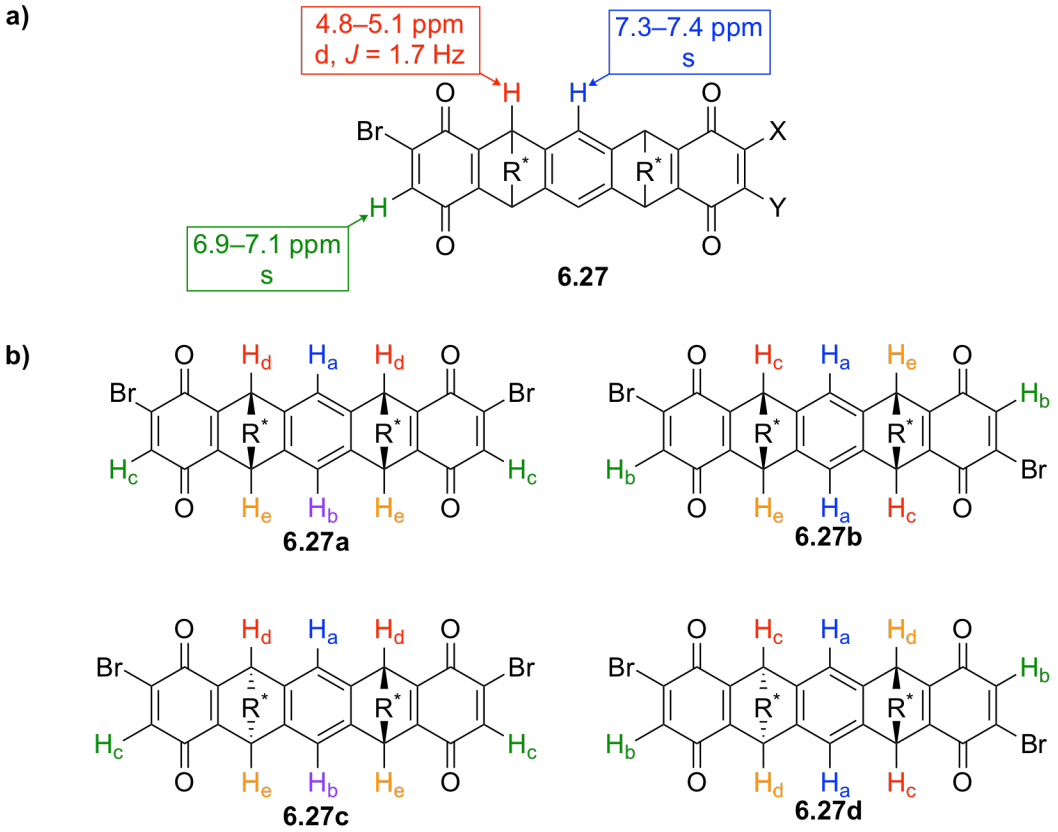

Figure 6.7 A guide for interpreting the ^{1}H NMRs of the biquinone 6.27 a) the region of the spectra and the splitting expected for each key proton and b) identification of equivalent protons and relative order from highest ppm to lowest ppm for each isomer.

Application of the above analysis to ^{1}H NMR spectra (Figure 6.8) of the major component of the double Diels–Alder cascade reaction appears to be only a mixture of *cis/trans* bromine isomers. Starting at the region of the bridgehead protons ($H_{d/e}$ and $H_{c'/d'}$), between 4.8 and 4.9 ppm there appears to be two triplets. However, it believed that each apparent triplet is actually two doublets (J = 1.9 Hz) that are overlapping. This is unsurprising as the protons on either side of the bridge are in extremely similar electronic environments and therefore should have extremely similar shifts. Based on this reasoning, there are a total of four doublets indicating there are two different isomers.

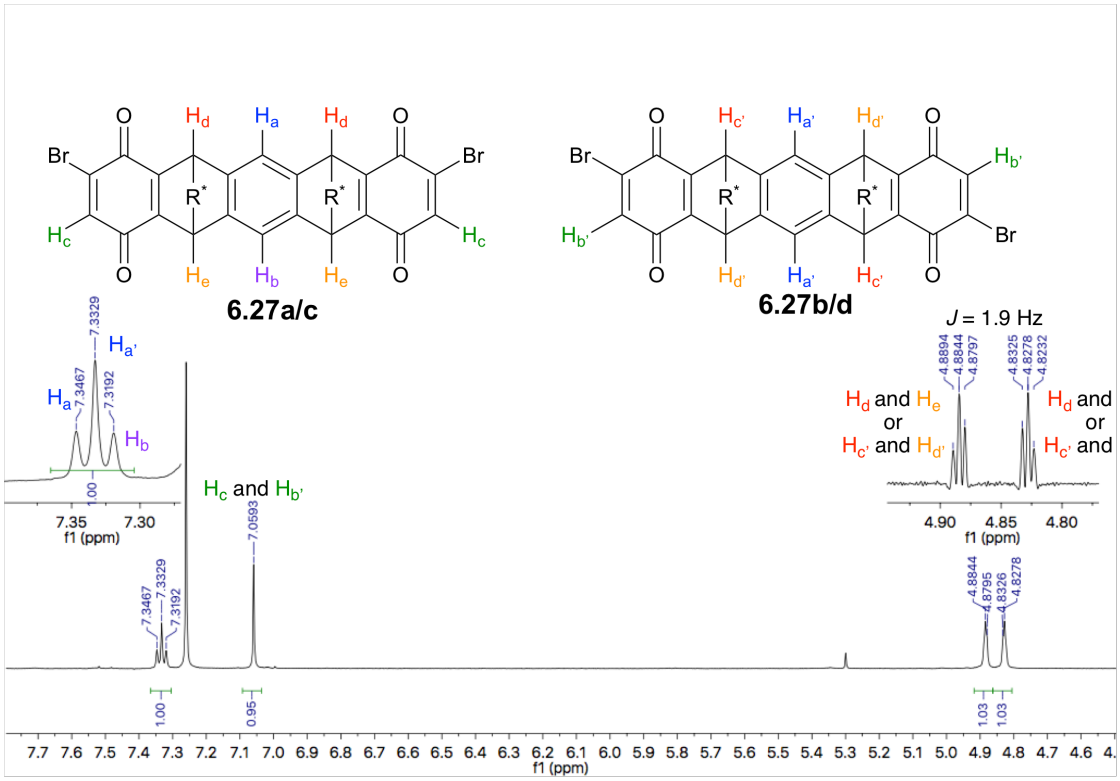

Figure 6.8 ^{1}H NMR of major isomer formed from attempt to form bisquinone 6.27. Note, the apparent triplets at 4.88 ppm and 4.83ppm are actually two separate doublets that are overlapping.

Moving to the protons of the quinone (H_c and $H_{b'}$) it is surprising to find that there is only one singlet at 7.06 ppm. This suggests that there is only one isomer total. We propose instead though that analogous protons of two isomers have exactly the same chemical shift. Comparison of the integration of the singlet (1H) and the total integration of the bridgehead region (2H) corresponds to the expected ratio for the presence of two isomers, supporting the above assumption.

Finally, at 7.33 ppm there appears to be another triplet for the protons of the central ring ($H_{a/b}$ and $H_{a'}$). This is a nonsensical splitting pattern though for these hydrogens. Instead, it is actually three different singlets where the central peak corresponds to $H_{a'}$ of **6.27$_{b/d}$** (the isomer where the hydrogens are equivalent) and the two outer peaks correspond to the inequivalent hydrogens H_a and H_b of **6.27a/c**. This is strong

evidence for the identifying the mixture as the two *cis/trans* bromine isomers rather than the *syn/anti* isomers. It is expected that these isomers would be formed in approximately a 1:1 ratio as there are no steric or electronic reasons for one to be formed preferentially over the other. Assuming a 1:1 ratio of *cis*/*trans* isomers were formed (confirmed by the 1:1 integration in the bridgehead region), this would then explain why the central signal is about twice the intensity of the outer signals as the area of the peak is directly related to the number of equivalent hydrogens.

Based on our prior experience in characterizing the *syn* and *anti* isomers of **4.32** we were worried that once again the *syn* and *anti* isomers would have near identical NMR spectra. This could make it difficult to tell if there is a mixture of *syn* and *anti* isomers or if just one is present. The ^{1}H NMR of the crude reaction mixture after elimination provided evidence for the presence of only one set of *syn/anti* isomers. As circled in Figure 6.9 there are very weak signals right next to or overlapping the key signals discussed above. Due to the similar chemical shifts, this indicates that the structures are similar but still distinctly different. Based on this observation we believed only **6.27a/b** or **6.27c/d** was formed.

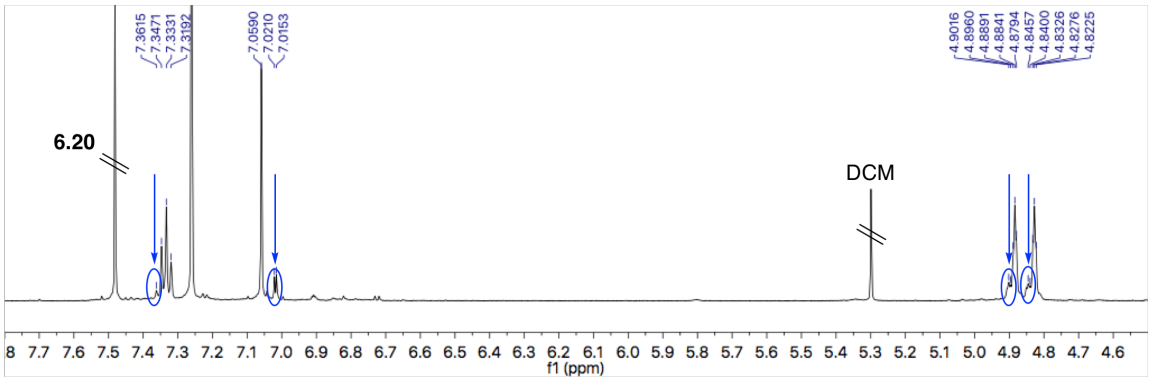

Figure 6.9 ^{1}H NMR of crude reaction mixture of a double cascade Diels–Alder reaction after elimination. Circled are the signals from of the minor *syn/anti* isomers.

Actually identifying if the *syn* or *anti* isomers of **6.27** were formed from the double Diels–Alder cascade reaction was slightly more challenging. Based on our previous work of determining the absolute structures of key intermediate **4.32a** and **4.32b**, we knew that the NMRs and IRs are nearly identical for *syn* and *anti* isomers and therefore not of much help. In fact, more basic comparison techniques are more useful if both isomers are present. First, the *anti* isomer has an inversion center and no dipole moment. Therefore, it should have a higher R_f value by TLC and elute from the column first. Conversely, for the *syn* isomer, the quinones induce a slight dipole and bind stronger to the silica gel. This reasoning is supported by the work of Larry L. Miller who studied similar structures.[9] Flash chromatography of the reaction mixture of the double Diels–Alder cascade reaction resulted in the major isomer eluting first indicating the undesired *anti* isomer was prepared almost exclusively.

At first, this seems like a devastating set back. However, after rationalizing why only the *anti* isomer was formed, a strategy could be developed to access the *syn* isomer. The first cascade Diels–Alder reaction produces almost exclusively the *syn/anti* endo dihydroquinone **6.29**. In the presence of excess tetrazine **6.5**, isobenzofulvene **6.30** is generated. As shown in Scheme 6.10a, this diene has two distinct faces. As drawn, the bottom face is blocked by the dihydroquinone moiety. Since the dienophile, dibromoquinone **6.20**, will prefer an endo approach sterics will control which face of **6.30** **6.20** will add to. The top face is significantly more accessible for proper diene-dienophile alignment resulting in the formation of the *anti* isomers of **6.27**.

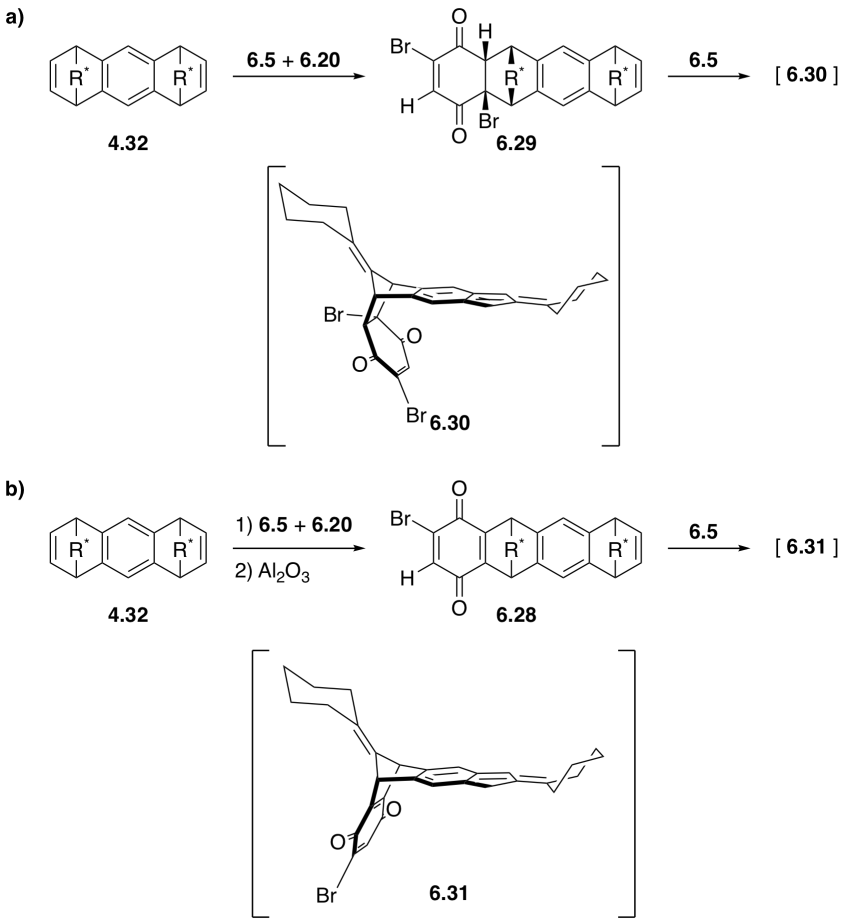

Scheme 6.10 A 3-dimensional image of the isobenzofulvene intermediate formed from a) dihydroquinone 6.29 and b) quinone 6.31.

We hypothesized that *syn*-**6.27** could be accessed if isobenzofulvene **6.31** was generated from quinone **6.28**. Looking at the 3-dimensional drawing of **6.31** Scheme 6.10b, both the top and bottom face of the diene have a similar steric environment. This could enable quinone **6.20** to approach in an endo fashion to the bottom face. Gratifyingly, this hypothesis was correct and allowed us to generate the **6.27** with a *syn* **6.27a**:*anti* **6.27b** ratio of about 1:1.6 in 58% yield over four steps as a red solid. Further confirming our assignment of the *syn* and *anti* isomers, we found **6.27b** to be less soluble than **6.27a**. Unfortunately, when attempting to measure melting points the compounds decomposed so we could not further confirm our assignment using melting point. Due to

the limited solubility of the **6.27b**, it is difficult to separate **6.27a** and **6.27b** by flash chromatography. However, if chromatography is performed before elimination, then the *syn* and *anti* isomers can be easily separated, and provided better separation than recrystallization. Before we could scale up the synthesis of *syn*-diquinone **6.27** we needed an efficient means to access monoquione **6.28**.

As stated earlier, the challenge in preparing monoquinone **6.28** is that tetrazine **6.5** does not selectively react with **4.32** over the norbornene of **6.21**, resulting in the formation of bisquinone **6.27** as a major by-product after elimination. Attempts were made to run the reaction in the presence of basic alumina with the hope that elimination would be faster than formation of the second isobenzofulvene to access the *syn* isomer. However, the tetrazine absorbed onto the alumina surface thereby slowing the rate of the reaction and the ratio of **6.27a**:**6.27b** did not change. Instead we found that when the ratio of **4.32**:**6.5** was 2:1, the ratio of monoquinone **6.28**:bisquinone **6.27** generated was about 4:1. Excess starting **4.32** could be readily recovered via flash chromatograpy. This method works as it is statistically more likely that tetrazine **6.5** will encounter **4.32** rather than the intermediate **6.29**. Using this methodology an inconsequential mixture of *syn/anti* monquinone **6.28** could be achieved with a 61% yield as an orange solid.

Interestingly, the stages for preparation of monoquinone **6.28** could be readily monitored by observation of the color of the reaction mixture. Tetrazine **6.5** is a bright magenta color in solution. At the start of the reaction, the mixture is a bright magenta color but once all of the tetrazine is consumed it turns a pale yellow color (Figure 6.10). Also, on large enough scale one can observe the formation of bubbles due to the expulsion of N_2. Then passing the crude reaction mixture through alumina results in a

bright orange solution indicating the elimination has occurred. ^{1}H NMR clearly established that only one quinone ring has been added Figure 6.11. At 7.01 and 7.03 ppm there are two singlets (one for *syn* and one for *anti*) indicating a quinone ring (H_b) has been incorporated. However, the apparent triplets at 6.91, 6.85, 4.30, and 4.29 ppm ($H_{c/c'}$ and $H_{e/e'}$ respectively) are diagnostic of a benzonorbornene olefin and bridgehead protons.

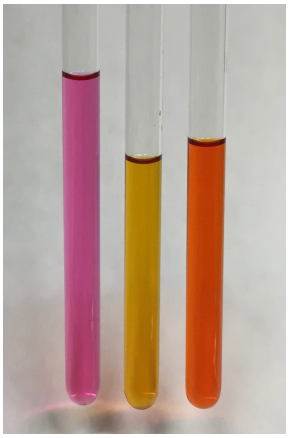

Figure 6.10 Representations of the colors observed during the cascade Diels–Alder reaction of tetrazine 6.5 with benzobisnorbornene 4.32 and after elimination. From left to right, the pink solution is tetrazine 6.5, the middle gold solution is the crude reaction mixture, the orange solution is after elimination.

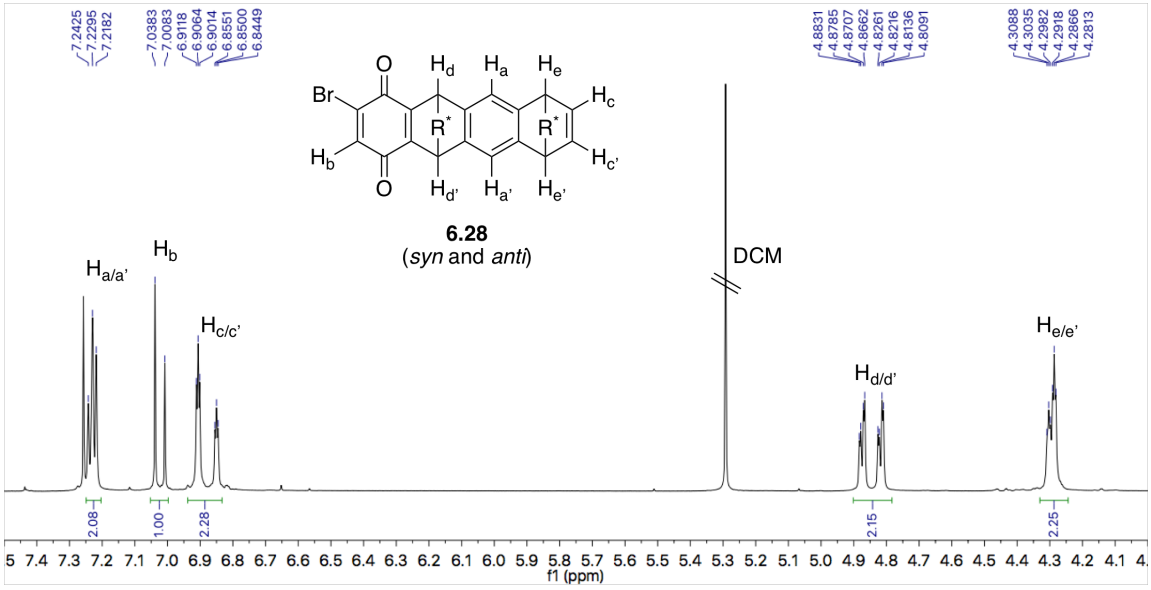

Figure 6.11 ^{1}H NMR of monoquinone 6.31 as a mixture of *syn* and *anti* isomers.

To gain more insight, both single and double Diels–Alder cascade reactions were monitored by ^{1}H NMR in 5 minute intervals. From these studies, the consumption of tetrazine **6.5** is rapid and it is consumed within 0.5 h at room temperature. Additionally, the only species observed in the spectra were bisbenzonorbornane starting material **4.32**, tetrazine, **6.5**, pyridazine by-product **6.8**, and dihydroquinone products. This indicated that the intermediate dihydropyridazine and isobenzofulvene, are very short lived and therefore the whole cascade process is rapid.

A control reaction was also performed and monitored by ^{1}H NMR, in which benzobisnorbornene **4.32** was treated with tetrazine **6.5** in the absence of a dieneophile to try and identify potential self-dimerization by-products. Within minutes the tetrazine **6.5** was consumed, pyridazine **6.8** was formed, indicating an isobenzofulvene had been generated, but no other by-products could be identified on the spectrum. In fact, there were no new peaks formed. Our best explanation for this outcome is that a polymerization occurred resulting in a low concentration of by-product that was not visible by ^{1}H NMR. Overall, we learned that these reactions need to be run in the presence of the dienophile and that decomposition of the isobenzofulvene can occur if the dienophile cannot be readily trapped.

With key intermediates bisquinone **6.27a** and monoquinone **6.28** in hand and a better understanding of our Diels–Alder cascade reaction, we were able to investigate macrocycle formation.

6.4.2. Attempts to Form a Macrocycle via Dimerization of Monoquinone 6.28 – Path A

Attempts at macrocycle formation were first made using the AB monomer monoquinone **6.28** as this appeared to be the most efficient route. Specifically, we targeted an [8]cyclacene precursor, which could be accessed through dimerization of **6.28** (Scheme 6.11a). We proposed this reaction could work if tetrazine **6.5** was slowly added to monoquinone **6.28,** thereby keeping the concentration of the intermediate isobenzofulvene **6.31** low relative to the dienophile **6.28**. Before the macrocycle could be closed, a dehydrohalogenation would need to be performed to bring the two end groups in closer proximity. While only the isomer where the internal benzonorborenes are *syn* can give macrocycle, we proposed that it would not need to be isolated as the *anti* isomer would likely polymerize upon introduction of **6.5** and be easily removed after the reaction.

Depending on the selectivity of the Diels–Alder reaction between **6.31** and **6.28** the probability of obtaining the necessary *syn* isomer could be rather low. In this case both the diene and dienophile have an EXO and ENDO face, Scheme 6.11b, plus theoretically the approach could be either exo or endo. Further complicating analysis of the outcome of the reaction, the bromine atoms of the quinones could end up either *cis* or *trans* from each other. Finally, if both *syn* and *anti* isomers of **6.28** are used this means there are two dienophiles in solution, further increasing the number of possible isomers. Using the 2^n rule (where $n = 5$ in this case), in total there are theoretically 32 different isomers of **6.32** that could be formed. By using only one isomer of **6.28** this number can be reduced to 16. Dehydrohalogenation then removes the *cis/trans* bromine isomer and

endo/exo isomer possibilities, further reducing this number to 4 different isomers of **6.33**. Due to the relative ease that *anti* **6.28b** could be isolated, it was used to investigate this dimerization.

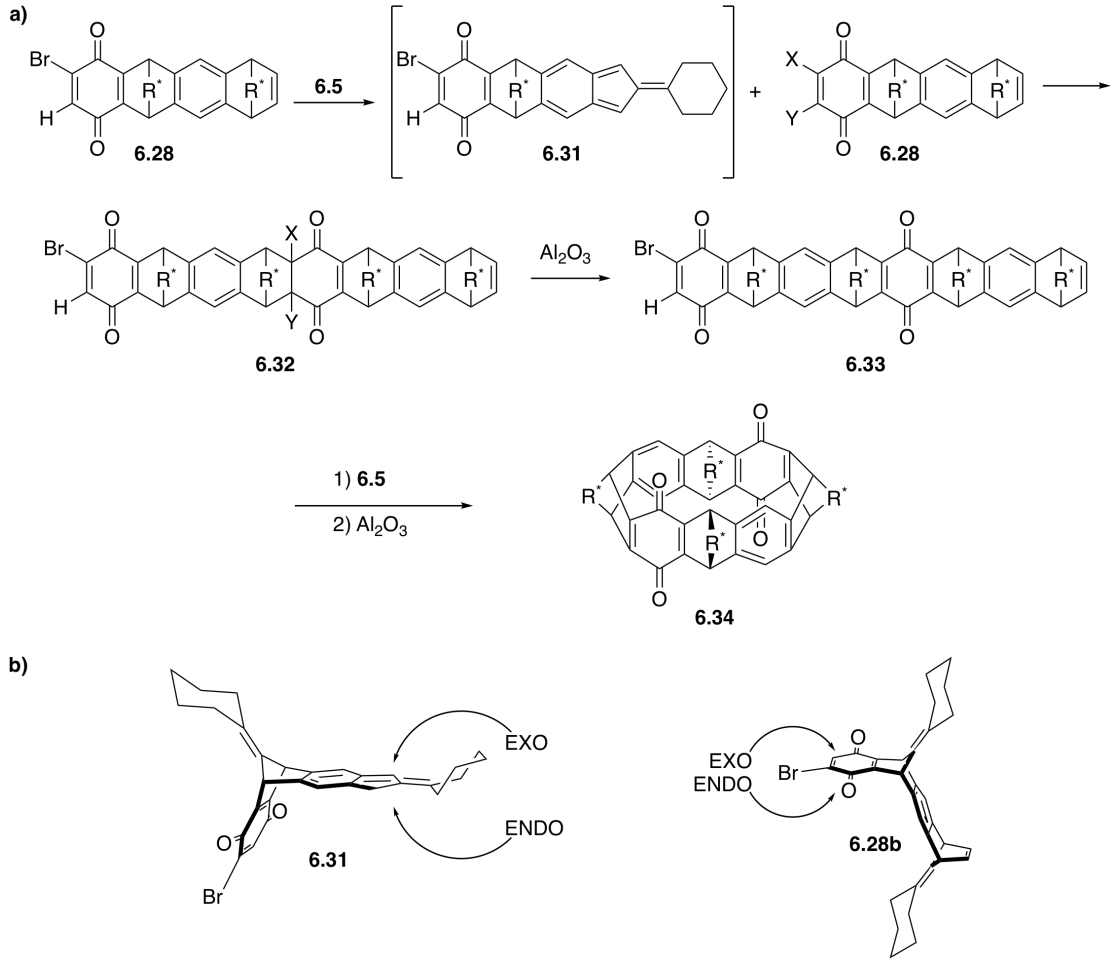

Scheme 6.11 Using AB monomer 6.31, a) proposed dimerization to form [8]cyclacene precursor, b) the EXO and ENDO faces of diene 6.32 and dienophile 6.31

Attempts were made to obtain ^{1}H NMR spectrum of dihydroquinone intermediate **6.32** to try and determine if there was a preference for endo or exo addition. However, the spectrum was not clean so no firm conclusions could be formed. Subjection of the crude reaction mixture to basic alumina resulted in a product with a promising ^{1}H NMR that had signals in the expected regions of the key diagnostic protons as shown in Figure 6.12. Gratifyingly LRMS also confirmed that a dimer had been formed.

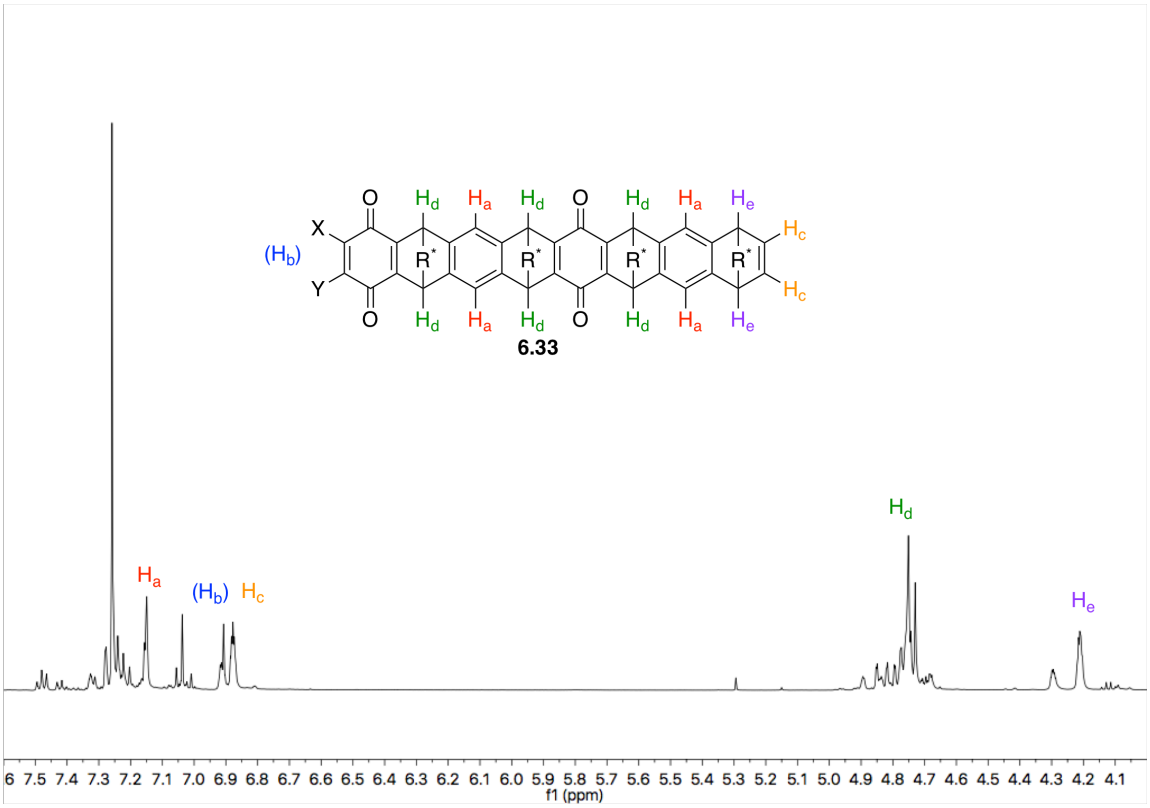

Figure 6.12 ^{1}H NMR of the dehydrohalogenated dimer of 6.28b. *Note, the labels H_{a-e} are for a general categories of key diagnostic regions, not for specific assignments.

Macrocyclization attempts using **6.33** were made, however, no evidence for the formation of macrocycle could be detected. We expected that the macrocycle would be easy to detect by ^{1}H NMR after elimination as all the bridgehead hydrogens would be equivalent, and all the hydrogens of the benzene rings would be equivalent, resulting in a spectrum with 2 strong singlets around the aromatic region. Rationalizing this outcome, there are two reasons the macrocycle may not have formed. First, it is possible that the two ends of the molecule were too far apart to come together in a Diels–Alder reaction. Building a model of the isobenzofulvene intermediate in Chem3D (shown in Figure 6.13) suggests this is a strong possibility. Second, it is possible that only the undesirable *anti* isomer was formed in appreciable quantities.

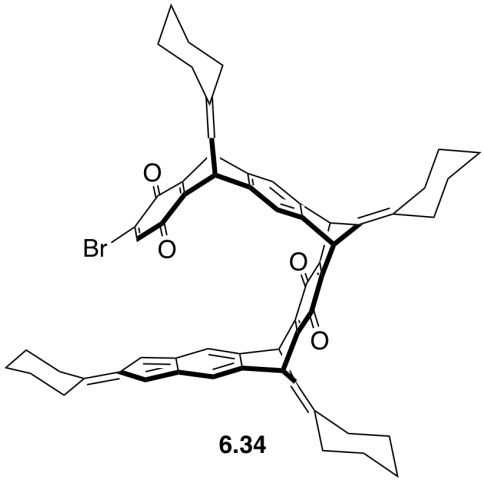

Figure 6.13 A 3-dimensional image of the isobenzofulvene intermediate generated from *syn* 6.33, generated using Chem3D, showing that there is too much space between the diene and dienophile for macrocycle closure.

We decided to reconsider the transition states for the formation of dimer **6.33** to try and assess which ones would be favored based on steric arguments. A few assumptions can be made to reduce the number of transition states to be considered. First, the relative orientation of the bromine atoms should have a negligible effect on the reaction pathway. Second, we assumed since we are bringing together a large diene and large dienophile an endo approach should be highly unlikely. A finding by Douglas group member Zhuoran Zhang, Figure 6.14, supports this assumption. He found that the Diels–Alder reaction between large isobenzofulvene **6.35** and large quinone **6.36** results in the formation of only exo products as determined by the ^{1}H NMR of the reaction mixture before elimination.

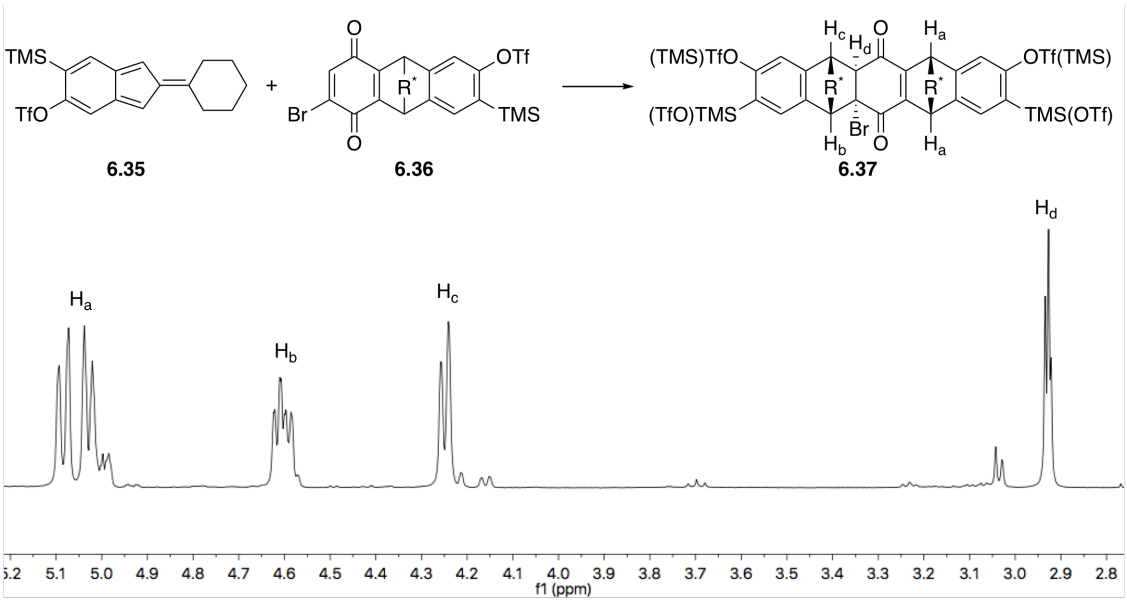

Figure 6.14 Zhuoran Zhang's Diels–Alder reaction between large isobenzofulvene 6.35 and large dienophile 6.36 to give only exo products as shown by the ^{1}H NMR spectrum.

Consideration of the remaining transition states is summarized in Figure 6.15. From these transitions states, the desired *syn* internal benzonorbornene isomer is only possible with an ENDO/EXO approach of the diene and dienophile respectively (first transition state). Based on our study of the preparation of bisquione **6.27**, we knew that both the EXO and ENDO faces of isobenzofulvene **6.31** are sterically accessible. We were hoping was that the ENDO face of quinone **6.28b** would be blocked by the bridge of the unsubstituted norbornene. This would then eliminate the second and fourth transition state both of which are unfavorable. However, after examining physical models and building these transition states in Chem3D all of the shown transition states look accessible. In fact, the ENDO face of **6.28b** actually looks less sterically encumbered. Therefore, with this reaction there is only probably a maximum of a 25% chance of obtaining the desired isomer.

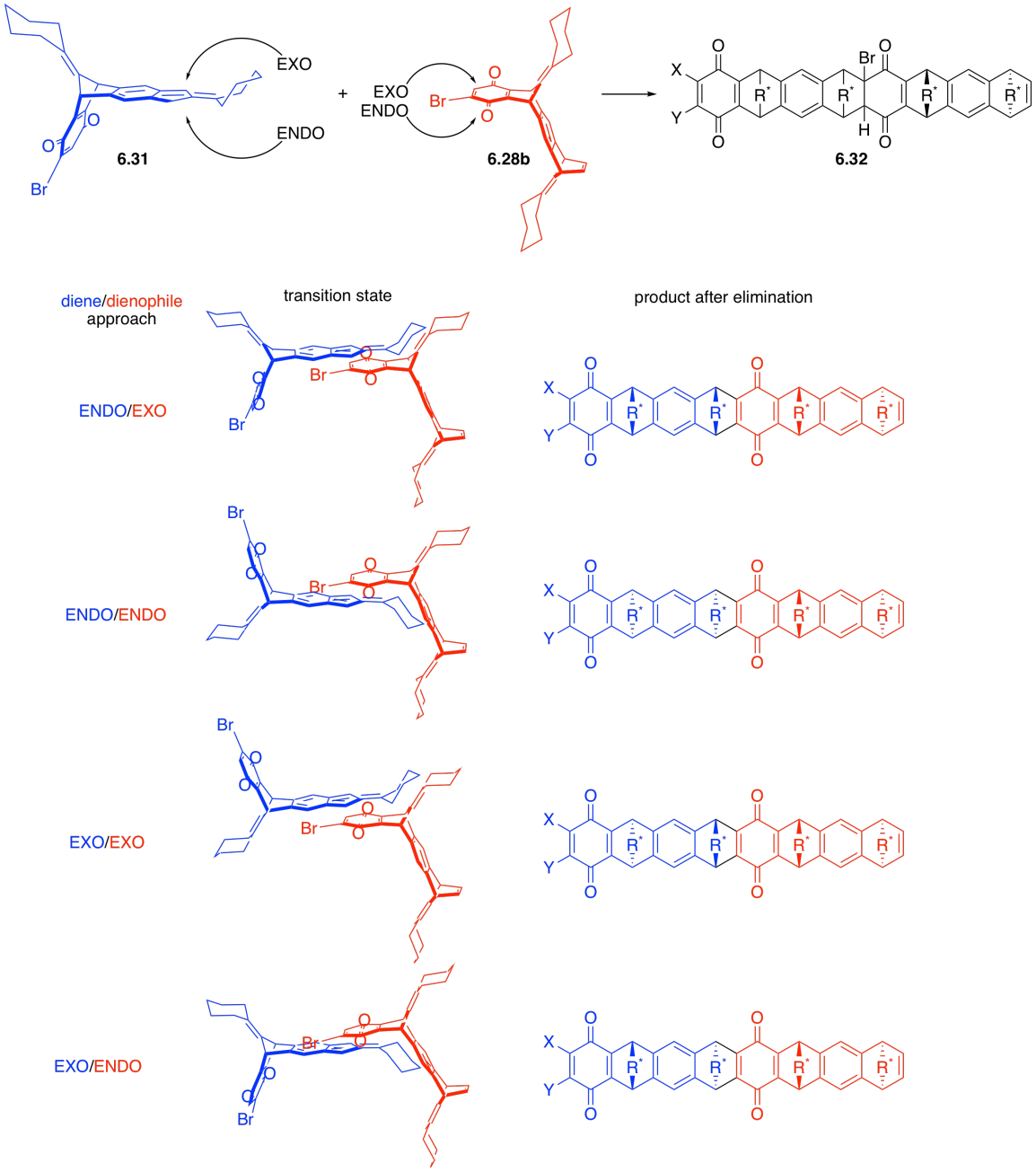

Figure 6.15 The proposed plausible transition states for the Diels-Alder reaction between large isobenzofulvene 6.31 and large quinone 6.28b.

Confirmation that the undesired isomer was formed was achieved by an independent synthesis of the desired *syn* isomer, Scheme 6.12. Coupling one equivalent of benzobisnorbornene **4.32** to bisquionone **6.27a** formed followed by treatment with basic alumina provided the *syn* isomer of **6.33**. Using this strategy, the norbornene rings

between the quinones are locked into a *syn* relationship. Once again assuming the isobenzofulvene from **4.32** is only able to approach by an exo orientation, there are eight different isomers of **6.32** (bromine atoms *cis/trans*, plus the diene and dienophile each have an EXO/ENDO face, 2^3) that could be formed, four of which have the desired *syn* relationship. Remarkably, the ^{1}H NMR of the product before elimination indicated only exo addition had taken place and 8 singlets could be seen around 2.7 ppm. Although the integrations are not completely correct, the rest of the spectrum looks extremely similar to what would be expected from such a structure, Figure 6.16.

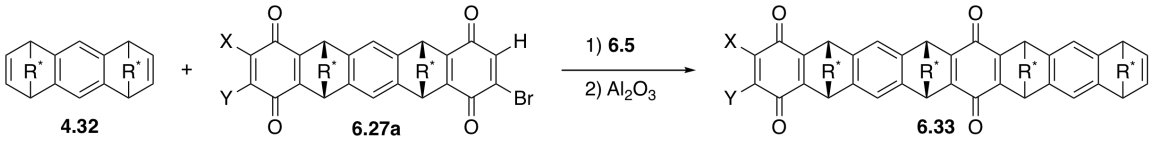

Scheme 6.12 Independent synthesis of the desired *syn* isomer of 6.32.

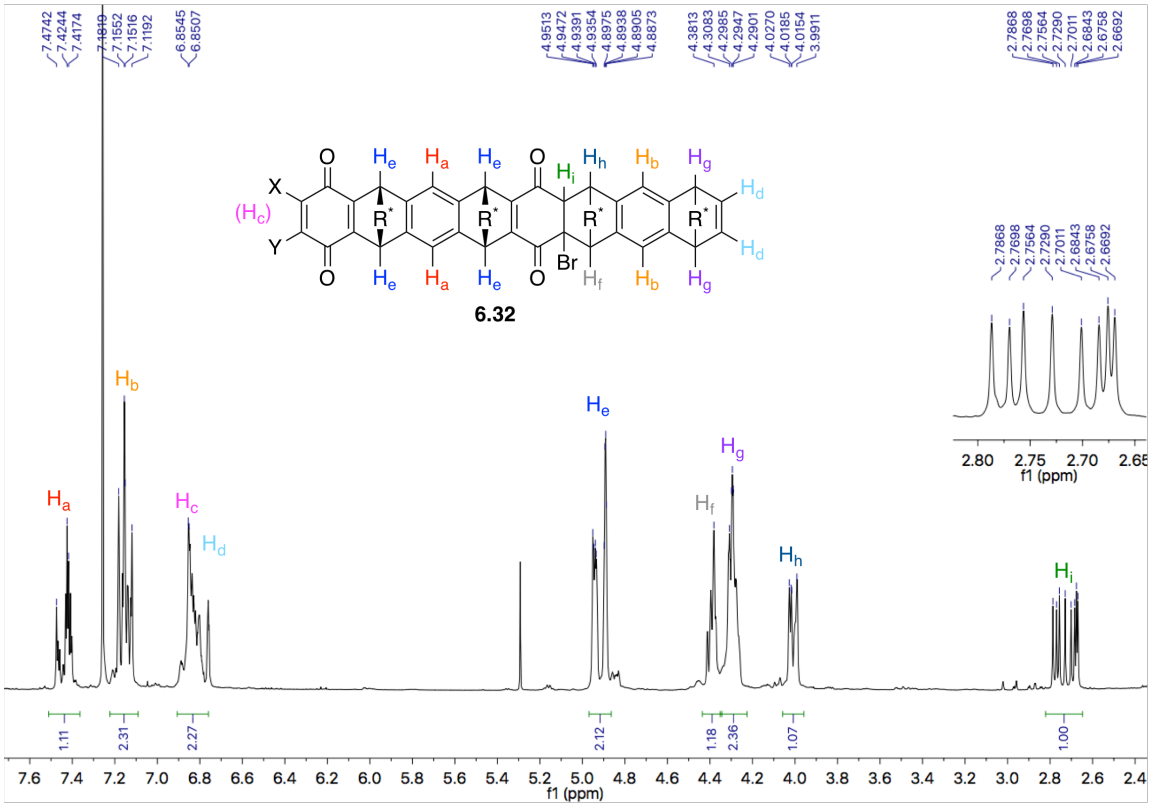

Figure 6.16 ^{1}H NMR of dihydroquinone 6.32 formed from the Diels–Alder cascade reaction of 4.32 and 6.27a.

Interestingly, after treatment with alumina all but two of those singlets disappeared suggesting two isomers are slow to undergo elimination. We assume this is a result of an increase in steric encumbrance of the HBr to be eliminated. As the systems get larger we have noticed that the elimination step takes longer (a couple of minutes vs overnight). After elimination of **6.32**, the 8 isomers should reduce to 4 different isomers of the **6.33**. Incredibly, 3 isomers can be distinctly seen based on the peaks corresponding to the terminal norbornene protons (H_d and H_f in Figure 6.17) supporting the assumption that two eliminations did not occur.

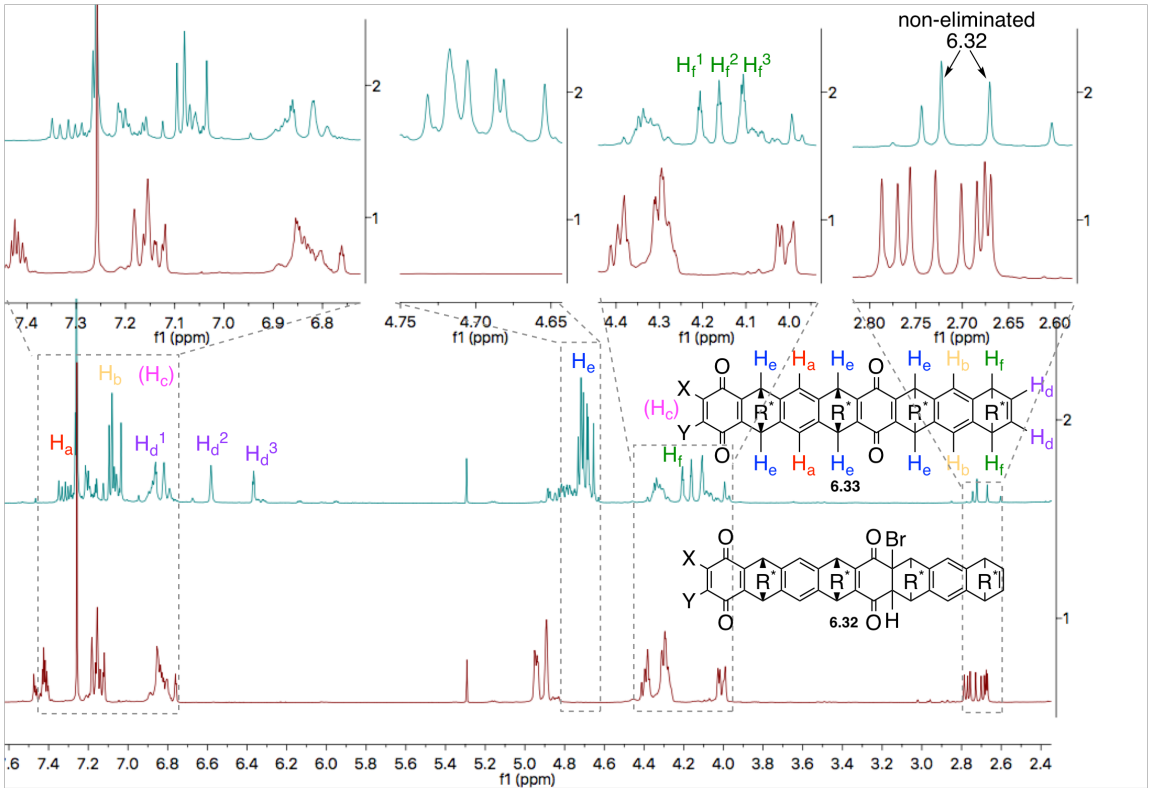

Figure 6.17 Comparison of the ^{1}H NMR spectra of 6.32 prepared from *syn*-bisquinone 6.27a with the eliminated product 6.33.

Unfortunately, the ^{1}H NMR spectrum of the eliminated products (**6.33**) from the dimerization attempt does not overlap with the reaction using **6.27a** (Figure 6.18). This suggests that the undesired *anti* isomers of **6.33** are favored when **6.28** is dimerized.

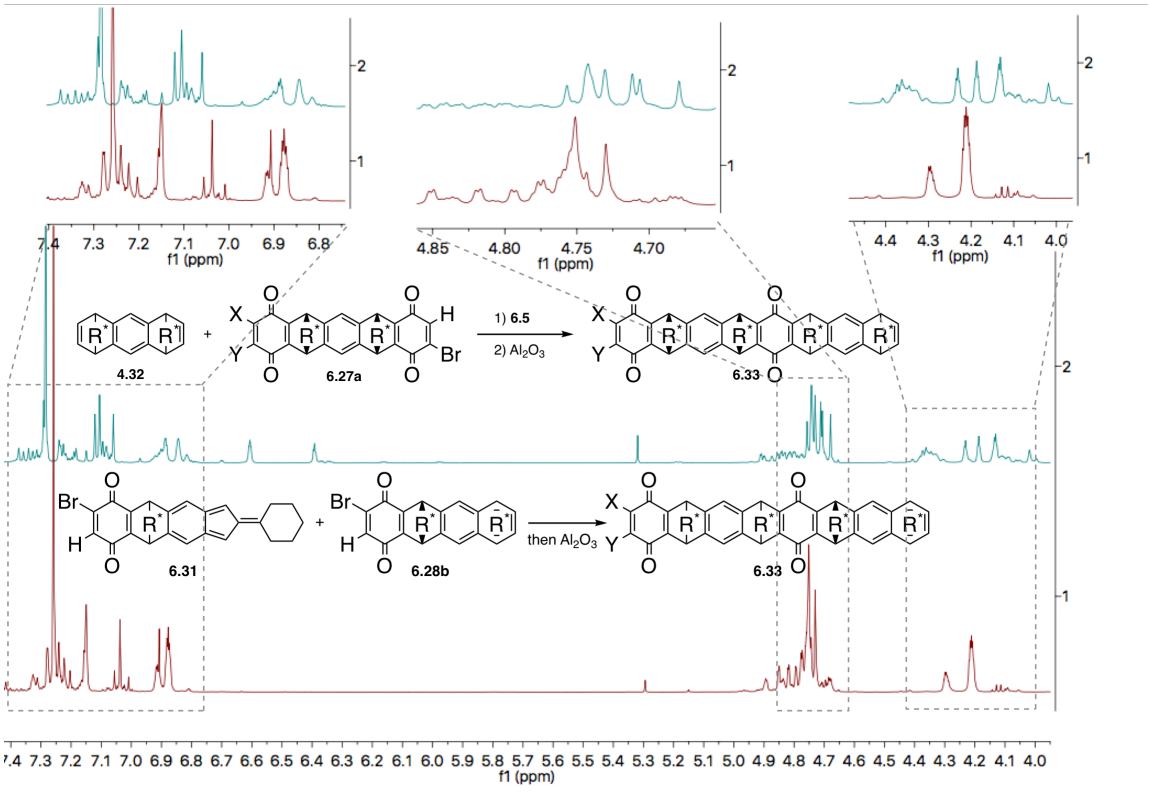

Figure 6.18 Comparison of the ^{1}H NMRs of the preparation of 6.32 from *syn*-bisquinone 6.27a (top) vs a dimerization of monoquinone 6.28b.

An attempt was made to form macrocycle from the promising product **6.33** generated from **6.27a** but the results were inconclusive. Two of the isomers of starting material **6.33** appeared to be consumed, and pyridazine by-product **6.8** peaks were observed, but no major new product emerged by ^{1}H NMR. We were at a loss for other ways to help determine the product as correlative techniques can be challenging to employ to study these reactions. For example these systems are difficult to monitor by MS as these quinones ionize poorly, have low solubility, and do not vaporize readily. IR is also not usually a viable option as there are multiple quinones making it difficult to

monitor the reaction by disappearance or formation of carbonyl signals. Since we did not observe macrocyle, we are worried that [8]macrocycle is too small of a ring to target using this chemistry as the diene and dienophile may be too far apart. In comparison, Stoddart's intermediates should have had similar curvature and he ended up making the framework for [12]cyclacene using high pressure.

Dimerization of monoquinone **6.28** appears to result in the formation of nonproductive *anti* isomers of **6.33**. Coupled with the observed low conversion of starting material to products, either from starting material decomposing or not reacting, we decided to set aside attempts to access macrocycle via dimerization or oligomerization reactions. However based on the described results, I would not recommend looking into oligomerization further.

6.4.3. Efforts to Form a Macrocycle from *syn*-bisquinone 6.27a – Path B

We next looked into advancing *syn*-bisquinone **6.27a** to a macrocycle precursor. In particular we wanted to work with a system in which at least two of the bridges are locked into place. The first reaction we tried was to couple monoquinone **6.28** onto **6.27a** (Scheme 6.13). A major benefit of this reaction is there is only one norbornene available for isobenzofulvene formation. Also, by slowly adding a solution of **6.28** to a mixture of **6.27a** with tetrazine **6.5** the relative concentration of **6.27a**, the intended dienophile, is high compared to **6.28**. This reduces the probability of self-dimerization of **6.28**. We proposed that triquione **6.38** could be transformed to [12]cyclacene precursor **6.41** by connecting the two terminal quinones through sequential Diels–Alder cascade and elimination reactions using key intermediate **4.32**.

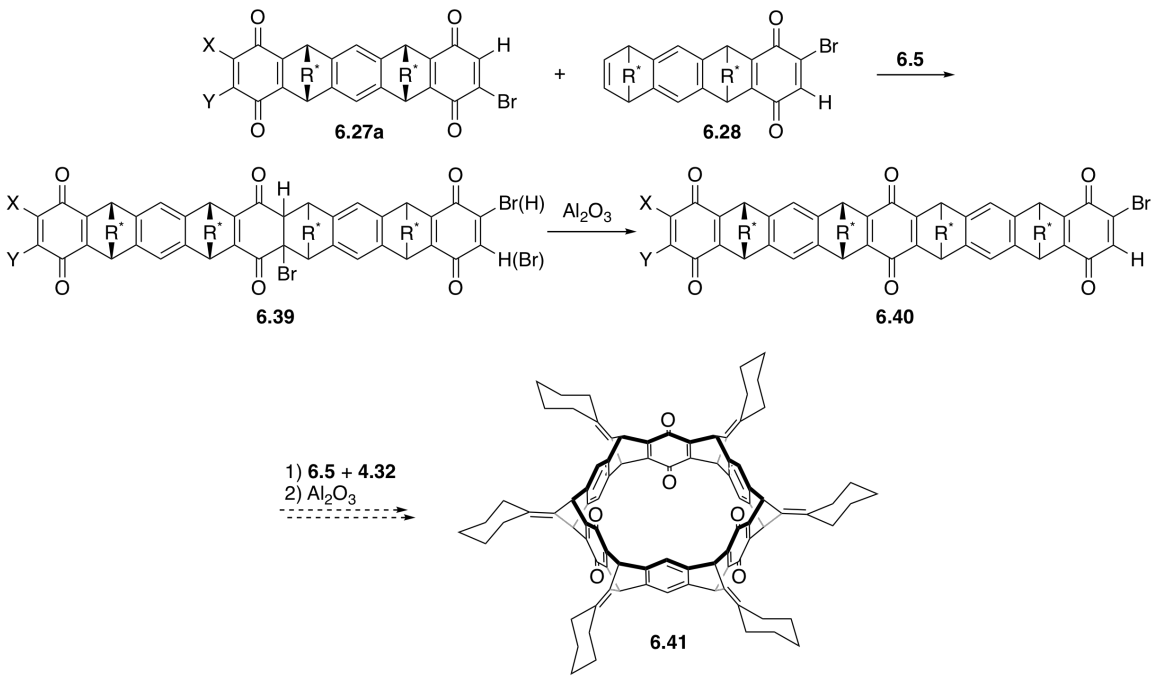

Scheme 6.13 Proposed synthesis to [12]cyclacene precursor 6.41 starting from 6.27a and 6.28.

The first Diels–Alder cascade reaction and elimination proceeded smoothly. By ^{1}H NMR there was no indication that **6.28** dimerized. Once again there are numerous isomers possible for this reaction. Assuming that the endo approach is inaccessible, there are still 16 possible isomers that could be formed. Both the diene and dienophile have an EXO and ENDO face, the bromine atoms of **6.27** could be *cis* or *trans*, and the bromine from **6.28** could end up on either side of the molecule (2^4, however two isomers are enantiomers so only 14 would be observed by ^{1}H NMR). Based on previous routes, we expect both the EXO and ENDO faces of the diene and dienophile to be accessible as the steric environments have not changed drastically.

The ^{1}H NMR spectrum for the products of this reaction (**6.39**, before elimination) shows that only exo addition occurred. Incredibly, through the use of apodization of the spectrum (exponential –3.10, Gaussian 1.00), all 14 singlets for the endo H (approximately 2.8 ppm) can be observed for each isomer (Figure 6.19)! Apodization is

needed as the isomers that vary only by the position of a bromine likely have extremely similar spectra. However, since all isomers appeared to have been formed in roughly equal amounts, this also means that only approximately 25% of the product mixture is the isomer in which all the bridges are *syn*.

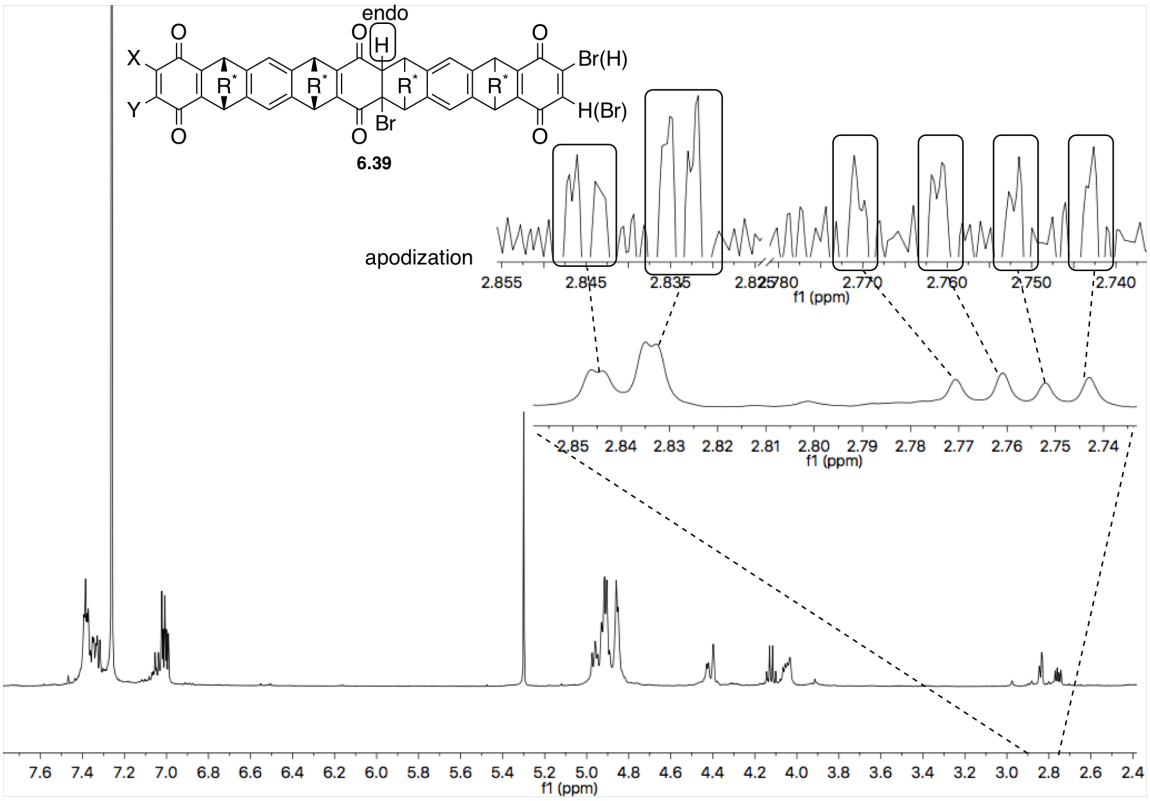

Figure 6.19 ^{1}H NMR of 6.39 highlighting the singlets for the endo H for each of the 16 anticipated isomers.

Dehydrohalogenation of **6.39** was readily achieved by stirring it in DCM with dry basic alumina overnight. The ^{1}H NMR confirmed the elimination was complete as the singlets around 2.8 ppm had disappeared. Determining the number of isomers represented in the spectrum though is less straightforward. If the bridges from **6.28** are *syn* relative to each other then there is a center of symmetry and some hydrogens on the molecule are equivalent. If instead they are *anti* then none of the hydrogens are equivalent. A diagnostic region for this analysis is around 7.0 ppm, where the hydrogens of the quinone

appear. Considering all the different isomers (Figure 6.20a) one would expect to see 12 singlets if all the isomers were present. Indeed, 12 singlets are observed in this region (Figure 6.20b, 7.0 ppm) further supporting that all of the EXO/ENDO combinations occurred.

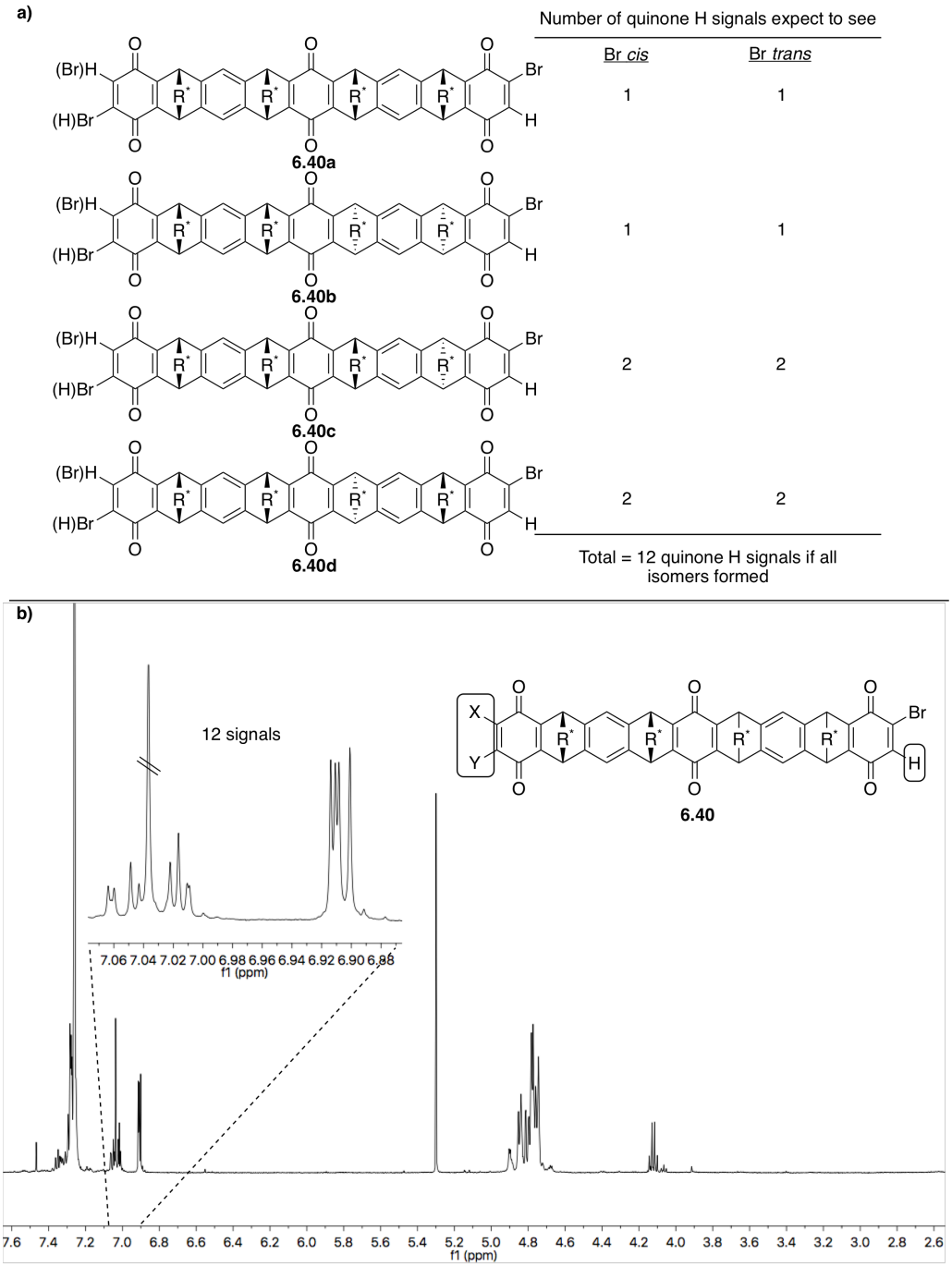

Figure 6.20 Considering the ^{1}H NMR spectrum expected for 6.40, a) the rational for the expected number of signals for the protons on the external quinones and b) the spectrum obtained after elimination of 6.39.

In addition to the low stereoselectivity of the reaction, unfortunately we also obtained a low yield of 27% for **6.39**. In monitoring this reaction by ^{1}H NMR, it appears that monoquinone **6.28** is rapidly consumed but a lot of the dienophile **6.27** is left

unreacted. This suggests that the generated isobenzofulvene is not efficiently trapped. Since both the diene and dienophile are bulky it is possible that they have a difficult time approaching each other. Although the ^{1}H NMR spectra from this reaction were remarkably clean this route was set aside.

For the next route we wanted to try to design a reaction that would yield a higher ratio of the *syn* isomer. We proposed that this could be achieved by coupling monobenzonorbornene **4.50** to *syn*-bisquinone **6.27a** (Scheme 6.14). By using **4.50** to generate isobenzofulvene **6.35**, the diene no longer has an EXO and ENDO face. Therefore the orientation of the new bridges will only depend on if **6.35** approaches from the EXO or ENDO face of **6.27a**. As a result, for each Diels–Alder cascade reaction, approximately 50% of the formed isomers should have the newly formed bridge *syn*. However, since this reaction would be performed on both sides, there is still only a 25% probability that the product with both new bridges *syn* to the existing ones will be formed. From **6.42**, we envisioned closing the all *syn* isomer to macrocycle **6.43** through double aryne formation and coupling using diazapyrone **3.8**.[10]

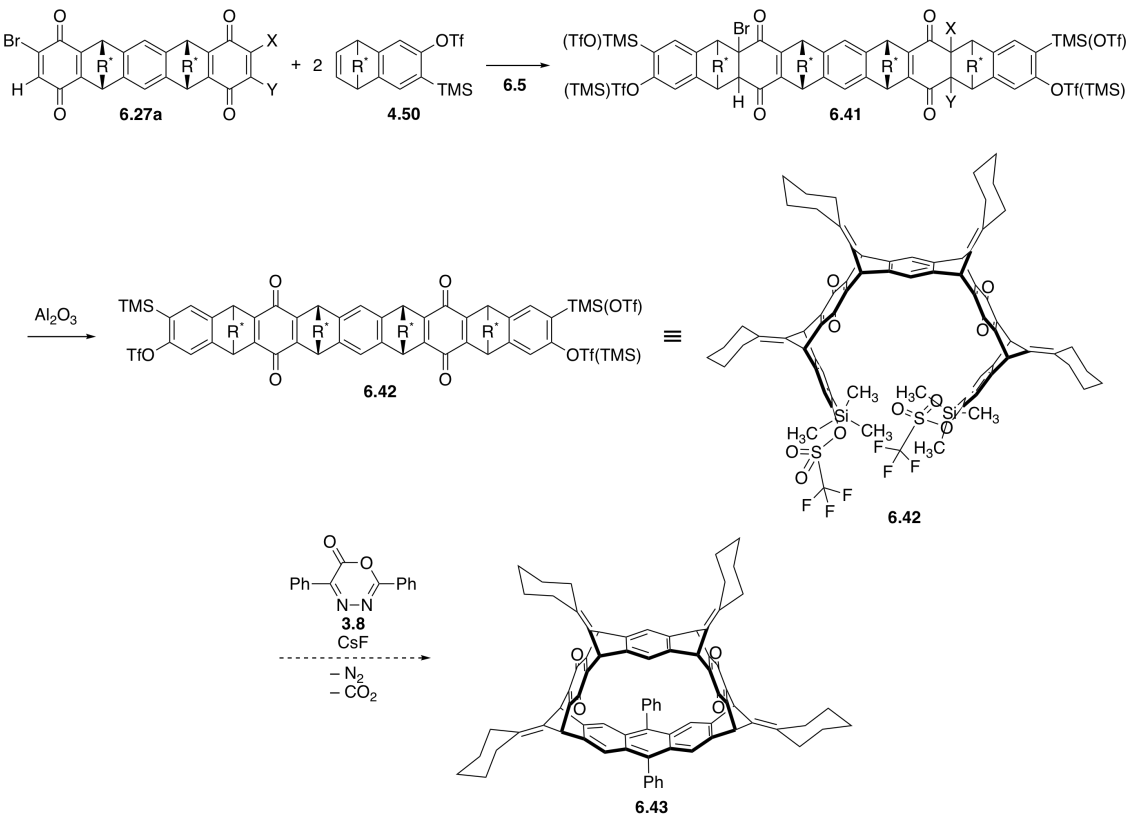

Scheme 6.14 Proposed synthesis of [10]cyclacene marcrocyclic framework.

In practice, we were easily able to add **4.50** to each side of **6.27a** using the Diels–Alder cascade reaction. We assumed that the quinones of **6.27a** were far enough apart to not influence the other's steric environment even after addition of the first isobenzofulvene **6.35**. However, since two Diels–Alder cascade reactions took place there were still a large number of isomers formed (each new bridge could be *syn* or *anti*, bromine atoms of **6.27a** were *cis* or *trans*, and the new TMS/OTf positions varied, leaving 2^5 or 64 isomers, but due to the symmetry of the molecule numerous isomers are equivalent or enantiomers). Due to the large number of products, looking at the ^{1}H NMR of the reaction mixture is primarily useful for identifying if both quinones of **6.27a** trapped an isobenzofulvene. The absence of singlets at or around 7.01 ppm and the

appearance of new signals around 2.7 ppm confirm that both quinones reacted and that the Diels–Alder occurred in an exo fashion.

Elimination using dry basic alumina proceeded to completion as indicated by the disappearance of the signals around 2.7 ppm. If both the EXO and ENDO faces of **6.27a** were accessible during the Diels–Alder reaction, then after elimination there should be 6 isomers distinguishable by ^{1}H NMR (the total number of isomers is higher but many are enantiomers of each other and therefore should have the same spectrum). These would result from a *cis/trans* relationship of the TMS groups when the new bridges are both *syn*, one *syn* one *anti*, and both *anti* to the existing bridges (Figure 6.21a **6.42a–f**). Surprisingly, looking in the TMS region of the ^{1}H NMR spectrum there appears to be only two major products (Figure 6.21b, 0.231 and 0.228 ppm).

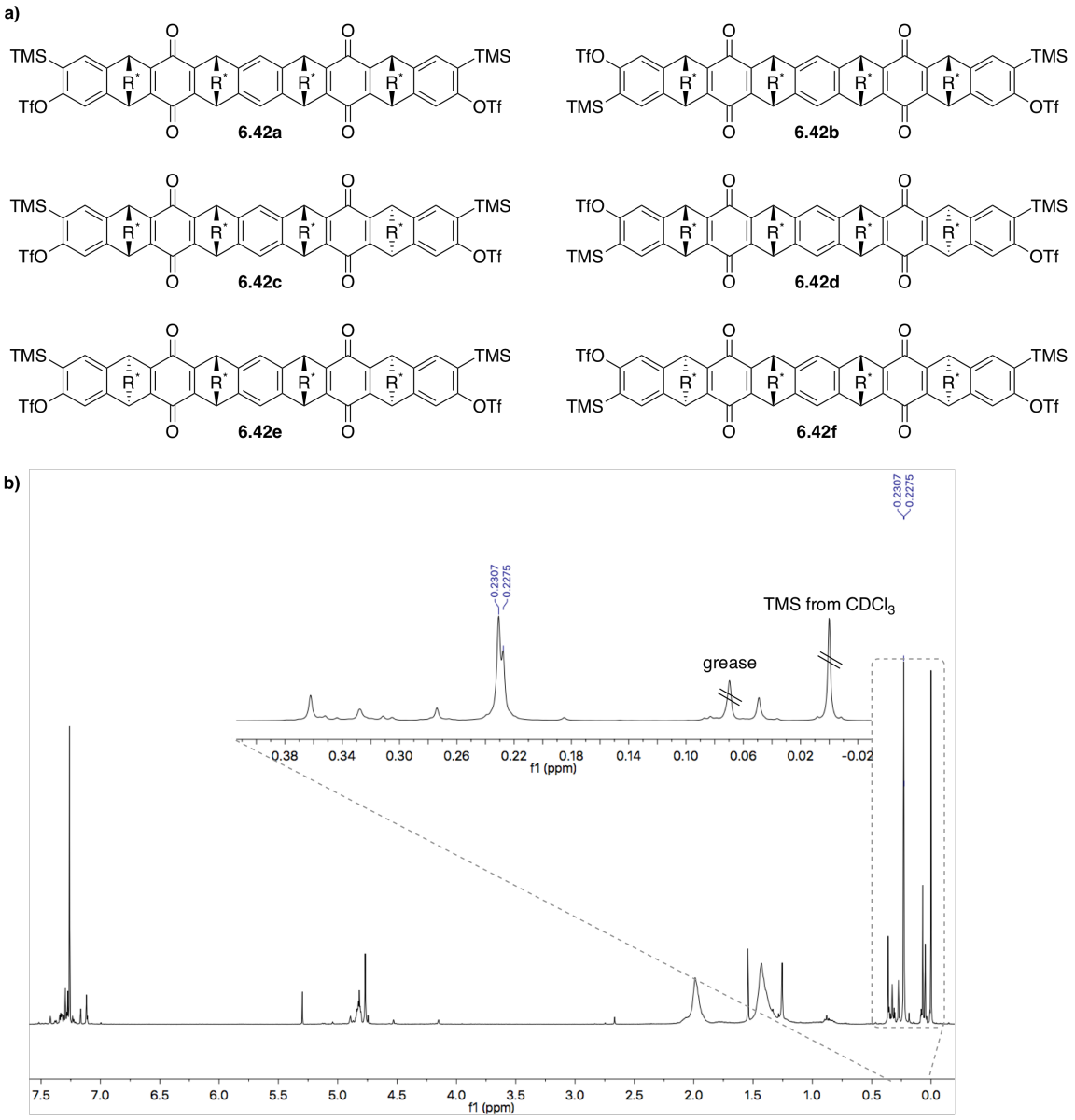

Figure 6.21 Analysis of the mixture of isomers of 6.42 a) the isomers that would have different NMR spectra and b) the observed ^{1}H NMR spectrum for the products after elimination of the product of the double Diels–Alder cascade reaction between 6.27a and 4.50.

It is highly possible that isobenzofulvene **6.35** selectively added to the EXO face of *syn*-bisquinone **6.27a**. When Zhuoran Zhang used this isobenzofulvene he observed that the Diels–Alder reaction proceeded with selectivity for EXO-exo addition (Figure 6.22). It can be assumed once again that endo addition is not possible due to the steric bulk of the isobenzofulvene. This means that the ENDO face of quinone **6.36** was

inaccessible. It was believed that this was a result of the steric encumbrance induced by the TMS and triflate group of the dienophile. However, there may be some other factors we are not yet aware of that induced this selectivity.

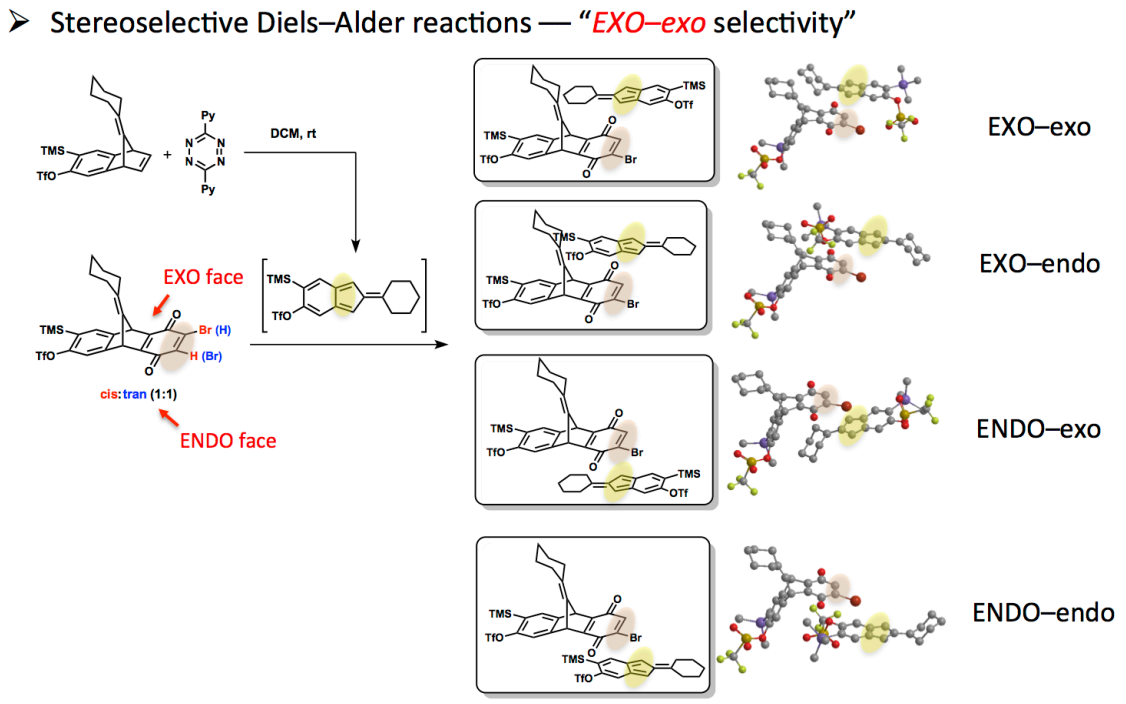

Figure 6.22[11] The steric analysis Zhuoran Zhang used to explain the observed EXO–exo selectivity when he used isobenzofulvene 6.35.

Encouraged by the possibility that the desired all *syn* isomer was formed, efforts were made to close the macrocycle. Treatment of bisaryne precursor **6.42** with CsF in the presence of diazapyrone **3.8** did not appear to yield the desired macrocycle. Interestingly though, both the ^{1}H NMR and ^{19}F NMR of the crude reaction mixture (Figure 6.23) appeared to be a pure sample of the major isomer **6.42** from the previous reaction. We hypothesize that the all *syn* isomer of **6.42** is very crowded around the TMS groups making it difficult for the fluoride to access them. However, all the other isomers have less steric hindrance, which may allow for faster aryne formation. If this is true, then it would be possible that the *anti* isomers reacted but the all *syn* isomer was not. The

product of this reaction then would be been oligomerization of *anti* **6.42**, which would not be visible by NMR. Potentially, further insight to determine if all the major isomers have the all *syn* relationship could be gained by reducing off the TMS and OTf groups.

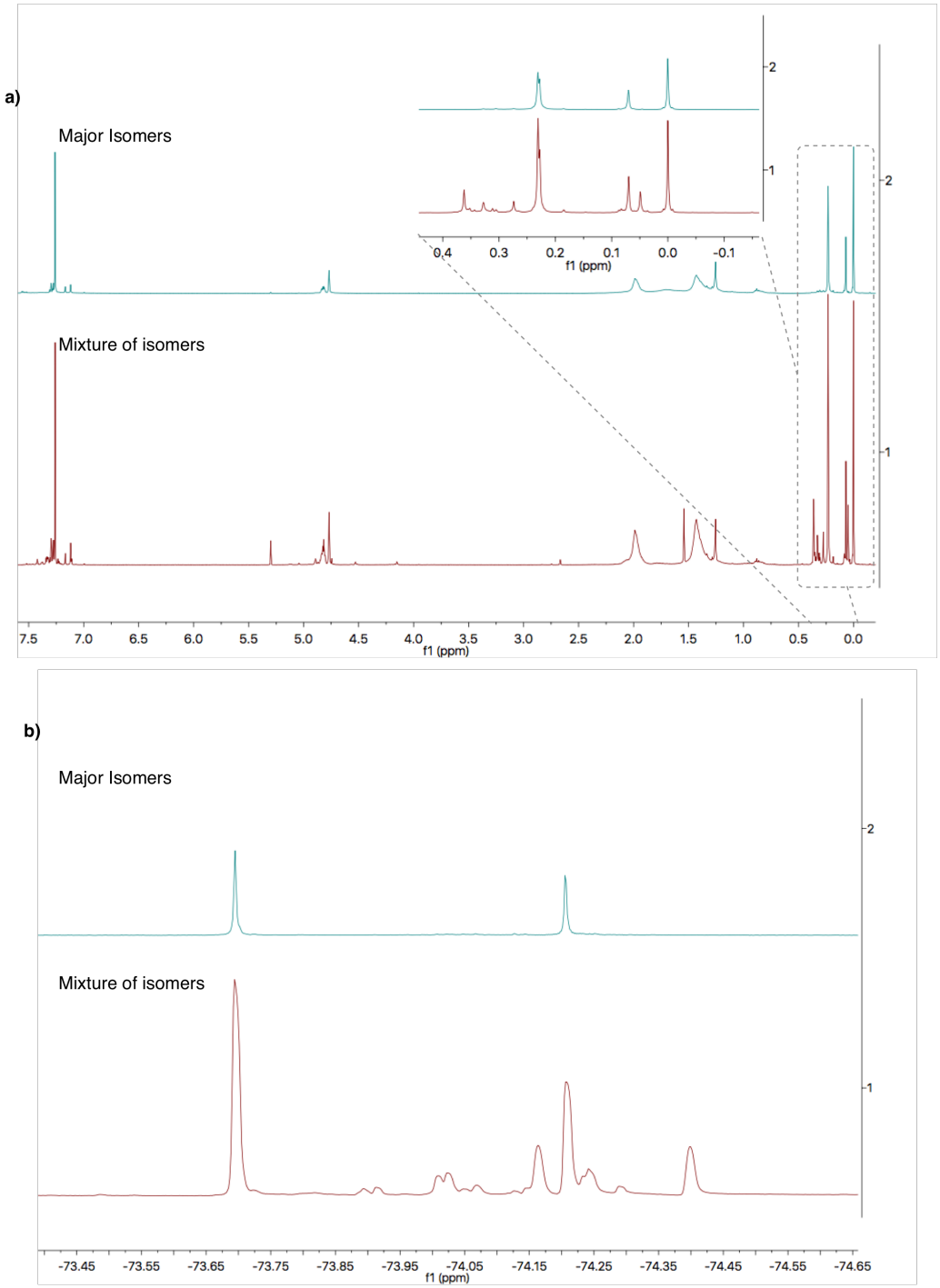

Figure 6.23 Comparison of the NMRs of the starting material 6.42 (bottom spectrum) and after macrocyle formation attempt (top spectrum) a) ^{1}H NMR and b) ^{19}F NMR.

Unfortunately, resubjection of the isolated starting material to the reaction conditions at 40 °C still resulted in no reaction. Zhuoran has also attempted to couple arynes attached to a norbornene ring via diazapyrone **3.8** but was been unable to detect

any indications of product formation. A model study was performed to probe how readily the Diels–Alder cascade of diazapyrone **3.8** and an aryne attached to a norbornene, as in **4.50**, occurs (Scheme 6.15). One concern was that the intermediate after the first Diels–Alder reaction **6.45** may undergo alternative retro Diels–Alder reactions or unexpected rearrangements. While running the reaction the solution turned from light yellow to bright orange which is an indicator for the formation of a conjugated system such as the anthracene of **6.44**. However, when a ^{1}H NMR spectrum of the reaction mixture was obtained a significant amount of the starting aryne precursor remained and no major product could be identified. As of right now, this model study is inconclusive and further investigations should be made.

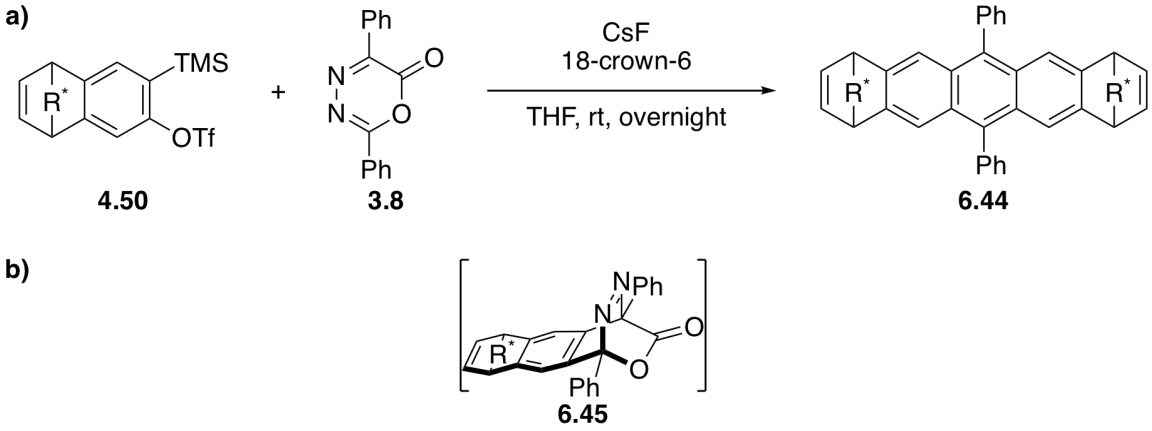

Scheme 6.15 Model study of Diels–Alder cascade using aryne generated from 4.50 and 3.8 a) the reaction scheme and b) the intermediate after the first Diels–Alder reaction.

6.4.4. Conclusions and Future Work

Efforts towards forming a macrocycle have been most successful using the Diels–Alder cascade reaction to generate isobenzofulvene moieties from benzonorbornenes and trapping them with dibromoquinone, followed by dehydrohalogenation using basic alumina. One major challenge though has been achieving stereoselective reactions to obtain the desired *syn* relationship of the bridges. In general, when the dienophile is

small, such as dibromoquinone **6.20**, endo addition will be favored. Once the quinone is substituted though, then exo addition predominates. If the dienophile has both an EXO and an ENDO face, it is desirable for EXO attack to occur. In most of our systems, the ENDO face is not significantly hindered and gets attacked as well. This unfortunately leads to a large loss of material. It also seems favorable to use dienes that do not have an EXO and ENDO face since these are rarely differentiated, but only ENDO will lead to the desired product.

It is strongly recommended that efforts towards a macrocycle should persist using this methodology. These reactions are exceptionally easy to perform and the products are readily identified by ^{1}H NMR. Moving forward, other deuterated solvents, such as benzene-d_6, should be explored as a means to obtain improved resolution of signals in the aromatic region of the ^{1}H NMRs. Future work should include a more thorough investigation into the model study shown in Scheme 6.15. If the arynes can be coupled via diazapyrone **3.8**, then efforts to close the [10]cyclacene precursor **6.42** should be performed. If however there is evidence that the arynes cannot be coupled using **3.8**, then the arynes should be trapped instead with fulvene **4.31**. These terminal benzonorbornenes could then be coupled to a single quinone using sequential Diels–Alder cascade/elimination reactions to give a [12]cyclacene precursor. Alternatively, we propose that a [12]cyclacene precursor could be obtained by coupling bisquinone **6.27a** with bis(isobenzofulvene) precursor **6.46** (Scheme 6.16).

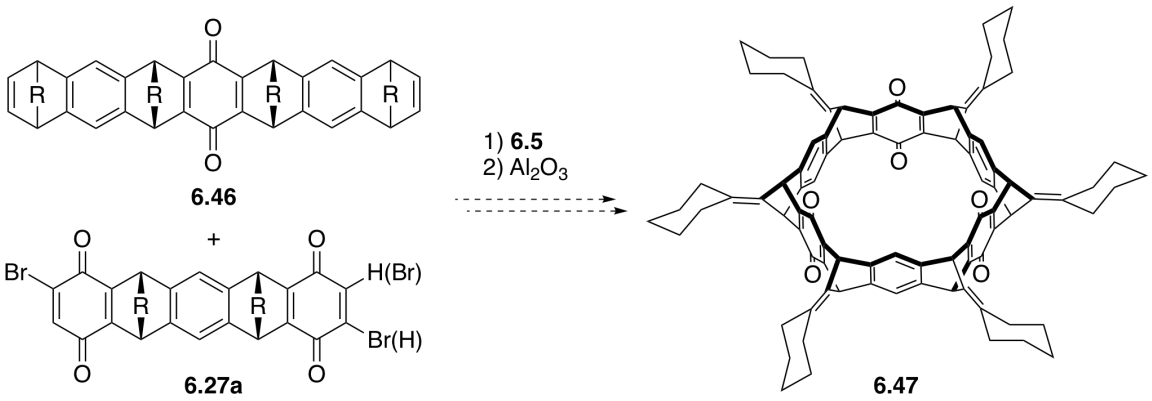

Scheme 6.16 Proposed preparation of a [12]cyclacene precursor

Future studies could also investigate methods to block the ENDO face of the dienophile. One idea would be to not perform the elimination after the addition of the second quinone to **6.28**. Since dibromoquinone **6.20** adds in an endo fashion, the newly added quinone would add steric bulk to the ENDO face of **6.48** (Figure 6.24). This additional bulk may be enough to block attack by an isobenzofulvene to the ENDO face. Additionally, a model study could be carried out to see if before elimination, the Diels–Alder between isobenzofulvene and dibromoquinone is reversible at high temperatures. If so perhaps more product could be obtained through equilibration reactions of the *anti* isomers.

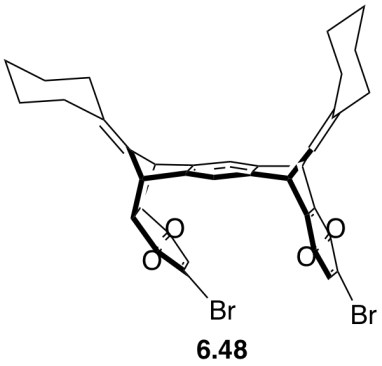

Figure 6.24 Proposed endo dihydroquinone 6.48. The ENDO face of the dienophile of this molecule could potentially be sterically hindered enough to prevent diene addition to this face.

Finally work also needs to be done to investigate the end game strategy. The difficulty with which the norbornene alkene was dihydroxylated using OsO_4 leaves us slightly worried that it will be difficult to oxidize the tetrasubstituted alkene bridges. A model study of our end game strategy could be readily carried out using *syn* **6.26a** (from Scheme 6.8). Along with investigating the oxidation of the alkene bridges, this compound could also be used to investigate conditions that will allow for addition into the quinones and subsequent oxidation.

While the formation of the macrocycle has proven to be challenging, I believe the Douglas group's end-game strategy for forming cyclacene is solid and should work. Additionally I believe that my group members, working as a team, will be able to achieve this goal. It is my hope that the work outlined in this dissertation will serve as a guide and has laid the groundwork for the first cyclacene to be prepared in the near future.

6.5. Experimentals

All reactions were carried out using flame-dried glassware under nitrogen atmosphere unless aqueous solutions were employed as reagents. Tetrahydrofuran (THF) was dried by distillation from benzophenone/sodium under nitrogen. Dichloromethane (DCM) was dried by distillation from CaH_2 under nitrogen. All other chemicals were used as received unless otherwise noted.

Analytical thin layer chromatography (TLC) was carried out using 0.25 mm silica plates from Silicycle. Eluted plates were visualized first with UV light then they were stained using $KMnO_4$. Flash chromatography was performed using 230–400 mesh (particle size 0.04–0.063 mm) silica gel purchased from Silicycle. ^{1}H NMR (500, 400 MHz), ^{13}C NMR (126 MHz), ^{19}F NMR (471 MHz) spectra were obtained on a Bruker FT

NMR instruments. NMR spectra were reported as δ values in ppm relative to TMS for ^{1}H (0.00 ppm), and chloroform for ^{13}C (77.16 ppm). ^{1}H NMR coupling constants are reported in Hz; multiplicity is indicated as follows; s (singlet); d (doublet); t (triplet); q (quartet); m (multiplet); dd (doublet of doublets); ddd (doublet of doublet of doublets); dt (doublet of triplets); app (apparent); br (broad).

Infrared (IR) spectra were obtained as films from DCM or $CDCl_3$ on sodium chloride plates or as KBr pellets on a Thermo Scientific FT-IR. High-resolution mass spectra (HRMS) for electrospray (ESI) experiments were performed on a Bruker BioTOF II. HRMS using GC-MS (QTOF) was performed on an Agilent 7200-QTOF GC/MS, GC column RTX-5MS 30 m length, 0.255 mm ID, 0.25 μm. Method: inlet temperature 250 °C, source temperature 280 °C. The initial column temperature was 120 °C and was held for 4 minutes after injection. Column temperature was ramped to 325 °C over 10 minutes and then held for 31 minutes. Alternatively, the column was bypassed using a solid injection probe. Method: Initial temperature of 80 °C was ramped at a rate of 45 °C/min up to 320 °C and held at 320 °C for 3 minutes.

Dibromoquinone 6.20

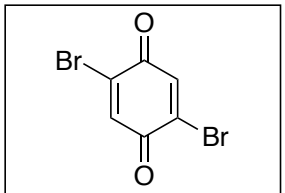

6.20

$C_6H_2{}^{79}Br^{81}BrO_2$

Exact Mass: 264.8450

Oxone (2.18 g, 7.1 mmol) was dissolved in a solution of acetonitrile (10.3 mL) and water (30.8 mL). At room temperature and while stirring, a suspension of dihydroquinone **4.46** (0.92 g, 3.4 mmol) in acetonitrile (4.1 mL) was added

to the solution. KBr (0.84 g, 7.1 mmol) was then added portionwise and the reaction was allowed to stir at room temperature for one hour.[9] The reaction mixture was then diluted with water (30 mL).[10] The product was extracted from the aqueous phase using diethyl ether (3 × 40 mL). The combined organic fractions were then washed with brine (1 × 50 mL), dried (Na_2SO_4), and concentrated to give a red solid (0.89 g). Purification by flash chromatography (15% EtOAc : 85% hexanes) provided **6.20** as a yellow solid (0.40 g, 1.5 mmol, 44%).

R_f = 0.63 (15% EtOAc : 85% hexanes).

^{1}H NMR (400 MHz, $CDCl_3$) δ 7.48 (s, 2H).

^{13}C NMR (100 MHz, $CDCl_3$) δ 177.1, 137.9, 137.2.

IR (film) 3059, 1668, 1587, 1312, 1191, 998, 902, 792, 675 cm^{-1}.

Mp 182–184 °C.

HRMS (QTOF) *m/z* 264.8446 (264.8450 calcd for $C_6H_2Br_2O_2$, (M^+)).

[9] On larger scale the resultant yellow precipitate, which is product, can be filtered and washed with large amounts of water.

[10] Caution: HBr is a by-product of the reaction; it can be removed with additional water washes as necessary

Dihydroquinone 6.22

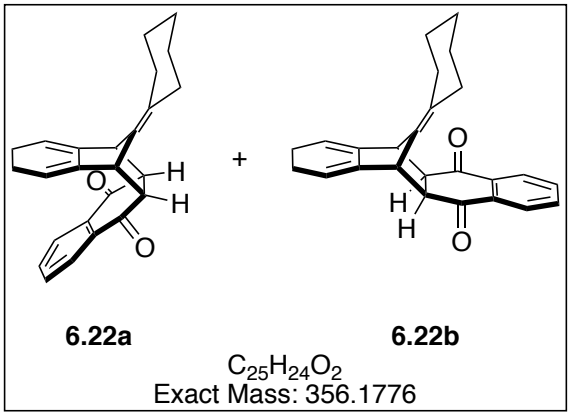

Norbornene **4.37** (11.1 mg, 0.05 mmol), naphthoquinone **6.21** (7.9 mg, 0.05 mmol), and tetrazine **6.5** (11.8 mg, 0.05 mmol) were placed in a round bottom flask. DCM (2.5 mL) was then added and the reaction was allowed to stir at room temperature for 3.5 h. The reaction mixture was then washed with 1M HCl (2 × 1 mL) and brine (1 × 1mL), dried ($MgSO_4$) and concentrated to give **6.22** (16.6 mg, 0.047 mmol, 94 %) as an orange-brown oil as a mixture of diastereomers. These diastereomers were unassigned and characterized as a mixture.

Major diastereomer of **6.22**:

^{1}H NMR (500 MHz, Chloroform-*d*) δ 7.72 (AA'BB', *J* = 6.4, 0.2, 7.7, 1.5 Hz, 2H) 7.46 (AA'BB', *J* = 7.3, 0.5, 7.9, 1.3 Hz, 2H), 6.96 (AA'BB', *J* = 7.7, 0.7, 6.8, 0.6 Hz, 2H), 6.73 (AA'BB', *J* = 7.6, 0.6, 7.4, 1.1 Hz, 2H), 4.48 (app dd, *J* = 2.8, 1.7 Hz, 2H), 3.60 (app dd, *J* = 2.8, 1.7 Hz, 2H), 2.25 – 2.29 (m, 2H), 2.11 – 2.06 (m, 2 H), 1.60 – 1.54 (m, 3H), 1.49 – 1.43 (m, 3H).

^{13}C NMR (126 MHz, Chloroform-*d*) δ 197.3, 143.0, 135.3, 133.8, 126.4, 126.4, 122.3, 50.4, 50.1, 31.0, 28.0, 26.7.

Minor diastereomer of **6.22**:

^{1}H NMR (500 MHz, Chloroform-*d*) δ 8.12 (AA'BB', *J* = 7.3, 0.4, 7.8, 1.3 Hz, 2H), 7.75 (AA'BB', *J* = 6.3, 0.2, 7.7, 1.4 Hz, 2H), 7.36 (AA'BB', *J* = 7.7, 0.6, 7.3, 1.1 Hz, 2H), 7.17 (AA'BB', *J* = 6.6, 0.3, 7.2, 1.2, 2H), 4.30 (s, 2H), 2.97 (s, 2H), 1.88–1.81 (m, 2H), 1.70 – 1.64 (m, 2H), 1.34 – 1.30 (m 3H), 1.16 – 1.12 (m 2H).

^{13}C NMR (126 MHz, Chloroform-*d*) δ 197.2, 141.6, 134.4, 127.2, 126.7, 123.2, 121.0, 51.9, 51.1, 30.5, 27.3, 26.1.

Mixture of isomers:

R_f = 0.48 (5% Toluene : 95% Hexanes).

IR (film) 3068, 3005, 2927, 2852, 1679, 1593, 1461, 1447, 1295, 1265, 9922, 310, 729 cm^{-1}.

Quinone 6.24

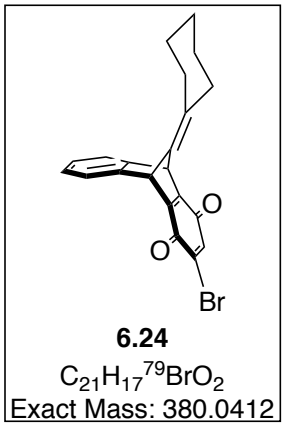

6.24

$C_{21}H_{17}{}^{79}BrO_2$

Exact Mass: 380.0412

Benzonorbornene **4.37** (111.2 mg, 0.5 mmol), dibromoquinone **6.20** (146.2 mg, 0.55 mmol), and tetrazine **6.5** (129.9 mg, 0.55 mmol) were placed in a round bottom flask. DCM (25 mL) was added and the reaction was allowed to stir at room temperature for 2.5 h. The reaction mixture was then washed with 1M HCl (2 × 15 mL), water (1 × 20 mL), and brine (1 × 20 mL), dried ($MgSO_4$) and concentrated to give

a gold foam (219.8 mg). Purification via flash chromatography (5% acetone : 95% hexanes) provided quinone **6.24** as a gold solid (180 mg, 0.39 mmol, 78%).

$\mathbf{R_f}$ = 0.21 (30% DCM : 70% hexanes).

^{1}H NMR (400 MHz, Chloroform-*d*) δ 7.34 – 7.37 (m, 2H), 6.99 (AA'BB', *J* = 7.7, 0.0, 7.3, 1.1 2H), 4.98 (d, *J* = 1.7 Hz, 1H), 4.92 (d, *J* = 1.8 Hz, 1H), 1.95 – 2.14 (m, 4H), 1.38 – 1.53 (m, 6H).

^{13}C NMR (126 MHz, Chloroform-*d*) δ 180.8, 175.4, 159.0, 157.8, 155.7, 147.3, 147.2, 137.1, 136.9, 125.8, 122.5, 117.1, 49.4, 48.8, 29.8, 29.7, 27.2, 27.2, 26.4.

IR (film) 3063, 2927, 2852, 1665, 1649, 1567, 1448, 1303, 1249, 1077, 1249, 1077, 884, 736 cm^{-1}.

HRMS (ESI) *m/z* 403.0308 (403.0309 calcd for $C_{21}H_{17}BrO_2$, $(M + Na)^+$).

Bis(benzonorbornene)quinone 6.26

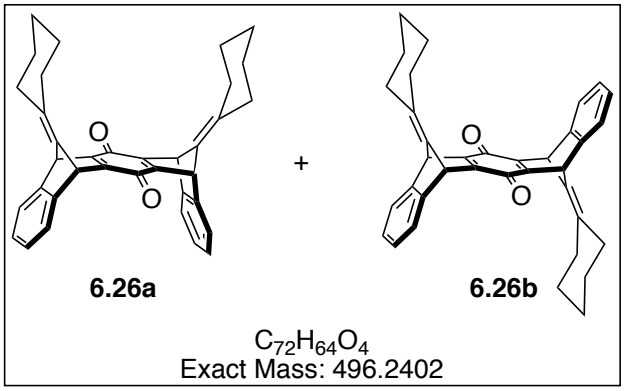

Benzonorbornene **4.37** (2.4 mg, 0.011 mmol), quinone **6.24** (2.9 mg, 0.011 mmol), and tetrazine **6.5** (2.6 mg, 0.011 mmol) were placed in a round bottom flask. CD_2Cl_2 (0.55 mL) was added and the reaction was allowed to stir at room temperature for 1.5 h. The reaction mixture was then washed with 1M HCl (2 × 0.75 mL), water (1 × 1 mL), and brine (1 × 1 mL), dried ($MgSO_4$) and

concentrated. The crude product was dissolved in $CDCl_3$ and passed five times through a 2 cm tall column of basic alumina in a pipet. It was then allowed to stir with basic alumina (140 mg) overnight. The solution was filtered then concentrated to give **6.26** (6 mg, 0.01 mmol, 99%) as a gold solid and as a mixture of diastereomers. These diastereomers were unassigned and characterized as a mixture.

Major diastereomer of **6.26**

^{1}H NMR (400 MHz, $CDCl_3$) δ 7.36 (AA'BB', *J* = 7.7, 0.6, 7.2, 1.1 Hz, 4H), 7.02 (AA'BB', *J* = 7.7, 0.6, 7.3, 1.1 Hz, 4 H), 4.87 (s, 4 H), 1.99 – 1.95 (m, 8H), 1.46 – 1.37 (m, 12 H).

Minor diastereomer of **6.26**

^{1}H NMR (400 MHz, $CDCl_3$) δ 7.26 (AA'BB', *J* = 7.7, 0.6, 7.0, 0.8 Hz, 4H), 6.94 (AA'BB', *J* = 6.3, 0.8, 7.1, 1.3 Hz, 4H), 4.88 (s, 4H), 2.04 – 2.01 (m, 8H), 1.46 – 1.37 (m, 12 H).

Mixture of diastereomers of **6.26**

IR (film) 3065, 2927, 2853, 1646, 1567, 1448, 1264, 1159, 938, 738, 701 cm^{-1}.

Monoquinone 6.28

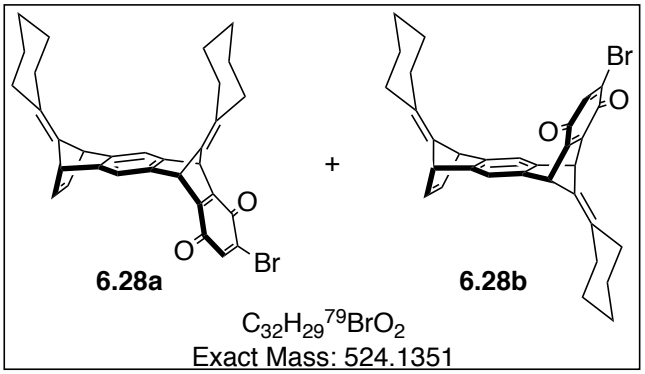

4.32 (89.7 mg, 0.24 mmol) and dibromoquinone **6.20** (35.1 mg, 0.13 mmol) were dissolved in DCM (12 mL). While

stirring at room temperature, a solution of tetrazine **6.5** (1.2 mL of a 0.1 M solution in DCM, 0.12 mmol) was added slowly to the solution of **4.32** and **6.20**. After the addition was complete, the reaction was allowed to stir for an additional 15 minutes, or until it was a clear golden solution. The reaction mixture was then diluted with DCM (5 mL) and washed with 1M HCl (2 × 10 mL), water (1 × 20 mL), and brine (1 × 20 mL), dried ($MgSO_4$) and concentrated to give a gold solid. The crude product was dissolved in freshly distilled DCM (5 mL), passed through a small column of dry basic alumina 5 times, and concentrated to give a red solid. Flash chromatography (50% DCM : 50 % hexanes) provided **6.28** as a red solid (33.8 mg, 0.06 mmol, 54%) and a mixture of *syn* and *anti* isomers.

6.28a

R_f = 0.10 (50% DCM : 50 % hexanes).

^{1}H NMR (400 MHz, Chloroform-*d*) δ 7.24 (s, 1H), 7.23 (s, 1H), 7.01 (s, 1H), 6.85 (app t, *J* = 2.1 Hz, 2H), 4.88 (d, *J* = 1.8 Hz, 1H), 4.82 (d, *J* = 1.8 Hz, 1H), 4.30 (app t, *J* = 2.2 Hz, 2H), 2.07 – 2.16 (m, 4H), 1.94 – 1.86 (m, 4H), 1.45 – 1.56 (m, 6H), 1.33 – 1.41 (m, 6H).

^{13}C NMR (126 MHz, Chloroform-*d*) δ 181.0, 175.5, 160.0, 159.4, 158.8, 156.1, 149.1, 149.1, 143.9, 143.7, 143.7, 137.0, 136.9, 116.6, 116.6, 115.3, 109.6, 50.2, 49.4, 48.8, 34.8, 31.7, 29.7, 29.7, 29.6, 27.4, 27.2, 27.2, 27.1, 26.8, 26.5, 25.4, 22.8, 14.3.

IR (film) 2927, 2852, 1664, 1649, 1566, 1440, 1304, 1249, 909, 785, 732 cm^{-1}.

HRMS (ESI) *m/z* 524.1334 (524.1351 calcd for $C_{32}H_{29}BrO_2$, $(M)^{\cdot-}$).

6.28b

R_f = 0.19 (50% DCM : 50 % hexanes).

^{1}H NMR (500 MHz, Chloroform-*d*) δ 7.23 (s, 1H), 7.22 (s, 1H), 7.04 (s, 1H), 6.91 (app t, *J* = 2.1 Hz, 2H), 4.87 (d, *J* = 1.8 Hz, 1H), 4.81 (d, *J* = 1.8 Hz, 1H), 4.29 (app t, *J* = 2.2 Hz, 2H), 2.09 – 2.04 (m, 4H), 1.95 – 1.80 (m, 4H), 1.53 – 1.43 (m, 6H), 1.41 – 1.29 (m, 6H).

^{13}C NMR (126 MHz, Chloroform-*d*) δ 181.1, 175.6, 160.0, 159.3, 158.8, 156.0, 149.1, 149.0, 143.8, 143.7, 143.6, 143.6, 137.1, 136.9, 116.4, 115.3, 109.5, 50.1, 49.4, 48.8, 34.8, 31.7, 29.6, 29.6, 27.4, 27.1, 27.1, 27.1, 26.7, 26.4, 25.4, 22.8, 20.9, 14.3.

IR (film) 3063, 2998, 2927, 2851, 1664, 1648, 1565, 1440, 1304, 1239, 1074, 909, 732 cm^{-1}.

HRMS (ESI) *m/z* 524.1390 (524.1351 calcd for $C_{32}H_{29}BrO_2$, $(M)^{\cdot-}$).

Bisquinone 6.27

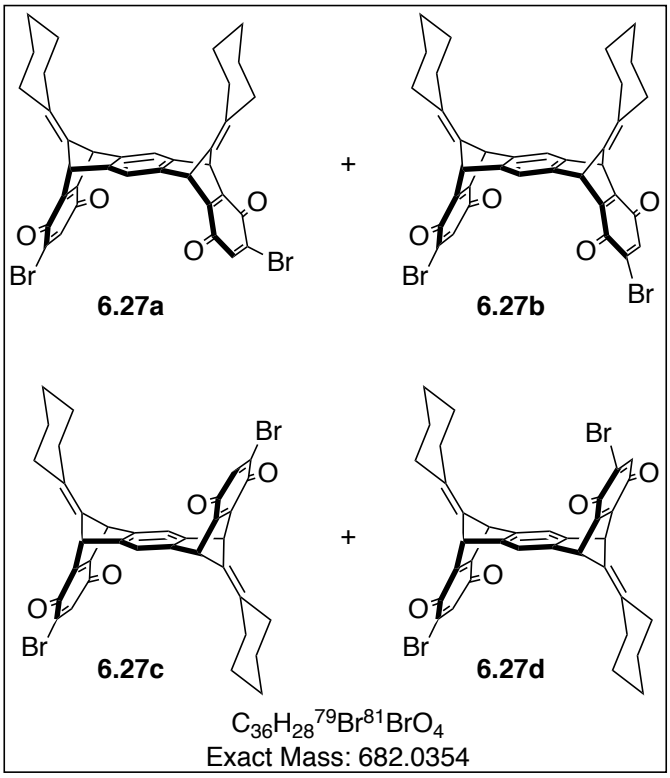

Dibromoquinone **6.20** (228.7 mg, 0.86 mmol) and tetrazine **6.5** (74.0 mg, 0.47 mmol) were dissolved in DCM (21.5 mL).

At room temperature and while stirring, quinone **6.28** (224.9 mg, 0.43 mmol) in DCM (4.3 mL) was added dropwise. The reaction was allowed to stir for 1 h. The reaction mixture was diluted with DCM (5 mL), washed with 1M HCl (2 × 20 mL), water (1 × 40 mL), brine (1 × 40 mL), dried ($MgSO_4$), and concentrated to give an orange solid (446 mg). Flash chromatography (70% DCM : 30% hexanes to 100% DCM) separated the *syn* **6.27a** and **6.27b** (97.6 mg) and *anti* **6.27c** and **6.27d** (156.8 mg) isomers of the dihydroquinone intermediate[11] as rusty-orange solids.

6.27a and **6.27b**

The *syn* isomers were dissolved in dry DCM (2.6 mL) and stirred with dry basic alumina (676 mg) for 40 minutes to give **6.27a** and **6.27b** (58.8 mg, 0.09 mmol, 20%) as a red solid.

R_f = 0.40 (100% DCM).

^{1}H NMR (500 MHz, $CDCl_3$)[12] δ 7.36 (s, 1H, **b**[13]), 7.35 (s, 2H, **a**), 7.34 (s, 1H, **b**), 7.02 (s, 2H), 7.01 (s, 2H), 4.91 (d, *J* = 1.9 Hz, 2H), 4.90 (d, *J* = 1.8 Hz, 2H), 4.85 (d, *J* = 1.8 Hz, 2H), 4.84 (d, *J* = 1.8 Hz, 2H), 2.13 – 2.09 (m, 8H), 1.95 – 1.91 (m, 8H), 1.52 – 1.51 (m, 12H), 1.40 – 1.38 (m, 12H).

^{13}C NMR (126 MHz, Chloroform-*d*) δ 180.6, 180.6, 175.2, 175.2, 159.5, 159.5, 158.3, 158.3, 155.8, 155.8, 145.6, 145.6, 145.5, 145.5, 137.1, 137.1, 136.8, 136.8, 117.8, 117.8, 117.7, 116.4, 116.4, 49.3, 48.7, 29.7, 29.7, 27.2, 27.2, 26.4.

IR (film) 2926, 2851, 1666, 1650, 1565, 1441, 1305, 1253, 1083, 882 cm^{-1}.

---

[11] During chromatography, some elimination takes place, so a pure sample of the dihydroquinone intermediate cannot be obtained.

[12] The diastereomers **6.27a** and **6.27b** were formed in a near to 1:1 ratio so integrations were reliable even though it is a mixture.

[13] Bold letter indicates which isomer the signal is from, however most are indistinguishable.

Mp sample began to decompose around 200 °C.

HRMS (ESI) *m/z* 682.0323 (682.0354 calcd for $C_{36}H_{28}Br_2O_4$, $(M)^{\cdot -}$).

6.27c and **6.27d**[14]

The *anti* isomers underwent a similar elimination reaction by passing a solution of the dihydroquinone through pipet columns of basic alumina.

$\mathbf{R_f}$ = 0.40 (70% DCM : 30% hexanes).

^{1}H NMR (400 MHz, $CDCl_3$)[15] δ δ 7.37 (s, 1H, **d**), 7.36 (s, 2H, **c**), 7.34 (s, 1H, **d**), 7.08 (s, 4H), 7.01 (s, 2H), 4.91 (d, *J* = 1.9 Hz, 2H), 4.90 (d, *J* = 1.9 Hz, 2H), 4.85 (d, *J* = 1.8 Hz, 2H), 4.84 (d, *J* = 1.9 Hz, 2H), 2.11 – 2.07 (m, 8H), 1.95 – 1.91 (m, 8H), 1.52 – 1.47 (m, 12H), 1.40 – 1.37 (m, 12H).

Mp sample began to decompose around 250 °C.

HRMS (ESI) *m/z* 682.0361 (682.0354 calcd for $C_{36}H_{28}Br_2O_4$, $(M)^{\cdot -}$).

[14] Elimination of the *anti* isomers to give **6.27c** and **6.27d** was performed for a different reaction so yields are not given.
[15] The diastereomers **6.27c** and **6.27d** were formed in a near to 1:1 ratio so integrations were reliable even though it is a mixture.

6.6. References

[1] Watanabe, M.; Chang, Y. J.; Liu, S. W.; Chao, T. H.; Goto, K.; Islam, M. M.; Yuan, C. H.; Tao, Y. T.; Shinmyozu, T.; Chow, T. J. *Nat. Chem.* **2012**, *4*, 574–578.

[2] Cory, R. M.; McPhail, C. L. *Tetrahedron Lett.* **1996**, *37,* 1987–1990.

[3] Watson, P. L.; Warrener, R. N. *Aust. J. Chem.* **1973**, *26*, 1725–1750.

[4] Boger, D. L. *Chemtracts: Org. Chem.* **1996**, *9*, 149–189.

[5] Butler, D. N.; Smits, R.; Evans, D. A. C.; Weerasuria, K. D. V.; Warrener, R. N. *Tetrahedron Lett.* **1996**, *37*, 2157–2160.

[6] Anthony, J. E.; Eaton, D. L.; Parkin, S. R. *Org. Lett.* **2002**, *4*, 15–18.

[7] McGarry, K. A.; Xie, W.; Sutton, C.; Risko, C.; Wu, Y.; Young, V. G.; Brédas, J.-L.; Frisbie, C. D.; Douglas, C. J. *Chem. Mater.* **2013**, *25*, 2254–2263.

[8] Tamhankar, B. V.; Desai, U. V.; Mane, R. B.; Wadgaonkar, P. P.; Bedekar, A. V. *Synth. Commun.* **2001**, *13*, 2021–2027.

[9] Thomas, A. D; Miller, L. L. *J. Org. Chem.* **1986**, *51*, 4160–4169.

[10] Miao, Q.; Chi, X.; Xiao, S.; Zeis, R.; Lefenfeld, M.; Siegrist, T.; Steigerwald, M. L.; Nuckolls, C. *J. Am. Chem. Soc.* **2006**, *128*, 1340–1345.

[11] Zhang, Z. Studies into the Synthesis of [12]cyclacene. Presented at the University of Minnesota Chemistry Department's Third Year Graduate Student Research Symposium, Minneapolis, MN, June 6th, 2016.

BIBLIOGRAPHY

1. Minkin, V. I.; Glukhovtsev, M. N.; Simkin, B. Y. *Aromaticity and Antiaromaticity: Electronic and Structural Aspects,* J. Wiley & Sons, New York, 1994.
2. Heilbronner, E. *Helv. Chim. Acta* **1954**, *37*, 921–935.
3. Tahara, K.; Tobe, Y. *Chem. Rev.* **2006**, *106*, 527–5290.
4. Chen, Z.; Jiang, D. E.; Lu, X.; Bettinger, H. F.; Dia, S.; Schleyer, P. V.; Houk, K. N. *Org. Lett.* **2007**, *9,* 5449–5452.
5. Iijima, S. *Nature* **1991**, *354,* 56–58.
6. Dia, H. J. *Acc. Chem. Res.* **2002**, *35,* 1035–1044.
7. Sgobba, V.; Guldi, D. M. *Chem. Soc. Rev.* **2009**, *38,* 165–184.
8. Dekker, C. *Physics Today* **1999**, *52,* 22–28.
9. Meo, M.; Rossi, M. *Composites Science and Technology* **2006**, *66,* 1597–1605.
10. Cory, R. M.; McPhail, C. L. *Tetrahedron Lett.* **1996**, *37,* 1987–1990.
11. Kohnke, F. H.; Slawin, A. M. Z.; Stoddart, J. F.; Williams, D. J. *Angew. Chem., Int. Ed.* **1987**, *26,* 892–894.
12. Cory, R. M.; McPhail, C. L.; Dikmans, A. J.; Vittal, J. J. *Tetrahedron Lett.* **1996**, *37,* 1983–1986.
13. Godt, A.; Enkelmann, V.; Schlüter, A. D. *Angew. Chem., Int. Ed.* **1989**, *28,* 1680–1682.
14. Anthony, J. E.; Eaton, D. L.; Parkin, S. R. *Org. Lett.* **2002**, *4,* 15–18.
15. Dresselhaus, M. S.; Dresselhaus, G.; Saito, R. *Carbon* **1995**, *33*, 883–891.
16. Baughman, R. H.; Zakhidov, A. A.; de Heer, W. A. *Science* **2002**, *297*, 787–792.
17. Jasti, R.; Bertozzie, C. R. *Chem. Phys. Lett.* **2010**, *494*, 1–7.
18. Liu, J.; Wang, C.; Tu, X.; Liu, B.; Chen, L.; Zheng, M.; Zhou, C. *Nature Commun.* **2012**, *3*, 1199–1206.
19. Omachi, H.; Nakayama, T.; Takahashi, E.; Segawa, Y.; Itami, K. *Nat. Chem.* **2013**, *5*, 572–576.
20. Alvarez, M. P.; Burrezo, P. M.; Kertesz, M.; Iwamoto, T.; Yamago, S.; Xia, J.; Jasti, R.; Navarrete, J. T. L.; Taravillo, M.; Baonza, V. G.; Casado, J. *Angew. Chem. Int. Ed.* **2014**, *53*, 7033–7037.
21. Hirst, E. S.; Jasti, R. *J. Org. Chem.* **2012**, *77*, 10473–10478.
22. Jasti, R.; Bhattacharjee, J.; Neaton, J. B.; Bertozzi, C. R. *J. Am. Chem. Soc.* **2008**, *130*, 17646–17647.
23. Xia, J.; Bacon, J. W.; Jasti, R. *Chem. Sci.* **2012**, *3*, 3018–3021.
24. Darzi, E. R.; Sisto, T. J.; Jasti, R. *J. Org. Chem.* **2012**, *77*, 6624–6628.
25. Sisto, T. J.; Golder, M. R.; Hirst, E. S.; Jasti, R. *J. Am. Chem. Soc.* **2011**, *133*, 15800–15802.
26. Xia, J.; Jasti, R. *Angew. Chem. Int. Ed.* **2012**, *51*, 2474–2476.

27. Evans, P. J.; Darzi, E. R.; Jasti, R. *Nature Chemistry* **2014**, *6*, 404–408.
28. Segawa, Y.; Šenel, P.; Matsuura, S.; Omachi, H.; Itami, K. *Chem. Lett.* **2011**, *40*, 423–425.
29. Segawa, Y.; Miyamoto S.; Omachi, H.; Matsuura, S.; Šenel, P.; Sasamori, T.; Tokitoh, N.; Itami, K. *Angew. Chem. Int. Ed.* **2011**, *50*, 3244–3248.
30. Takaba, H.; Omachi, H.; Yamamoto, Y.; Bouffard, J.; Itami, K. *Angew. Chem. Int. Ed.* **2009**, *48*, 6112–6116.
31. Ishii, Y.; Nakanishi, Y.; Omachi, H.; Matsuura, S.; Matsui, K.; Shinohara, H.; Segawa, Y.; Itami, K. *Chem. Sci.* **2012**, *3*, 2340–2345.
32. Omachi, H.; Matsuura, S.; Segawa, Y.; Itami, K. *Angew. Chem. Int. Ed.* **2010**, *49*, 10202–10205.
33. Sibbel, F.; Matsui, K.; Segawa, Y.; Studer, A.; Itami, K. *Chem. Commun.* **2013**, *50*, 954–956.
34. Kayahara, E.; Sakamoto, Y.; Suzuki, T.; Yamago, S. *Org. Lett.* **2012**, *14*, 3284–3287.
35. Kayahara, E.; Iwamoto, T.; Suzuki, T.; Yamago, S. *Chem. Lett.* **2013**, *42*, 621–623.
36. Yamago, S.; Watanabe, Y.; Iwamoto, T. *Angew. Chem. Int. Ed.* **2010**, *49*, 757–759.
37. Iwamoto, T.; Watanabe, Y.; Sadahir, T.; Haino, T.; Yamago, S. *Angew. Chem. Int. Ed.* **2011**, *50*, 8342–8344.
38. Kivelson, S.; Chapman, O. L. *Phys. Rev. B* **1983**, *28*, 7236–7243.
39. Bendikov, M.; Duong, H. M.; Starkey, K.; Houk, K. N.; Carter, E. A.; Wudl, F. *J. Am. Chem. Soc.* **2004**, *126*, 7416–7417.
40. Sadowsky, D.; McNeill, K.; Cramer, C. J. *Faraday Discussions* **2010**, *145*, 507–521.
41. Evans, P. J.; Jasti, R. Molecular Belts. In *Polyarenes*, Siegel J. S.; Wu, Y. T.; Topics in Current Chemistry; Springer-Verlag Berlin Heidelberg, **2014**, *349*, 249–290.
42. Kintzel, O.; Luger, P.; Weber, M.; Schlüter, A. –D. *Eur. J. Org. Chem.* **1998**, 99–105.
43. Stoddart, J. F. *J. Inclusion Phenom. And Molecular Recognition in Chem.* **1989**, *7*, 227–245.
44. Houk, K. N. *Stereochemistry and Reactivity of Systems Containing π-Electrons*; Watson, W. H., Ed.; Verlag-Chemie: Deerfield Beach, FL, 1983; 1–40.
45. Alder, K.; Stein, G. *Liebigs Ann. Chem.* **1931**, *485*, 211–222.
46. Alder, K; Stein, G. *Liebigs Ann. Chem.* **1935**, *515*, 185–200.
47. Schleyer, P. v. R. *J. Am. Chem. Soc.* **1967**, *89*, 701–703.
48. Brown, H. C.; Hammer, W. J.; Kawakami, J. H.; Rotberg, I.; Van Der Jugt, D. L. *J. Am. Chem. Soc.* **1967** *89*, 6381–6382.
49. Brown, H. C.; Kawakami, J. H.; Liu, K.-T. *J. Am. Chem. Soc.* **1973**, *95*, 2209-2216.
50. Watson, W. H.; Galloy, J.; Bartlett, P. D.; Roof, A. A. M. *J. Am. Chem. Soc.* **1981**, *103*, 2022-2031.
51. Bartlett, P. D.; Combs, G. L., Jr.; Thi Li, A.-X.; Watson, W. H.; Galloy, J.; Kimura, M. *J. Am. Chem. Soc.* **1982**, *104*, 3131–3138.

52. Pinkerton, A. A.; Schwarzenbach, D.; Stibbard, J. H. A.; Carrupt, P.-A.; Vogel, P. *J. Am. Chem. Soc.* **1981**, *103*, 2095–2096.
53. Hagenbuch, J.-P.; Vogel, P.; Pinkerton, A. A.; Schwarzenbach, D. *Helv. Chim. Acta* **1981**, *64*, 1818–1832.
54. Paquette, L. A.; Carr, R. V. C.; Böhm, M. C.; Gleiter, R. *J. Am. Chem. Soc.* **1980**, *102*, 1186–1188.
55. Böhm, M. C.; Carr, J. V. C.; Gleiter, R.; Paquette, L. A. *J. Am. Chem. Soc.* **1980**, *102*, 7218–7228.
56. Paquette, L. A.; Carr, R. V. C.; Arnold, E.; Clardy, J. *J. Org. Chem.* **1980**, *45*, 4907–4913.
57. Paquette, L. A.; Charumilind, P.; Kravetz, T. M.; Böhm, M. C.; Gleiter, R. *J. Am. Chem. Soc.* **1983**, *105*, 3126–3135.
58. Paquette L. Al; Schaefer, A. G.; Blount, J. F. *J. Am. Chem. Soc.* **1983**, *105*, 3642–3649.
59. Paquette, L. A.; Green, K. E.; Hsu, L.-Y. *J. Org. Chem.* **1984**, *49*, 3650–3652.
60. Paquette, L. A.; Kravetz, T. M.; Böhm, M. C.; Gleiter, R. *J. Org. Chem.* **1983**, *48*, 1250–1257.
61. Ashton, P. R.; Isaacs, N. S.; Kohnke, F. H.; Slawin, A. M. Z.; Spencer, C. M.; Stoddart, J. F.; Williams, D. J. *Angew. Chem. Int. Ed.* **1988**, *27*, 966–969.
62. Xing, Y. D.; Huang, N. Z. *J. Org. Chem.* **1982**, *47*, 140–142.
63. Ashton, P. R.; Girreser, U.; Giuffrida, D.; Kohnke, F. H.; Mathias, J. P.; Raymo, F. M.; Slawin, A. M. Z.; Stoddart, J. F.; Williams, D. J. *J. Am. Chem. Soc.* **1993**, *115*, 5422–5429.
64. Cory, R. M.; McPhail, C. L.; Dikmans, A. J. *Tetrahedron Lett.* **1993**, *34*, 7533–7536.
65. Watanabe, M.; Chen, K.-Y.; Chow, T. J. *Acc. Chem. Res.* **2013**, *46*, 1606–1615 and references therein.
66. Watanabe, M.; Chang, Y. J.; Liu, S. W.; Chao, T. H.; Goto, K.; Islam, M. M.; Yuan, C. H.; Tao, Y. T.; Shinmyozu, T.; Chow, T. J. *Nat. Chem.* **2012**, *4*, 574–578.
67. Irie, T.; Tanida, H. *J. Org. Chem.* **1979**, *44*, 1002–1003.
68. Yankelevich, S.; Fuchs, B. *Tetrahedron Lett.* **1967**, *8*, 4945–4949.
69. McCulloch, R.; Rye, A. R.; Wege, D. *Tetrahedron Lett.* **1969**, *10*, 5231–5234.
70. Meinwald, J.; Miller, E. G. *Tetrahedron Lett.* **1961**, *2*, 253–258.
71. Lai, C.-H.; Li, E. Y.; Chen, K.-Y.; Chow, T. J.; Chou, P.-T. *J. Chem. Theory Comput.* **2006**, *2*, 1078–1084.
72. Miao, Q.; Chi, X.; Xiao, S.; Zeis, R.; Lefenfeld, M.; Siegrist, T.; Steigerwald, M. L.; Nuckolls, C. *J. Am. Chem. Soc.* **2006**, *128*, 1340–1345.
73. Wissinger, J. E. *Laboratory Manual for Organic Chemistry 2311*. Eighth Ed.; Cengage Learning: Mason, Ohio, 2008; pp 67–69.
74. Purushothaman, B.; Bruzek, M.; Parkin, S. R.; Miller, A.-F.; Anthony, J. E. *Angew. Chem. Int. Ed.* **2011**, *50*, 7013–7017.

75. Terao, Y.; Satoh, T.; Miura, M.; Nomura, M. *Bull. Chem. Soc. Jpn.* **1999**, *72*, 2345–2350.
76. Holland, J. M.; Jones, D. W. *J. Chem. Soc. C: Organic* **1971**, 608–612.
77. Kitamura, T.; Yamane, M.; Inoue, K.; Todaka, M.; Fukatsu, N.; Meng, Z. H.; Fujiwara *J. Am. Chem. Soc.* **1999**, *121*, 11674–11679.
78. Chen, Y. L.; Sun, J. Q.; Wei, X.; Wong, W. Y.; Lee, A. W. M. *J. Org. Chem.* **2004**, *69*, 7190–7197.
79. Butler, D. N.; Smits, R.; Evans, D. A. C.; Vinidra Weerasuria, K. D.; Warrener, R. N. *Tetrahedron Lett.* **1996**, *37*, 2157–2160.
80. Lorbach, A.; Reus, C.; Bolte, M.; Lerneer, H. W.; Wagner, M. *Adv. Synth. Catal.* **2010**, *352*, 3443–3449.
81. Satoh, T.; Inoh, J.; Kawamura, Y.; Kawanura, Y.; Miura, M.; Nomura, M *Bull. Chem. Soc. Jpn.* **1998**, *71*, 2239–2246.
82. Cao, C.; Wang, L.; Cai, Z.; Zhang, L.; Guo, J.; Pang, G.; Shi, Y. *Eur. J. Org. Chem.* **2011**, 1570–1574.
83. Hellal, M.; Singh, S.; Cuny, G. D. *J. Org. Chem.* **2012**, *77*, 4123–4130.
84. Inagaki, S.; Fujimoto, H.; Fukui, K *J. Am. Chem. Soc.* **1976**, *98*, 4054-4061.
85. Ashton, P. R.; Brown, G. R.; Isaacs, N.S; Giuffrida, D.; Kohnke, F. H.; Mathias, J. P.; Slawin, A. M. Z.; Smith, D. R.; Stoddart, J. F.; Williams, D. J. *J. Am. Chem. Soc.* **1992**, *26,* 6330–6353, and references therein.
86. Cava, M. P.; Napier, D. R. *J. Am. Chem. Soc.* **1957**, *79*, 1701–1709.
87. Cava, M. P.; Shirley, R. L. *J. Am. Chem. Soc.* **1960**, *82*, 654–656.
88. Paddon-Row, M. N.; Patney, H. K.; Harish, K. *Synthesis* **1986**, 328–330.
89. Boger, D. L.; Panek, J. S.; Meier, M. M. *J. Org. Chem.* **1982**, *47*, 895–897.
90. Boger, D. L. *Chemtracts: Org. Chem.* **1996**, *9*, 149–189.
91. Alper, H.; Laycock, D. E. *Synthesis* **1980**, 799.
92. Hart, H.; Lai, C.-Y.; Nwokogu, G. C.; Shamouilian, S. *Tetrahedron* **1987**, *43*, 5203–5224.
93. Reynaud, C; Fall, Y.; Feuerstein, M.; Doucet, H.; Santelli, M. *Tetrahedron* **2009**, *65*, 7440–7448.
94. Bhojgude, S. S.; Kaicharia, T.; Bhunia, A.; Biju, A. T. *Org. Lett.* **2012**, *14*, 4098–4101, and references therein.
95. Himeshima, Y.; Sonoda, T.; Kobayashi, H. *Chem. Lett.* **1983**, 1211.
96. Bock, H.; Nick, S.; Ruppert, K. Z. *Naturforsch* **1995**, *50*, 595–602.
97. Duong, H. M.; Bendikov, M.; Steiger, D.; Zhang, Q.; Sonmez, G.; Yamada, J.; Wudl, F. *Org. Lett.* **2003**, *5*, 4433–4436.
98. Wu, Q. –C.; Li, B.-S.; Shi, C.-Q; Chen, Y.-X. *Hecheng Huaxue*, **2007**, *15*, 111.
99. Bronner, S. M.; Garg, N. K. *J. Org. Chem.* **2009**, *74*, 8842–8843.
100. Atkinson, D. J.; Sperry, J.; Brimble, M. A. *Synthesis* **2010**, 911–913.

101. Tietze, L. F.; Eicher, T.; Diederichsen, U.; Speicher, A. *Reactions and Syntheses in the Organic Chemistry Laboratory*; Wiley-VCH Verlag GmbH & Co. KGaA: Weinheim, Germany, 2007; pp 174.
102. Breton, G. W. *J. Org. Chem.* **1997**, *62*, 8952–8954.
103. Douglas, C. J. Evaluation of Ferrocenyloxazoline Palladacyclic Catalysts for the Asymmetric Allylic Imidate Rearrangement and Studies toward an Enantioselective Synthesis of Sarain A. Ph.D. Dissertation, University of California at Irvine, 2005.
104. Pretsch, E.; Bühlmann, P.; Badertscher, M. *Stucture Determination of Organic Compounds Tables of Spectral Data*; Springer: Verlag Berlin Heidelberg, 2009; 174.
105. Jansen, G.; Kahler, B.; Klärner, F.-G.; Boese, R.; Bläser, D. *J. Am. Chem. Soc.* **2010**, *132*, 8581–8592.
106. Schleyer, P. V.; Jiao, H. J. *Pure Appl. Chem.* **1996**, *68*, 209–218.
107. Bergmann, E. D. *Chem. Rev.* **1968**, *68*, 41–84.
108. Rodríguez-Lojo, D.; Peña, D.; Pérez, D.; Guitián, E. *Synlett* **2015**, *26*, 1633–1637.
109. Segura, J. L.; Martin, N. *Chem. Rev.* **1999**, *99*, 3199–3246.
110. Bornhöft, J.; Siegwarth, J.; Näther, C.; Herges, *Eur. J. Org. Chem.* **2008**, *9*, 1619–1624.
111. Winstein, S.; Trifan, D. S. *J. Am. Chem. Soc.* **1949**, *71*, 2953–2953.
112. Anslyn, E. V.; Dougherty, D. A. Organic Reaction Mechanisms, Part 2 *Modern Physical Organic Chemistry*; University Science Books, 2006, 662 and references therein.
113. Parakka, J. P.; Sadanandan, E. V.; Cava, M. P. *J. Org. Chem.* **1994**, *59*, 4308–4310.
114. Michael, J. P.; Maqutu, T. L.; Howard, A. S. *J. Chem. Soc., Perkin Trans, 1* **1989**, 2389–2395.
115. Boger, D. L.; Lerner, R. A.; Cravatt, B. F. *J. Org. Chem.* **1994**, *59*, 5078–5079.
116. Schulze A.; Pagona, G.; Giannis, A. *Syn. Comm.* **2006**, *36*, 1147–1156.
117. Scarso, A.; Pellizzaro, L.; De Lucchi, O.; Linden, A.; Fabris, F. *Angew. Chem. Int. Ed.* **2007**, *46*, 4972.
118. Yates, M. H. *Tetrahedron Lett.* **1997**, *38*, 2813–2816.
119. Pashkovskii, F. S.; Lakhvich, F. A.; Koval'skaya, S. S.; Kozlov, N. G. *Russ. J. Org. Chem.* **2001**, *37*, 375–381.
120. Carlson, R.; Nilsson, Å. *Acta Chemica Scandinavica* **1985**, *39B*, 181–186.
121. Carlson, R.; Nilsson, Å. *Acta Chemica Scandinavica* **1984**, *38B*, 49–53.
122. Becker, H.; Soler, M. A.; Sharpless, B. K. *Tetrahedron* **1995**, *51*, 1345–1376.
123. Français, A.; Bedel, O.; Haudrechy, A. *Tetrahedron* **2008**, *64*, 2495–2524.
124. Regen, S. L.; Whitesides, G. M. *J. Org. Chem.* **1972**, *37*, 1832–1833.
125. Jain, S. L.; Sharma, V. B.; Sain, B. *Tetrahedron Lett.* **2004**, *45*, 1233–1235.
126. Lokan, N.; Paddon-Row, M. N.; Smith, T. A.; La Rosa, M.; Ghiggino, K. P.; Speiser, S. *J. Am. Chem. Soc.* **1999**, *121*, 2917–2918.

127. Burgstahler, A. W.; Boger, D. L.; Naik, N. C. *Tetrahedron* **1976**, *32*, 309–315.
128. Greenfield, S.; Mackenzie, K. *J. Chem. Soc., Perkin Trans. 2* **1986**, 1651–1666.
129. Kolb, H. C.; VanNieuwenhze, M. S.; Sharpless, K. B. *Chem. Rev.* **1994**, *94*, 2483–2547.
130. Takano, S.; Yoshimitsu, T.; Ogasawara, K. *J. Org. Chem.* **1994**, *59*, 54–57.
131. Sharpless, B. K.; Amberg, W.; Bennani, Y. L.; Crispino, G. A.; Hartung, J.; Jeong, K.-S.; Kwong, H.-L.; Morikawa, K.; Wang, Z.-M.; Xu, D.; Zhang, X.-L. *J. Org. Chem.* **1992**, *57*, 2768.
132. Wu, F.; Mandadapu, V.; Day, A. I. *Tetrahedron* **2013**, *70*, 9957–9965.
133. Ray, R.; Matteson, D. S. *Tetrahedron Lett.* **1980**, *21*, 449–450.
134. Russell, R. A.; Harrison, P. A.; Warrener, R. N. *Aust. J. Chem.* **1984**, *37*, 1035–1041.
135. Mondal, R.; Adhikari, R. M.; Shah, B. K.; Neckers, D. C. *Org. Lett.* **2007**, *9*, 2505–2508.
136. Maliakal, A.; Raghavachari, K.; Katz, H.; Chandross, E.; Siegrist, T. *Chem. Mater.* **2004**, *16*, 4980–4986 and references therein.
137. Warrener, R. N.; Harrison, P.A.; Russell, R.A. *J. Chem. Soc., Chem. Commun.*, **1982**, 1134-1136.
138. Johnson, J. R.; Grummitt, O. *Org. Syn.* **1955**, *3*, 806.
139. Watson, P. L.; Warrener, R. N. *Aust. J. Chem.* **1973**, *26*, 1725–1750.
140. McGarry, K. A.; Xie, W.; Sutton, C.; Risko, C.; Wu, Y.; Young, V. G.; Brédas, J.-L.; Frisbie, C. D.; Douglas, C. J. *Chem. Mater.* **2013**, *25*, 2254–2263.
141. Tamhankar, B. V.; Desai, U. V.; Mane, R. B.; Wadgaonkar, P. P.; Bedekar, A. V. *Synth. Commun.* **2001**, *13*, 2021–2027.
142. Thomas, A. D; Miller, L. L. *J. Org. Chem.* **1986**, *51*, 4160–4169.
143. Zhang, Z. Studies into the Synthesis of [12]cyclacene. Presented at the University of Minnesota Chemistry Department's Third Year Graduate Student Research Symposium, Minneapolis, MN, June 6th, 2016.

APPENDIX 1.

NMR Spectra Chapter 4

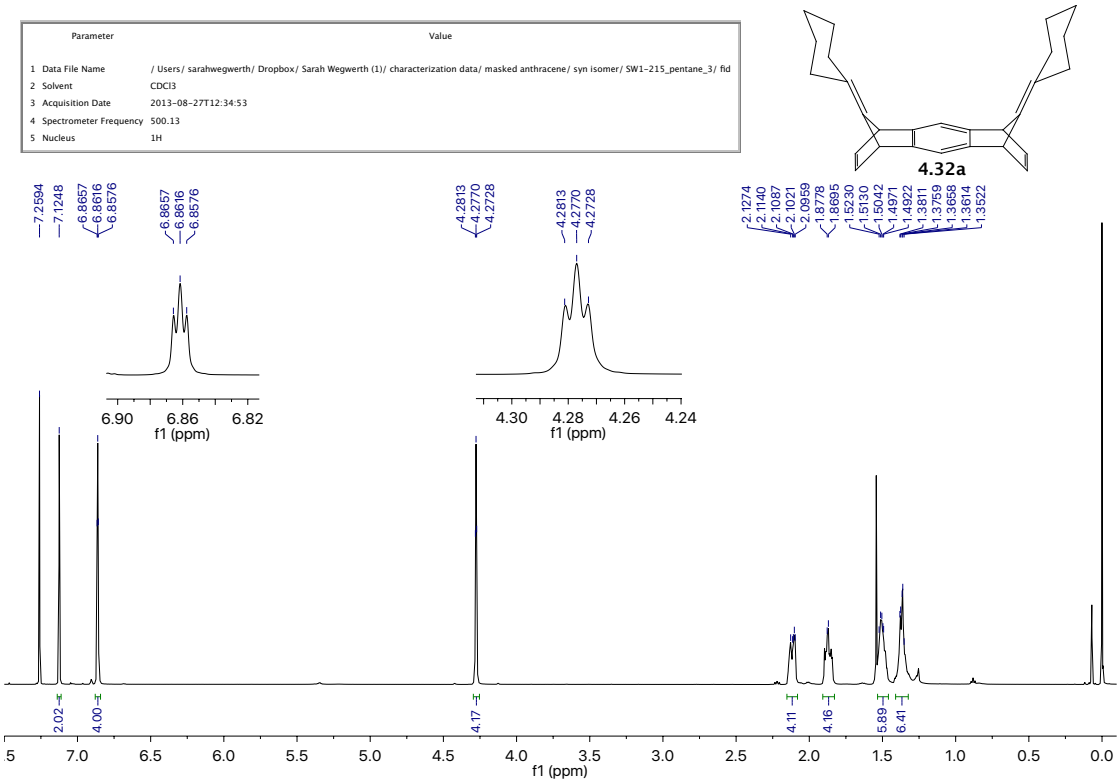

Parameter	Value
1 Data File Name	/ Users/ sarahwegwerth/ Dropbox/ Sarah Wegwerth (1)/ characterization data/ masked anthracene/ syn isomer/ SW1-215_1D(13C)/ fid
2 Solvent	CDCl3
3 Acquisition Date	2013-08-04T13:12:50
4 Spectrometer Frequency	125.77
5 Nucleus	13C

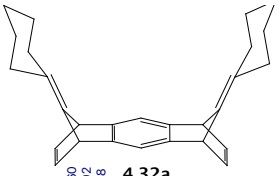

4.32a

159.5614
147.2773
143.7512
115.2558
108.3731
50.1171
29.6260
27.3692
26.8128

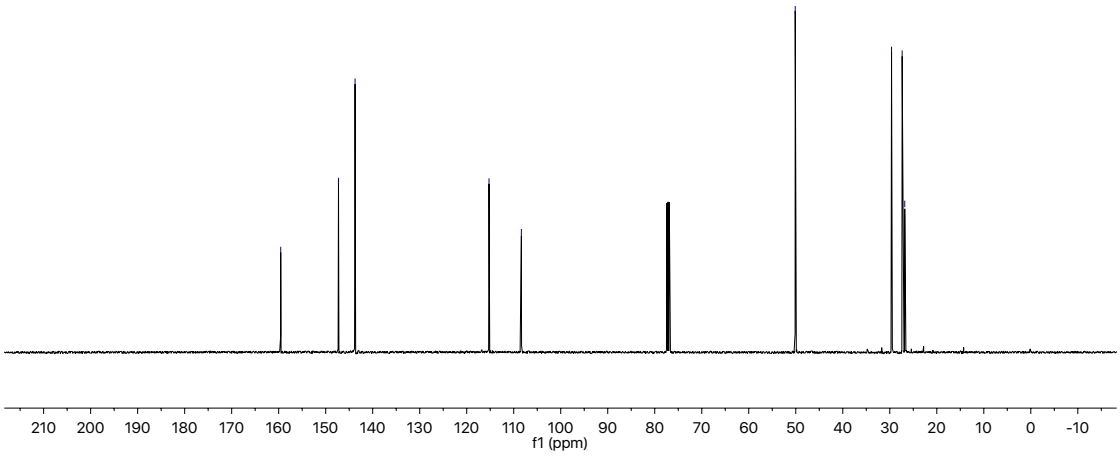

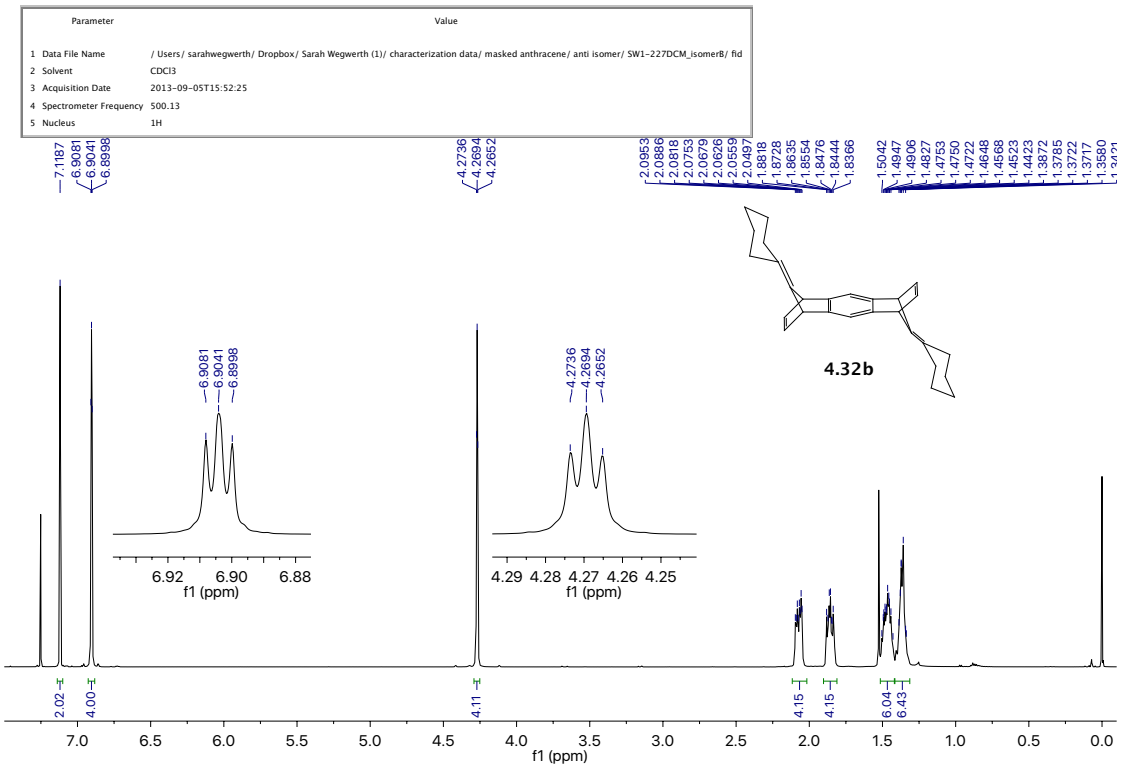
Parameter
Value
1 Data File Name
/ Users/ sarahwegwerth/ Dropbox/ Sarah Wegwerth (1)/ characterization data/ masked anthracene/ anti isomer/ SW1-227DCM_isomerB/ fid
2 Solvent
CDCl3
3 Acquisition Date
2013-09-05T15:52:25
4 Spectrometer Frequency
500.13
5 Nucleus
1H
7.1187
6.9081
6.9041
6.8998
4.2736
4.2694
4.2652
2.0953
2.0886
2.0818
2.0753
2.0679
2.0626
2.0559
2.0497
1.8818
1.8728
1.8635
1.8554
1.8476
1.8444
1.8366
1.5042
1.4947
1.4906
1.4827
1.4753
1.4750
1.4722
1.4648
1.4568
1.4523
1.4423
1.3872
1.3785
1.3722
1.3717
1.3580
4.32b
6.92 6.90 6.88
f1 (ppm)
4.29 4.28 4.27 4.26 4.25
f1 (ppm)
2.02
4.00
4.11
4.15
4.15
6.04
6.43
7.0 6.5 6.0 5.5 5.0 4.5 4.0 3.5 3.0 2.5 2.0 1.5 1.0 0.5 0.0
f1 (ppm)

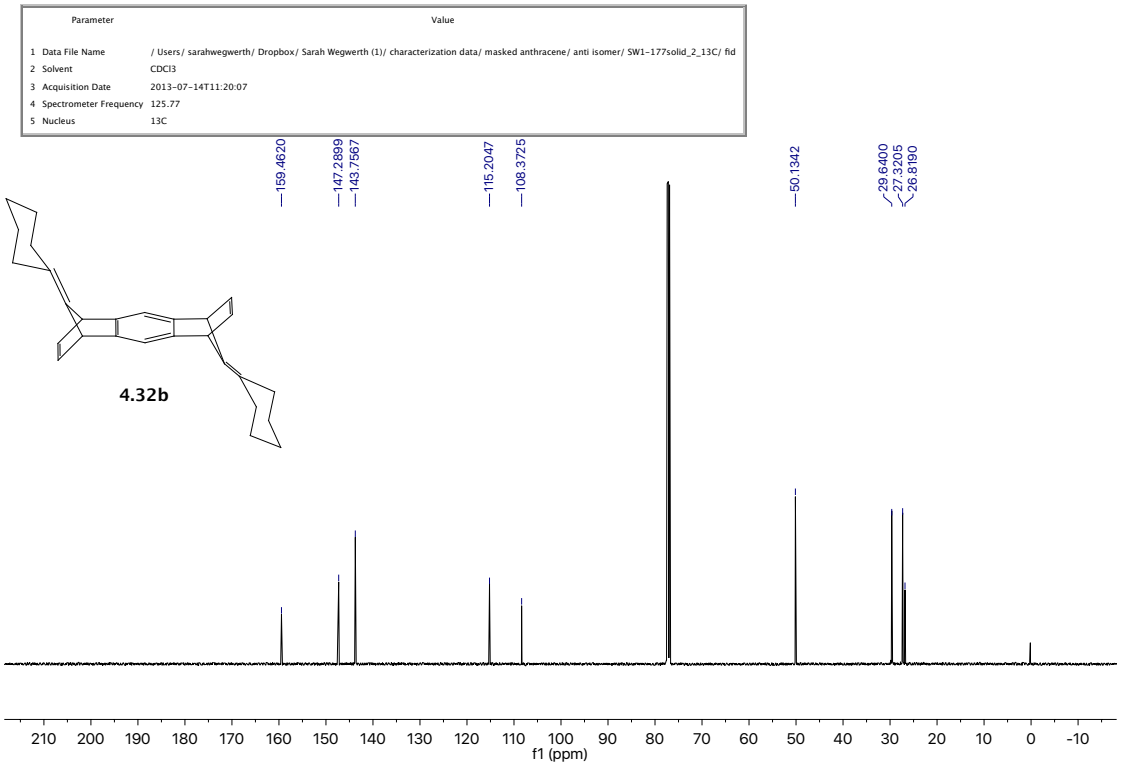
Parameter
Value
1 Data File Name
/ Users/ sarahwegwerth/ Dropbox/ Sarah Wegwerth (1)/ characterization data/ masked anthracene/ anti isomer/ SW1-177solid_2_13C/ fid
2 Solvent
CDCl3
3 Acquisition Date
2013-07-14T11:20:07
4 Spectrometer Frequency
125.77
5 Nucleus
13C
159.4620
147.2899
143.7567
115.2047
108.3725
50.1342
29.6400
27.3205
26.8190
4.32b
210 200 190 180 170 160 150 140 130 120 110 100 90 80 70 60 50 40 30 20 10 0 -10
f1 (ppm)

Parameter	Value
1 Data File Name	/ Users/ sarahwegwerth/ Dropbox/ Sarah Wegwerth (1)/ characterization data/ bisbenzyne precursor prep/ bisbenzyne precursor/ SW1-212B1 (1H)/ fid
2 Solvent	CDCl3
3 Acquisition Date	2013-07-26T16:34:35
4 Spectrometer Frequency	500.13
5 Nucleus	1H

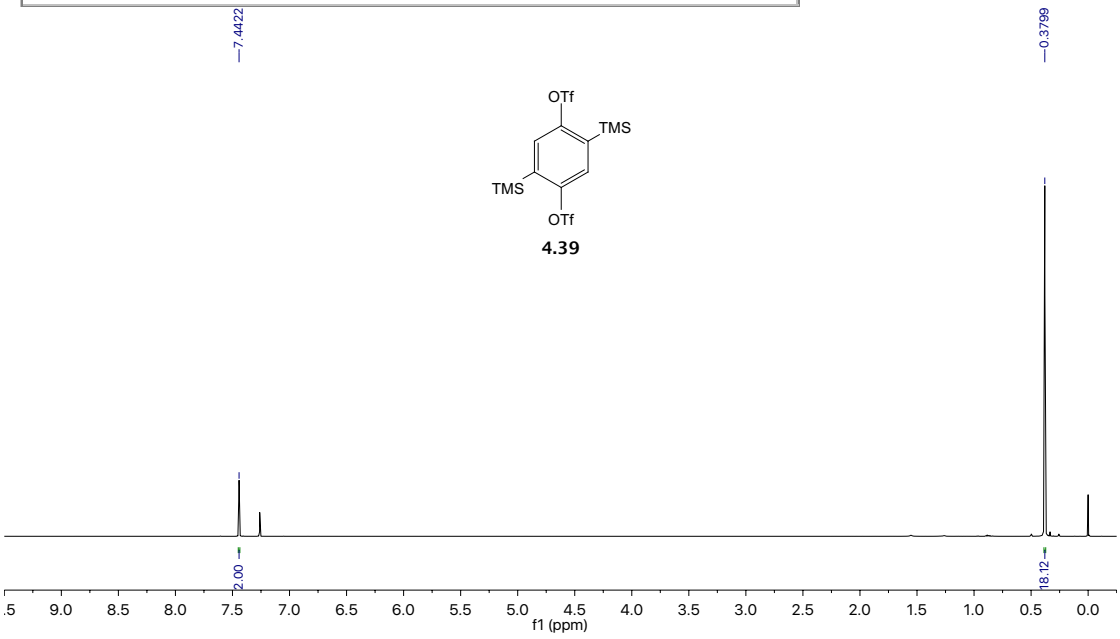

4.39

Parameter	Value
1 Data File Name	/ Users/ sarahwegwerth/ Dropbox/ Sarah Wegwerth (1)/ characterization data/ bisbenzyne precursor prep/ bisbenzyne precursor/ SW1-212B1 (13C)/ fid
2 Solvent	CDCl3
3 Acquisition Date	2013-07-26T16:42:20
4 Spectrometer Frequency	125.77
5 Nucleus	13C

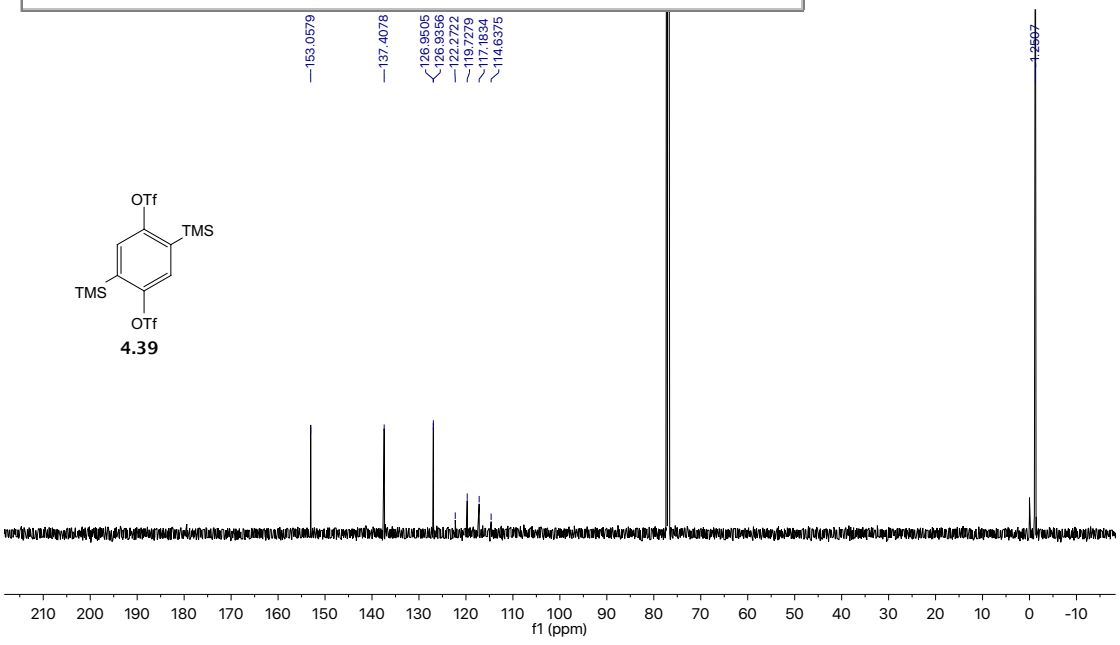

4.39

Parameter	Value
1 Data File Name	/ Users/ sarahwegwerth/ Dropbox/ Sarah Wegwerth (1)/ characterization data/ bisbenzyne precursor prep/ bisbenzyne precursor/ SW1-212B1_19F/ fid
2 Solvent	CDCl3
3 Acquisition Date	2013-07-29T14:54:17
4 Spectrometer Frequency	470.55
5 Nucleus	19F

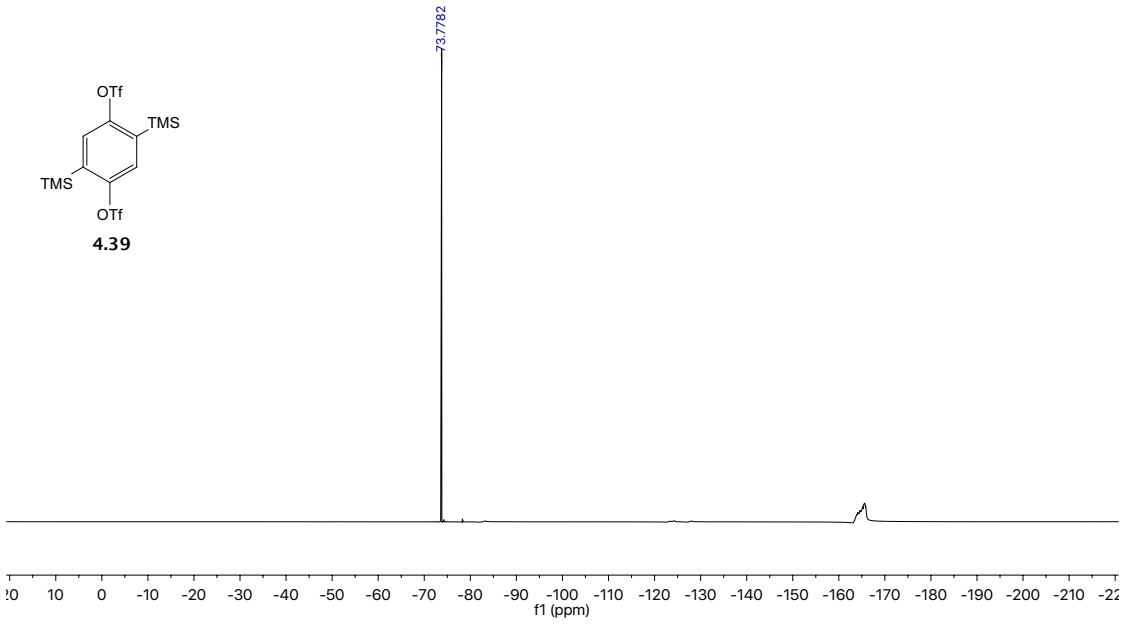

4.39

Parameter	Value
1 Data File Name	/ Users/ sarahwegwerth/ Dropbox/ Sarah Wegwerth (1)/ characterization data/ bisbenzyne precursor prep/ dibromohydroquinone/ SW1-157crude.fid/ fid
2 Solvent	dmso
3 Acquisition Date	2013-04-08T14:14:59
4 Spectrometer Frequency	499.87
5 Nucleus	1H

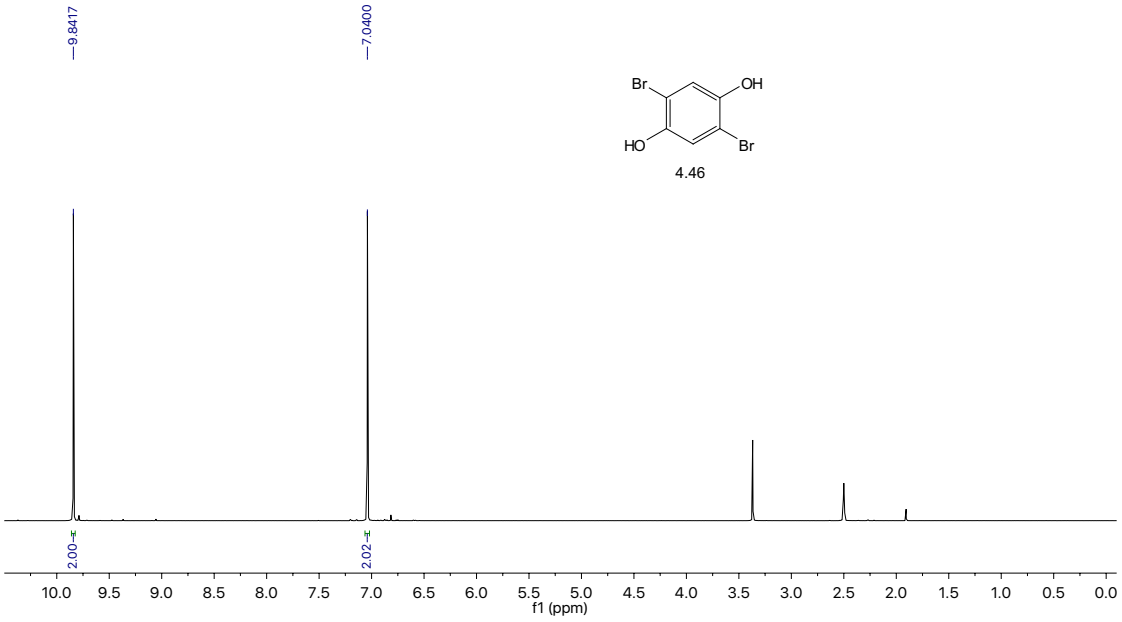

Parameter	Value
1 Data File Name	/ Users/ sarahwegwerth/ Dropbox/ Sarah Wegwerth (1)/ characterization data/ bisbenzyne precursor prep/ dibromohydroquinone/ JAM1-20_recyrstallized(13C)/ fid
2 Solvent	DMSO
3 Acquisition Date	2013-07-30T11:18:26
4 Spectrometer Frequency	125.77
5 Nucleus	13C

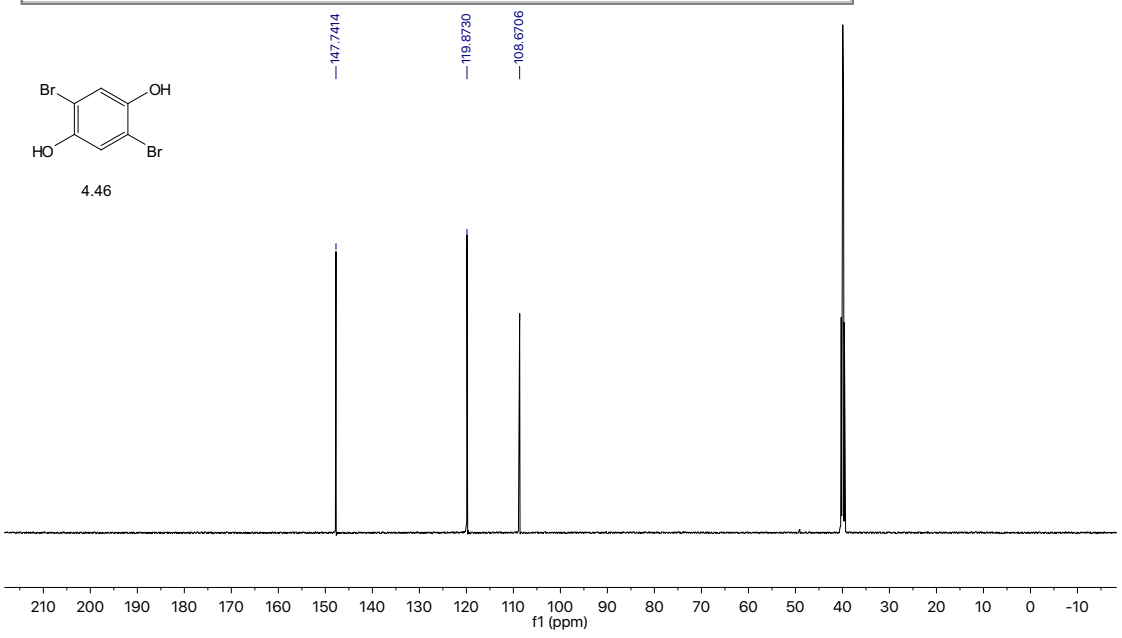

Parameter	Value
1 Data File Name	/ Users/ sarahwegwerth/ Dropbox/ Sarah Wegwerth (1)/ characterization data/ bisbenzyne precursor prep/ dibromo,bis(TMS)benzene/ 1H NMR/ SW1-162recrystallized.fid/ fid
2 Solvent	cdcl3
3 Acquisition Date	2013-04-16T16:24:42
4 Spectrometer Frequency	499.87
5 Nucleus	1H

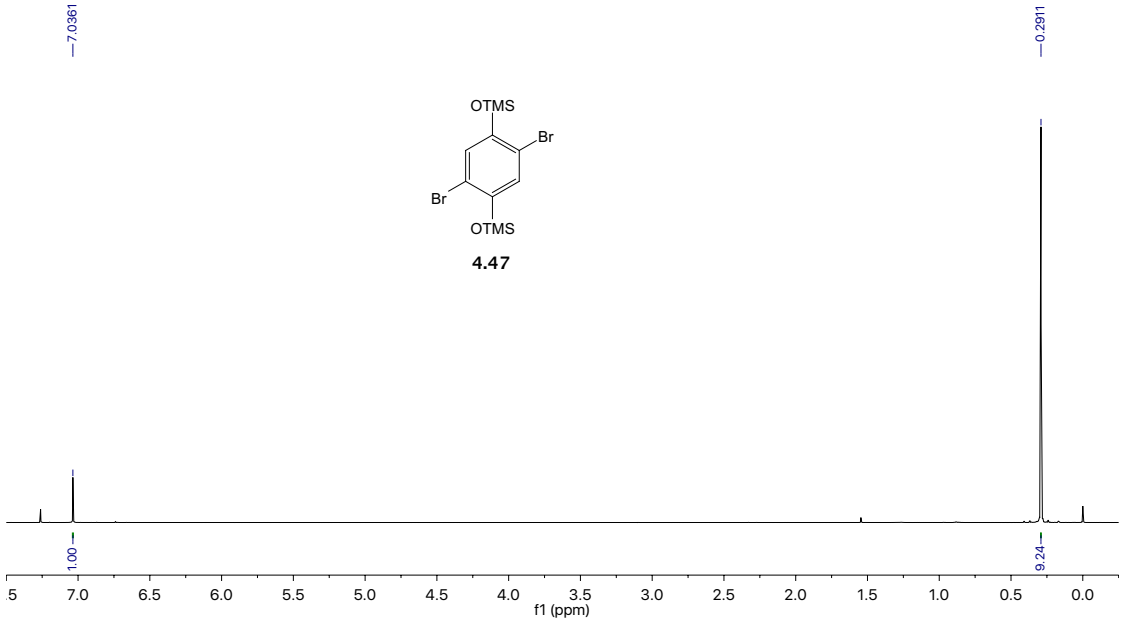

4.47

Parameter	Value
1 Data File Name	/ Users/ sarahwegwerth/ Dropbox/ Sarah Wegwerth (1)/ characterization data/ bisbenzyne precursor prep/ dibromo,bis(TMS)benzene/ 13C NMR/ SW1-209(13C)/ fid
2 Solvent	CDCl3
3 Instrument	spect
4 Acquisition Date	2013-07-30T11:50:03
5 Spectrometer Frequency	125.77
6 Nucleus	13C

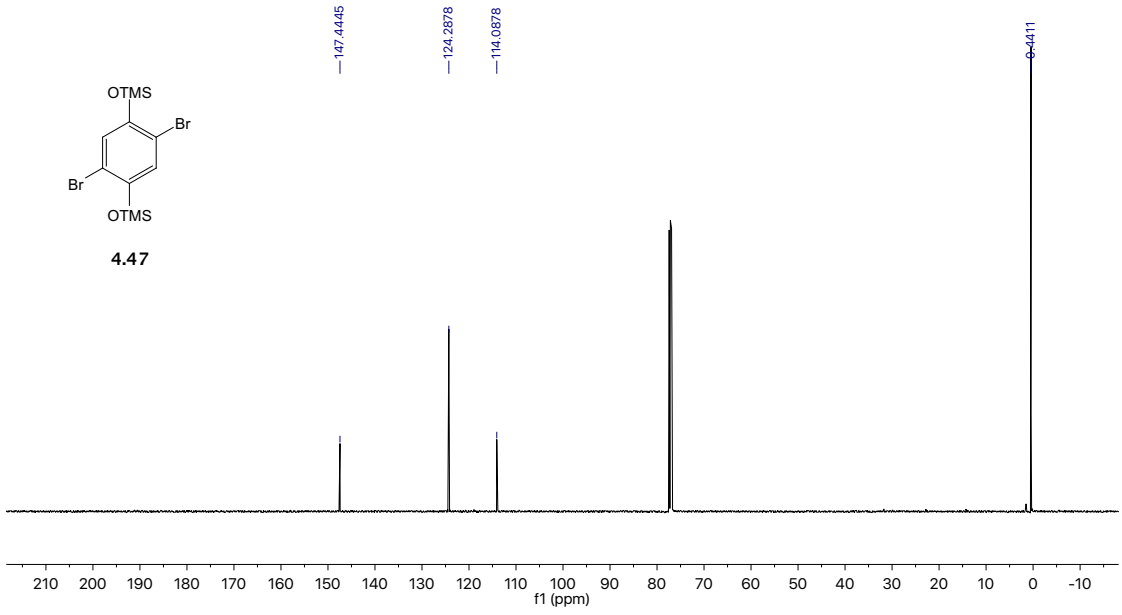

4.47

	Parameter	Value
1	Data File Name	/ Users/ sarahwegwerth/ Dropbox/ Sarah Wegwerth (1)/ characterization data/ bisbenzyne precursor prep/ bisTMS,bisOTMS benzene/ 1H NMR/ SW1-210 (1H)/ fid
2	Solvent	CDCl3
3	Acquisition Date	2013-07-29T08:05:43
4	Spectrometer Frequency	500.13
5	Nucleus	1H

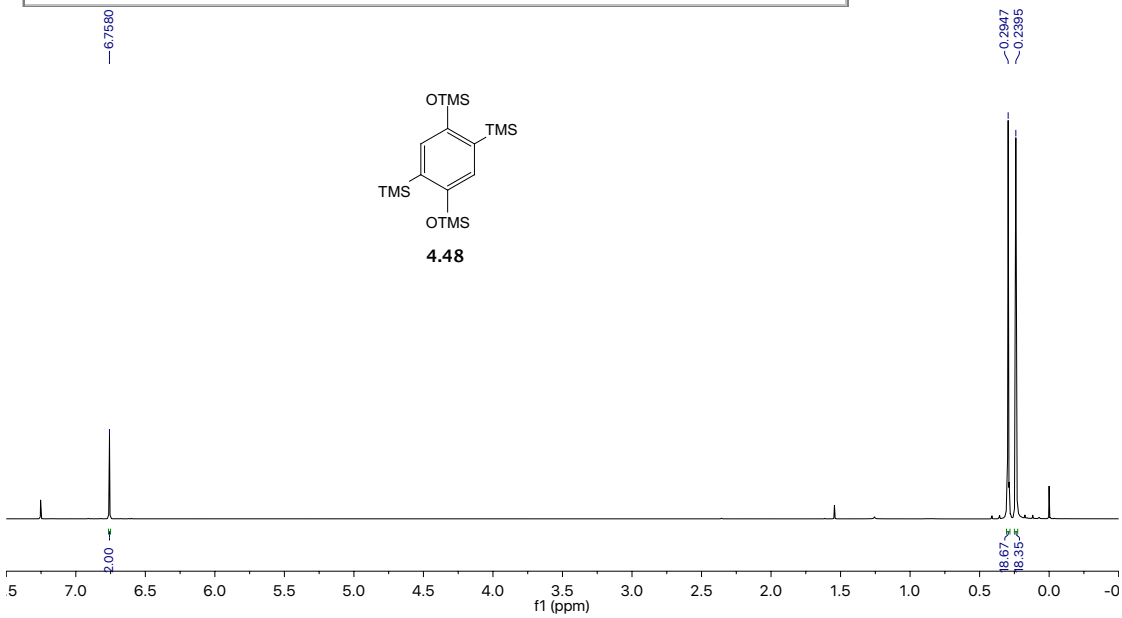

4.48

	Parameter	Value
1	Data File Name	/ Users/ sarahwegwerth/ Dropbox/ Sarah Wegwerth (1)/ characterization data/ bisbenzyne precursor prep/ bisTMS,bisOTMS benzene/ 13C NMR/ SW1-210 (13C)/ fid
2	Solvent	CDCl3
3	Acquisition Date	2013-07-29T08:33:43
4	Spectrometer Frequency	125.77
5	Nucleus	13C

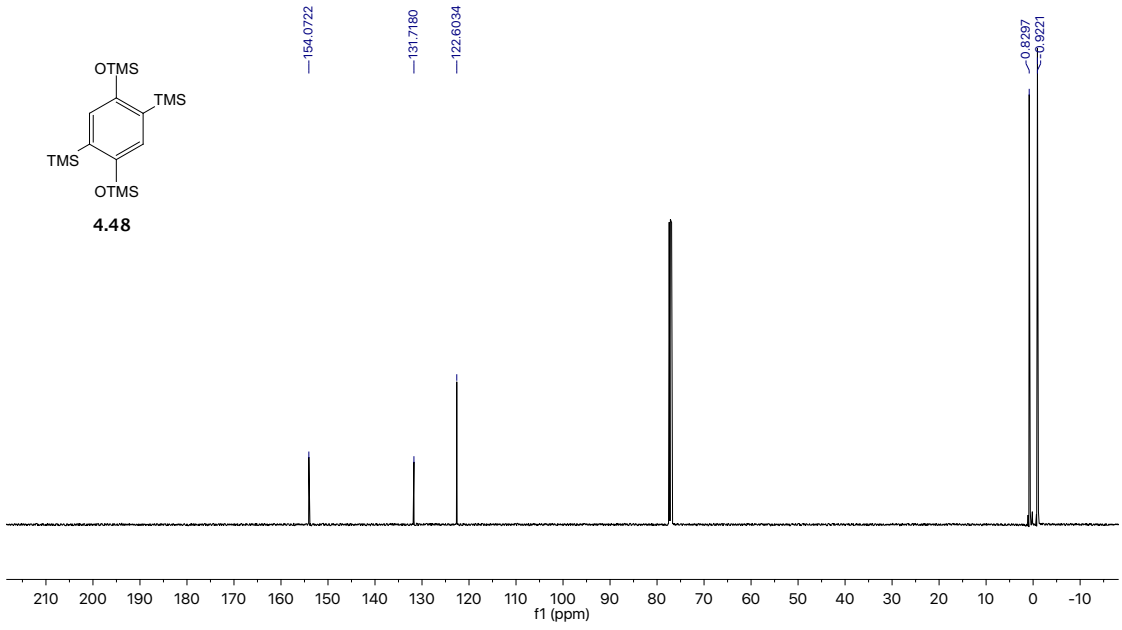

4.48

Parameter	Value
1 Data File Name	/ Users/ sarahwegwerth/ Dropbox/ Sarah Wegwerth (1)/ characterization data/ bisbenzyne precursor prep/ bisTMS, diol/ SW1-211crude.fid/ fid
2 Solvent	cdcl3
3 Acquisition Date	2013-07-25T09:35:12
4 Spectrometer Frequency	499.87
5 Nucleus	1H

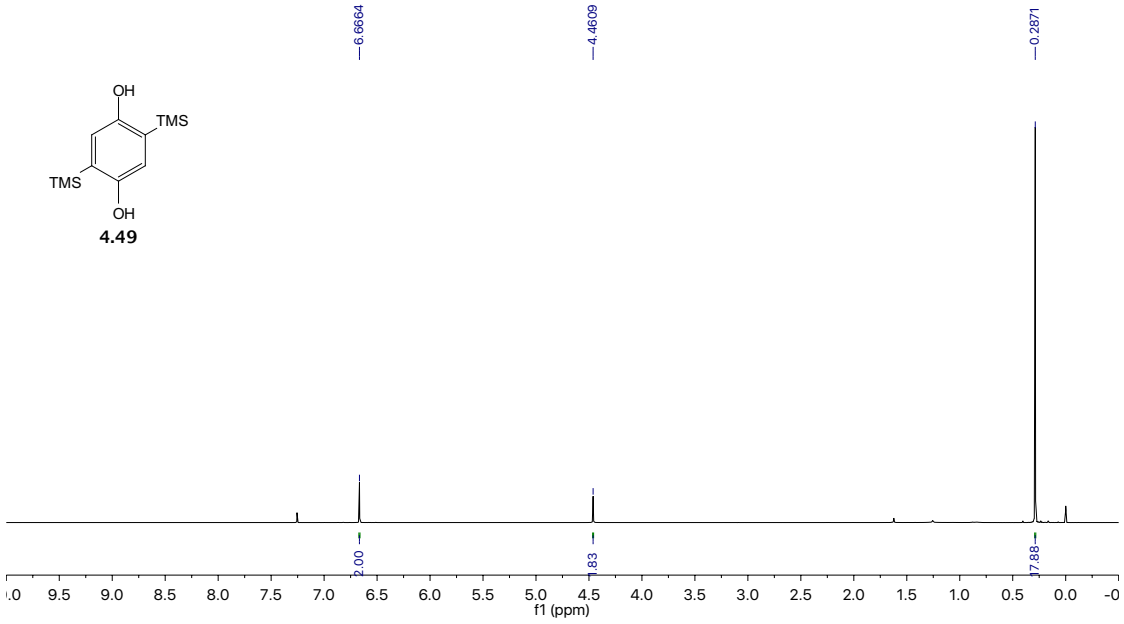

4.49

Parameter	Value
1 Data File Name	/ Users/ sarahwegwerth/ Dropbox/ Sarah Wegwerth (1)/ characterization data/ bisbenzyne precursor prep/ bisTMS, diol/ cdosew-161117-7 SEW1-185 13C, 19F/ 10/ fid
2 Solvent	CDCl3
3 Acquisition Date	2016-11-18T04:38:53
4 Spectrometer Frequency	125.78
5 Nucleus	13C

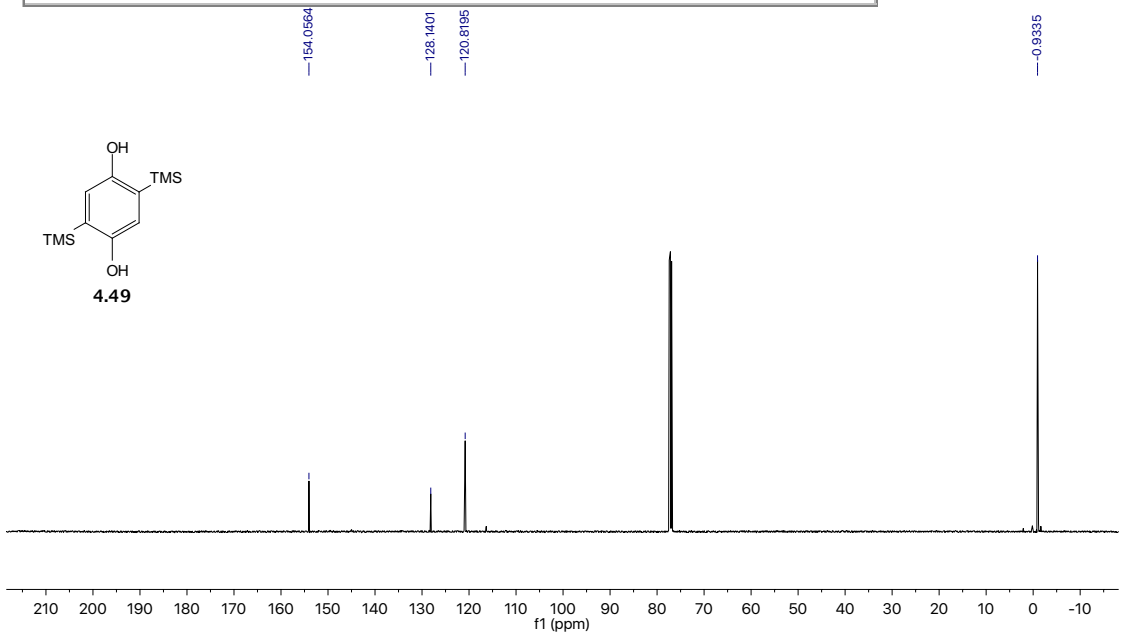

4.49

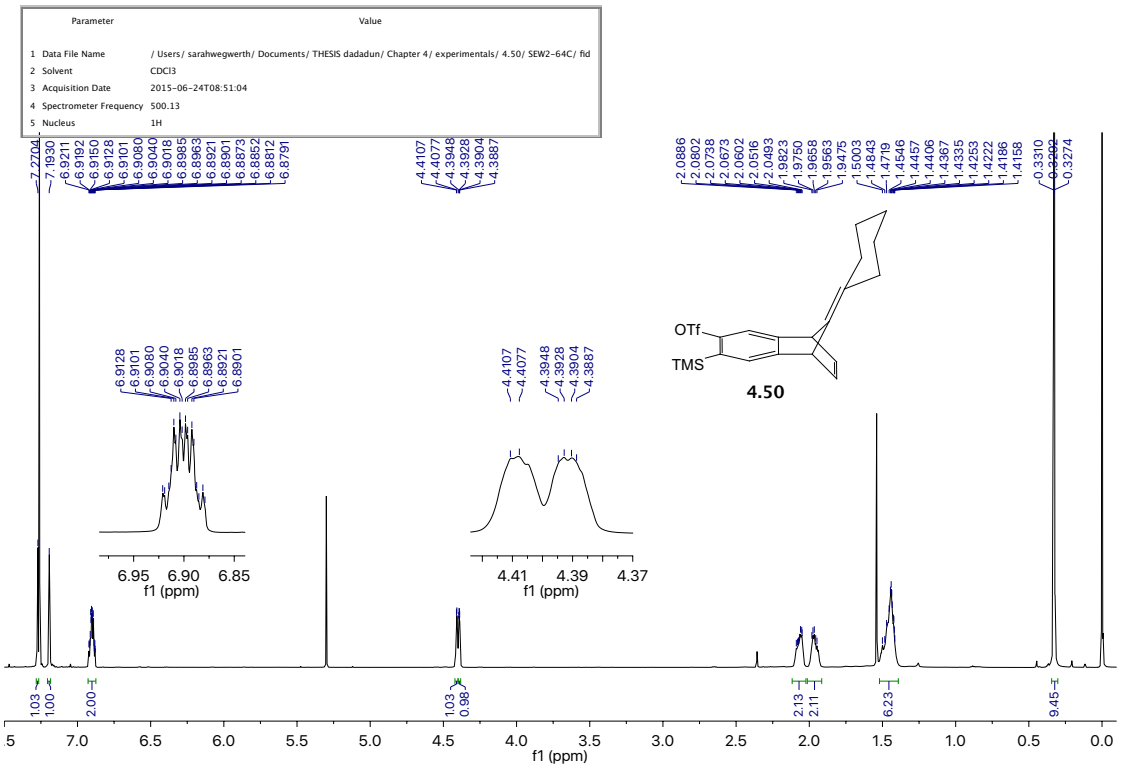
Parameter
Value
1 Data File Name / Users/ sarahwegwerth/ Documents/ THESIS dadadun/ Chapter 4/ experimentals/ 4.50/ SEW2-64C/ fid
2 Solvent CDCl3
3 Acquisition Date 2015-06-24T08:51:04
4 Spectrometer Frequency 500.13
5 Nucleus 1H
OTf
TMS
4.50
f1 (ppm)

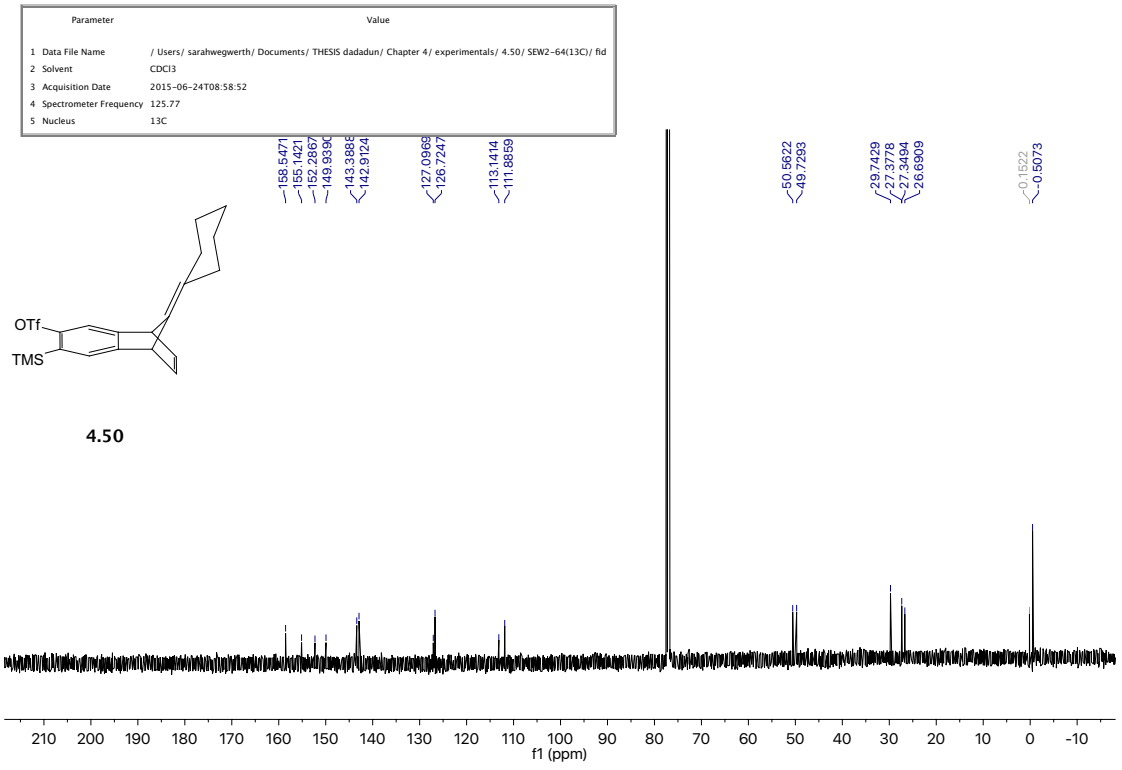
Parameter
Value
1 Data File Name / Users/ sarahwegwerth/ Documents/ THESIS dadadun/ Chapter 4/ experimentals/ 4.50/ SEW2-64(13C)/ fid
2 Solvent CDCl3
3 Acquisition Date 2015-06-24T08:58:52
4 Spectrometer Frequency 125.77
5 Nucleus 13C
OTf
TMS
4.50
f1 (ppm)

Parameter	Value
1 Data File Name	/ Users/ sarahwegwerth/ Documents/ THESIS dadadun/ Chapter 4/ experimentals/ 4.50/ SEW2-64(19F)/ fid
2 Solvent	CDCl3
3 Acquisition Date	2015-06-24T09:00:44
4 Spectrometer Frequency	470.55
5 Nucleus	19F

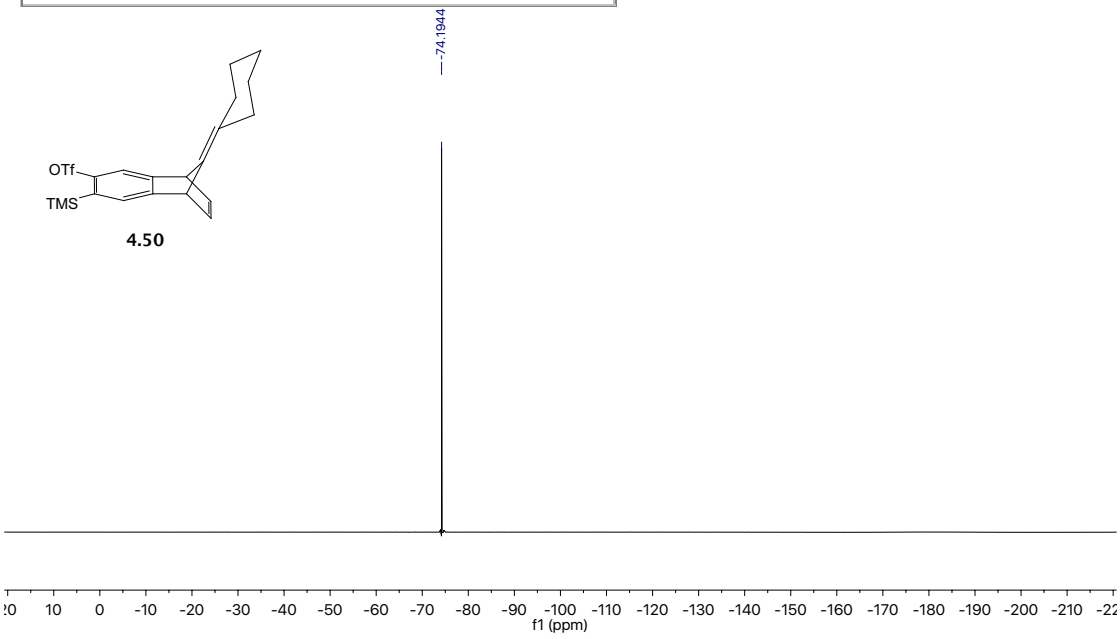

NMR Spectra Chapter 5

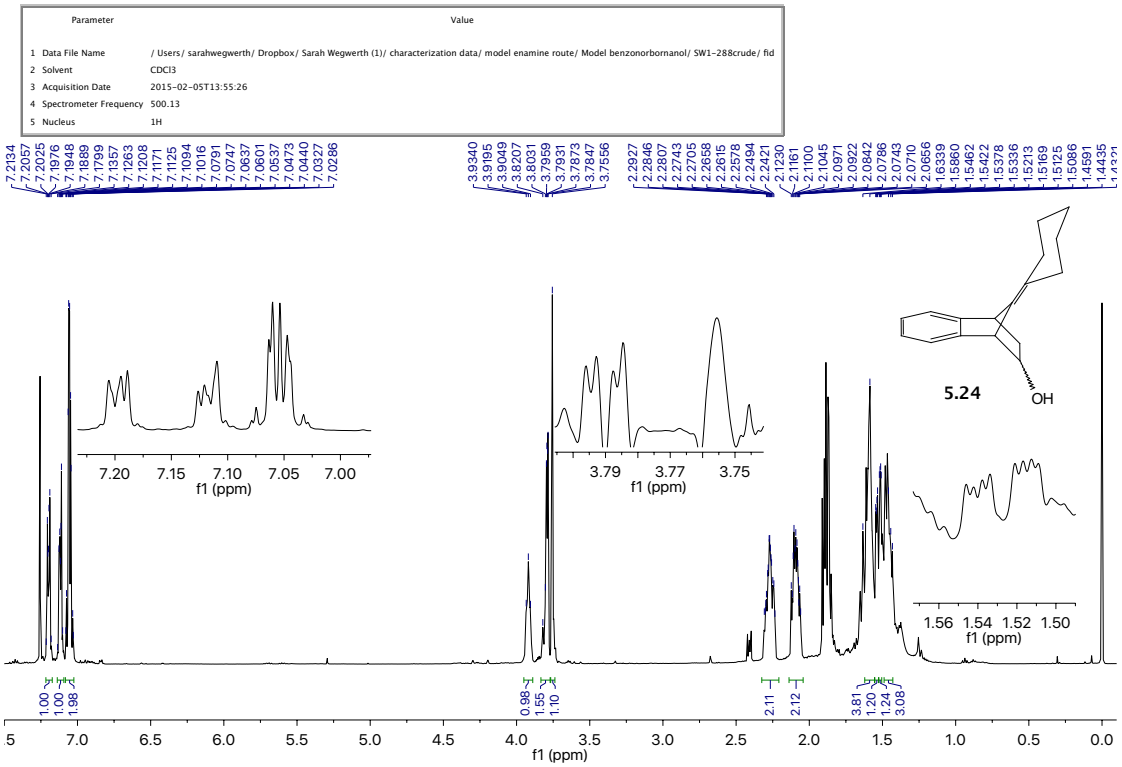

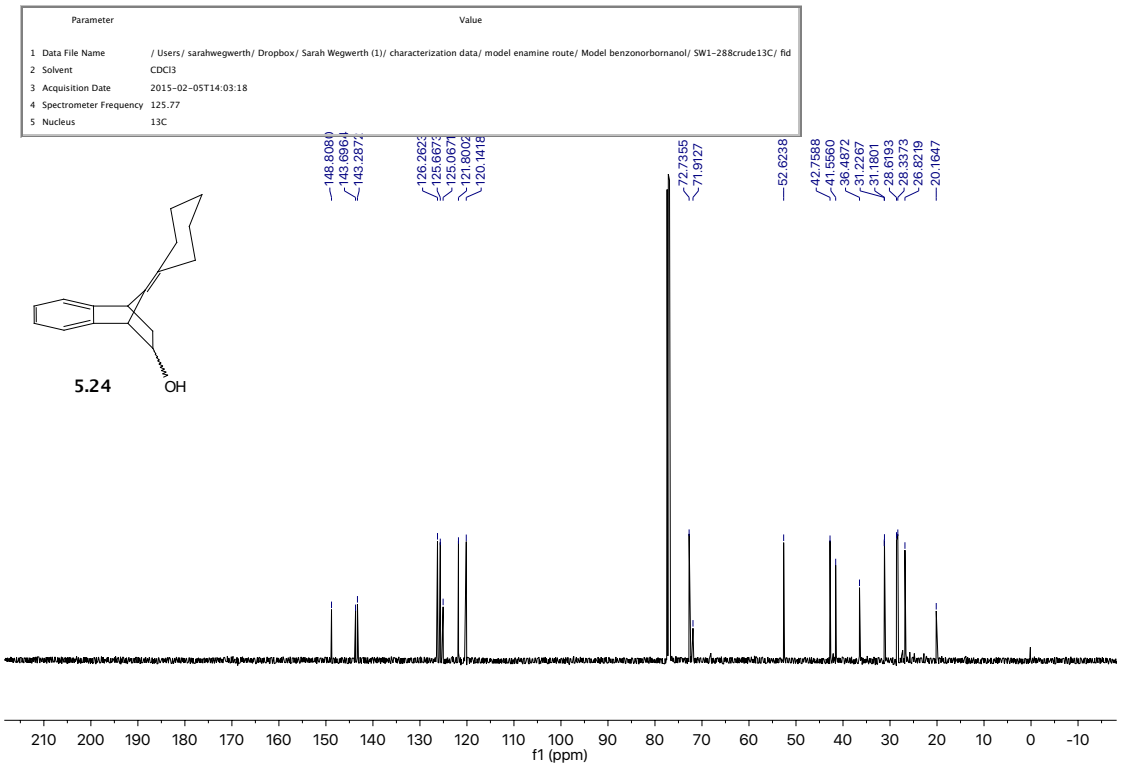

Parameter	Value
1 Data File Name	/ Users/ sarahwegwerth/ Dropbox/ Sarah Wegwerth (1)/ characterization data/ model enamine route/ Model benzonorbornannone/ SEW2-21B/ fid
2 Solvent	CDCl3
3 Acquisition Date	2015-03-17T19:14:31
4 Spectrometer Frequency	500.13
5 Nucleus	1H

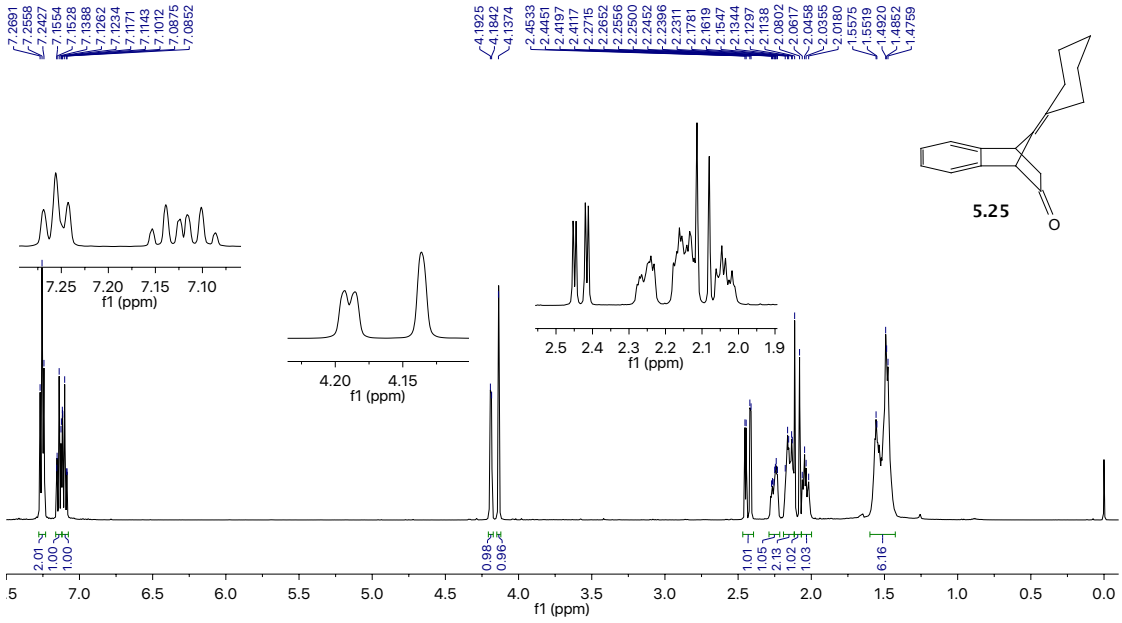

Parameter	Value
1 Data File Name	/ Users/ sarahwegwerth/ Dropbox/ Sarah Wegwerth (1)/ characterization data/ model enamine route/ Model benzonorbornannone/ SEW2-21B_13C/ fid
2 Solvent	CDCl3
3 Acquisition Date	2015-03-18T13:10:18
4 Spectrometer Frequency	125.77
5 Nucleus	13C

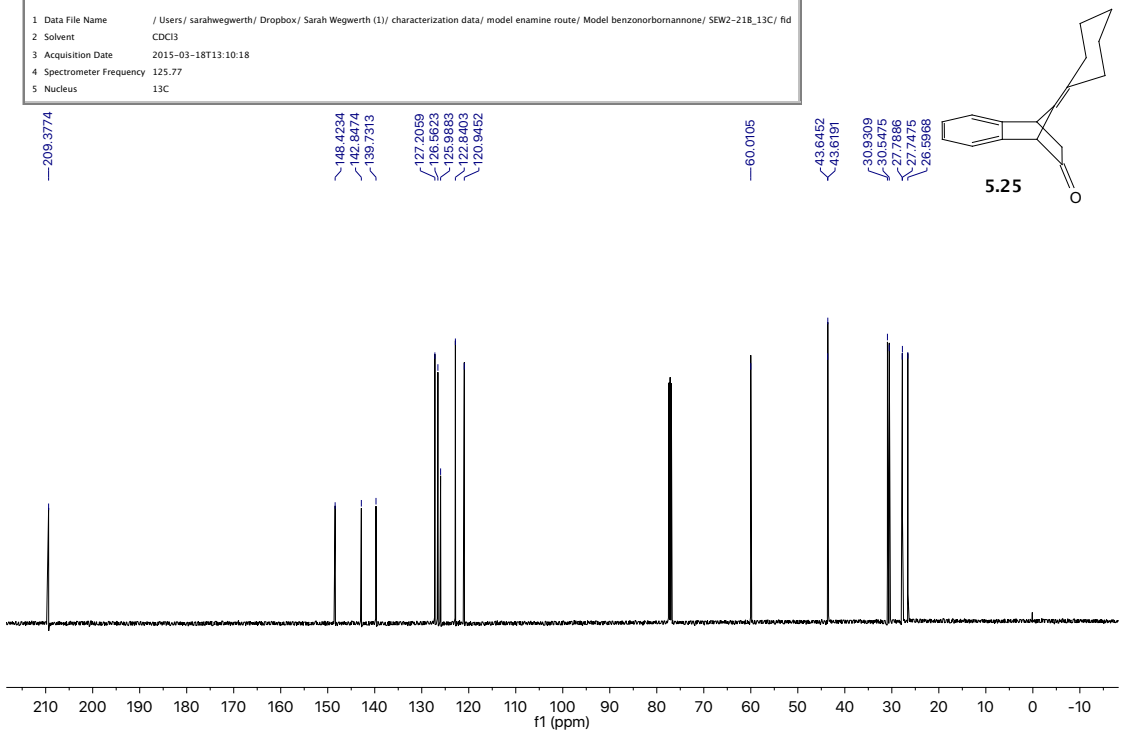

Parameter	Value
1 Data File Name	/ Users/ sarahwegwerth/ Dropbox/ Sarah Wegwerth (1)/ characterization data/ model cyclopentadienone/ model diol (SEW2-67B)/ NMRs/ SEW2-67B/ fid
2 Solvent	CDCl3
3 Acquisition Date	2015-08-05T13:38:38
4 Spectrometer Frequency	500.13
5 Nucleus	1H

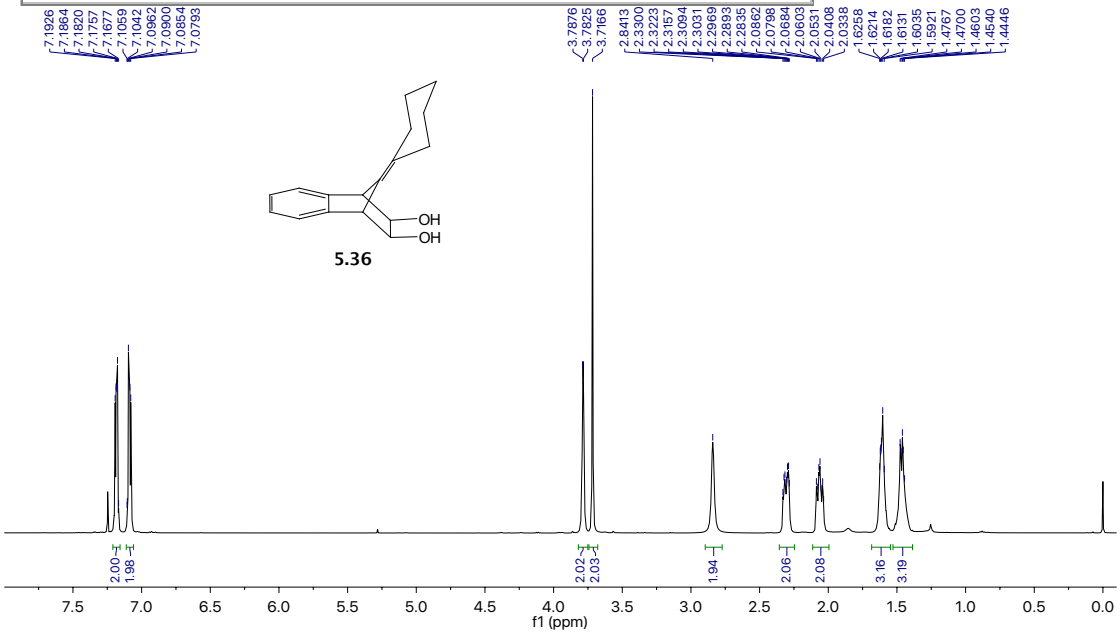

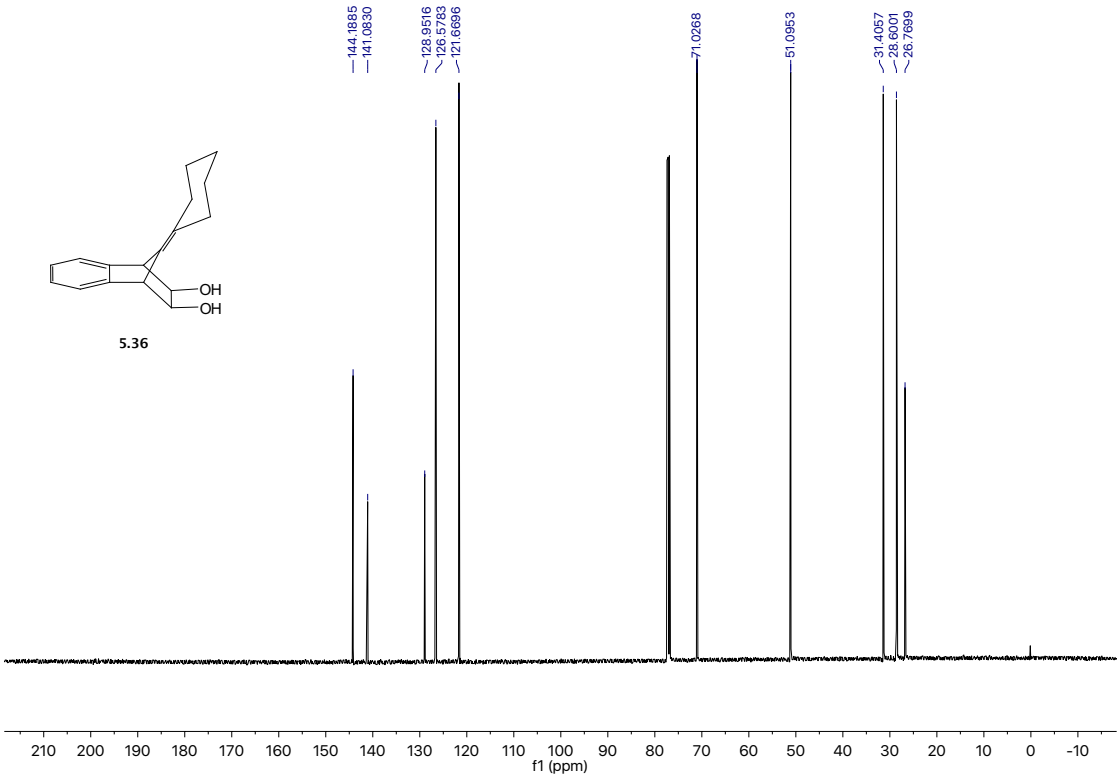

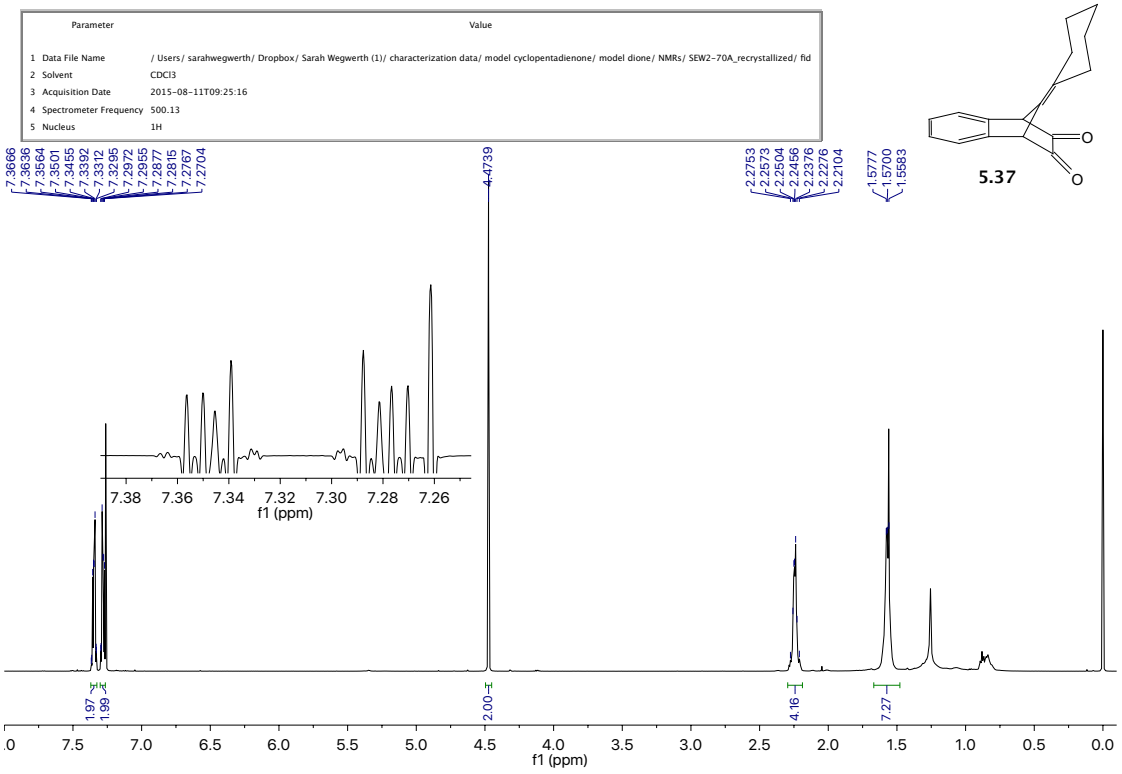
Parameter
Value
1 Data File Name / Users/ sarahwegwerth/ Dropbox/ Sarah Wegwerth (1)/ characterization data/ model cyclopentadienone/ model dione/ NMRs/ SEW2-70A_recrystallized/ fid
2 Solvent CDCl3
3 Acquisition Date 2015-08-11T09:25:16
4 Spectrometer Frequency 500.13
5 Nucleus 1H
7.3666
7.3636
7.3564
7.3501
7.3455
7.3392
7.3312
7.3295
7.2972
7.2955
7.2877
7.2815
7.2767
7.2704
4.4739
2.2753
2.2573
2.2504
2.2456
2.2376
2.2276
2.2104
1.5777
1.5700
1.5583
5.37
O
O
7.38 7.36 7.34 7.32 7.30 7.28 7.26
f1 (ppm)
1.97
1.99
2.00
4.16
7.27
.0 7.5 7.0 6.5 6.0 5.5 5.0 4.5 4.0 3.5 3.0 2.5 2.0 1.5 1.0 0.5 0.0
f1 (ppm)

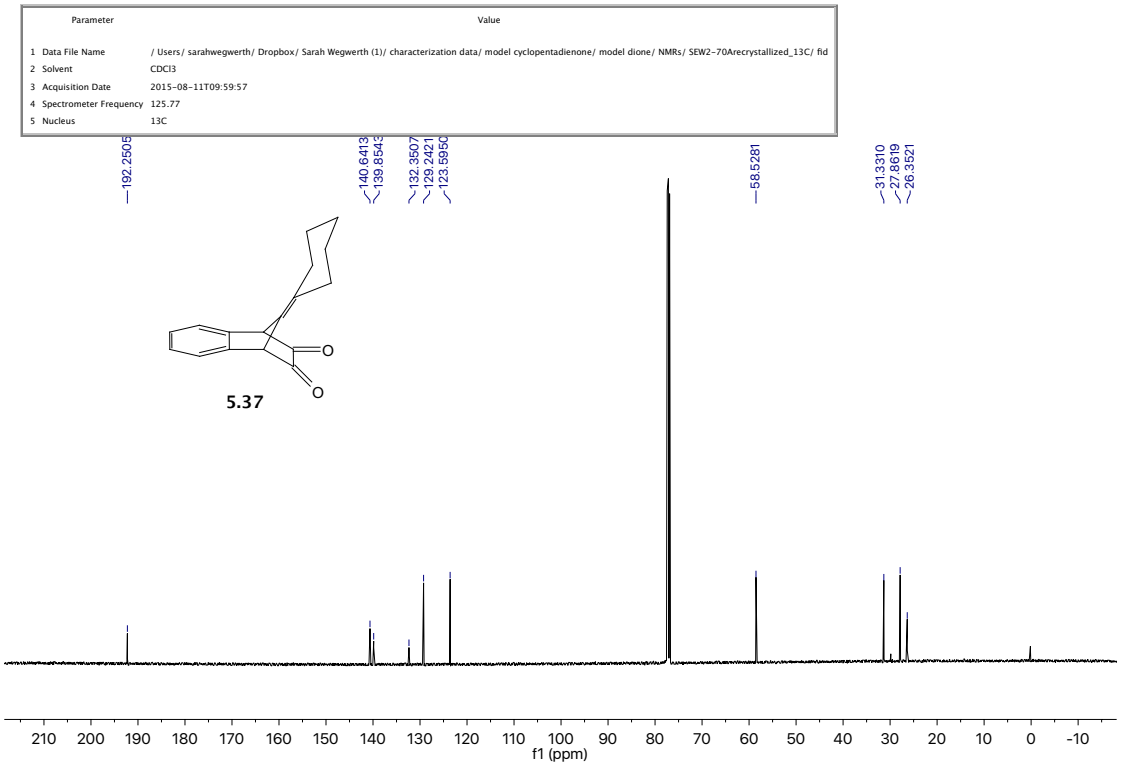
Parameter
Value
1 Data File Name / Users/ sarahwegwerth/ Dropbox/ Sarah Wegwerth (1)/ characterization data/ model cyclopentadienone/ model dione/ NMRs/ SEW2-70Arecrystallized_13C/ fid
2 Solvent CDCl3
3 Acquisition Date 2015-08-11T09:59:57
4 Spectrometer Frequency 125.77
5 Nucleus 13C
192.2505
140.6413
139.8543
132.3507
129.2421
123.5950
58.5281
31.3310
27.8619
26.3521
O
O
5.37
210 200 190 180 170 160 150 140 130 120 110 100 90 80 70 60 50 40 30 20 10 0 -10
f1 (ppm)

Parameter	Value
1 Data File Name	/ Users/ sarahwegwerth/ Dropbox/ Sarah Wegwerth (1)/ characterization data/ model cyclopentadienone/ rearranged dione/ SEW2-74recryst-3hlight/ fid
2 Solvent	CDCl3
3 Acquisition Date	2015-09-30T11:27:47
4 Spectrometer Frequency	500.13
5 Nucleus	1H

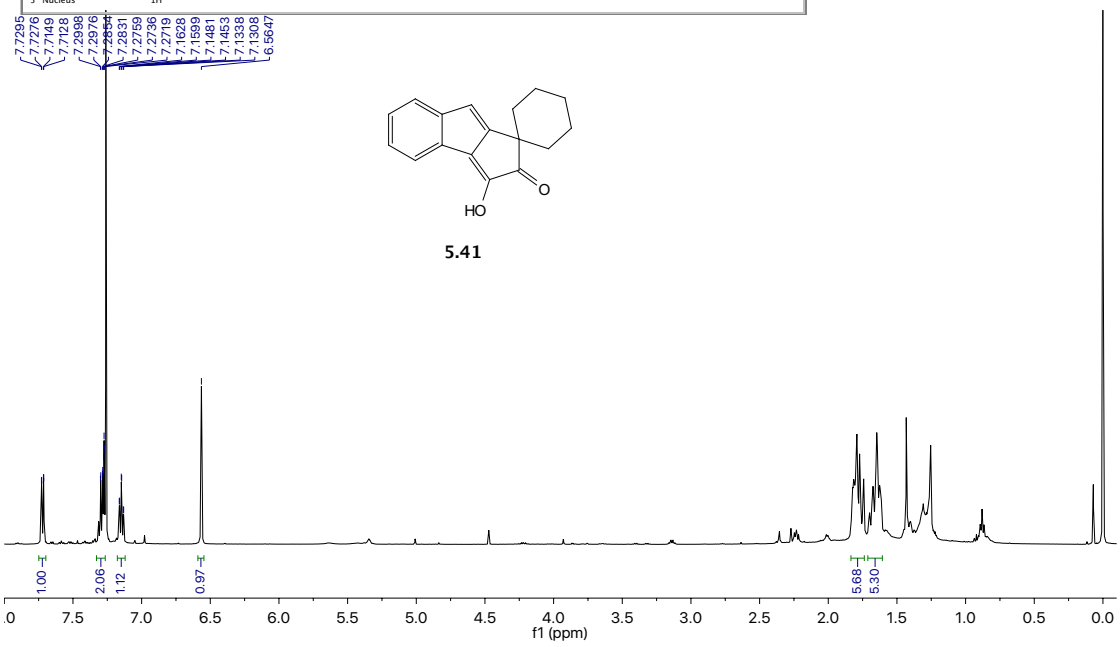

5.41

Parameter	Value
1 Data File Name	/ Users/ sarahwegwerth/ Dropbox/ Sarah Wegwerth (1)/ characterization data/ model cyclopentadienone/ rearranged dione/ SEW2-74recryst-3hlight13C/ fid
2 Solvent	CDCl3
3 Acquisition Date	2015-09-30T12:03:06
4 Spectrometer Frequency	125.77
5 Nucleus	13C

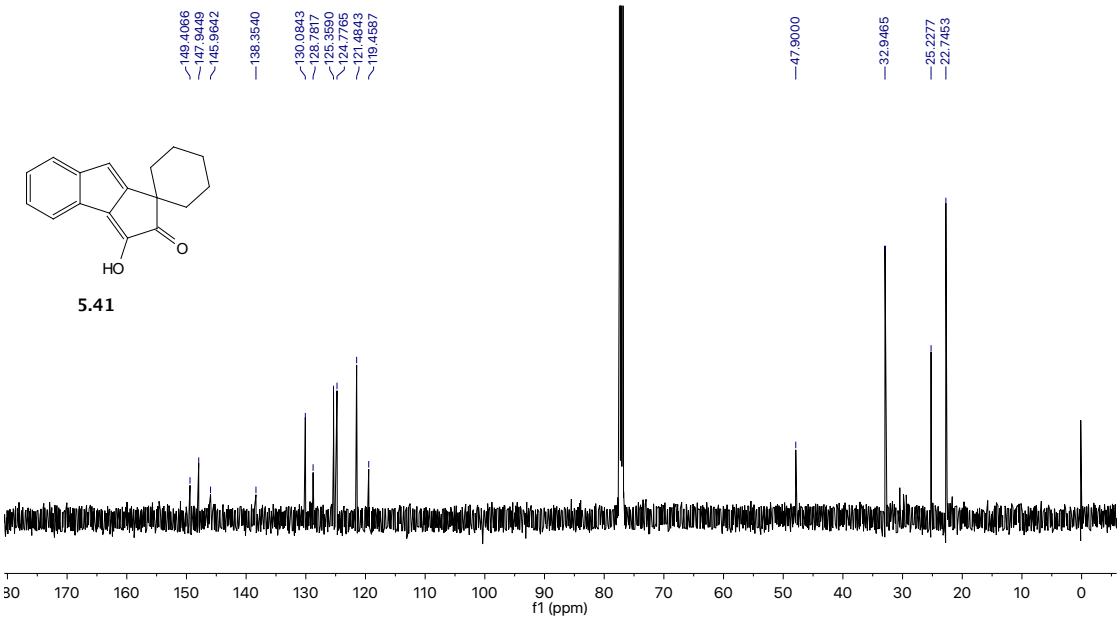

5.41

NMR Spectra Chapter 6

	Parameter	Value
1	Data File Name	/ Users/ sarahwegwerth/ Dropbox/ Sarah Wegwerth (1)/ characterization data/ tetracene route/ Model Study Tetracene/ dibromoquinone/ cdosew-170711-20/ 10/ fid
2	Solvent	CDCl3
3	Acquisition Date	2017-07-11T12:26:06
4	Spectrometer Frequency	400.13
5	Nucleus	1H

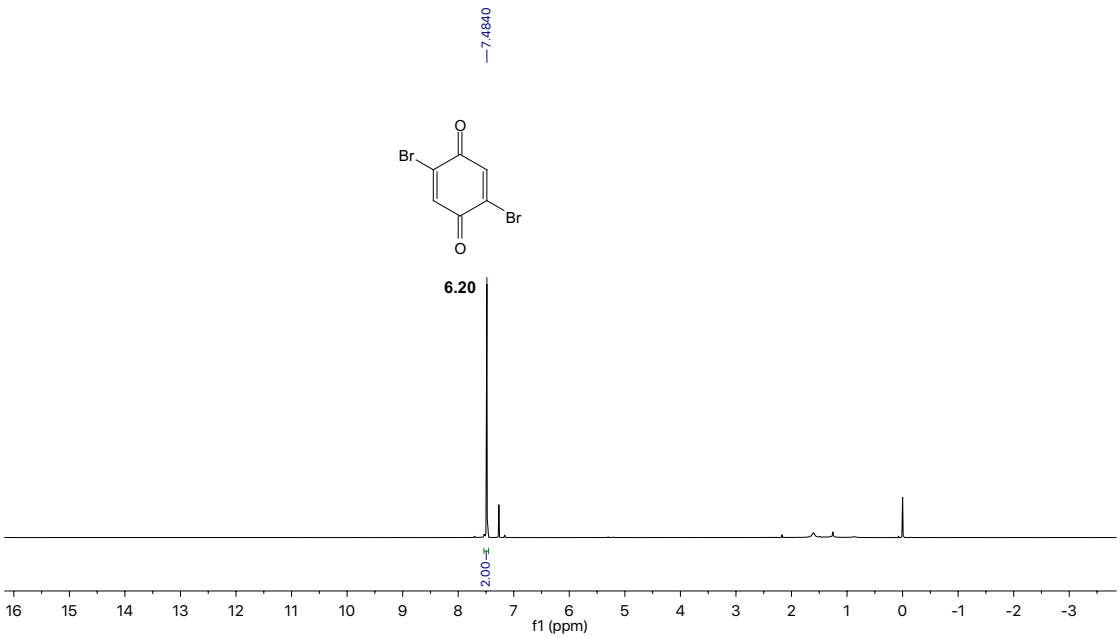

	Parameter	Value
1	Data File Name	/ Users/ sarahwegwerth/ Dropbox/ Sarah Wegwerth (1)/ characterization data/ tetracene route/ Model Study Tetracene/ dibromoquinone/ cdosew-170711-20/ 11/ fid
2	Solvent	CDCl3
3	Acquisition Date	2017-07-11T12:34:45
4	Spectrometer Frequency	100.62
5	Nucleus	13C

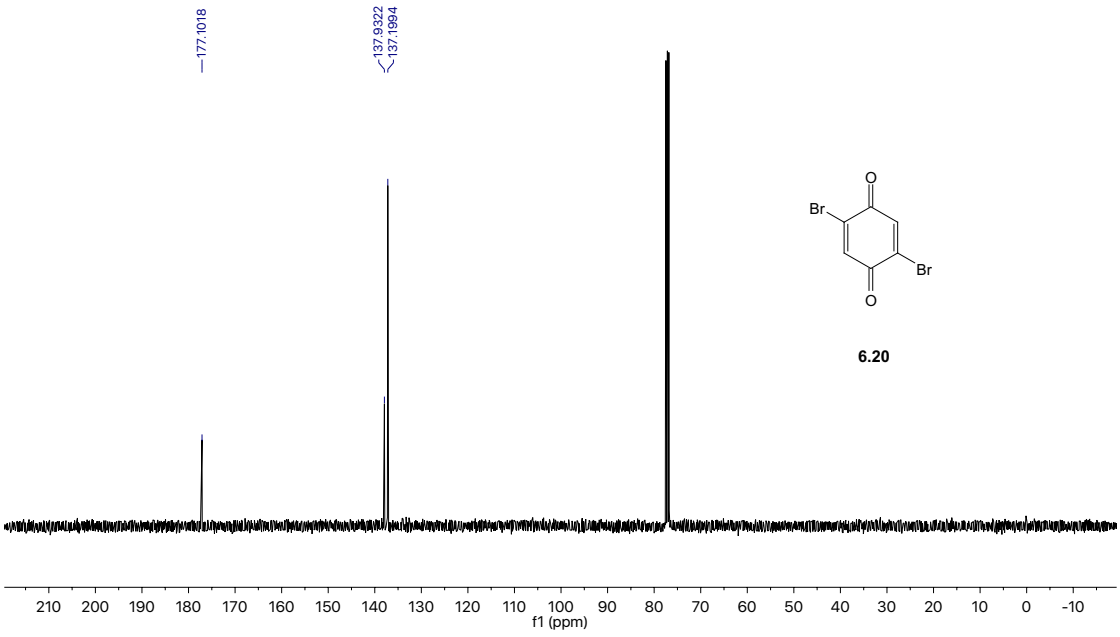

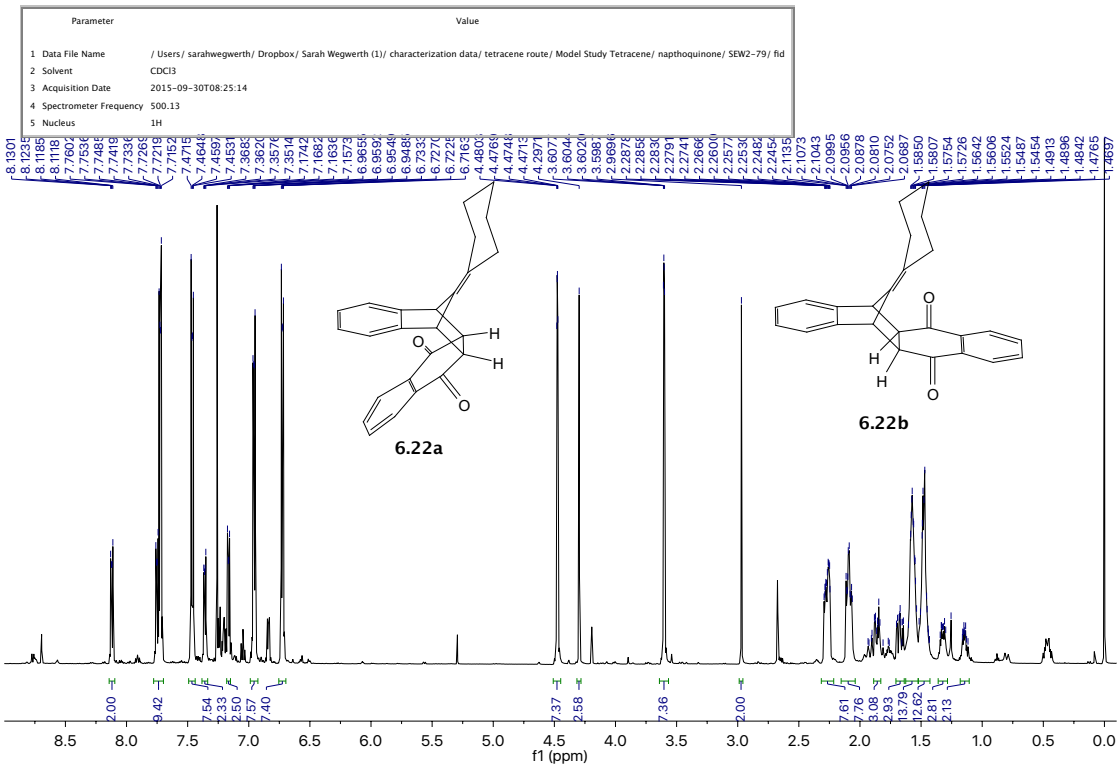
Parameter
Value
1 Data File Name / Users/ sarahwegwerth/ Dropbox/ Sarah Wegwerth (1)/ characterization data/ tetracene route/ Model Study Tetracene/ napthoquinone/ SEW2-79/ fid
2 Solvent CDCl3
3 Acquisition Date 2015-09-30T08:25:14
4 Spectrometer Frequency 500.13
5 Nucleus 1H
6.22a
6.22b
f1 (ppm)

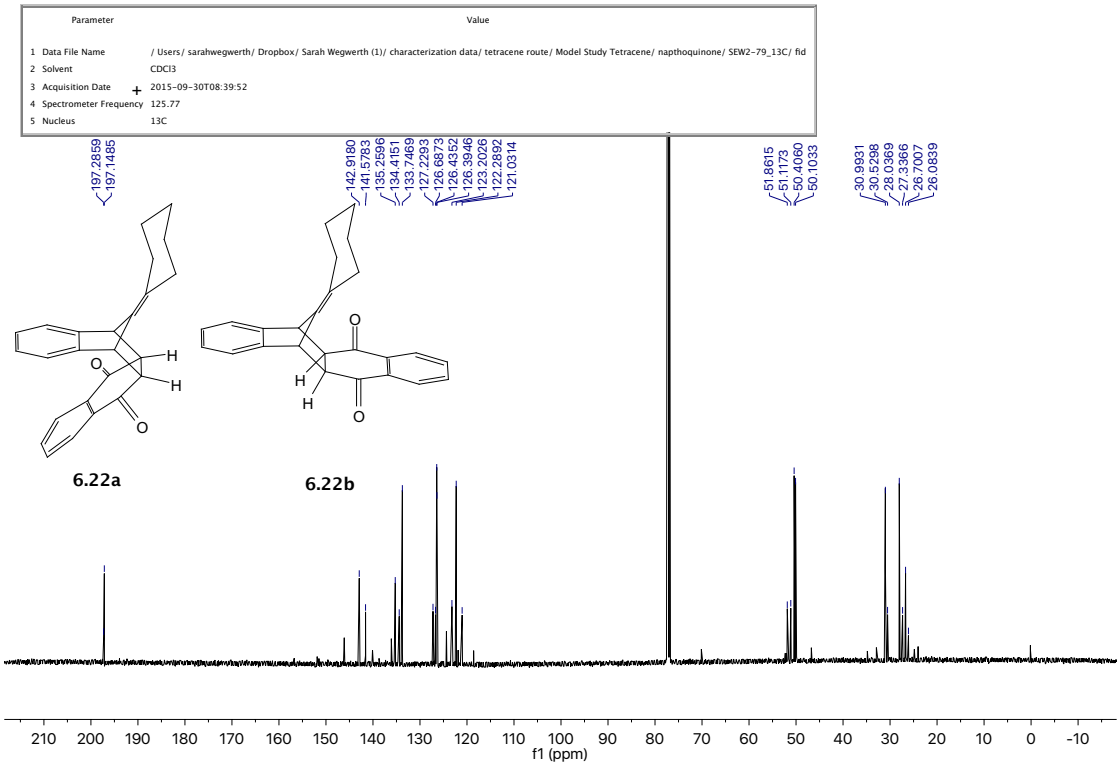
Parameter
Value
1 Data File Name / Users/ sarahwegwerth/ Dropbox/ Sarah Wegwerth (1)/ characterization data/ tetracene route/ Model Study Tetracene/ napthoquinone/ SEW2-79_13C/ fid
2 Solvent CDCl3
3 Acquisition Date 2015-09-30T08:39:52
4 Spectrometer Frequency 125.77
5 Nucleus 13C
6.22a
6.22b
f1 (ppm)

Parameter	Value
1 Data File Name	/ Users/ sarahwegwerth/ Dropbox/ Sarah Wegwerth (1)/ characterization data/ tetracene route/ Model Study Tetracene/ 1st addition post elimination/ SEW2-99-3columns/ fid
2 Solvent	CDCl3
3 Acquisition Date	2015-11-11T12:55:44
4 Spectrometer Frequency	399.87
5 Nucleus	1H

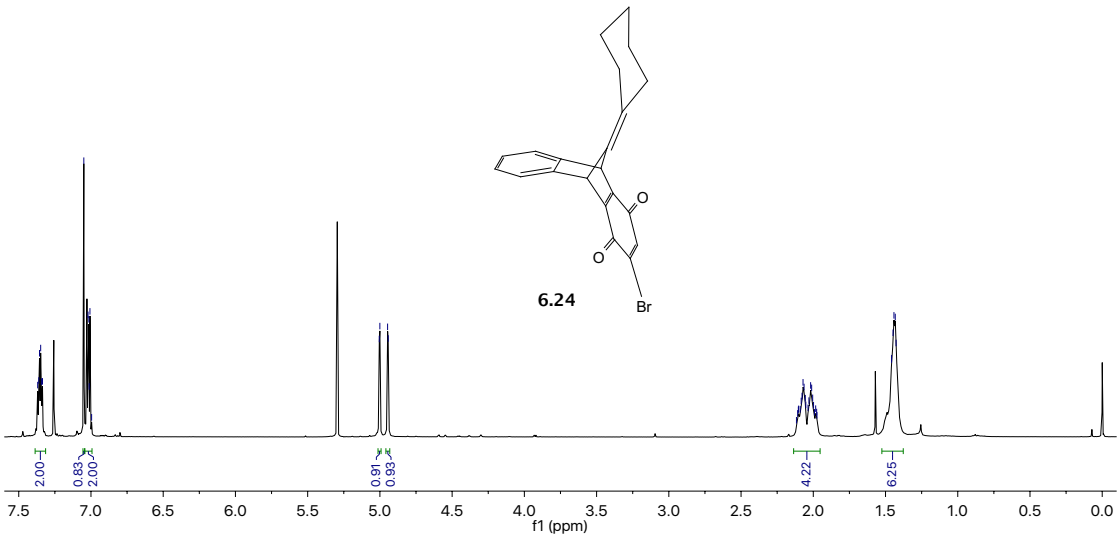

Parameter	Value
1 Data File Name	/ Users/ sarahwegwerth/ Documents/ THESIS dadadun/ Chapter 6/ Ch 6 Experimentals/ 6.24/ SEW2-99-13C/ fid
2 Solvent	CDCl3
3 Acquisition Date	2015-11-12T08:34:10
4 Spectrometer Frequency	125.77
5 Nucleus	13C

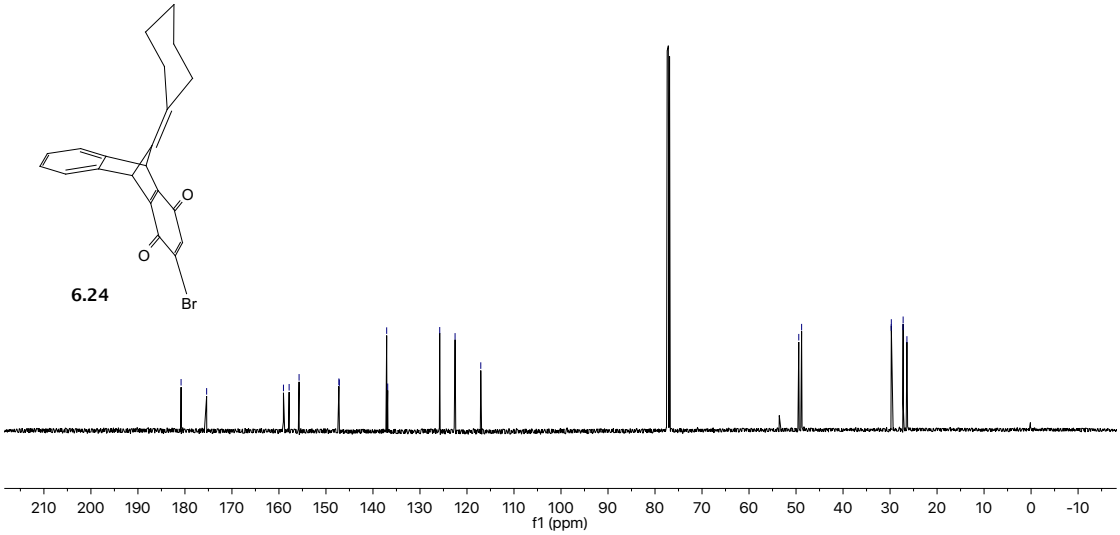

Parameter	Value
1 Data File Name	/ Users/ sarahwegwerth/ Dropbox/ Sarah Wegwerth (1)/ characterization data/ tetracene route/ Model Study Tetracene/ 2nd addition post elimination/ SEW2-102-post-alumina/ fid
2 Solvent	CDCl3
3 Acquisition Date	2015-11-13T14:59:05
4 Spectrometer Frequency	399.87
5 Nucleus	1H

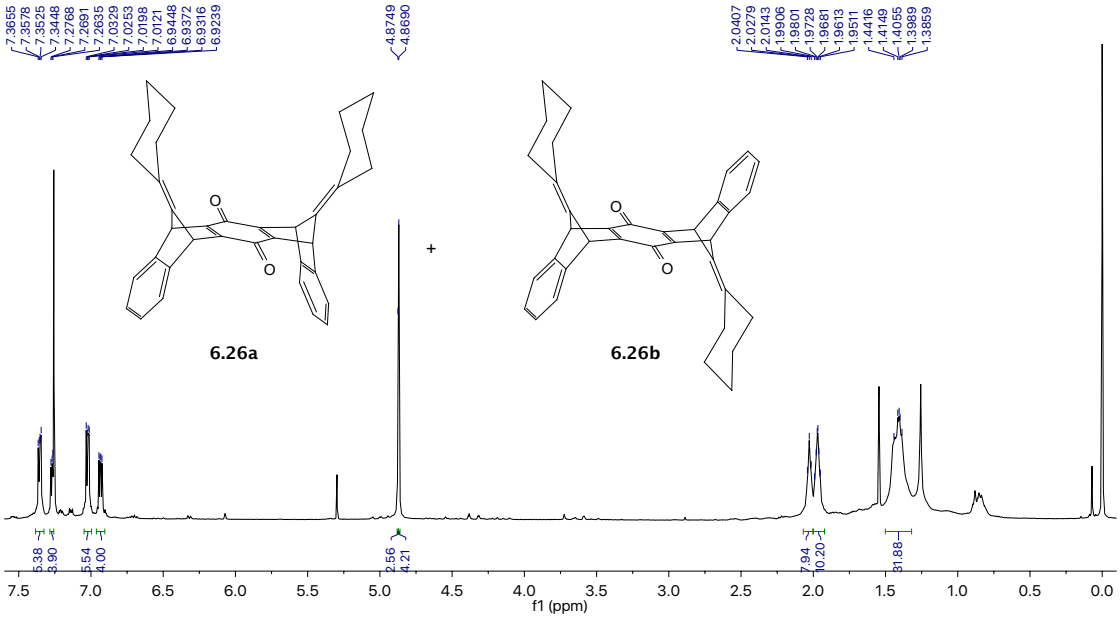

Parameter	Value
1 Data File Name	/ Users/ sarahwegwerth/ Dropbox/ Sarah Wegwerth (1)/ characterization data/ tetracene route/ bisquinone/ syn/ SEW2-139DA/ fid
2 Solvent	CDCl3
3 Acquisition Date	2016-03-25T02:12:28
4 Spectrometer Frequency	500.13
5 Nucleus	1H

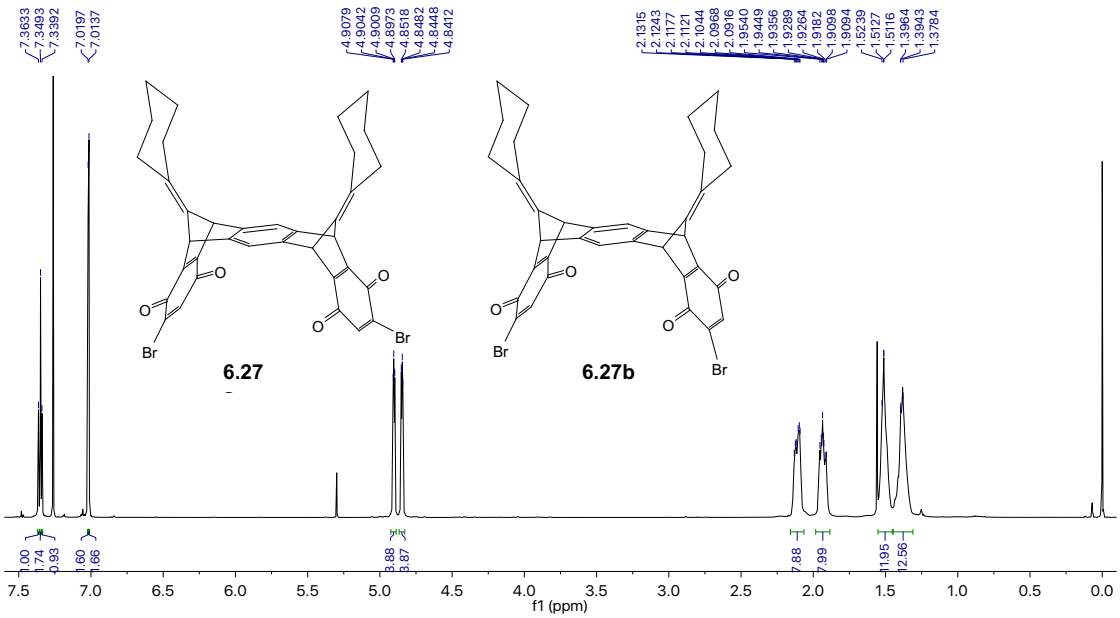

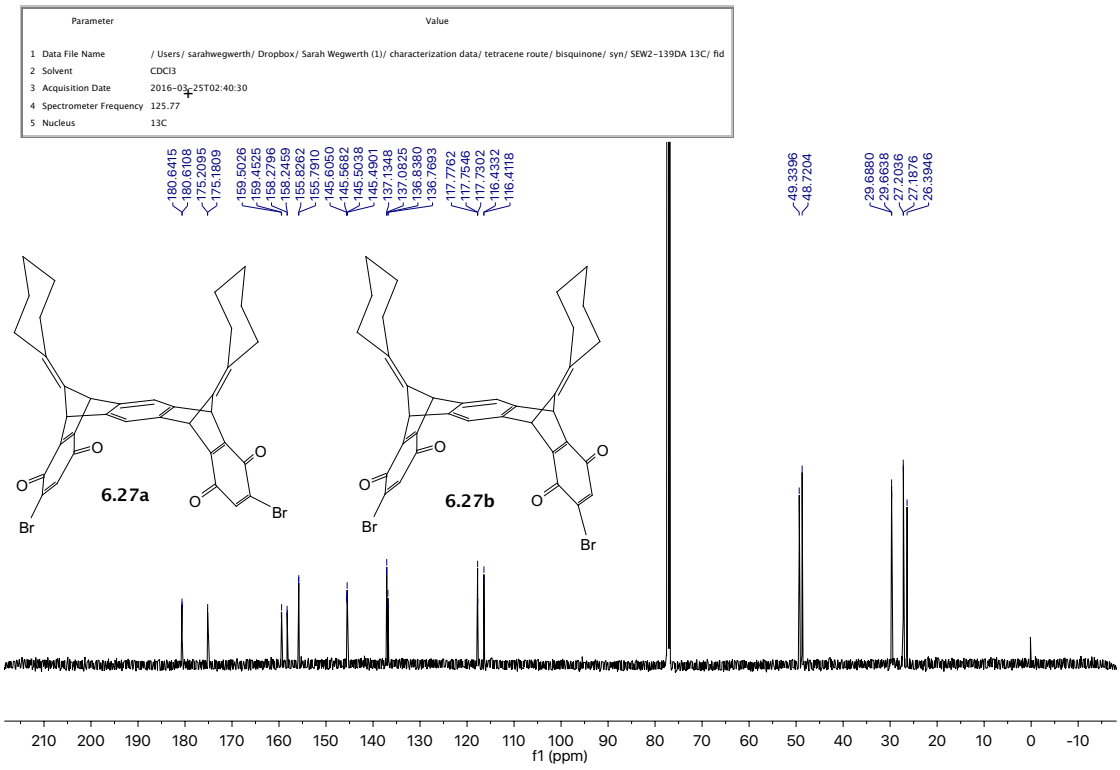
Parameter
Value
1 Data File Name / Users/ sarahwegwerth/ Dropbox/ Sarah Wegwerth (1)/ characterization data/ tetracene route/ bisquinone/ syn/ SEW2-139DA 13C/ fid
2 Solvent CDCl3
3 Acquisition Date 2016-03-25T02:40:30
4 Spectrometer Frequency 125.77
5 Nucleus 13C
180.6415
180.6108
175.2095
175.1809
159.5026
159.4525
158.2796
158.2459
156.8262
155.7910
145.6050
145.5682
145.5038
145.4901
137.1348
137.0825
136.8380
136.7693
117.7762
117.7546
117.7302
116.4332
116.4118
49.3396
48.7204
29.6880
29.6638
27.2036
27.1876
26.3946
6.27a
6.27b
f1 (ppm)

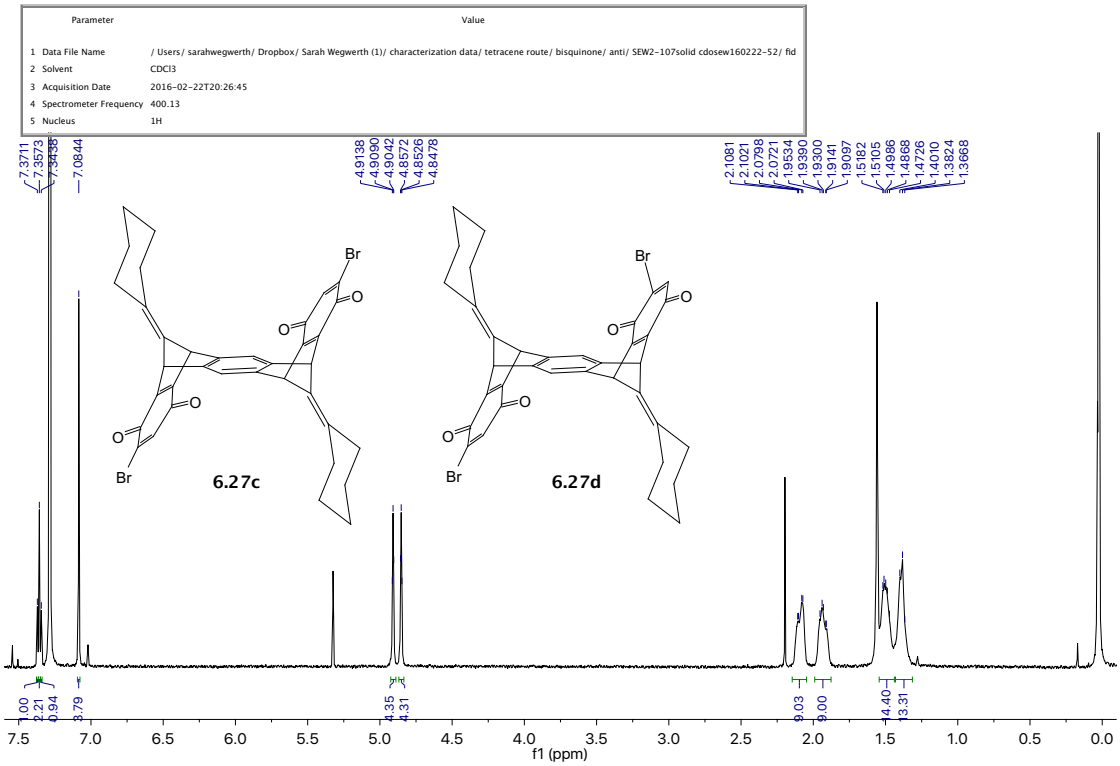
Parameter
Value
1 Data File Name / Users/ sarahwegwerth/ Dropbox/ Sarah Wegwerth (1)/ characterization data/ tetracene route/ bisquinone/ anti/ SEW2-107solid cdosew160222-52/ fid
2 Solvent CDCl3
3 Acquisition Date 2016-02-22T20:26:45
4 Spectrometer Frequency 400.13
5 Nucleus 1H
7.3711
7.3573
7.3438
7.0844
4.9138
4.9090
4.9042
4.8572
4.8526
4.8478
2.1081
2.1021
2.0798
2.0721
1.9534
1.9390
1.9300
1.9141
1.9097
1.5182
1.5105
1.4986
1.4868
1.4726
1.4010
1.3824
1.3668
6.27c
6.27d
1.00
2.21
0.94
3.79
4.35
4.31
9.03
9.00
14.40
13.31
f1 (ppm)

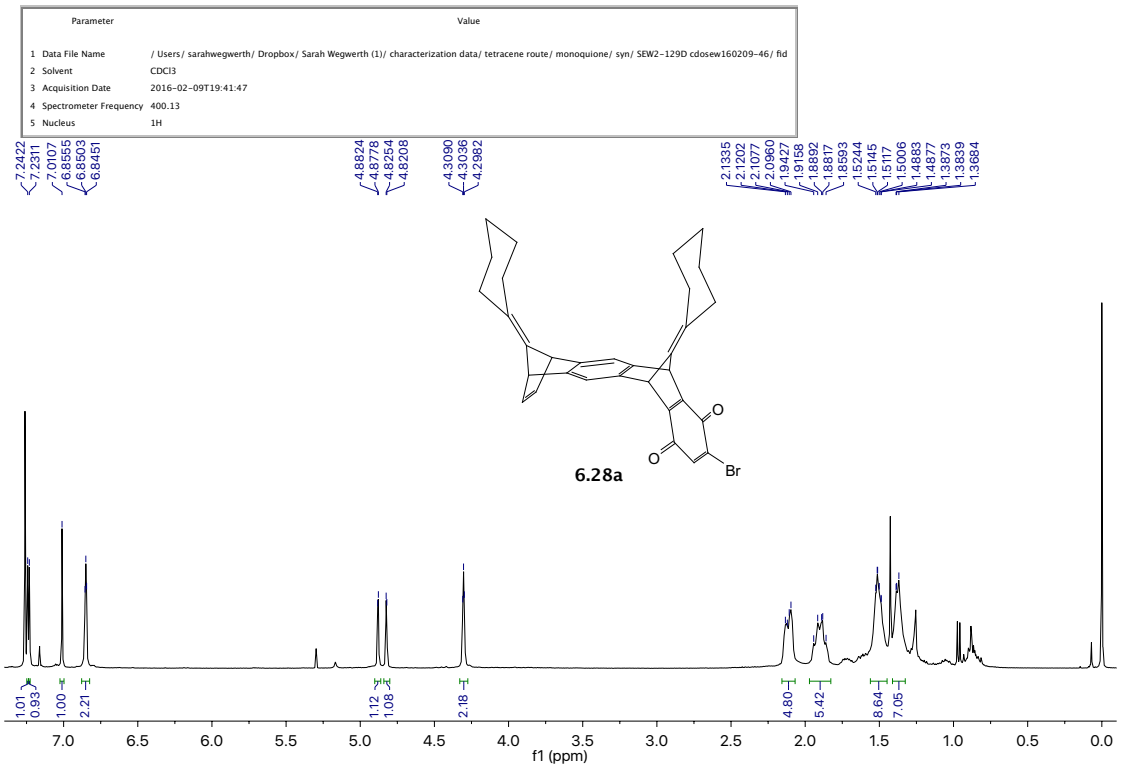
Parameter
Value
1 Data File Name / Users/ sarahwegwerth/ Dropbox/ Sarah Wegwerth (1)/ characterization data/ tetracene route/ monoquione/ syn/ SEW2-129D cdosew160209-46/ fid
2 Solvent CDCl3
3 Acquisition Date 2016-02-09T19:41:47
4 Spectrometer Frequency 400.13
5 Nucleus 1H
7.2422
7.2311
7.0107
6.8555
6.8503
6.8451
4.8824
4.8778
4.8254
4.8208
4.3090
4.3036
4.2982
2.1335
2.1202
2.1077
2.0960
1.9427
1.9158
1.8892
1.8817
1.8593
1.5244
1.5145
1.5117
1.5006
1.4883
1.4877
1.3873
1.3839
1.3684
O
O
Br
6.28a
1.01
0.93
1.00
2.21
1.12
1.08
2.18
4.80
5.42
8.64
7.05
7.0
6.5
6.0
5.5
5.0
4.5
4.0
3.5
3.0
2.5
2.0
1.5
1.0
0.5
0.0
f1 (ppm)

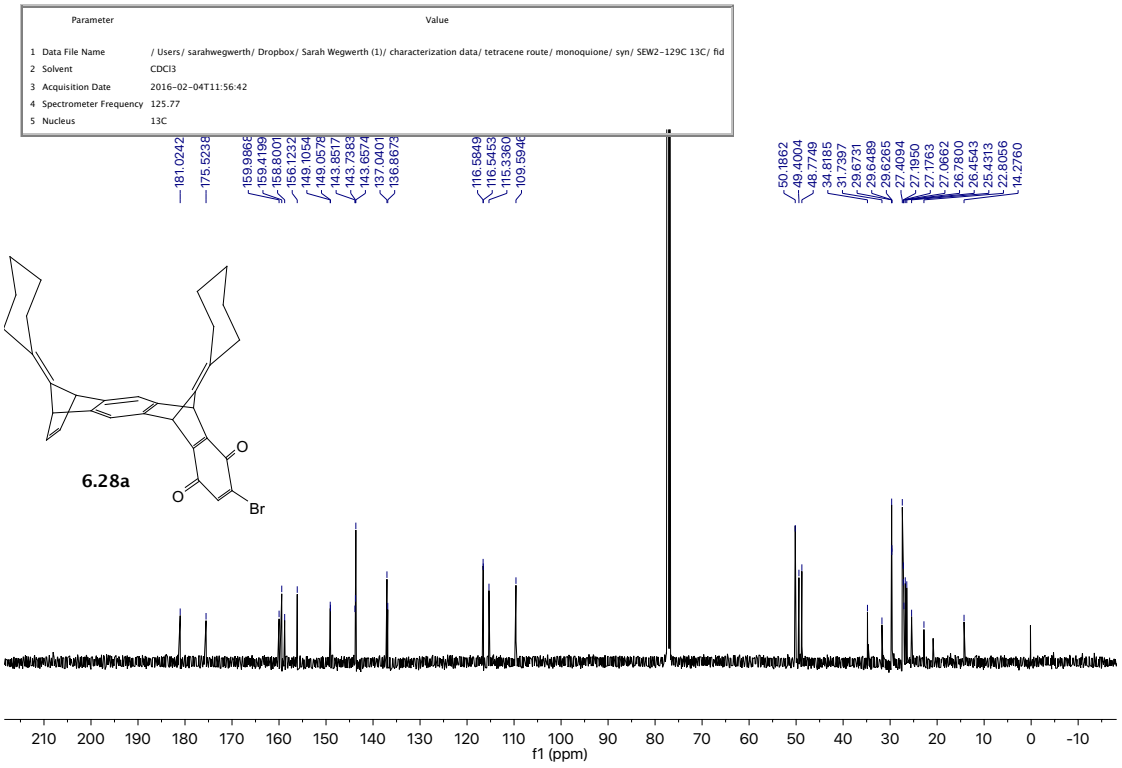
Parameter
Value
1 Data File Name / Users/ sarahwegwerth/ Dropbox/ Sarah Wegwerth (1)/ characterization data/ tetracene route/ monoquione/ syn/ SEW2-129C 13C/ fid
2 Solvent CDCl3
3 Acquisition Date 2016-02-04T11:56:42
4 Spectrometer Frequency 125.77
5 Nucleus 13C
181.0242
175.5238
159.9865
159.4199
158.8001
156.1232
149.1054
149.0578
143.8517
143.7383
143.6574
137.0401
136.8673
116.5849
116.5453
115.3360
109.5946
50.1862
49.4004
48.7749
34.8185
31.7397
29.6731
29.6489
29.6265
27.4094
27.1950
27.1763
27.0662
26.7800
26.4543
25.4313
22.8056
14.2760
O
O
Br
6.28a
210
200
190
180
170
160
150
140
130
120
110
100
90
80
70
60
50
40
30
20
10
0
-10
f1 (ppm)

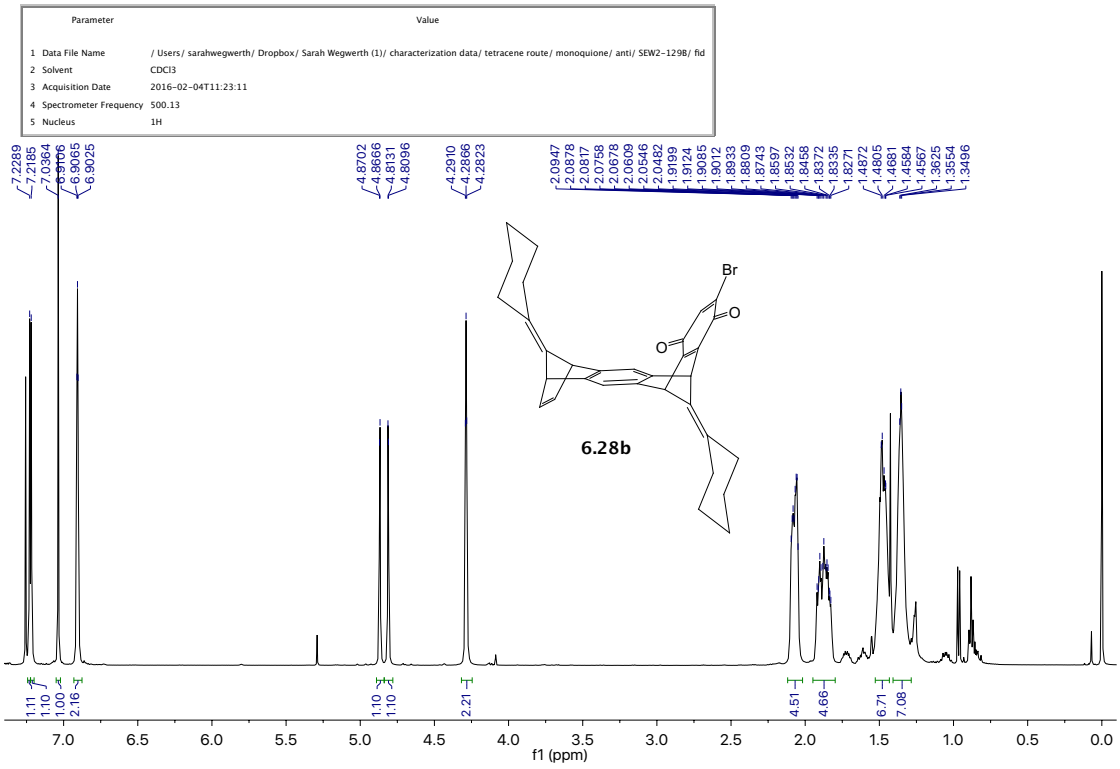
Parameter
Value
1 Data File Name / Users/ sarahwegwerth/ Dropbox/ Sarah Wegwerth (1)/ characterization data/ tetracene route/ monoquione/ anti/ SEW2-129B/ fid
2 Solvent CDCl3
3 Acquisition Date 2016-02-04T11:23:11
4 Spectrometer Frequency 500.13
5 Nucleus 1H
7.2289
7.2185
7.0364
6.9176
6.9065
6.9025
4.8702
4.8666
4.8131
4.8096
4.2910
4.2866
4.2823
2.0947
2.0878
2.0817
2.0758
2.0678
2.0609
2.0546
2.0482
1.9199
1.9124
1.9085
1.9012
1.8933
1.8809
1.8743
1.8597
1.8532
1.8458
1.8372
1.8335
1.8271
1.4872
1.4805
1.4681
1.4584
1.4567
1.3625
1.3554
1.3496
Br
O
O
6.28b
1.11
1.10
1.00
2.16
1.10
1.10
2.21
4.51
4.66
6.71
7.08
f1 (ppm)

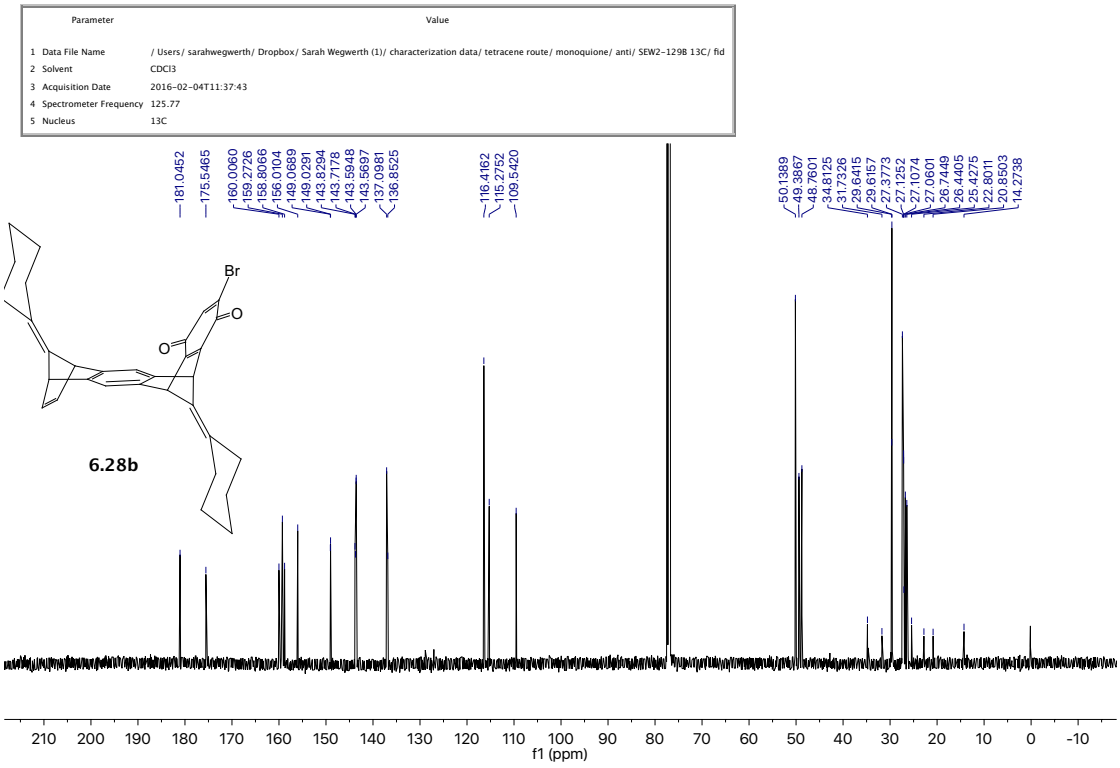
Parameter
Value
1 Data File Name / Users/ sarahwegwerth/ Dropbox/ Sarah Wegwerth (1)/ characterization data/ tetracene route/ monoquione/ anti/ SEW2-129B 13C/ fid
2 Solvent CDCl3
3 Acquisition Date 2016-02-04T11:37:43
4 Spectrometer Frequency 125.77
5 Nucleus 13C
181.0452
175.5465
160.0060
159.2726
158.8066
156.0104
149.0689
149.0291
143.8294
143.7178
143.5948
143.5697
137.0981
136.8525
116.4162
115.2752
109.5420
50.1389
49.3867
48.7601
34.8125
31.7326
29.6415
29.6157
27.3773
27.1252
27.1074
27.0601
26.7449
26.4405
25.4275
22.8011
20.8503
14.2738
Br
O
O
6.28b
f1 (ppm)